

**Rho GTPases and their regulators in cell
polarity of the filamentous ascomycete
*Neurospora crassa***

Dissertation
zur Erlangung des mathematisch-naturwissenschaftlichen Doktorgrades
"Doctor rerum naturalium"
der Georg-August-Universität Göttingen

vorgelegt von
Corinna Richthammer
aus Nürnberg

Göttingen 2011

Mitglied des Betreuungsausschusses: Dr. Stephan Seiler (Referent)

Abteilung Molekulare Mikrobiologie und Genetik, Institut für Mikrobiologie und Genetik,
Georg-August-Universität Göttingen

Mitglied des Betreuungsausschusses: Prof. Dr. Stefanie Pöggeler (Referentin)

Abteilung Genetik eukaryotischer Mikroorganismen, Institut für Mikrobiologie und Genetik,
Georg-August-Universität Göttingen

Mitglied des Betreuungsausschusses: Prof. Dr. Andreas Wodarz

Abteilung Stammzellbiologie, Göttinger Zentrum für Molekulare Biowissenschaften, Georg-
August-Universität Göttingen

Tag der mündlichen Prüfung:

I hereby confirm that this thesis has been written independently and with no other sources and aids than quoted.

Göttingen, 31.01.2011

Corinna Richthammer

Parts of this work have been or will be published in:

Justa-Schuch, D., Heilig, Y., Richthammer, C., and Seiler, S. (2010). Septum formation is regulated by the RHO4-specific exchange factors BUD3 and RGF3 and by the landmark protein BUD4 in *Neurospora crassa*. *Mol. Microbiol* 76, 220-235.

Riquelme, M., Yarden, O., Bartnicki-Garcia, S., Bowman, B., Castro-Longoria, E., Free, S. J., Fleißner, A., Freitag, M., Lew, R. R., Mouriño-Pérez, R., Plamann, M., Rasmussen, C., Richthammer, C., Roberson, R. W, Sanchez-Leon, E., Seiler, S., and Watters, M. K. Architecture and development of the *Neurospora crassa* hypha – a model cell for polarized growth. (Article in press, to appear in *Fungal Biol.*, 2011)

Table of Contents

1. Summary	1
2. Zusammenfassung	3
3. Introduction	5
3.1 Structure and mechanism of Rho GTPases	5
3.2 General regulation of Rho GTPases	6
3.3 Effector pathways, cellular functions and fine-tuning of Rho GTPase signalling	8
3.4 Rho GTPases and polarized growth in yeasts.....	9
3.4.1 Rho GTPases in yeasts: An overview	9
3.4.2 Polarized growth and its characteristics in yeasts	10
3.4.3 The Cdc42 GTPase module and its role in establishment of polarity	11
3.4.3.1 The Cdc42p module in <i>S. cerevisiae</i>	11
3.4.3.2 The Cdc42 module in <i>S. pombe</i>	12
3.4.4 The Rho1 GTPase module as a guardian of cell wall integrity	13
3.4.4.1 The Rho1p module in <i>S. cerevisiae</i>	13
3.4.4.2 The Rho1 module in <i>S. pombe</i>	16
3.5 Rho GTPases and polarized growth in filamentous fungi.....	18
3.5.1 Characteristics of hyphal growth in filamentous fungi	18
3.5.2 The roles of Rac and Cdc42 homologues in filamentous fungi.....	20
3.5.3 The functions of Rho1 homologues in filamentous fungi.....	23
3.6 Rho GTPases and their regulators in <i>N. crassa</i>	25
3.7 Aims of this work.....	26
4. Materials and Methods	27
4.1 Suppliers of chemicals.....	27
4.2 Media and growth conditions for microorganisms	27
4.3 Transformation of microorganisms.....	27
4.4 Plasmid construction.....	28
4.4.1 General procedure and overview.....	28
4.4.2 Full-length cDNA constructs of putative RhoGEFs and RhoGAPs	35
4.4.3 Plasmids encoding MBP- and GST-tagged RhoGEF constructs.....	35
4.4.4 Plasmids encoding MBP-tagged GAP constructs	36
4.4.5 Plasmids for yeast two-hybrid analyses.....	37
4.4.6 Plasmids for analysis of subcellular fusion protein localization.....	39
4.4.7 Plasmids for overexpression of epitope-tagged fusion proteins for phenotypic ... rescue and coimmunoprecipitation experiments	41
4.5 Strains	42

4.6	General molecular biological techniques	45
4.6.1	Isolation and analysis of nucleic acids	45
4.6.2	Reverse transcription of RNA.....	45
4.6.3	Polymerase chain reaction (PCR).....	46
4.6.4	DNA agarose gel electrophoresis	46
4.6.5	Enzymatic restriction and modification of DNA.....	46
4.6.6	Ligation	47
4.7	Biochemical and immunological methods	47
4.7.1	Preparation of <i>N. crassa</i> crude extracts for protein analysis.....	47
4.7.2	Separation of proteins by SDS polyacrylamide gel electrophoresis (PAGE)....	47
4.7.3	Western blotting.....	48
4.7.4	Immunoprecipitation	48
4.7.5	Analysis of MAK1 phosphorylation status.....	49
4.7.6	Protein expression and purification from <i>E. coli</i>	50
4.7.7	<i>In vitro</i> GEF activity assays.....	51
4.7.8	Copurification experiments.....	52
4.8	Yeast two-hybrid assays.....	52
4.9	Microscopy.....	52
4.10	Bioinformatic tools	53
4.10.1	DNA and protein sequence analysis.....	53
4.10.2	Phylogenetic analysis and alignment.....	53
5.	Results	55
5.1	Analysis of Rho regulator specificity in <i>N. crassa</i>	55
5.1.1	Comparison with the yeast Rho regulatory machinery	55
5.1.2	Heterologous expression and purification of RhoGAP and RhoGEF	58
5.1.3	<i>In vitro</i> GEF activity assays.....	60
5.2	Analysis of the CDC42/RAC/CDC24 module in <i>N. crassa</i>	64
5.2.1	Morphological characterization of mutants	64
5.2.2	<i>In vitro</i> GEF activity of mutant CDC24 versions	68
5.2.3	Analysis of the subcellular localization of RAC and CDC42	71
5.3	Analysis of the RHO1/RHO2/NCU00668 module in <i>N. crassa</i>	73
5.3.1	Potential autoregulatory effect of the DEP domain on GEF activity of..... NCU00668.....	73
5.3.2	Morphological characterization of <i>rho-1</i> , <i>rho-2</i> and NCU00668 mutants.....	75
5.3.3	Effector pathways regulated by RHO1 and RHO2 in <i>N. crassa</i>	78
5.3.4	Analysis of the subcellular localization of NCU00668, RHO1 and RHO2.....	83

6. Discussion	87
6.1 Lessons from the <i>in vitro</i> assays.....	87
6.2 CDC42 and RAC have overlapping functions in polarized growth of <i>N. crassa</i>	90
6.3 CDC24 acts as a GEF of RAC and CDC42	92
6.4 RHO1 and RHO2 share a function in maintaining cell wall integrity in <i>N. crassa</i>	94
6.5 NCU00668 is a RHO1-specific GEF and might be autoregulated.....	98
7. Supplemental material	103
8. References	121
9. Acknowledgements	135
10. Curriculum vitae	137

List of Abbreviations

aa	amino acid
<i>A. gossypii</i>	<i>Ashbya gossypii</i>
<i>A. fumigatus</i>	<i>Aspergillus fumigatus</i>
<i>A nidulans</i>	<i>Aspergillus nidulans</i>
<i>A. niger</i>	<i>Aspergillus niger</i>
a.u.	arbitrary units
AD	activation domain
APS	ammonium persulfate
ATP	adenosine triphosphate
BAR domain	Bin/amphyphysin/Rvs domain
BD	DNA-binding domain
BiFC	bimolecular fluorescence complementation
BLAST	Basic Local Alignment Search Tool
bp	base pair
<i>C. albicans</i>	<i>Candida albicans</i>
cDNA	complementary DNA
CNH domain	citron homology domain
cp.	compare
<i>C. purpurea</i>	<i>Claviceps purpurea</i>
CRIB domain	Cdc42/Rac-interactive binding domain
<i>C. trifolii</i>	<i>Colletotrichum trifolii</i>
CZH	CDM (CED-5, DOCK180, Myoblast city)-zizimin homology
Ded_cyto domain	dedicator of cytokinesis domain
DEP domain	domain found in Dishevelled, Egl-10, and Pleckstrin
DA	dominant active
DH	Dbl homology domain
DN	dominant negative
DHR-2	DOCK homology region 2
DNA	deoxyribonucleic acid
dNTP	deoxyribonucleotide triphosphate
DTT	dithiothreitol
<i>E. coli</i>	<i>Escherichia coli</i>
EDTA	ethylenediaminetetraacetic acid
FCH domain	Fes/CIP4 homology domain
FGSC	Fungal Genetics Stock Center
<i>F. oxysporum</i>	<i>Fusarium oxysporum</i>
GAP	GTPase activating protein
GBD	GTPase binding domain
GDI	GDP dissociation inhibitor
GDP	guanosine diphosphate
GEF	GDP/GTP (or guanine nucleotide) exchange factor
GFP	green fluorescent protein
G protein	guanine nucleotide-binding protein
GST	glutathione S-transferase
GTP	guanosine triphosphate
GTPase	guanosine triphosphatase

HA	hemagglutinin
HC	heavy chain
IgG	immunoglobulin G
IP	immunoprecipitation
kD	kiloDalton
LG	linkage group
mant-...	2'/3'-O-(N'-methylantraniloyl)-...
MAPK	mitogen-activated protein kinase
MBP	maltose binding protein
MW	molecular weight
NCBI	National Center for Biotechnology Information
<i>N. crassa</i>	<i>Neurospora crassa</i>
nd	nucleotide
NETO	new end take off
NLS	nuclear localization signal
NP-40	Nonidet P-40
OD	optical density
PAGE	polyacrylamide gel electrophoresis
PAK	p21-activated kinase
PB1 domain	Phox and Bem1p domain
PCR	polymerase chain reaction
PH domain	pleckstrin homology domain
<i>P. marneffeii</i>	<i>Penicillium marneffeii</i>
PMSF	phenylmethylsulfonyl fluoride
RBD	Rho binding domain
RIP	repeat induced point mutation
RNA	ribonucleic acid
ROS	reactive oxygen species
<i>S. cerevisiae</i>	<i>Saccharomyces cerevisiae</i>
SD	standard deviation
SDS	sodium dodecyl sulfate
<i>S. pombe</i>	<i>Schizosaccharomyces pombe</i>
TEMED	tetramethylethylenediamine
<i>U. maydis</i>	<i>Ustilago maydis</i>
UTR	untranslated region
UV	ultraviolet
VMM	Vogel's Minimal Medium
WB	Western blot
YFP	yellow fluorescent protein
<i>Y. lipolytica</i>	<i>Yarrowia lipolytica</i>

1. Summary

Rho GTPases are small G proteins of the Ras superfamily that function as molecular switches, activating a variety of effector proteins when in the GTP-bound state and returning to inactivity upon hydrolysis of GTP. They play a key role in several signal transduction pathways regulating fundamental cellular processes including cell migration, cell cycle progression and cell polarity. Rho guanine nucleotide exchange factors (RhoGEFs) and Rho GTPase-activating proteins (RhoGAPs) enhance nucleotide binding and hydrolysis by Rho GTPases, respectively, and are increasingly acknowledged as crucial determinants of spatio-temporal Rho signalling activity. Concise orchestration of Rho GTPase function is thought to be one of the decisive factors allowing the formation of widely different polarized structures in distinct cell types and organisms, and thus investigations on the Rho regulatory machinery are pivotal for understanding morphogenetic processes.

While the unicellular yeasts *Saccharomyces cerevisiae* and *Schizosaccharomyces pombe* are the paradigms for polarized growth, many members of the fungal kingdom, among them important human pathogens, are distinguished from their well-studied yeast relatives by their ability to grow in a filamentous mode, leading to the formation of highly elongated hyphae. Knowledge about the molecular mechanisms underlying this extreme form of polarized extension is only slowly beginning to accumulate, but Rho GTPases and their regulators appear to play an essential role in directing hyphal morphogenesis.

The filamentous ascomycete *Neurospora crassa* is a widely acknowledged model organism, whose genome encodes six Rho GTPases and numerous putative regulators, most of which were uncharacterized at the start of this study. I have employed *in vitro* GEF activity assays to determine the target specificity of the predicted RhoGEFs of the fungus. CDC24 exhibits dual specificity towards the GTPases RAC and CDC42, while NCU10282 preferentially stimulates nucleotide exchange in the latter GTPase. BUD3 is identified as an activator of RHO4, and NCU00668 is established as a RHO1-specific GEF, which might be autoregulated by an intramolecular interaction.

In subsequent experiments, I demonstrate that CDC24 is an essential protein required for the establishment and maintenance of polarized growth in *N. crassa*. Moreover, RAC and CDC42 must share an essential function, as their simultaneous depletion leads to synthetic-lethal defects that mimic loss of CDC24 function; their common localization to the apex and septa of growing hyphae further supports the notion of partial overlap in function between the two GTPases.

Likewise, the absence of functional NCU00668 or its target GTPase RHO1 is lethal, resulting in cells that are unable to establish polarity. In accordance with the knockout phenotype, temperature-sensitive mutants compromised in RHO1 activity exhibit polarity defects, which are severely exacerbated by concomitant loss of *rho-2*, whose single deletion is associated with mild morphological aberrancies. Inhibitor growth tests and MAK1 activity assays indicate that the observed synthetic defects are most likely due to functional redundancy of the two GTPases in maintaining cell wall integrity. Initial characterization of effector interactions suggests that only RHO1, but not RHO2, directs activity of *N. crassa* protein kinase C and the formin BNI1. Preliminary analysis of the subcellular localization patterns of NCU00668, RHO1 and RHO2 overall corroborate the proposed overlap and distinctness in function among the components of this GTPase module, but further work is needed to elucidate the signalling pathways used by the two GTPases to maintain a protective cell wall structure during hyphal growth.

2. Zusammenfassung

Rho-GTPasen sind kleine G-Proteine der Ras-Superfamilie, die als molekulare Schalter wirken: Im GTP-gebundenen Zustand aktivieren sie eine Vielzahl von Effektorproteinen, wohingegen sie durch die Hydrolyse des GTPs wieder inaktiviert werden. Rho-GTPasen nehmen eine Schlüsselstellung in zahlreichen Signaltransduktionswegen ein, die so grundlegende zelluläre Prozesse wie Zellmigration, Zellzyklusfortschritt und Zellpolarität regulieren. Rho-Guaninnukleotid-Austauschfaktoren (RhoGEFs) und Rho-GTPase-aktivierende Proteine (RhoGAPs) beschleunigen die Bindung von Nukleotiden bzw. deren Hydrolyse durch Rho-GTPasen und bestimmen, wie zunehmend deutlich wird, in erheblichem Maß das räumliche und zeitliche Aktivitätsmuster von Rho-GTPasen. Man geht heute davon aus, dass eine präzise Regulierung von Rho-GTPasen einer der entscheidenden Faktoren ist, die die Ausbildung höchst unterschiedlicher polarer Strukturen in verschiedenen Zelltypen und Organismen ermöglichen. Daher ist die Untersuchung von Faktoren, die die Aktivität von Rho-GTPasen kontrollieren, essentiell für das Verständnis morphogenetischer Prozesse.

Während die einzelligen Hefen *Saccharomyces cerevisiae* und *Schizosaccharomyces pombe* die Grundmodelle für polares Wachstum darstellen, unterscheiden sich viele Pilze, darunter auch wichtige humanpathogene Arten, von ihren beiden gut untersuchten Verwandten durch die Fähigkeit zu filamentösem Wachstum, das zur Bildung lang ausgestreckter Hyphen führt. Die molekularen Mechanismen, die dieser extremen Form polaren Wachstums zugrunde liegen, werden erst in jüngster Zeit allmählich deutlicher, aber Rho-GTPasen und ihre Regulatoren scheinen bei der Steuerung der Hyphenmorphogenese eine wesentliche Rolle zu spielen.

Das Genom des filamentösen Ascomyceten *Neurospora crassa*, eines anerkannten Modellorganismus, kodiert für sechs Rho-GTPasen und eine große Zahl mutmaßlicher Regulatoren, von denen der Großteil zu Beginn dieser Arbeit noch nicht charakterisiert war. Mittels *in vitro* GEF-Aktivitätstests wurde hier die Spezifität der RhoGEFs des Pilzes bestimmt. CDC24 zeigt ausgeglichene GEF-Aktivität gegenüber RAC und CDC42, während NCU10282 bevorzugt den Nukleotidaustausch in letzterer GTPase stimuliert. BUD3 aktiviert spezifisch RHO4, und NCU00668 wirkt als RHO1-spezifischer GEF, der möglicherweise durch eine intramolekulare Wechselwirkung autoreguliert wird.

Weiterhin wird gezeigt, dass CDC24 ein essentielles Protein ist, das für die Etablierung und die Aufrechterhaltung polaren Wachstums in *N. crassa* benötigt wird. Außerdem müssen sich RAC und CDC42 eine essentielle Funktion teilen, da ihr gleichzeitiges Fehlen synthetisch letale Defekte bedingt, die denjenigen gleichen, die bei Verlust der Funktion ihres GEFs auftreten. Die gemeinsame Lokalisation von RAC und CDC42 am Apex und an Septen wachsender Hyphen unterstützt die Vorstellung, dass sich die Funktionen der beiden GTPasen teilweise überschneiden.

Auch das Fehlen von NCU00668 oder RHO1 ist letal und verhindert in den betroffenen Zellen die Ausbildung von Polarität. Übereinstimmend damit weisen temperatursensitive Mutanten, deren RHO1-Aktivität beeinträchtigt ist, Polaritätsdefekte auf, die durch gleichzeitigen Verlust von *rho-2* erheblich verschlimmert werden; die einfache Deletion von *rho-2* führt zu milden morphologischen Anomalien. Wachstumstests in Gegenwart verschiedener Inhibitoren und MAK1-Aktivitätsbestimmungen lassen vermuten, dass die beobachteten synthetischen Defekte auf eine Redundanz der Funktionen beider GTPasen im Erhalt der Zellwandintegrität zurückzuführen sind. Erste Wechselwirkungsanalysen

deuten darauf hin, dass die Aktivität der Proteinkinase C und des Formins BNI1 nur von RHO1, nicht aber von RHO2, kontrolliert wird. Parallel stützen Untersuchungen zur subzellulären Lokalisation von NCU00668, RHO1 und RHO2 die Annahme, dass die Komponenten dieses GTPase Moduls sowohl gemeinsame als auch individuelle Funktionen erfüllen; allerdings sind noch weitere Analysen nötig, um die Signalwege aufzudecken, mit deren Hilfe die beiden GTPasen den Erhalt einer schützenden Zellwandstruktur während des Hyphenwachstums sicherstellen.

3. Introduction

The first genes encoding Rho guanosine triphosphatases (GTPases) were identified as *ras* homologues - hence their name - in a complementary DNA (cDNA) library from the abdominal ganglia of the marine mollusc *Aplysia*, and their evolutionary conservation among eukaryotic organisms ranging from yeast to humans was immediately recognized (Madaule and Axel, 1985).

Early studies already emphasized the role of Rho GTPases in control of polarized growth and cell morphology in yeast and mammalian cells (Adams et al., 1990; Johnson and Pringle, 1990; Paterson et al., 1990), and soon their involvement in regulation of the actin cytoskeleton was revealed (Chardin et al., 1989; Ridley and Hall, 1992; Ridley et al., 1992; Kozma et al., 1995). Since then, it has become obvious that the ability of Rho GTPases to activate a wide range of effector proteins makes them important regulators of an astonishing variety of further cellular functions and pathways (reviewed in (Etienne-Manneville and Hall, 2002)); nevertheless, their role as key regulators of polar growth has never been challenged.

3.1 Structure and mechanism of Rho GTPases

Rho GTPases such as Rho, Rac and Cdc42 belong to the Ras superfamily of small GTPases and function as molecular switches, activating downstream effectors when they are in their active, GTP-bound state and becoming inactive upon hydrolysis of bound GTP to GDP (Figure 1). While cycling between the two nucleotide binding states seems to be a prerequisite for efficient activation of the majority of output pathways (Irazoqui et al., 2003; Vanni et al., 2005; Barale et al., 2006; Fidyk et al., 2006), it has been shown to be dispensable for other functions (Qadota et al., 1996; Roumanie et al., 2005).

The G domain, the ca. 20 kD core region of small GTPases which binds and hydrolyzes guanine nucleotides, is characterized by a common fold in which a six-stranded β -sheet is surrounded by five α -helices (reviewed in (Vetter and Wittinghofer, 2001; Hakoshima et al., 2003)). Rho GTPase domains are distinguished from other G domains of Ras superfamily members by a 13-residue mainly helical insertion located between β -strand 5 and α -helix 4 (Ihara et al., 1998). Five conserved sequence elements designated G1 to G5 mark regions of small GTPase interaction with the bound guanine nucleotide and the Mg^{2+} cofactor (Bourne et al., 1991; Wennerberg et al., 2005); the P loop (or phosphate binding loop) indicated by the G1 signature motif is thought to make the most important contribution to nucleotide coordination within the binding pocket (Vetter and Wittinghofer, 2001).

Comparison of crystal structures of human RhoA in the GDP- versus GTP-bound state (Wei et al., 1997; Ihara et al., 1998) confirmed that, besides the overall fold, the structural mechanism underlying the cycle of alternating signal transduction activity of Ras proteins is conserved among Rho GTPases: Dependent on the the nucleotide-binding state of the GTPase, two exposed flexible surface loops known as switch I (or effector region) and switch II, which overlap with the above-mentioned G2 and G3 motifs, respectively, adopt markedly different conformations compatible or not with activation of downstream effector proteins (Vetter and Wittinghofer, 2001; Hakoshima et al., 2003).

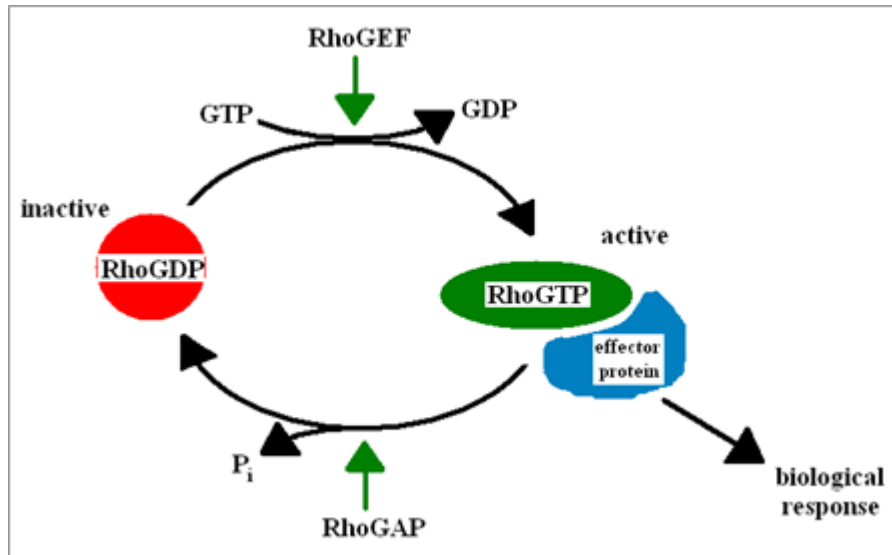


Figure 1: Rho GTPases act as molecular switches. Schematic representation of the Rho GTPase cycle and its regulation by RhoGEFs and RhoGAPs. See text for details.

Most Rho proteins require subcellular localization to membranes to perform their biological functions. Membrane association is achieved by a series of posttranslational modifications involving the attachment of a geranyl-geranyl or farnesyl moiety to the C-terminus of the Rho protein. The modification is triggered by a prenylation motif found at the C-terminus of the majority of Rho GTPases, the so-called CaaX box (whereby C = cysteine, a = aliphatic and X = any amino acid) (reviewed in (Bustelo et al., 2007)). Additionally, a polybasic amino acid region or one or more palmitoylated cysteines upstream of the CaaX box have been shown to be required for proper plasma membrane targeting of several small GTPases (Hancock et al., 1991; Adamson et al., 1992; Pechlivanis and Kuhlmann, 2006).

3.2 General regulation of Rho GTPases

Intrinsic rates of GTP hydrolysis and, in accordance with their high affinity for both GDP and GTP, guanine nucleotide exchange by small GTPases are usually low. However, transition between the “on” and “off” state of the GTPase is accelerated significantly by GAPs (GTPase activating proteins) and GEFs (GDP/GTP or guanine nucleotide exchange factors), respectively, which ensures efficient function of GTPases in signal transduction processes requiring fast response reactions (Vetter and Wittinghofer, 2001).

RhoGAPs enhance the rate of GTP hydrolysis by several orders of magnitude (Bos et al., 2007). The decisive feature within their characteristic all-helical GAP domain is a conserved arginine finger, which inserts into the nucleotide binding pocket of the GTPase, aids indirectly in positioning of the attacking water molecule and stabilizes the transition state of the hydrolysis reaction, thus facilitating inactivation of the GTPase and concomitant disruption of signal transmission (reviewed in (Hakoshima et al., 2003; Bos et al., 2007)).

Classical RhoGEFs are characterized by the presence of a Dbl homology (DH) domain, which contains three conserved regions referred to as CR1 to CR3 and assumes an all-helical fold. They function by remodelling the switch regions of their target GTPases in such a way that the nucleotide binding pocket is disorganized. Thereby, interactions of the switch regions and the P loop with the Mg²⁺ cofactor and the bound GDP are disrupted, and their dissociation is encouraged (reviewed in (Rossman et al., 2005)). Rebinding of Mg²⁺ and

GTP - its cytoplasmic concentration being ten times higher than that of GDP (Bourne et al., 1991) - then restores the active state of the GTPase.

In many RhoGEFs, the DH domain is followed by a pleckstrin homology (PH) domain. Initially, such PH domains were ascribed a function in membrane anchoring and protein-protein interactions of the RhoGEFs. In the meantime, however, increasing evidence suggests that rather they have a supportive effect on GEF activity by cooperating with the DH domain in facilitating nucleotide exchange (reviewed in (Hakoshima et al., 2003; Rossman et al., 2005)).

More recently, a second family of RhoGEFs has been discovered (Brugnera et al., 2002; Meller et al., 2002; Côté and Vuori, 2002). So far, only Rac and Cdc42 and their distant plant homologues have been shown to be targets of this kind of RhoGEFs (Meller et al., 2005). The DH-unrelated signature domain mediating GEF activity of this family has become known as Docker, CZH2 (CDM (CED-5, DOCK180, Myoblast city)-zizimin homology domain 2) or DHR-2 (Dock Homology Region-2). Sequence conservation of the domain is low (ibid.), but mutational and structural analyses have identified residues important for its GEF activity (Yang et al., 2009). In the cited study, solution of the crystal structure of the human exchange factor DOCK9 in complex with its target GTPase Cdc42 in different nucleotide binding states also revealed the overall topology and mechanism of action of the DHR2 domain, which appears to act as a dimer. Each DHR2 domain forms two α -helical and one β -stranded lobe and contacts both switch regions of the GTPase. In contrast to DH-type GEFs, however, the conformational changes associated with destabilization of nucleotide binding interactions evoked in the GTPase are restricted to switch I and the P loop; the DHR2 inserts a conserved loop, the α 10 insert with a valine at its tip, directly into to the newly exposed nucleotide binding site, thereby displacing Mg^{2+} . As a consequence, GDP and the cofactor are released and replaced by the more abundant GTP and Mg^{2+} , rendering the GTPase once more competent for effector interaction.

Strikingly, many RhoGAPs and RhoGEFs are multidomain proteins. Additional domains besides the catalytic ones are thought to mediate cross-talk of Rho GTPases with other signalling pathways or allow fine-tuning of regulator activity and localization. An additional level of complexity is achieved by the fact that both activators and inactivators are subject to regulation by protein-protein interactions, second messengers and posttranslational modifications (reviewed in (Tcherkezian and Lamarche-Vane, 2007; Bos et al., 2007)).

GDP dissociation inhibitor (GDIs) form a third class of regulators directly involved in control of the GTPase cycle. They function by burying the isoprenoid tail of GTPases within a hydrophobic pocket, thereby facilitating extraction of GTPases from membranes and allowing their intracellular relocation. Through conformational changes resulting from their interaction with the switch regions of the GTPase, they prevent both GDP dissociation and GTP hydrolysis by the G protein. This interference with the GDP/GTP cycle, however, is now widely viewed as a by-product of their binding mode, their main function being the supply of a cytoplasmic pool of prenylated GTPases (reviewed in (Vetter and Wittinghofer, 2001; Hakoshima et al., 2003)).

In addition to the control exercised by GAPs, GEFs and GDIs, Rho GTPase function can be further modulated by changes in subcellular localization or release of autoinhibition by protein-protein interactions, transcriptional regulation, differential degradation or posttranslational modification such as phosphorylation (reviewed in (Bustelo et al., 2007)).

3.3 Effector pathways, cellular functions and fine-tuning of Rho GTPase signalling

The ability of Rho GTPases to control a wide range of intracellular signalling pathways depends on their specific interaction with a multitude of effector proteins. Suitable conformation of the switch regions, indicators of the nucleotide binding state of the GTPase, is critical for binding of effectors. Mutational and structural studies investigating Rho-effector interactions suggest that the binding interface usually includes the switch I region, aptly termed effector region, in combination with further surface areas of the G protein (reviewed in (Hakoshima et al., 2003; Karnoub et al., 2004; Dvorsky and Ahmadian, 2004)). Discrimination between different, often highly similar, GTPases is achieved by specific contacts with variable residues located within switch I, the Rho-specific helical insert and other regions (Karnoub et al., 2004). On the side of the effectors, most domains mediating interaction with Rho GTPases (GTPase binding domains or GBDs) seem to be of diverse sequence and topology (Dvorsky and Ahmadian, 2004); this precludes the existence of a universal recognition and binding mechanism, but at the same time increases potential specificity of interaction. As an exception, several effectors of the Rho GTPases Cdc42 and/or Rac possess a conserved binding domain known as Cdc42/Rac-interactive binding (CRIB) domain; this domain exhibits a characteristic binding mode involving the formation of an intermolecular β -sheet, primarily with the switch I region of the GTPase (Karnoub et al., 2004). Probably due to the diversity of interactions, little is known so far about the exact mechanisms by which target proteins are rendered active upon GTPase binding (Dvorsky and Ahmadian, 2004).

The interaction with a multitude of different effector molecules allows Rho GTPases to control diverse biochemical pathways involved in the most fundamental cellular processes (reviewed in (Etienne-Manneville and Hall, 2002; Jaffe and Hall, 2005)). For instance, the classical Rho family members Rho, Rac and Cdc42 each influence the actin cytoskeleton in distinctive ways. For this, they orchestrate proteins regulating actin polymerization and organization such as the microfilament-nucleating formins, the filament cross-linking Arp2/3 complex or the myosin kinase ROCK. Likewise, they govern microtubule dynamics and arrangement by interaction with several microtubule-binding proteins. While these effects on the cytoskeleton probably constitute the best-known and most prominent function of Rho GTPases, it is becoming increasingly evident that they are also considerably involved in control of gene expression via activation of a multitude of corresponding signal transduction pathways, many of them including a mitogen-activated protein kinase (MAPK) cascade. Moreover, Rho GTPases have been implicated in the regulation of vesicular transport and secretion and have been shown to influence additional enzymatic activities ranging from reactive oxygen species (ROS) production to lipid metabolism and cell wall synthesis (ibid.).

Through coordinated control of the described biochemical pathways, Rho GTPases are key factors in the regulation of many major biological functions of eukaryotic cells including cell cycle progression, mitosis, cytokinesis, cell migration and, above all, morphology and polar growth (ibid.). In all these processes, their outstanding position as supreme regulators of the cytoskeleton and morphogenetic machinery of the cell plays a decisive role.

In light of the significant influence exerted by Rho GTPases as signal integrators on the most vital cell functions, it is not surprising that in all organisms analyzed so far, putative regulators outnumber Rho GTPases. In humans, for instance, over 60 GEFs and more than 70 GAPs (Etienne-Manneville and Hall, 2002) are opposed to 22 Rho proteins (Rossman et al., 2005).

It is becoming increasingly clear that this majority of GEFs and GAPs provides the basis for a sophisticated modulation and spatio-temporal fine-tuning of the activity of Rho GTPases, ensuring proper biological response to a variety of upstream signals. For instance, both RhoGAPs and RhoGEFs have been implicated in selective regulation of specific Rho GTPase output pathways; many have been shown to act as scaffolds linking upstream and downstream components of signalling cascades or mediating cross-talk to other Rho modules and further cellular pathways (reviewed in (Rossman et al., 2005; Tcherkezian and Lamarche-Vane, 2007)). Although it has become a major focus of research in recent years, general principles regarding the spatio-temporal modularity of Rho-GTPase signalling are only gradually emerging and require new experimental approaches (reviewed in (Pertz, 2010)).

The confusingly large number of Rho GTPase signalling components present in higher eukaryotes - in humans, for example, an astonishing 1% of the genome is estimated to encode proteins that are regulators of Rho GTPases or are directly regulated by them (Jaffe and Hall, 2005) - further aggravates the already complex challenge to elucidate the subtly wired signalling network. Therefore, it is not surprising that the simpler yeasts *S. pombe* and especially *S. cerevisiae* still remain the best-studied models for almost all aspects of Rho GTPase signalling. This makes them valuable sources of reference for the investigation of polarized growth and other Rho GTPase functions in any eukaryotic organism. Moreover, they are well suited to illustrate general modulatory principles of Rho signalling such as amplification of its localized activity by positive feedback loops and the use of scaffold proteins or outcome-specificity and promiscuity of Rho regulators.

3.4 Rho GTPases and polarized growth in yeasts

3.4.1 Rho GTPases in yeasts: An overview

The genomes of both *S. cerevisiae* and *S. pombe* each encode six Rho GTPases, Rho1(p) to Rho5(p) and Cdc42(p). As in other organisms, the numbers of putative Rho-specific regulators surpass that of Rho proteins and amount to eleven or ten RhoGAPs and seven or eight RhoGEFs, respectively (for a summary of their target specificities determined so far see Figure 4 and Figure 5 in section 5.1.1.). Interestingly, only *S. cerevisiae* appears to possess a CZH-type GEF. In addition, one RhoGDI is present in both yeasts.

Great progress has been made in the elucidation of the biological roles and interaction partners of most yeast Rho GTPases (reviewed in (García et al., 2006b; Park and Bi, 2007; Perez and Rincón, 2010)). The functions and signalling networks of Cdc42 and Rho1 have certainly been best characterized, probably owing to their outstanding influence on cell morphology. They will be considered in more detail in separate sections after short overviews of Rho GTPase functions and polarized growth in yeasts.

RHO1 is an essential gene in *S. cerevisiae* and encodes a GTPase performing a pivotal role in morphogenesis, primarily by controlling maintenance of cell wall integrity and the actin cytoskeleton (Madaule et al., 1987; Drgonová et al., 1996; Kohno et al., 1996). The highly similar Rho2p is thought to have overlapping functions with Rho1p (Ozaki et al., 1996). Likewise, Rho3p and Rho4p are presumed to have partially redundant functions in regulating the actin cytoskeleton and polarized secretion (Matsui and Toh-e, 1992a; Imai et al., 1996; Robinson et al., 1999; Adamo et al., 1999). Rho5p has been implicated in downregulation of the cell integrity pathway and, more recently, in cellular responses to osmotic and oxidative

stress (Schmitz et al., 2002; Singh et al., 2008; Annan et al., 2008). Cdc42p is essential and was early shown to be a key factor in the establishment of cell polarity (Adams et al., 1990; Johnson and Pringle, 1990).

The functions of the respective *S. pombe* Rho GTPases are widely conserved. Also in fission yeast, Rho1 is essential and controls cell wall integrity and polarization of the actin cytoskeleton (Arellano et al., 1996; Nakano et al., 1997). Interestingly, Rho2 has been shown to regulate cell wall α -D-glucan synthesis (Calonge et al., 2000). Similarly to their budding yeast counterparts, Rho3 and Rho4 influence cytoskeletal polarization and secretion, especially during cytokinesis (Nakano et al., 2002, 2003; Santos et al., 2003, 2005; Wang et al., 2003). Rho5 exhibits overlapping functions with Rho1 and might be important for stress resistance (Nakano et al., 2005; Rincón et al., 2006), whereas Cdc42 is essential and controls polarized cell growth (Miller and Johnson, 1994).

3.4.2 Polarized growth and its characteristics in yeasts

Establishment and maintenance of polarity, i.e. the ordered and asymmetric arrangement of structures along one or several axes, is a fundamental requirement for correct morphogenesis of single cells, tissues and ultimately entire organisms. Polarized growth on the cellular level can be divided in three main steps (reviewed in (Harris and Momany, 2004; Perez and Rincón, 2010)). First, prospective sites of polarization are marked by “landmark proteins” in response to internal or external cues. The second step, the establishment of polarity, involves Rho GTPases and their regulators as key players; they recognize the polarization site and signal to the cytoskeleton, inducing its localized asymmetric organization. Finally, in the third step, polar growth is achieved and maintained by asymmetric distribution of further components of the morphogenetic machinery in combination with polarized secretion.

S. cerevisiae forms slightly elongated round cells and divides by formation of a single bud. Budding is closely coupled to the cell cycle. In the early G₁ phase, the bud grows in an apical manner until it reaches a critical size; then, it switches to isotropic expansion and becomes round. After mitosis, mother and daughter cells are physically separated by formation of a septum and its subsequent degradation. Generally, the bud site is selected adjacent to the bud scar of the previous cell cycle (axial pattern) or opposite of it (bipolar pattern) (reviewed in (Perez and Rincón, 2010)).

S. pombe forms rod-shaped cells which grow through tip extension. Their growth and division, too, is tightly coordinated with the cell cycle. During G₁, tip growth is restricted to the old end of the cell, while at the onset of G₂, when cells have reached a critical size, they switch from mono- to bipolar growth following conclusion of a process known as new end take off (NETO). Upon entry into mitosis, tip growth stops and later cytokinesis is completed by division at a medial septum (ibid.).

While the nature and modes of positioning of “landmark proteins” for determination of growth sites differ between the two yeasts, the ensuing processes of signal transduction, cytoskeletal reorganization and recruitment of the morphogenetic machinery as well as the cellular components involved are mostly conserved (ibid.). In both yeasts, the local activation of Cdc42 and its subsequent asymmetric remodelling of the actin cytoskeleton represent the decisive steps towards polarized cell growth. Rho1 appears to play a subordinate role in actin polarization and is essential for cell wall integrity during growth.

3.4.3 The Cdc42 GTPase module and its role in establishment of polarity

3.4.3.1 The Cdc42p module in *S. cerevisiae*

Activity of *S. cerevisiae* Cdc42p is thought to be controlled by only one GEF, Cdc24p (Zheng et al., 1994), and six GAPs, Rga1/2p, Bem2/3p, Rgd2p and Lrg1p (Zheng et al., 1993; Stevenson et al., 1995; Roumanie et al., 2001; Smith et al., 2002a), although assignment of the latter two relies solely on *in vitro* data. Additionally, the RhoGDI Rdi1p has been shown to interact with the GTPase (Koch et al., 1997; Tiedje et al., 2008).

The only GEF Cdc24p is essential (Coleman et al., 1986) and plays a key role in local activation of Cdc42p, which initiates the budding process (reviewed in (Park and Bi, 2007; Perez and Rincón, 2010)). As stated, budding is closely linked to the cell cycle. In G₁ cells, Cdc24p is anchored in the nucleus by interaction with the protein Far1p. In late G₁, Far1p phosphorylation by the G₁ cyclin/Cdc28p kinase complex triggers its degradation and allows Cdc24p release from the nucleus (Henchoz et al., 1997; Nern and Arkowitz, 1999; Toenjes et al., 1999; Shimada et al., 2000). Oligomerization of Cdc24p via its DH domain might also affect its localization and increase nuclear sequestration (Mionnet et al., 2008).

Once exported from the nucleus, Cdc24p is thought to be recruited by the activated Ras-type GTPase Rsr1p (alias Bud1p) (Zheng et al., 1995; Park et al., 1997), which resides together with its GEF Bud5p and GAP Bud2p at the incipient bud site and thereby transmits the position of deposited landmark proteins to the Rho module (Bender and Pringle, 1989; Chant and Herskowitz, 1991; Park et al., 1993; Kang et al., 2001; Nelson, 2003). Rsr1p has also been shown to interact with Cdc42p and might thus be involved in its clustering at the bud site (Kozminski et al., 2003; Kang et al., 2010). It is assumed that at the same time, Bem2p and Bem3p, and possibly also the other Cdc42-specific GAPs, globally restrict Cdc42 activity during G₁ until their inactivation by G₁ cyclin/Cdc28p-mediated phosphorylation (Knaus et al., 2007). Upon relief of the inactivating effect, local activation of Cdc42p by Cdc24p becomes possible.

In addition to the role of the Rsr1 GTPase module, other factors are expected to be involved in establishing a local accumulation of Cdc24p and Cdc42p. The scaffold protein Bem1p, which is able to bind Cdc24p, activated Cdc42p and the effector Cla4p, seems to have a parallel function in clustering Cdc24p and Cdc42p to a single cortical site (Bender and Pringle, 1991; Chenevert et al., 1992; Bose et al., 2001). A positive feedback loop in which activated Cdc42p recruits Bem1p, which in turn stabilizes the Cdc42p activator Cdc24p at the polarization site, is thought to contribute to efficient establishment of Cdc42p-GTP polarization (Butty et al., 2002). Interestingly, Bem1p is also considered to be involved in facilitating another positive feedback loop, in which Cla4p activates Cdc24p by phosphorylation and thus leads to the amplification of the Cdc42p signal at the budding site (Bose et al., 2001). However, the biological significance of Cdc24p phosphorylation by Cla4p and other kinases involved in the budding process is challenged by the finding that abolition of Cdc24p phosphorylation sites has no morphological consequences (Wai et al., 2009). Although the initial polarization of Cdc42p is independent of actin, yet another putative positive feedback loop acting at later stages during the budding process might involve the actin cables polarized by Cdc42p: They could serve as tracks for targeted secretion of Cdc42p, which counteracts the dispersing effects of endocytosis of the GTPase, and thus contribute to maintaining its stable polarization (Irazoqui et al., 2005).

Once localized activation of Cdc42p has been achieved by the mechanisms described, the GTPase in turn locally activates several effectors, which induce an asymmetric organization of the actin cytoskeleton and the septins and set the basis for targeted secretion (reviewed in (Johnson, 1999; Park and Bi, 2007; Perez and Rincón, 2010)).

Cdc42p is thought to regulate the localization of Bni1p, one of the two *S. cerevisiae* formins, by direct interaction, thereby polarizing the nucleation of actin filaments assembled into cables; it might also play a minor role in activating the formin, although in this respect Rho3p and Rho4p are considered more important (Matsui and Toh-e, 1992b; Evangelista et al., 1997; Ozaki-Kuroda et al., 2001; Dong et al., 2003). Bni1p has also been reported to link Cdc42p signalling to the actin filament-branching Arp2/3 complex, which is responsible for the formation of actin patches that are also polarized towards growth sites (Adams and Pringle, 1984; Lechler et al., 2001). Another link is provided by the members of the p21-activated kinase (PAK) family by their phosphorylation of type I myosins (Wu et al., 1996, 1997; Evangelista et al., 2000; Lechler et al., 2000). Ste20p, Cla4p and Skm1p all possess a CRIB domain that mediates their interaction with Cdc42p (Cvrcková et al., 1995; Leberer et al., 1997a; Johnson, 1999). In addition to their putative influence on actin patch dynamics, Ste20p is thought to play a role in activation of the pheromone response MAPK pathway during mating (Peter et al., 1996), while Cla4p has been implicated in septin organization (Dobbelaere et al., 2003; Versele and Thorner, 2004). The recruitment of septins, GTP-binding filament-forming proteins mainly involved in cytokinesis (Park and Bi, 2007), to the bud site is also regulated by Cdc42p via its activation of the CRIB-domain containing effectors Gic1p and Gic2p (Brown et al., 1997; Chen et al., 1997; Iwase et al., 2006). Moreover, Cdc42p controls polarized exocytosis and thus targeted delivery of components required for active cell growth: Besides its role in directing the nucleation of actin cables, which are thought to serve as tracks along which secretory vesicles are moved (Pruyne et al., 1998; Karpova et al., 2000; Bretscher, 2003), it interacts with Sec3p, a subunit of the exocyst complex mediating vesicle tethering to the membrane during exocytosis in yeast, and seems to be necessary for its proper localization (Zhang et al., 2001).

3.4.3.2 The Cdc42 module in *S. pombe*

In *S. pombe*, the Cdc42 module consists of the GTPase itself, its two GEFs Scd1 and Gef1 (Chang et al., 1994; Coll et al., 2003; Hirota et al., 2003) and the GAP Rga4 (Tatebe et al., 2008). Deletion mutant characteristics indicate that Scd1, a homologue of *S. cerevisiae* Cdc24p, is the main GEF controlling Cdc42 activity in cell polarization, while Gef1 plays a role in NETO and cytokinesis (Chang et al., 1994; Murray and Johnson, 2001; Coll et al., 2003; Hirota et al., 2003). Interaction of Cdc42 with the RhoGDI Rdi1 has been shown, which might add further regulatory potential (Nakano et al., 2003).

In *S. pombe* the microtubule cytoskeleton plays an important role in defining the site of polarized growth by positioning polarity factors (reviewed in (Chang and Martin, 2009; Martin, 2009)), but the ensuing processes of local activation of Cdc42 and the actin assembly machinery that lead to cell polarization are quite similar to those observed in budding yeast (reviewed in (García et al., 2006b; Chang and Martin, 2009; Perez and Rincón, 2010)).

The *S. pombe* Ras1, a homologue of Rsr1p, and the scaffold protein Scd2 are thought to enhance interaction between the RhoGEF Scd1 and Cdc42 at sites of growth (Chang et al., 1994). In analogy to its homologue Bem1p, Scd2 has also been implicated in facilitating the interaction of Cdc42 with one of its effectors, the PAK kinase Shk1 (Endo et al., 2003). Consistent with its localization to the sides of cells and to nongrowing tips, the GAP Rga4

has been proposed to play a role in spatially restricting Cdc42 activity to the sites of growth (Das et al., 2007; Tatebe et al., 2008).

Once activated, fission yeast Cdc42 controls the assembly of polarized actin cables by relieving the autoinhibition of one of the three *S. pombe* formins, For3 (Martin et al., 2007). There are indications that Cdc42 also plays a role in regulating actin patch formation by the conserved Arp2/3 complex, but its exact modes of action in this context remain to be determined (García et al., 2006b; Chang and Martin, 2009; Perez and Rincón, 2010). Like its *S. cerevisiae* counterpart, *S. pombe* Cdc42 interacts with and activates CRIB-domain containing PAK kinases (Marcus et al., 1995; Otilie et al., 1995; Yang et al., 1998). One of them, Shk2, has been implicated in cell wall integrity signalling and shown to interact with Mkh1, the first kinase of the corresponding MAPK cascade; however, its significance in activation of this pathway is controversial (Merla and Johnson, 2001; Madrid et al., 2006). Substrates of Shk1, in contrast, appear to link Cdc42 to the control of cytokinesis and, possibly, microtubule dynamics (Qyang et al., 2002; Kim et al., 2003; Loo and Balasubramanian, 2008). Interestingly, Shk1-mediated phosphorylation of the Rho1-specific GAP Rga8 could provide a close connection between the Cdc42 and Rho1 GTPase modules of *S. pombe* (Yang et al., 2003). In contrast to budding yeast, no direct involvement of Cdc42 in regulation of polarized secretion has been reported so far.

3.4.4 The Rho1 GTPase module as a guardian of cell wall integrity

In budding yeast and other fungi, polarized growth requires dynamic remodelling of the relatively rigid cell wall at sites of growth. The two-layered cell wall, which derives its mechanical strength from the inner layer mainly composed of glucan polymers and chitin, must be weakened there just enough to allow incorporation of new cell wall material for growth to proceed; at the same time, rupture must be avoided, and cell wall growth must be coordinated with expansion of the plasma membrane (reviewed in (Levin, 2005)). The Rho1 GTPase module is thought to be a key player in maintaining cell integrity by its ability to coordinately regulate activity of cell wall biosynthetic enzymes and the pivotal processes focussing cell growth on a particular region, namely polarized actin organization and directed secretion (Levin, 2005; Park and Bi, 2007; Perez and Rincón, 2010).

3.4.4.1 The Rho1p module in *S. cerevisiae*

In *S. cerevisiae*, the Rho1p GDP/GTP cycle has been shown to be regulated by three GEFs, Rom1p, the closely related Rom2p and Tus1p (Ozaki et al., 1996; Schmelzle et al., 2002), and by four GAPs, Bem2p (which also inactivates Cdc42p), Sac7p, Bag7p and Lrg1p (Peterson et al., 1994; Schmidt et al., 1997; Roumanie et al., 2001; Fitch et al., 2004). The numerous Rho1p regulators are thought to have differential, although in some cases overlapping roles in regulating distinct Rho1p-mediated processes (reviewed in (Levin, 2005; Park and Bi, 2007; Perez and Rincón, 2010)). Rho1p signalling activity also appears to be influenced by the RhoGDI Rdi1p, which interacts with the GTPase and extracts it from the membrane (Koch et al., 1997; Tiedje et al., 2008).

Together with its regulators, Rho1p constitutes the core of the cell wall integrity signalling network, linking cell surface sensors to a set of five effectors involved in cell wall biosynthesis, cell wall-related gene expression, actin organization and targeted secretion (Levin, 2005). The main Rho1p effector pathways are summarized in Figure 2.

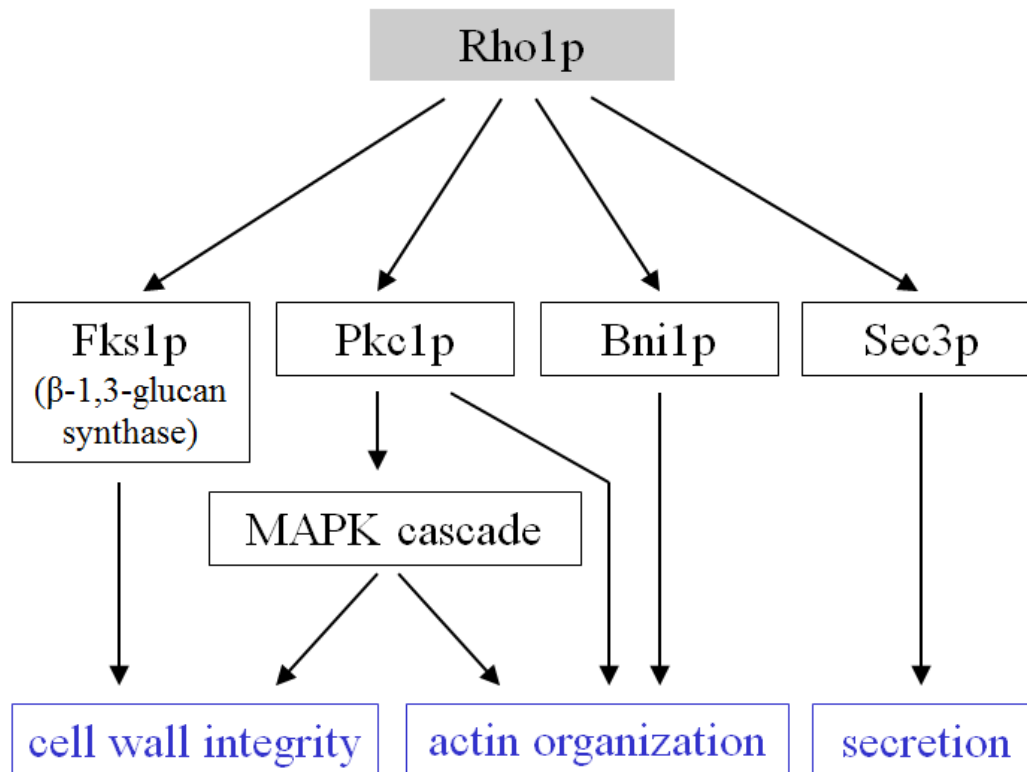


Figure 2: Overview of main *S. cerevisiae* Rho1p effectors and their proposed roles in cell wall integrity maintenance and related processes during polarized growth. See text for details.

The most important of the at least five transmembrane cell wall stress sensors whose signals converge on Rho1p are Wsc1p and Mid1p (ibid.). They have been shown to interact with Rom2p and are thought to stimulate its GEF activity towards Rho1p (Philip and Levin, 2001).

In response to upstream signals transmitting cell wall perturbation, Rho1p governs synthesis of cell wall components in two distinct ways (Drgonová et al., 1996; Levin, 2005), which can be genetically separated from each other by specific *RHO1* mutations (Saka et al., 2001).

First, Rho1p is supposed to function as a regulatory subunit of the β -1,3-glucan synthase complex, stimulating the activity of the two similar alternative catalytic subunits Fks1p and Fks2p in production of the main cell wall component in a GTP-dependent manner (reviewed in (Levin, 2005)). This notion is based on findings that extracts prepared from temperature-sensitive *rho1* mutants exhibit decreased glucan synthase activity which can be specifically restored by addition of wild type extracts or recombinant Rho1p in combination with GTP; the requirement for GTP can be circumvented by providing a constitutively active Rho1p protein (Drgonová et al., 1996; Qadota et al., 1996). Direct interaction of Rho1p with Fks1p has been shown by its concomitant enrichment with Fks1p during product entrapment purification and by coimmunoprecipitation with partially purified Fks1p (Mazur and Baginsky, 1996; Qadota et al., 1996). In addition, Fks1p and Rho1p have been shown to both be transported to the plasma membrane in secretory vesicles, in which the GTPase is thought to be kept in its inactive state by absence of GEFs; in addition, the two proteins colocalize at sites of polarized growth, i.e. bud tips and bud necks, where Rho1p is presumably switched on by its membrane associated activators (Qadota et al., 1996; Abe et al., 2003). Interestingly, a recent *in vitro* study also suggests that Rho1p might directly regulate the enzyme complex synthesizing β -1,6-glucan, the branched polymer mainly responsible for connecting the inner cell wall layer to the outer mannoprotein layer (Vink et al., 2004).

The second pathway emanating from Rho1p that controls production of cell wall polymers leads via its effector Pkc1p on to the tripartite cell wall integrity MAPK cascade composed of the MAPK kinase kinase Bck1p, the functionally redundant MAPK kinases Mkk1/2p and the MAPK Mpk1p (also known as Slt2p). Upon its activation, Mpk1p activates at least two transcription factors, Rlm1p and the Swi4p/Swi6p complex, which regulate the expression of several genes whose products are involved in cell cycle progression and cell wall synthesis, such as Fks1p, Fks2p or the catalytic subunit of chitin synthase 3, Chs3p (reviewed in (Levin, 2005; Park and Bi, 2007)). This branch of Rho1p signalling is supposed to be especially important and highly active in response to cell wall stress sensed by the surface receptors, while the direct regulation of glucan synthase activity is considered the main mode in which Rho1p controls cell wall biosynthesis during normal growth (Levin, 2005). Rho1p has been shown to interact with Pkc1p, the sole protein kinase C in *S. cerevisiae*, and to confer upon the kinase the ability to be activated by its cofactor phosphatidylserine (Nonaka et al., 1995; Kamada et al., 1996). Moreover, Pkc1p localization to sites of polarized growth depends on functional Rho1p (Andrews and Stark, 2000). *In vitro* studies have revealed that Pkc1p phosphorylates Bck1p (Levin et al., 1994), and the activating signal is then passed on along the cascade by sequential phosphorylation of its component kinases, resulting in adaptive gene expression alterations counteracting cell wall instability (reviewed in (Levin, 2005)).

The finding that depletion of the essential Pkc1p results in a more severe cell lysis phenotype than that of mutants lacking any of the constituents of its downstream MAPK cascade suggests that Pkc1p might regulate additional targets besides Bck1p important for cell wall integrity (*ibid.*). A potential candidate is Chs3p, whose translocation from internal stores to the plasma membrane appears to be controlled by Rho1p and Pkc1p (Valdivia and Schekman, 2003). However, the exact mechanisms of this control as well as the influence of Pkc1p on the activity of further alternative substrates remain largely elusive (reviewed in (Levin, 2005)).

Similar to its role in regulation of cell wall polymer production, Rho1p exerts dual control on organization of the actin cytoskeleton.

The first, possibly branched, route used by Rho1p to influence the actin cytoskeleton involves the Pkc1p-MAPK pathway. It has been shown that this pathway is required for actin organization, as mutants lacking Mpk1p, the last kinase in the MAPK cascade, not only display a lysis phenotype but also are affected in polarization of the actin cytoskeleton (Mazzoni et al., 1993). Moreover, the actin defect observed in certain *rho1* mutants can be specifically suppressed by upregulation of Pkc1p and Mpk1p, but not other Rho1p effectors (Helliwell et al., 1998). The mechanisms by which the Pkc1p/MAPK pathway drives polarization of the cytoskeleton, however, are still widely unknown (Levin, 2005). An actin-related function of the cell wall integrity pathway could be especially important under heat stress conditions associated with cell wall defects. In response to such stress, the actin cytoskeleton is depolarized and, later, repolarized; in combination with other cellular responses such as concomitant redistribution of Rho1p, its GEF Rom2p and its effector Fks1p to the cell periphery, this is presumed to allow the cell to counterbalance adversities before resuming polarized growth at the bud (Delley and Hall, 1999; Audhya and Emr, 2002; Park and Bi, 2007). For regulation of this stress-induced de- and repolarization of actin structures, the pathway has been suggested to bifurcate at Pkc1p: The upper part including Wsc1p, Rom2p, Rho1p and Pkc1p, together with one or more unknown Pkc1p targets, is apparently sufficient for depolarization, while reconstitution of polarity also requires the downstream MAPK cascade (Delley and Hall, 1999). Recently, the discovery of a negative

feedback control of Mpk1p on Rom2p (Guo et al., 2009) has shed some light on how the phases of this stress response might be regulated. Nevertheless, as stated, the exact impact of Rho1p on actin polarization via the Pkc1p/MAPK route is far from being understood (Levin, 2005).

The second way in which Rho1p influences the organization of the actin cytoskeleton is more straightforward: It shares with Cdc42p the effector Bni1p, a nucleator of actin filaments which can be assembled into higher order structures such as cables, patches and the contractile actin ring acting in cytokinesis. Rho1p has been shown to physically interact with Bni1p (Kohno et al., 1996). Nevertheless, localization of Bni1p to the bud tip is absolutely dependent on Cdc42p, but scarcely on Rho1p (Ozaki-Kuroda et al., 2001). In accordance with this finding, another study indicates that Rho1p regulation of Bni1p-mediated filament nucleation might mainly be important in controlling the assembly of the contractile actomyosin ring, while Cdc42p is dispensable for this process (Tolliday et al., 2002). Still, Rho1p appears necessary for formin-stimulated assembly of polarized actin cables at least at elevated temperatures (Dong et al., 2003). Interestingly, evidence from the same report suggests that in spite of the direct binding interaction of the two proteins, regulation of Bni1p by Rho1p could be indirect through activation of Pkc1p.

Like Cdc42p, Rho1p does not only influence the formation of polarized actin cables, which serve as tracks for targeted delivery of secretory vesicles, via the routes just described, but it is also presumed to spatially regulate vesicle fusion with the plasma membrane by its interaction with the exocyst subunit Sec3p. Mislocalization of Sec3p has been observed in certain conditional *rho1* mutants, and interaction between Sec3p and Rho1p proved *in vitro* turns out to be necessary for proper localization of Sec3p *in vivo* (Guo et al., 2001). Obviously, therefore, both Cdc42p and Rho1p collaborate as key regulators of directed exocytosis.

Skn7p, finally, is the fifth effector of Rho1p known so far. It interacts with activated Rho1p in yeast two-hybrid assays, and interaction between the two proteins appears to be required for the *in vivo* functions of Skn7p (Alberts et al., 1998). Skn7p is a transcription factor with homology to response regulators of bacterial two-component signalling pathways and has been implicated in processes such as adaptation to hypoosmotic and oxidative stress, morphogenesis and G1 cyclin synthesis (reviewed in (Alberts et al., 1998; Levin, 2005)). The product of its only target gene identified so far, *OCH1* (Li et al., 2002), is a mannosyltransferase required for maturation of cell wall glycoproteins, underlining its proposed involvement in maintenance of cell wall integrity. There are also indications that Skn7p could participate indirectly in controlling expression of *FKS2*; meanwhile, the significance of its interaction with Rho1p and its role in other signalling pathways are yet to be elucidated (reviewed in (Levin, 2005)).

3.4.4.2 The Rho1 module in *S. pombe*

Signalling activity of *S. pombe* Rho1 is presumed to be regulated, in part in an output-specific manner, by three GEFs, Rgf1, Rgf2 and Rgf3 (Tajadura et al., 2004; Mutoh et al., 2005; García et al., 2006a), three GAPs, Rga1, Rga5 and Rga8 (Nakano et al., 2001; Calonge et al., 2003; Yang et al., 2003) and by the GDI Rdi1 (Nakano et al., 2003).

In *S. pombe*, too, Rho1 appears to play a pivotal role in safeguarding cell wall integrity. In comparison to *S. cerevisiae*, however, fewer details about the effector pathways of the GTPase are known. Likewise, no cell surface sensors signalling to Rho1p have been

identified so far (Perez and Rincón, 2010). Strikingly, Rho2, a close relative of Rho1, is thought to contribute considerably to cell integrity signalling, although it is not essential for cell viability (Calonge et al., 2000; Ma et al., 2006). Proposed effectors of the two GTPases are depicted in Figure 3.

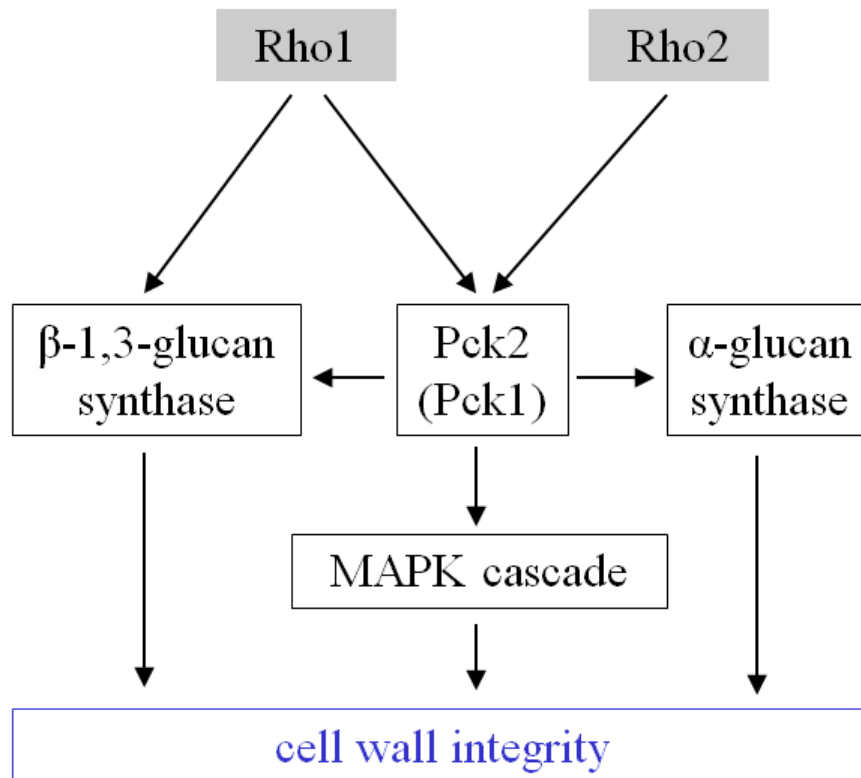


Figure 3: Overview of *S. pombe* Rho1 and Rho2 effector pathways regulating cell wall integrity. See text for details.

Like its budding yeast homologue, *S. pombe* Rho1 is supposed to act as a regulatory subunit of the enzyme complex synthesizing the main cell wall polymer β -1,3-glucan (reviewed in (García et al., 2006b)). This notion is based on the findings that overexpression of *rho1*⁺ leads to abnormally thick cell walls and an increased activity of β -1,3-glucan synthase in the wild type background, as verified by *in vitro* experiments; the stimulatory effect on enzyme activity becomes independent of GTP if a constitutively active variant of Rho1 is used (Arellano et al., 1996).

Pck1 and Pck2, the two protein kinase C family members sharing overlapping roles in cell viability (Toda et al., 1993; Arellano et al., 1999), have been identified as further effectors of *S. pombe* Rho1. Activated Rho1 interacts with both kinases, and this interaction results in their stabilization (Arellano et al., 1999). In the same study, the two kinases have also been shown to interact with activated Rho2. In addition, the authors present evidence that besides its direct stimulation of β -1,3-glucan synthase, Rho1 (but not Rho2) exerts an additional indirect influence on the activity of this enzyme through Pck2 and, possibly, Pck1. Rho2, acting through Pck2, positively regulates biosynthesis of α -D-glucan, the second most abundant structural component of the fission yeast cell wall (Calonge et al., 2000); thus, Rho1 and Rho2 coordinately control production of the most important cell wall polymers.

In addition, the two Rho GTPases are presumed to cooperatively regulate signalling through the conserved cell wall integrity MAPK cascade of *S. pombe*. The cascade consists of the MAPK kinase kinase Mkh1, the MAPK kinase Pek1 (alias Shk1) and the MAPK Pmk1

(reviewed in (Perez and Rincón, 2010)). Pmk1 becomes phosphorylated under cell wall and a variety of other stresses (Madrid et al., 2006) and in turn phosphorylates the transcription factor Atf1, whose lack renders cells hypersensitive towards cell wall damaging agents (Takada et al., 2007). Two putative Atf1 target genes possibly involved in maintenance of cell integrity have been identified, but their exact roles remain to be studied (Takada et al., 2007, 2010).

Pck2, but not Pck1, interacts with Mkh1 and activates the MAPK cascade, and Rho2 has been shown to act upstream of Pck2 in this signalling pathway (Ma et al., 2006). This view is supported by the finding that the (exclusively) Rho2-specific GAP Rga2 negatively regulates Pmk1 activity (Villar-Tajadura et al., 2008).

In contrast, the role of Rho1 within the cell integrity pathway is not yet entirely clear. Based on the finding that double deletion of *pck1*⁺ and *pck2*⁺ results in a lethal cell lysis phenotype similar to that of a mutant devoid of *rho1*⁺, it has been suggested that one of the main role of Rho1 within the cell integrity pathway might be the local stabilization of the otherwise unstable two kinases (Arellano et al., 1999). However, a recent study has placed the Rho1-specific GEF Rgf1 (but not the other two GEFs) upstream of the cell integrity Pck2-MAPK pathway and presented compelling evidence that Rho1 is indeed directly involved in stimulation of the pathway (Garcia et al., 2009).

The cellular targets of the the other effector shared by Rho1 and Rho2, Pck1, are still unknown, but it has been shown to be required for cell integrity, presumably acting in parallel to the Pck2-Mkh1-Pek1-Pmk1 signalling pathway (Arellano et al., 1999; Ma et al., 2006). Notably, a recent report indicates that Pck1 and Pck2 could play opposing roles in the regulation of the MAPK cascade, with Pck1 negatively modulating the basal activity of Pmk1 by an as yet unknown mechanism (Barba et al., 2008).

Based on phenotypes of strains with diminished or excessive Rho1 activity levels, fission yeast Rho1, in analogy to its budding yeast relative, is expected to play additional roles in polarization of the actin cytoskeleton and general cell polarity, as well as in septation and cell division (Arellano et al., 1997; Nakano et al., 1997). However, the effectors mediating these functions are still unknown.

3.5 Rho GTPases and polarized growth in filamentous fungi

3.5.1 Characteristics of hyphal growth in filamentous fungi

The study of polarized growth in unicellular yeasts, especially during budding in *S. cerevisiae*, has established the groundwork for the elucidation of the fundamental principles underlying this vital process. However, while it is now widely presumed that the core mechanisms used to generate cell polarity are conserved from yeasts to mammals, it is also becoming evident that they must be adapted to create a variety of specific morphogenetic outcomes (reviewed in (Nelson, 2003; Harris et al., 2005; Harris, 2006)).

Filamentous fungi have a tremendous impact, both disadvantageous and advantageous, on human welfare: Among them are devastating pathogens, affecting crop plants and humans alike, while various species are highly valued as cell factories in biotechnology and producers of potent antibiotics and other medically important compounds (reviewed in (Adrio and Demain, 2003; Harris et al., 2005)). Nevertheless, the molecular mechanisms underlying

their defining hallmark, hyphal growth, are still poorly understood, although it is acknowledged as the basis of their astonishing success in quickly colonizing and exploiting new substrates (Harris and Momany, 2004).

Polarized growth in filamentous fungi is distinguished in many aspects from that in their unicellular relatives (reviewed in (Momany, 2002, 2005; Harris and Momany, 2004)). In contrast to budding yeast, where phases of isotropic and polar growth alternate throughout the budding cycle, a short period of isotropic expansion of the spore during germination is followed by a permanent switch to persistent polarized growth in filamentous fungi. In the latter, extremely rapid apical extension (up to $\geq 1 \mu\text{m}/\text{second}$ (Seiler and Plamann, 2003)) leads to the formation of a germ tube which ultimately grows into a highly elongated multicellular hypha. Unlike in *S. cerevisiae*, multiple axes of polarity are established and simultaneously maintained when branches emerge from the main hypha, creating a ramified mycelium. All these differences imply that the basic polarity machinery must be adapted and regulated differently to meet the challenges presented by the hyphal growth mode.

In accordance with this notion, the limited data about molecular aspects of morphogenesis in filamentous fungi suggest that the microtubule cytoskeleton, not unlike the situation in fission yeast but in stark contrast to the budding process in *S. cerevisiae*, might play a pivotal role in polarized growth; it appears to provide the tracks for long-distance transport of secretory vesicles to the hyphal tip (reviewed in (Harris and Momany, 2004; Harris et al., 2005; Fischer et al., 2008)).

Another adaptation to the needs of rapid apical growth unique to filamentous fungi is the so-called Spitzenkörper, a phase-dark structure found at actively growing hyphal tips (Girbardt, 1957; Borkovich et al., 2004; Harris et al., 2005; Virag and Harris, 2006; Fischer et al., 2008). It is thought to serve as a vesicle supply center safeguarding the directed delivery of compounds to the growing tip, where up to 40,000 vesicles per minute (Collinge and Trinci, 1974) are estimated to fuse with the plasma membrane. While its molecular composition has not been fully elucidated yet, it is thought to be made up of vesicles, microfilaments and polarity-related proteins; some of these are homologues of components of the yeast polarisome, a multiprotein complex including Bni1p, which is involved in the formation of polarized actin cables (Sheu et al., 1998; Pruyne and Bretscher, 2000; Harris et al., 2005; Virag and Harris, 2006). However, the exact relationship between Spitzenkörper and the polarisome remains to be determined (Harris et al., 2005; Virag and Harris, 2006).

Recently, genome surveys have revealed that the components of the signal transduction pathways and the morphogenetic machinery involved in polarized growth in the two model yeasts are largely conserved in various filamentous fungi (Wendland, 2001; Borkovich et al., 2004; Harris and Momany, 2004; Momany, 2005; Banuett et al., 2008; Harris et al., 2009). Nevertheless, homologues of some key proteins, many of them serving as cortical landmark proteins in yeasts, appear to be absent or highly diverged; other proteins possibly playing a role in polar morphogenesis, such as a homologue of the Rac GTPase found in higher eukaryotes, have been identified in filamentously growing fungi only, suggesting their specific involvement in the formation of hyphal structures (ibid.).

With this knowledge, it is now a major challenge to clarify how conserved and novel components of the polarity toolbox interact and how they are wired and regulated to achieve the singular temporal and spatial patterns characteristic of hyphal growth.

3.5.2 The roles of Rac and Cdc42 homologues in filamentous fungi

As expected, many of the recent studies investigating the molecular mechanisms of truly filamentous fungal growth have focused on the roles of Rho GTPases therein. Consequently, in the last decade some progress has already been achieved in understanding the roles of these key signalling switches in hyphal growth. Nevertheless, the data collected so far are still far from unfolding a picture as detailed and comprehensive as that in the two model yeasts, and in particular the distinct regulation of Rho signalling remains largely unknown.

Special attention has been paid to the fact that, as stated above, most filamentous fungi, in contrast to budding and fission yeast, possess a homologue of Rac. In mammalian systems, Rac and the relatively similar Cdc42 are best known for their control of different actin-based cell projections involved in cell motility: While Rac is the main regulator of lamellipodia formation, Cdc42 is required for formation of the slender filopodia. In these and other individual and common cellular functions, the two GTPases appear to regulate both unique and shared effector proteins (reviewed in (Bishop and Hall, 2000; Ridley, 2001)). A similar tendency to employ Rac and Cdc42 for both overlapping and distinct morphogenetic functions is observed in filamentous fungi, too. Already with the limited data available, however, it is clear that the degree of specialization between the two GTPases and their relative contributions to hyphal growth vary widely between different species, although in all cases at least one of them has an important influence on polarized growth.

In the filamentous ascomycete *Aspergillus nidulans*, Cdc42 is supposed to play the major role in hyphal morphogenesis (Virag et al., 2007). RacA and Cdc42 are proposed to share a function in establishing the primary axis of polarity, which might explain the synthetic lethality of the double deletion mutant. Cdc42 appears solely responsible for maintaining directed elongation and regulating subsequent polarization events for lateral branch formation. SepA, the sole formin of *A. nidulans*, is thought to act as an effector of Cdc42 in actin polarization. RacA appears to play the prominent role in asexual development, i.e. formation of conidiophores (ibid.), but both Cdc42 and RacA are probably involved in localized ROS production (Semighini and Harris, 2008). In filamentous fungi, ROS and Ca²⁺ tip-high gradients are presumed to be responsible for apical dominance, i.e. suppression of secondary polarity axes close to growing hyphal tips, and unlike yeasts, many filamentous fungi possess homologues of NADPH oxidases (Nox), whose ROS synthesis activity is controlled by a regulatory subunit, NoxR (reviewed in (Jackson and Heath, 1993; Takemoto et al., 2007; Scott and Eaton, 2008)). In several filamentous fungi an involvement of Rac in regulation of ROS production has been proposed (see below), and in *A. nidulans*, too, Rac seems to activate Nox; exceptionally, however, in this fungus Cdc42 appears to play an equally important part by contributing to Nox localization in cooperation with NoxR and, possibly, the scaffold protein Bem1 (Semighini and Harris, 2008).

Only recently it has been shown that in *Aspergillus niger*, contrasting clearly to the situation in its close relative *A. nidulans*, RacA has a prominent role in regulating actin polarization and hyphal growth, especially maintenance of established polarity axes, while the Cdc42-homologue CftA appears largely dispensable (Kwon et al., 2010). Again, however, the two GTPases must share an essential function, possibly in actin filament elongation, as their simultaneous depletion is lethal. Tip-high ROS gradients are observed in the fungus, but, again in contrast to *A. nidulans*, neither the RacA-interacting RiaA/NoxR nor NoxA appear to play a decisive role in their generation (ibid.).

The opportunistic human pathogen *Candida albicans* is a dimorphic fungus, i.e. it switches between yeast-like and truly filamentous growth; in this fungus Rac1 and Cdc42 have distinct roles in hyphal growth triggered by different stimuli and cannot substitute for each other (Bassilana and Arkowitz, 2006). Deletion of *rac1* does not interfere with viability (ibid.), but *cdc42* is an essential gene (Ushinsky et al., 2002; Bassilana et al., 2003). Rac1 and its GEF Dck1 are required for matrix-induced filamentous growth and appear to be involved in cell wall integrity (Bassilana and Arkowitz, 2006; Hope et al., 2008, 2010). On the other hand, specific regulation of Cdc42 and its essential GEF Cdc24 allows serum-induced filament formation, and a positive feedback loop has been shown to transiently promote Cdc24 expression, thereby contributing to increasing levels of active Cdc42 at the hyphal tip (Bassilana et al., 2003, 2005). Polarizing activity of Cdc42, which is altogether considered the major player in hyphal development (Court and Sudbery, 2007), is in addition positively regulated by the RhoGDI Rdi1 and negatively influenced by the GAPs Rga2, Bem3 and Rgd1 (Court and Sudbery, 2007; Zheng et al., 2007; Ness et al., 2010). Cdc42 interacts *in vitro* with the CRIB domains of the PAK-family kinases Cla4 and Cst20 (Su et al., 2005), both of which have been clearly implicated in formation of hyphae and virulence of the fungus (Leberer et al., 1996, 1997b), and genetic interaction between Cdc42 and Cst20 indicates relevance of their relationship *in vivo* (Ushinsky et al., 2002).

In contrast to the majority of filamentous fungi, *Ashbya gossypii*, a close relative of budding yeast, possesses no Rac (Boyce et al., 2003). Like their *S. cerevisiae* counterparts, both AgCdc42p and its putative GEF AgCdc24p are essential proteins required for polarized growth and actin polarization; this is evident in the inability of deletion mutant spores to accomplish the isotropic-polar switch and to correctly localize actin patches (Wendland and Philippsen, 2001). One of the three *A. gossypii* formins, the essential AgSepAp, has been suggested to act as an effector of the GTPase for formation of actin cables in hyphal growth (Schmitz et al., 2006).

Both Rac and Cdc42 homologues are involved in regulating growth and development in the fungal phytopathogens *Claviceps purpurea* and *Colletotrichum trifolii*. In the first one, Rac1 has the major influence on hyphal growth, with deletion mutants exhibiting excessive hyperbranching and loss of polarity, sporulation and the ability to penetrate the plant surface (Rolke and Tudzynski, 2008). Rac1 and its effector Cla4 seem to have an impact on oxidative stress response and ROS homeostasis required for differentiation, but the exact mechanisms are still unclear (ibid.). Cdc42 of *C. purpurea* appears to exercise accessory control on branch formation, and while deletion mutant strains still penetrate the plant, invasive growth is soon arrested (Scheffer et al., 2005). In *C. trifolii*, hyphal growth is abolished altogether in strains expressing a dominant negative version of CtRac1, and the GTPase is thought to function in ROS production and MAPK activation downstream of CtRas (Chen and Dickman, 2004). CtCdc42 is proposed to be essential, and expression of a dominant negative form affects spore germination and hyphal morphology and promotes pathogenic development; interestingly, reminiscent of *A. nidulans*, CtCdc42 appears to play a role in ROS generation, presumably acting in the same pathway as CtRas (Chen et al., 2006).

ROS produced by NoxA are also important factors in maintaining a mutualistic symbiotic relationship between the fungus *Epichloë festucae* and its ryegrass host *Lolium perenne*; RacA is needed for activation of the NADPH oxidase, and in interaction with NoxR it appears to spatially regulate ROS production, thus preventing hyphal hyperbranching and excessive

colonization of the plant, which would result in premature senescence of the host (Takemoto et al., 2006; Tanaka et al., 2008).

In the dimorphic fungus *Yarrowia lipolytica* deletion of *YIRAC1* affects cell morphology in yeast cells and completely abolishes hyphal growth, although actin polarization appears unaltered (Hurtado et al., 2000). A similar, although more severe mutant phenotype has fuelled speculation that the PAK kinase YICla4p might be a YIRac1p effector (Szabo, 2001), but so far this hypothesis has not been tested, just as the role of YICdc42p (Hurtado et al., 2000) remains to be determined.

Penicillium marneffe represents a prime example for shared and individual functions of Rac and Cdc42. In this thermally dimorphic fungus the Cdc42-homologue CflA and the Rac-like CflB coordinately regulate hyphal cell polarization, while they have unique functions in yeast-like growth and development of asexual structures, respectively (Boyce et al., 2001, 2003, 2005). *cfIA* appears to be an essential gene, and phenotypes of strains expressing a dominant negative allele suggest that CflA is needed for both initiation and maintenance of polarized hyphal growth, for proper septation and for determining cell shape of yeast cells (Boyce et al., 2001). A strain deleted for *cfIB* is viable but exhibits loss of polarized growth, inappropriate septation, distortion of the actin cytoskeleton and the absence of conidiophores; later, swollen hyperbranched apical and subapical cells are observed (Boyce et al., 2003). Consistent with an only partial overlap of functions, overexpression of a constitutively active form of CflA partially suppresses the hyphal aberrancies of a $\Delta cfIB$ strain but cannot restore the conidiation defects (Boyce et al., 2005). Genetic evidence suggests that CflA acts downstream from RasA and upstream of its putative effector kinase PakA to control conidial germination (Boyce et al., 2005; Boyce and Andrianopoulos, 2007), but further components of the signalling network around CflA and CflB have not been elucidated so far.

In the dimorphic basidiomycete *Ustilago maydis*, the causative agent of corn smut disease, the roles of Cdc42 and Rac1 have strongly diverged, and consistently the two GTPases cannot substitute for each other (Hlubek et al., 2008). Nevertheless, despite the high degree of specialization, the two GTPases must have retained at least one common essential function, as evident in the synthetically lethal effect of their combined depletion (Mahlert et al., 2006). Both GTPases appear to be required for pathogenicity of the fungus (ibid.). Strikingly, cells lacking Cdc42 have almost normal morphology, but they are unable to separate, and further studies have revealed that Cdc42 and its GEF Don1 coordinately regulate cytokinesis and cell separation in parallel to the Ste20-like germinal center kinase Don3 (Weinzierl et al., 2002; Mahlert et al., 2006; Böhmer et al., 2008; Schink and Bölker, 2009). In contrast, Rac1 clearly controls polarized growth; yeast cells devoid of the GTPase are enlarged and have unusually round tips, and the deletion strain is unable to form filaments (Mahlert et al., 2006); conversely, overexpression of *rac1* suffices to induce hyphal growth (ibid.). Rac1 activity is thought to be regulated by the essential GEF Cdc24, which appears to be localized to hyphal tips by the adaptor protein Bem1 (Castillo-Lluva et al., 2007; Alvarez-Tabarés and Pérez-Martín, 2008). Several lines of evidence suggest that the PAK-family member Cla4 acts as an effector of Rac1 in hyphal morphogenesis, but further downstream targets are supposed to exist (Leveleki et al., 2004; Mahlert et al., 2006).

As evident in the examples outlined, there appears to be no general scheme of Cdc42 and Rac utilization in different species of filamentous fungi. However, a tendency to employ both

GTPases for controlling various aspects of hyphal growth, often in polarization of the actin cytoskeleton and ROS generation, seems to exist.

3.5.3 The functions of Rho1 homologues in filamentous fungi

As stated, in the two yeasts *S. cerevisiae* and *S. pombe* Rho1 is mainly known for its pivotal functions in maintaining cell wall integrity, while it also plays a role, albeit subordinate to Cdc42, as a regulator of actin cytoskeleton polarization. Based on the results from few studies, both of these major functions appear to be conserved in several filamentous fungi, whose fast apical extension rates pose a special challenge to the cell wall integrity machinery. Indeed, Rho1 seems to have acquired an even more prominent position in securing establishment and continuity of polarized growth. However, as observed for Rac and Cdc42 homologues, clear differences in Rho1 contributions to viability and hyphal growth appear to have evolved between species.

In the close *S. cerevisiae* relative *A. gossypii* tandem duplication is thought to have generated a second copy of Rho1, thus producing two paralogous genes denoted as *AgRHO1a* (alias *AgRHOH*) and *AgRHO1b* (also known as *AgRHO1*) that have overlapping functions (Walther and Wendland, 2005; Köhli et al., 2008). *AgRho1bp* is the more important factor and able to substitute for *S. cerevisiae* Rho1p, and its deletion leads to the formation of slow-growing colonies, which exhibit high rates of non-osmoremedial cell lysis and die within few days; in addition to the strong lysis phenotype, cells are slightly affected in actin polarization and exhibit irregular shapes (Wendland and Philippsen, 2001; Köhli et al., 2008). In contrast, *AgRho1ap* is not essential for viability, although its lack results in weak actin abnormalities and minor cell wall defects evident in occasional tip lysis and hypersensitivity towards cell wall damaging agents (Walther and Wendland, 2005; Köhli et al., 2008). The overlap in functions of the two paralogues is emphasized by the exacerbated defect of a double deletion strain, whose spores are entirely unable to germinate (Walther and Wendland, 2005). Both GTPases show almost identical yeast two-hybrid interactions with putative effectors *AgBni1p*, *AgPkc1p* and *AgSec3p*; however, their subcellular localization and presumed functions differ, probably due to differential regulation by the two GAPs *AgLrg1p* and *AgSac7p*, which in turn is effected by an atypical switch I region of *AgRho1ap* (Köhli et al., 2008).

In the dimorphic fungus *C. albicans* Rho1 is essential for viability during yeast-like growth, its depletion leading to cell lysis and cell aggregation, as well as during hyphal growth both in culture and in mammalian hosts (Smith et al., 2002b). Rho1 has been shown to directly regulate β -1,3-glucan synthesis, and consistent with a conservation of functions between species, expression of *RHO1* is able to rescue *S. cerevisiae rho1* null mutants (Kondoh et al., 1997).

In the *Aspergilli* Rho1 homologues have likewise been implicated in polarized growth and cell wall maintenance. *A. fumigatus* *AfRho1p* copurifies with *AfFks1p* during product entrapment, and the two putative components of the β -1,3-glucan synthase complex are known to localize predominantly to hyphal tips (Beauvais et al., 2001; Dichtl et al., 2010). In *A. niger* deletion of *rhoA* prevents polarized growth and is ultimately lethal, with most spores swelling apolarly and only few developing into malformed germlings that soon stop growing (Kwon et al., 2010). Similarly, *A. nidulans* RhoA influences polar growth, branching and cell wall synthesis (Guest et al., 2004). Expression of a dominant negative *rhoA* allele leads to faster emergence of secondary and tertiary germ tubes as well as lateral branches in an abnormal

pattern; later, tip lysis occurs, indicating cell wall defects also suggested by hypersensitivity towards cell wall disrupting agents and alterations in cell wall composition (ibid.).

In contrast to the examples just outlined and to the two yeast species, *Fusarium oxysporum* strains deleted for *rho1* are viable, although they exhibit severe colony phenotypes associated with cell wall aberrancies (Martínez-Rocha et al., 2008). While cell morphology is largely unaffected in $\Delta rho1$ loss of function mutants, hyphal growth is markedly slowed on solid medium, lysis is observed, and cells exhibit altered sensitivity towards cell wall stressing agents. Expression of *chsV*, encoding a chitin synthase, and *fks1* is upregulated in the deletion strain; however, while chitin synthase activity is consistently enhanced, glucan synthase activity is reduced, indicating lack of positive posttranslational regulation in the absence of Rho1. Rho1 appears to be dispensable for virulence of *F. oxysporum* in mammals but not in plants, where alterations in cell wall structure of $\Delta rho1$ strains are thought to elicit strong host defense responses (ibid.).

YIRHO1 is another non-essential homologue of *RHO1*, although it is able to complement lethality of a *S. cerevisiae rho1 Δ strain (León et al., 2003). *Y. lipolytica* strains deleted for *YIRHO1* are less resistant to some cell wall damaging agents but exhibit otherwise normal cell and colony morphology, growth rates and morphological transition; the existence of a further similar GTPase with redundant functions has been suggested to account for the mild effects of *YIRHO1* deletion (ibid.).*

Replacing wild type *CnRHO1* by a temperature-sensitive mutant allele in the dimorphic opportunistic pathogen *Cryptococcus neoformans* results in an osmoremedial phenotype characterized by slow growth and lysis-induced death (Chang and Penoyer, 2000). As in other fungi, strong evidence suggests that glucan synthase is directly regulated by CnRho1 (ibid.).

Its differential expression during spore germination, peaking during germ tube formation and branching, in conjunction with its localization to the spore plasma membrane, accumulating at sites of tube emergence, indicates the involvement of RhoA in polarized growth of the filamentous zygomycete *Phycomyces blakesleeanus* (Ramírez-Ramírez et al., 1999). However, none of the molecular functions of the GTPase have been analyzed so far.

Only recently, *U. maydis* Rho1 has been shown to be essential for viability and involved in regulation of cell polarity and, notably, cytokinesis, the two processes also controlled by Rac1 and Cdc42, respectively (see above and (Pham et al., 2009)). Prior to death, cells depleted for Rho1 exhibit abnormal budding patterns, septation and cell separation defects as well as irregular chitin deposition. Interestingly, Rho1 interacts with the presumed Rac1 GEF Cdc24, and based on epistasis experiments it is predicted to negatively modulate the function of Rac1 and its effector kinase Cla4 in filament formation, although the exact mechanisms remain unknown. Pdc1, the sole and essential *U. maydis* homologue of 14-3-3 proteins, which are mainly known for their ability to interact with phosphoserine and phosphothreonine motifs, has been proposed to act as an upstream component of Rho1 signalling, possibly serving as a scaffold to safeguard localized Rho1 activity at the hyphal tip (ibid.).

Collectively, these examples demonstrate that Rho1 homologues in many filamentously growing fungi, similar to their yeast counterparts, are required for proper composition and integrity of the cell wall and for establishment and maintenance of polarized growth.

However, the regulatory circuits orchestrating their functions in hyphal growth as well as their downstream targets are only slowly beginning to emerge.

3.6 Rho GTPases and their regulators in *N. crassa*

The filamentous ascomycete *Neurospora crassa* has a remarkable history as a model organism in genetic, biochemical and molecular biological research (reviewed in (Davis, 2000)), and the publication of its genome sequence (Galagan et al., 2003) has opened up new opportunities for a comprehensive investigation of the molecular basis underlying the most fundamental cellular processes such as filamentous growth.

Like other filamentous fungi, *N. crassa* appears to possess a widely conserved polarity machinery (Borkovich et al., 2004), and based on the findings in yeasts and other eukaryotes, Rho GTPases and their regulators are expected to represent key factors in the establishment and maintenance of polarized growth in this filamentous fungus, too.

Besides six Rho GTPases, RHO1 to RHO4, CDC42 and RAC, all of which, except RAC, are homologues of their respective yeast counterparts (ibid.), the genome of *N. crassa* encodes seven putative RhoGEFs (six of them belonging to the classical Dbl homology family, one with similarity to the CZH-family), ten RhoGAPs and one RhoGDI.

At the start of this study, little was known about the roles of the GTPases or their regulators in hyphal morphogenesis of *N. crassa*.

Some hints came from a large-scale genetic screen to identify conditional mutants defective in cell polarity (Seiler and Plamann, 2003). In this study, mutations in the genes encoding CDC42, its putative GEF CDC24 and the homologue of the *S. cerevisiae* scaffold protein Bem1p had resulted in phenotypes implicating these factors in establishment and maintenance of cell polarity. Based on the close resemblance of some of the mutants to an actin-deficient strain, a potential role in regulation of the actin organization had been proposed, but a detailed analysis of the mutants was lacking.

The RHO1-specific LRG1 is the only Rho GAP characterized so far in *Neurospora* (Vogt and Seiler, 2008). Like *rho-1*, *lrg-1* is an essential gene. As in many other filamentous fungi, functional RHO1 seems to be necessary for the establishment of polarity, with homokaryotic deletion mutants predominantly germinating in a completely isotropical manner; on the other hand, lack of negative regulation of the GTPase in a conditional *lrg-1* mutant leads to the development of pointed, needle-like tips and cessation of tip elongation accompanied by excessive subapical hyperbranching. When LRG1 function is compromised putative RHO1 downstream effectors including β -1,3-glucan synthase, protein kinase C and the actin cytoskeleton appear to be misregulated (ibid.).

Similar to its homologues in other filamentous fungi (Dünkler and Wendland, 2007; Si et al., 2010), *N. crassa* RHO4, which interacts with the sole RhoGDI RDI1 (Rasmussen and Glass, 2007), has been shown to be involved in the control of hyphal septation (Rasmussen and Glass, 2005, 2007; Rasmussen et al., 2008).

In contrast, no functional data at all had been gathered so far for RHO2, RHO3 and RAC, nor for the vast majority of putative Rho regulators.

3.7 Aims of this work

Given the presumed significance of Rho regulatory proteins in adapting Rho signalling to the requirements of highly different morphogenetic outcomes and the scarce knowledge about their roles in filamentous fungi, one of the aims of this study was to obtain a comprehensive overview of the RhoGAP and RhoGEF repertoire of *N. crassa* in comparison to its yeast relatives. This phylogenetic approach was complemented by *in vitro* assays to experimentally determine the target specificity of all putative RhoGEFs present in *N. crassa*. Based on the results from this more general examination, I intended to characterize the *in vivo* functions of selected Rho GTPases and their GEFs in the regulation of polarized growth by analyzing mutant phenotypes, subcellular localization patterns and interactions with putative effectors. In this, special focus was placed on discerning overlapping and distinct functions of the closely related Rho proteins RAC/CDC42 and RHO1/RHO2, respectively.

4. Materials and Methods

4.1 Suppliers of chemicals

Standard chemicals of grade p.a. and culture media components used in this study were obtained from AppliChem GmbH, Carl Roth GmbH & Co. KG, Invitrogen GmbH, Merck KGaA, Oxoid Deutschland GmbH, Roche Diagnostics GmbH, SERVA Electrophoresis GmbH and Sigma-Aldrich Chemie GmbH (all Germany).

4.2 Media and growth conditions for microorganisms

General procedures for growth and manipulation of *Neurospora crassa* were as described in (Davis and de Serres, 1970) or in the collection of protocols provided by the Fungal Genetics Stock Center at <http://www.fgsc.net/Neurospora/NeurosporaProtocolGuide.htm>.

Neurospora crassa strains were cultured on solid (with 1.5-2% (w/v) agar) or in liquid Vogel's Minimal Medium (VMM), i.e. "Vogel's Medium" (Medium N) (Vogel, 1956, 1964) with 2% (w/v) sucrose. For colonial growth on solid Vogel's medium, sucrose was replaced by 2% L-sorbose and 0.05% glucose and fructose each (Brockman and de Serres, 1963; Mishra and Tatum, 1972). Crosses were made on solid medium containing 2% Difco cornmeal agar (BD, USA) and 0.1% glucose to restrict formation of conidia and induce protoperithecia formation in the female parent before inoculation with the male parent (Shear and Dodge, 1927). For auxotrophic strains, culture media were supplemented with 8 µg/ml nicotinamide, 200 µg/ml tryptophane and/or 150 µg/ml histidine, and for selection of resistant strains, 200 µg/ml hygromycin B (InvivoGen, USA) were used. Cultures were routinely grown at 37°C, although temperature sensitive strains were usually propagated at 20-25°C unless stated otherwise. For inhibitor growth tests, reagents were added to culture media as stated in the respective figure legend.

Escherichia coli DH5α cells were grown on solid (with 1.5% agar) or in liquid LB medium (1% NaCl, 0.5% yeast extract, 1% tryptone) modified from (Bertani, 1951). Cultures were incubated at 37°C.

For protein expression, *E. coli* Rosetta2 (DE3) cultures were propagated at 20°C in enriched LB medium (LB⁺: 1% NaCl, 0.8% yeast extract, 1.8% peptone, 2% glucose).

When required, 100 µg/ml ampicillin, 50 µg/ml kanamycin and/or 50 µg/ml chloramphenicol (all Sigma-Aldrich Corporation, USA) were added as selecting agents.

Saccharomyces cerevisiae cultures were grown at 30°C as outlined in section 4.8.

4.3 Transformation of microorganisms

Initially, the spheroplast method was employed for transformation of *N. crassa* with plasmid DNA. Preparation and transformation of spheroplasts were carried out as described in (Vollmer and Yanofsky, 1986) except that Lysing Enzymes from *Trichoderma harzianum* (Sigma-Aldrich Corporation, USA) were used for cell wall digestion and spermidine·3HCl was omitted from the transformation mix.

Alternatively, transformation was achieved by electroporation of conidia as described in (Margolin et al., 1997) with minor modifications: Routinely, conidia were harvested after 9-11 days already, and electroporation was performed in cuvettes obtained from PEQLAB Biotechnologie GmbH (Germany) using a Bio-Rad Gene Pulser® II (Bio-Rad Laboratories GmbH, Germany) with slightly different settings (voltage 1.5 kV; capacitance: 50 μ F; resistance: 200 Ω). If dominant markers were used for selection of positive transformants, conidia were resuspended in VMM after electroporation, incubated at room temperature for three hours and then plated on selective medium as desired.

Transformants were identified by their ability to grow on medium lacking supplemented histidine (when histidine-auxotrophic strains had been transformed with plasmids allowing restoration of histidine prototrophy) or their resistance towards hygromycin B in the medium (in case strains had been transformed with plasmids carrying the antibiotic resistance cassette; see section 4.5 for details). Expression of the desired protein was verified by immunodetection in Western blots (see section 4.7.3).

Preparation and transformation of chemically competent *E. coli* cells followed the procedure presented in (Inoue et al., 1990).

For transformation of *S. cerevisiae* cells the method provided in (Schiestl and Gietz, 1989) was adopted (see section 4.8).

4.4 Plasmid construction

4.4.1 General procedure and overview

DNA cloning projects were planned, documented and analyzed using DNASTAR® SeqBuilder (version 8.0.3(1); DNASTAR, Inc., USA). Sequences of predicted genes were obtained from the Broad *Neurospora crassa* Database at <http://www.broadinstitute.org/annotation/genome/neurospora/MultiHome.html>. Primer design for construction of partial cDNA constructs was based on conserved domain predictions by InterProScan Sequence Search (European Bioinformatics Institute of European Molecular Biology Laboratory; available at <http://www.ebi.ac.uk/Tools/InterProScan/index.html>) performed on protein sequences downloaded from the Broad *Neurospora crassa* Database (assembly 7, version .3 annotation) unless stated otherwise.

In all cases of plasmid construction described in the following sections, DNA fragments amplified by polymerase chain reaction (PCR) were first subcloned into vector pJet1.2 blunt of the CloneJET™ PCR Cloning Kit (Fermentas GmbH, Germany); note that the resulting plasmids are not listed in Table 2. Consistency of resulting plasmids with intended theoretical sequence was ensured by analyzing results of suitable restriction digests and complete sequencing of inserts. After ligation of inserts with the respective end vector, at least the region of transitions between insert and vector was sequenced and restriction pattern was checked.

DNA was sequenced by the Göttingen Genomics Laboratory (G2L) at the Institute of Microbiology and Genetics, University of Göttingen, Germany. Results were analyzed using 4Peaks (version 1.7.2; Mekentosj B.V., The Netherlands) and the alignment mode bl2seq of BLAST (Basic Local Alignment Search Tool; (Altschul et al., 1990)) at the National Center for Biotechnology Information (NCBI) (accessible via <http://blast.ncbi.nlm.nih.gov/Blast.cgi>).

Primers and plasmids used in this study are summarized in Table 1 and Table 2, respectively.

Table 1: Primers used in this study. Restriction enzyme recognition sites are underlined, and mismatched nucleotides for insertion of mutations are depicted in lower case.

Primer	Sequence
Cdc42_3_Spe	GACTAGTCGCCCTATGCCGTTTAAATGTCC
Cdc42_5_Bgl	GAAGATCTGTGACGGGAAGTATCAAGTATGC
CoS_00196_1	GTCTCGAGCACGTCCGCCGCCGCTGCC
CoS_00196_2	GTGCGGCCGCTTAGTCATCTAGATCCATGTGCC
CoS_00196_3	TCTCGAGCGTAGCAGAACC GCCAAAGG
CoS_00196_4	TGCGGCCGCTTAGAGGAAATGATCCTGGTTCTC
CoS_00553_1	GTATTTAAATTATCTCTAGGAGATGCGTCTGCC
CoS_00553_2	GTGCGGCCGCTCAGTCATCATCATCGAAGATCTG
CoS_00668_3	GTATTTAAATTAGCCGACTATCATCAAGACCCC
CoS_00668_5	ACCCGGGAGTCAAATCAGGATGCCTCTGG
CoS_00668_6	ACCCGGGAGAAGGAAAAGCCGCGGTCAAC
CoS_00668_7	CGGATCCTACGCATCCGCCAACTTTTTTC
CoS_00668_8	CGGATCCTAGGCAAAGTAACCATACGATATTATC
CoS_00668_9	AACTAGTGGATGGCCGACTATCATCAAGACC
CoS_00668_10	GGTTAATTAACGCATCCGCCAACTTTTTCTG
CoS_00668_11	TGCGGCCGCTATCCCTTCAGGTTGAGCTTGGC
CoS_00668_12	AACCATGGTCAAATCAGGATGCCTCTGG
CoS_00668_13	GACACGTGCATGGCCGACTATCATCAAGACC
CoS_00668_14	GTTAATTAACTACGCATCCGCCAACTTTTTTC
CoS_01431_1	GGGCCATGGAGGCCTCCTCCACGACAAGAATGG
CoS_01431_9	GACACGTGTCAGCCCTTGGTGGCATTGGAGG
CoS_01431_11	GTA CTAGTATGTCTCCACGACAAGAATG
CoS_01431_12	GCTTAATTAATCCTGTTGTTTCTTTACTTTCTTC
CoS_01472_1	GTATTTAAATCGGAGGCTACTCCGATGCAG
CoS_01472_2	GTGCGGCCGCTTACTCGATTCCGATCTCCGCA
CoS_01472_3	ATGTGACCCAGCGAAGCGAGACATTCTG
CoS_01472_4	TGCGGCCGCTTACAGATCACCAACCAGGAGCG
CoS_02524_1	GGAATTCTGTGCGAGCTTGCTCACCCGGC
CoS_02524_3	GATGTCGACTTAGAACCATTATCGTCCCTCAT
CoS_02524_3b	ATGTGACCCAGACCTGTGTTTGGTGGGCC
CoS_02524_4	TGCGGCCGCTTAAAGCTCATATTGCGCGGGGTC
CoS_02764_1	GGAATTCTGGCAGCCCCTGGACCCAATGT
CoS_02764_3	GTGCGGCCGCTCATTCTCTTTCTCTCCGGA
CoS_02764_3b	ATGTGACCCCGGAGCGACAGTTGATGG
CoS_02764_4	TGCGGCCGCTTAGAGAAACACGAGTTTCCAGGA
CoS_02764_7	TGCGGCCGCTTAAAGGAAACACCAGACGGTCTTG
CoS_02915_1	GGAATTCTGGCGACCACGGCGCTTCACC
CoS_02915_3	GTGCGGCCGCTCAAAAAGCAGCCGGACTTCTC
CoS_02915_4	ATGTGACCCAGCTCCCCAACCAGTCTC
CoS_06544_1	GGGCCATGGAGGCCAACGACGAAGACAAGGTCC
CoS_06544_2	GACACGTGTTACTCAAAGTCGGCCGTG
CoS_06544_5	GACACGTGTTACCCCGGCCTAAGGGTAC
CoS_06544_6	GACACGTGCATGAACGACGAAGACAAGGTCC
CoS_06544_7	GTTAATTAATTA ACTCAAAGTCGGCCGTGTAC
CoS_06579_1	GCCCGGGTTCGTGTACGGAGGAACTG
CoS_06579_2	GCCCGGGTCATGACCCGTCAACCCCATC
CoS_06579_3	ATGTGACCCCTTCGCGGCCCTCTTCAT
CoS_06579_4	TGCGGCCGCTTAGGCCTTGGCGATTCTTCAC

Primer	Sequence
CoS_06871_1	GACATATGGGTTCTCGATCTGGACTCC
CoS_06871_2	GGAAATTCCTAGTTGTTCAAGTGGAAACCGGG
CoS_06871_3	ATCTAGAATGTCGGGATATCCTCAGCAAG
CoS_06871_4	CGGATCCGAAATGCCATCCTCCTTTTCAGCC
CoS_07622_2	GGAAATTCAGCGTCACCGCCAGTCCCTC
CoS_07622_3	GTGCGGCCGCTCACGAATAACTTTGGCCCCC
CoS_09492_1	GTATTTAAATTACCCTGGCAACCACTGCCCC
CoS_09492_2	GTGCGGCCGCTATTCTCATCCAGTGCCCC
CoS_09492_3	TCTCGAGCCCCATTGTTGAGCTTTGTCTTAG
CoS_09492_4	TGCGGCCGCTTAGGGTGGTGGTGTGAAGATTGC
CoS_09492_10	TCTCGAGCATTGTCAGCGAGTGGACCCTG
CoS_09492_11	TGCGGCCGCTTACCCATGTTTCCTCACCATCTC
CoS_09537_1	GGAAATTCGCCGGGCTTCGCGGACTCCT
CoS_09537_3	GTGCGGCCGCTAGTCATCCATTGGAGCGTCC
CoS_09537_4	ATGTCGACCCCAAGGTTGTGACCTACG
CoS_09537_5	TGCGGCCGCTTAGAAGATGGCATCCTTATGCG
CoS_10282_1	GTATTTAAATTAGATCACGGCAGCATCCGGATC
CoS_10282_2	GTGCGGCCGCTACTCCGCCAGCTTGGCGA
CoS_10282_3	TCTCGAGCACAGATAACTTGACGCAGGAG
CoS_10282_4	TGCGGCCGCTTACGGAATCTCGGGGGTGTGG
CoS_10647_1	GTCTCGAGCGCCCGAAAAGGCGTACCGCA
CoS_10647_2	GTAAAGCTTTTCAGTACAACAGCGTGATGGTC
CoS_10647_3	ATGTCGACCCCGCTCGTTGAGCAGACGC
CoS_10647_4	TGCGGCCGCTTAGAATAGCGCATACTCCTCCTC
CoS_myc9_1	TGGATGGAAGATCTATGAGAGGTGAAC
CoS_myc9_2	CTCTAAGGGCGGTTCTGATAC
CoS_Pgpd_1	AGCGGCCGCGAGCTCTGTACAGTGACCG
CoS_Pgpd_2	CTTCTGCTTGCCATGGTGTATGTCTGCTCAAG
CoS_Pgpd_3	AGGGCCCCGAGCTCTGTACAGTGACCG
CoS_Pgpd_4	CCTTGCTCACCATGGTGTATGTCTGCTCAAG
CoS_Rho1_1	GACATATGTCTGCTGAACTCCGCCGAAAG
CoS_Rho1_2	GGAAATTCCTAGACCGAGCTCTTGCTtAaGCCCTC
CoS_Rho1_5	CCTTAATTA ACTCTGCTGAACTCCGCCGAAAG
CoS_Rho1_6MCS	GGAAATTCACGTGAGATCTTAATTAATTAGACCGAGCTCTTGCA GAG
CoS_Rho1_9	GGAGATCTGCTGAACTCCGCCGAAAG
CoS_Rho1_10	CTGAATTCCTAGACCGAGCTCTTGCAAG
CoS_Rho1_11	GGTTAATTA ACTCTGCTGAACTCCGCCGAAAG
CoS_Rho1_12	GCTCTAGATTAGACCGAGCTCTTGCAAG
CoS_Rho1_13	GCACTCGGTGAATTCGAGAGTCATGTTCCGGGAG
CoS_Rho1_14	GTAGATCTGGCGTCCGTTTGGTGGTTG
CoS_Rho2_1	GACATATGGCATCAGGCAGCCCTCAG
CoS_Rho2_2	GGAAATTCATAGAATCACAgAGCtCCCGCTTC
CoS_Rho2_3	GGAGATCTGCATCAGGCAGCCCTCAG
CoS_Rho2_4	CTGAATTCATAGAATCACACAGCACCC
CoS_Rho2_5	GGTTAATTAACGCATCAGGCAGCCCTCAG
CoS_Rho2_6	GCTCTAGATCATAGAATCACACAGCACCC
CoS_Rho2_7	GACTAGTATGGCATCAGGCAGCCCTC
CoS_Rho2_8	GTTAATTAATCATAGAATCACACAGCACCC
CoS_Rho2_9	CGAATTCACCGTTACCTCTGGGAGTC
CoS_Rho2_10	CGGATCCTTTGGGTAATGGCTGTAAATATC
CoS_Rho2_DAfor	CATTATCGGCGACGtGCTTGCGGAAAAAC
CoS_Rho2_DArev	GTTTTCCGCAAGCgaCGTCGCCGATAATG

Primer	Sequence
CoS_YFP_1	GACATCACCATGGTGAGCAAGGGCGAGG
CoS_YFPC_1	GACATCACCATGGACAAGCAGAAGAACGGCATC
CoS_YFPC_2MCS	AGCGGCCGCGAGAATTCAGGCATTTAAATGCAGATCTCTTGAC AGCTCGTCCATGC
CS_NCU02689_1	CCTCGAGCGCCAGCTCAGACTACGGC
NV_00668_1	ACCCGGGGTCAAAATCAGGATGCCTCTGG
NV_00668_2	AGCGGCCGCTACGCATCCGCCAACTTTTTTC
NV_CDC24_5	CCCGTCCGACGCCGGGTTCTAAGATGACCCATC
NV_CDC24_6	CCCGCGGCCGCTCAAGCAACTGGGGCCGCTTGC
NV_lrg7	CAAGCGGCCGCTCATGCAGTGCCAGTAG
NV_NCU07688_2	CGCGGCCGCTTATTCTCAAAGATGAGCGCAC
NV_NCU07688_4	CGAATTCGAAGCCCCACTACTCTCTTC
NV_NCU07688_5	CGAATTCGATGACTATCTTGACGCCCC
pGADT7_adh1_as	CGGCGGTACCCAATTGACC
pGADT7_adh1_s	GTCCTGCAGGCAACTTCTTTTCTTTTTTTTTCTTTTC
pGBKT7_adh1_as	TCTTCTCGAGGAAAATCAGTAG
pGBKT7_adh1_s	GTCACTACGTGCAACTTCTTTTCTTTTTTTTTCTTTTC
Rac_3_Spe	GACTAGTGGATGAATGGATGCACTTCACAC
Rac_5_Bgl	GAAGATCTGCTGCTATCGGAGGCGTGCAGTC
Rho1_DN1	GTCTACGTCCCTACCGTTTTcattAAATACGTGCGCCGATGT
Rho1_DN2	AACCTCGACATCGGCGACGTAaTTaatGAAAACGGTAGGGA
Rho1_GV1	CGTCATCGTTGGCGAcGtcGCCTGCGGCAAGACC
Rho1_GV2	GGTCTTGCCGCAGGCgaCgTCGCCAACGATGACG
Rho2_DN1short	CCCCACCGTGTTcattAATTACGTTACCGACTGCC
Rho2_DN2short	GGCAGTCGGTAACGTAATTaatGAACACGGTGGGG
SB_cdc24_3_pacl	GCTTAATTAACTCCAACAGTTCCCCTTCGC
SB_cdc24_5_speI	GTA TAGTATGAGCCTGTCCAACGCCG
SB_cdc42_3_EcoRI	GTGAATTCTCACAGAATCAAGCACTTCTTG
SB_cdc42_5_BglII	CTAGATCTATGGTGACGGGA ACTATCAAG
SB_rac_3_EcoRI	CAGAATTCTTAGAGGATAGTGCACTTGGAC
SB_rac_5_BglII	CGAGATCTATGGCTGCTATCGGAGGCG

Table 2: Plasmids used in this study. Note that construction intermediates, i.e. DNA fragments inserted into pJet1.2 blunt (Fermentas GmbH, Germany) for subcloning and sequencing, are not listed. See text in ensuing sections for details. Amino acid (aa) positions indicated refer to annotation version .4 of Broad *Neurospora crassa* Database.

Plasmid	Short description	Reference/source
pBiFC	Fungal expression vector for N-terminal YFPC and C-terminal YFPN fusion proteins under control of P _{gpdA} or P _{ccg-1} , respectively; targeted to <i>his-3</i> locus	this study
pBiFC_00668	pBiFC; NCU00668	this study
pBiFC_Cdc42_Cdc24	pBiFC; <i>cdc-42</i> , <i>cdc-24</i>	this study
pBiFC_Rac_Cdc24	pBiFC; <i>rac</i> , <i>cdc-24</i>	this study
pBiFC_Rho1	pBiFC; <i>rho-1</i>	this study
pBiFC_Rho1_00668	pBiFC; <i>rho-1</i> , NCU00668	this study
pBiFC_Rho2	pBiFC; <i>rho-2</i>	this study
pBiFC_Rho2_00668	pBiFC; <i>rho-2</i> , NCU00668	this study
pBScpcmyc3hyg	pBScpcmyc3hyg_Cdc42 with insert removed	this study
pBScpcmyc3hyg_Cdc42	derived from pNV83, NCU01431 (<i>bni-1</i>) _{aa1-824} replaced by <i>cdc-42</i>	this study

Plasmid	Short description	Reference/source
pBSpcmyc3hyg_Rac	derived from pNV83, NCU01431 (<i>bni-1</i>) _{aa1-824} replaced by <i>rac</i>	this study
pCCG::C-Gly::3xFLAG	Fungal expression vector for C-terminal 3xFLAG fusion proteins under control of P _{ccg-1} ; targeted to <i>his-3</i> locus	(Honda and Selker, 2009)
pCCG_C_Gly_3xFLAG_01431	pCCG::C-Gly::3xFLAG; NCU01431 (<i>bni-1</i>)	this study
pCCG_C_Gly_3xFLAG_06871	pCCG::C-Gly::3xFLAG; NCU06871 (<i>gls-1</i>)	this study
pCCG::N-3xMyc	Fungal expression vector for N-terminal 3xmyc fusion proteins under control of P _{ccg-1} ; targeted to <i>his-3</i> locus	(Honda and Selker, 2009)
pCCG_N_3xMyc_Rho1	pCCG::N-3xMyc; <i>rho-1</i>	this study
pCCG_N_3xMyc_Rho2	pCCG::N-3xMyc; <i>rho-2</i>	this study
pCCG_N_12xMyc_Rho1	pCCG_N_3xMyc_Rho1, epitope tag extended to 12xmyc	this study
pCCG_N_12xMyc_Rho2	pCCG_N_3xMyc_Rho2, epitope tag extended to 12xmyc	this study
pCCG::N-GFP	Fungal expression vector for N-terminal GFP fusion proteins under control of P _{ccg-1} ; targeted to <i>his-3</i> locus	(Honda and Selker, 2009)
pCCG_N_GFP_Rho1	pCCG::N-GFP; <i>rho-1</i>	this study
pCCG_N_GFP_Rho2	pCCG::N-GFP; <i>rho-2</i>	this study
pCSN44	Plasmid carrying <i>hyg</i> ^R cassette (<i>hph</i> ^R under control of <i>Aspergillus</i> P _{trpC} and t _{trpC})	(Staben et al., 1989)
pEHN1-nat	fungal expression vector carrying the <i>egfp</i> gene under control of P _{gpdA} and t _{trpC} ; contains <i>nat1</i> gene	(Dreyer et al., 2007), kind gift of S. Pöggeler
pETM30	<i>E. coli</i> expression plasmid for N-terminal GST fusion proteins	Protein Expression and Purification Core Facility, EMBL, Germany
pETM30_00668DEP	pETM-30; NCU00668 _{aa366-510} cDNA	this study
pFLAGN1	Fungal expression vector for N-terminal 3xFLAG fusion proteins under control of P _{ccg-1} ; targeted to <i>his-3</i> locus	(Kawabata and Inoue, 2007)
pFLAGN1_00668	pFLAGN1; NCU00668	this study
pFLAGN1_06544	pFLAGN1; NCU06544 (<i>pkc-1</i>)	this study
pGADT7	Yeast two-hybrid vector for expression of N-terminal GAL4 activation domain fusion proteins under control of full-length P _{ADH1} ; carrying <i>LEU2</i>	Clontech, USA
pGADT7_06544	pGADT7; NCU06544 (<i>pkc-1</i>) cDNA	this study
pGADT7_06871icd	pGADT7; NCU06871 (<i>gls-1</i>) _{aa762-1352} cDNA	this study
pGADT7-T	pGADT7; SV40 largeT- antigen _{aa86-708} cDNA	Clontech, USA
pGADT7adh1sht	pGADT7 with truncated P _{ADH1}	this study

Plasmid	Short description	Reference/source
pGADT7adh1sht_00668DGC	pGADT7adh1sht; NCU00668 _{aa366-1251} cDNA	this study
pGADT7adh1sht_00668GC	pGADT7adh1sht; NCU00668 _{aa517-1251} cDNA	this study
pGADT7adh1sht_00668GEF	pGADT7adh1sht; NCU00668 _{aa517-928} cDNA	this study
pGADT7adh1sht_01431N	pGADT7adh1sht; NCU01431 (<i>bni-1</i>) _{aa2-824} cDNA	this study
pGADT7adh1sht_06544	pGADT7adh1sht; NCU06544 (<i>pkc-1</i>) cDNA	this study
pGADT7adh1sht_06544N	pGADT7adh1sht; NCU06544 (<i>pkc-1</i>) _{aa2-612} cDNA	this study
pGADT7adh1sht_06871icd	pGADT7adh1sht; NCU06871 (<i>gls-1</i>) _{aa762-1352} cDNA	this study
pGADT7adh1sht_T	pGADT7adh1sht; SV40 largeT-antigen _{aa86-708} cDNA	this study
pGADT7Rec-ΔN-RanBPM	pGADT7Rec; murine RanBPM _{aa51-654} cDNA	(Tucker et al., 2009), kind gift of S. Pöggeler
pGBKT7	Yeast two-hybrid vector for expression of N-terminal GAL4 DNA binding domain fusion proteins under control of truncated P _{ADH1} ; carrying <i>TRP1</i>	Clontech, USA
pGBKT7-53	pGBKT7; murine p53 _{aa72-390} cDNA	Clontech, USA
pGBKT7-Lam	pGBKT7; human lamin C cDNA	Clontech, USA
pGBKT7adh1sht	pGBKT7 with truncated P _{ADH1}	this study
pGBKT7adh1sht_p53	pGBKT7adh1sht; murine p53 _{aa72-390} cDNA	this study
pGBKT7adh1sht_Rho1DA	pGBKT7adh1sht; <i>rho-1</i> _{G15V,C191S} cDNA	this study
pGBKT7adh1sht_Rho1DN	pGBKT7adh1sht; <i>rho-1</i> _{E41I,C191S} cDNA	this study
pGBKT7adh1sht_Rho2DA	pGBKT7adh1sht; <i>rho-2</i> _{G20V,CC196/197SS} cDNA	this study
pGBKT7adh1sht_Rho2DN	pGBKT7adh1sht; <i>rho-2</i> _{E46I,CC196/197SS} cDNA	this study
pHAN1	Fungal expression vector for N-terminal HA fusion proteins under control of P _{ccg-1} ; targeted to <i>his-3</i> locus	(Kawabata and Inoue, 2007)
pHAN1_Rho1	pHAN1; <i>rho-1</i>	this study
pHAN1_Rho2	pHAN1; <i>rho-2</i>	this study
pJet1.2 blunt	vector for subcloning of PCR fragments	Fermentas GmbH, Germany
pJV_16_2_1	Fungal expression vector carrying <i>mCherry</i> and <i>gfp</i> under control of P _{ccg-1} ; targeted to <i>his-3</i> locus	kind gift of M. Riquelme
pJV16_Rho1MCS	pJV_16_2_1 with <i>gfp</i> replaced by <i>rho-1</i> -multiple cloning site; for expression of mCherry-RHO1	this study
pMalc2xL_Cdc42	pNV72; <i>cdc-42</i> cDNA	(Vogt, 2008)
pMalc2xL_Rac	pNV72; <i>rac</i> cDNA	(Vogt, 2008)
pMalc2xL_Rho1	pNV72; <i>rho-1</i> cDNA	(Vogt, 2008)
pMalc2xL_Rho2	pNV72; <i>rho-2</i> cDNA	(Vogt, 2008)

Plasmid	Short description	Reference/source
pMalc2xL_Rho3	pNV72; <i>rho-3</i> cDNA	(Vogt, 2008)
pMalc2xL_Rho4	pNV72; <i>rho-4</i> cDNA	(Vogt, 2008)
pMalc2xL_00196GAP	pNV72; NCU00196 _{aa224-455} cDNA	this study
pMalc2xL_00553GAP	pNV72; NCU00553 _{aa531-742} cDNA	this study
pMalc2xL_00668DEP	pNV72; NCU00668 _{aa366-510} cDNA	this study
pMalc2xL_00668DGC	pNV72; NCU00668 _{aa366-1251} cDNA	this study
pMalc2xL_00668GC	pNV72; NCU00668 _{aa517-1251} cDNA	this study
pMalc2xL_00668GEF	pNV72; NCU00668 _{aa517-928} cDNA	this study
pMalc2xL_01472GAP	pNV72; NCU01472 _{aa88-308} cDNA	this study
pMalc2xL_02524GAP	pNV72; NCU02524 _{aa1120-1317} cDNA	this study
pMalc2xL_02764GEF	pNV72; NCU02764 _{aa244-626} cDNA	this study
pMalc2xL_02764GEFonly	pNV72; NCU02764 _{aa244-530} cDNA	this study
pMalc2xL_02915GAP	pNV72; NCU02915 _{aa441-678} cDNA	this study
pMalc2xL_07622GAP	pNV72; NCU07622 _{aa110-626} cDNA	this study
pMalc2xL_07688GAP	pNV72; NCU07688 _{aa972-1169} cDNA	this study
pMalc2xL_09492DHR	pNV72; NCU09492 _{aa1290-1846} cDNA	this study
pMalc2xL_09492DHRsht	pNV72; NCU09492 _{aa1314-1824} cDNA	this study
pMalc2xL_09537GAP	pNV72; NCU09537 _{aa453-669} cDNA	this study
pMalc2xL_10282GEFBAR	pNV72; NCU10282 _{aa1425-1911} cDNA	this study
pMalc2xL_10647GAP	pNV72; NCU10647 _{aa369-572} cDNA	this study
pMalc2xL_BUD3GEF	pNV72; <i>bud-3</i> _{aa230-637} cDNA	this study
pMalc2xL_CDC24GEFPH	pNV72; <i>cdc-24</i> _{aa204-544} cDNA	(Vogt, 2008)
pMalc2xL_CDC24GEFPH(10-19)	pNV72; <i>cdc-24</i> _{aa204-544} cDNA derived from <i>cdc-24</i> (10-19)	this study
pMalc2xL_CDC24GEFPH(19-3)	pNV72; <i>cdc-24</i> _{aa204-544} cDNA derived from <i>cdc-24</i> (19-3)	this study
pMalc2xL_CDC24GEFPH(24-21)	pNV72; <i>cdc-24</i> _{aa204-544} cDNA derived from <i>cdc-24</i> (24-21)	this study
pME2865	Yeast expression vector carrying 9xmyc and <i>PCL5</i>	(Bömeke et al., 2006), kind gift of G. Braus
pMF272	Fungal expression vector for C-terminal GFP fusion proteins under control of P_{ccg-1} ; targeted to <i>his-3</i> locus	(Freitag et al., 2004)
pMF272_00668	pMF272; NCU00668	this study
pMF272_Cdc24	pMF272; <i>cdc-24</i>	this study
pNV28	pETM30; <i>rho-1</i> cDNA	(Vogt, 2008)
pNV29	pETM30; <i>rho-2</i> cDNA	(Vogt, 2008)
pNV33	pETM30; <i>cdc-42</i> cDNA	(Vogt, 2008)
pNV70	pNV72; <i>lrg-1</i> _{aa650-1035} cDNA	(Vogt, 2008)
pNV72	<i>E. coli</i> expression plasmid for N-terminal MBP (MalE) fusion proteins	(Vogt, 2008)
pNV83	Fungal expression vector; pBluescript SK+ carrying <i>hyg</i> ^R cassette, P_{opc-1} 3xmyc-NCU01431 (<i>bni-1</i>) _{aa1-824}	(Vogt, 2008)
pPgpd_YFP	Fungal expression vector for N-terminal YFP fusion proteins under control of P_{gpdA} ; targeted to <i>his-3</i> locus	this study
pPgpdYFP_Cdc42	pPgpd_YFP; <i>cdc-42</i>	this study
pPgpdYFP_Rac	pPgpd_YFP; <i>rac</i>	this study

Plasmid	Short description	Reference/source
pPgpdYFP_Rho1	pPgpd_YFP; <i>rho-1</i>	this study
pPgpdYFP_Rho2	pPgpd_YFP; <i>rho-2</i>	this study
ppRho1_N_GFP_Rho1	pCCG_N_GFP_Rho1 with <i>his-3</i> flank and P _{<i>ccg-1</i>} replaced by <i>rho-1</i> 5' UTR; EcoRI/NotI fragment targeted to <i>rho-1</i> locus for expression of GFP-RHO1 under control of endogenous promoter	this study
ppRho2_N_GFP_Rho2	pCCG_N_GFP_Rho2 with P _{<i>ccg-1</i>} replaced by <i>rho-2</i> 5' UTR; EcoRI/NotI fragment targeted to <i>rho-2</i> locus for expression of GFP-RHO2 under control of endogenous promoter	this study
pYFP	Fungal expression vector for C-terminal YFP fusion proteins under control of P _{<i>ccg-1</i>} ; targeted to <i>his-3</i> locus	(Bardiya et al., 2008)
pYFP_00668	pYFP; NCU00668	this study
pYFP_Cdc24	pYFP; <i>cdc-24</i>	this study
pYFPC	Fungal expression vector for C-terminal YFPC fusion proteins under control of P _{<i>ccg-1</i>} ; targeted to <i>his-3</i> locus	(Bardiya et al., 2008)
pYFPN	Fungal expression vector for C-terminal YFPN fusion proteins under control of P _{<i>ccg-1</i>} ; targeted to <i>his-3</i> locus	(Bardiya et al., 2008)

4.4.2 Full-length cDNA constructs of putative RhoGEFs and RhoGAPs

Full-length cDNA (excluding translation start codon; based on Broad *Neurospora crassa* Database (assembly 7, version .3 annotation) of selected *N. crassa* putative Rho regulators was amplified from reaction products of reverse transcriptions (see section 4.6.2) and inserted into pJet1.2blunt (Fermentas GmbH, Germany) for sequencing and further cloning projects. The following primer pairs (5-digit numbers in middle of primer names give NCU number of the amplified genes) were used: CoS_00668_3/NV_00668_2; CoS_02764_1/_3; CoS_06579_1/_2; CoS_09492_1/_2; CoS_10282_1/_2; CoS_00196_1/_2; CoS_00553_1/_2; CoS_01472_1/_2; CoS_02524_1/_3; CS_NCU02689_1/NV_lrg7; CoS_02915_1/_3; CoS_07622_2/_3; NV_NCU07688_5/_2; CoS_09537_1/_3; CoS_10647_1/_2.

Details on cDNA sequencing results can be found in Supplementary Table 1 (p.104).

4.4.3 Plasmids encoding MBP- and GST-tagged RhoGEF constructs

cDNA encoding RhoGEF domains and/or other conserved domains of *N. crassa* putative Rho regulators was amplified from the full-length cDNA constructs described in the previous section or directly from reaction products of reverse transcriptions (see section 4.6.2). For convenience, amino acid (aa) positions given in the following outline refer to the current annotation version .4 of the Broad *Neurospora crassa* Database (see Supplementary Table 1, p.104) for further details on cDNA annotation versions). cDNA was inserted into plasmids pNV72 or pETM30 to create vectors for expression of N-terminally tagged MBP or GST fusion proteins, respectively, by *E. coli*.

cDNA fragments for NCU00668DGC constructs (DEP-GEF-CNH domains; aa 366-1251, i.e. end) were amplified using primers NV_00668_1/_2, cut with SmaI/NotI and inserted into pNV72 opened with PmlI/NotI, creating pMalc2xL_00668DGC. For generation of NCU00668GC constructs (GEF-CNH domains; aa 517-1251, i.e. end) and NCU00668GEF constructs (GEF domain, aa 517-928), primer combinations CoS_00668_6/_7 or CoS_00668_6/_8, respectively, were used. Inserts were released from subcloning vectors by digestion with SmaI/BamHI and ligated with pNV72 opened with BamHI/Ecl136II to create pMalc2xL_00668GC and pMalc2xL_00668GEF, respectively. For generation of NCU00668DEP domain constructs (DEP domain; aa 366-510), primer pairs NV_00668_1/CoS_00668_11 or CoS_00668_12/_11, respectively, were used in cDNA amplification. Fragment ends were made compatible for insertion into pNV72 via PmlI/NotI sites or pETM30 via NcoI/NotI sites by digestion with SmaI/NotI or NcoI/NotI, respectively. Resulting plasmids were named pMalc2xL_00668DEP and pETM30_00668DEP.

The longer and shorter cDNA constructs encoding the putative RhoGEF domain of NCU02764 (aa 244-626 or 244-530, respectively), were generated by PCR with primers CoS_02764_3/_4 or CoS_02764_3/_7, respectively. They were inserted into pNV72 using Sall/NotI restriction sites present both in insert and vector, resulting in plasmids pMalc2xL_02764GEF and pMalc2xL_02764GEFonly, respectively.

cDNA encoding wildtype and mutant versions of RhoGEF and PH domain regions of CDC24 (NCU06067; aa 204-544) were amplified from the respective templates using primers NV_CDC24_5/_6. Sall/NotI sites were used for ligation with pNV72 to produce pMalc2xL_CDC24GEFPH and its respective mutant analogues.

The NCU06759 (*bud-3*) cDNA construct intended for expression of the RhoGEF domain (aa 230-637) was amplified using primers CoS_06579_3,_4 and inserted into pNV72 via Sall/NotI sites, thereby creating pMalc2xL_BUD3GEF.

For generation of two cDNA fragment variants encoding the DHR-2 (or Docker) domain of NCU09492 (aa 1290-1846 or aa 1314-1824), primer combinations CoS_09492_3/_4 or CoS_09492_10/_11 were used. Inserts were released after subcloning using XhoI/NotI and ligated with pNV72 opened at Sall/NotI sites, giving rise to pMalc2xL_09492DHR and pMalc2xL_09492DHRsht, respectively.

The same restriction and ligation scheme was used for creation of pMalc2xL_10282GEFBAR following amplification of cDNA encoding GEF and BAR domains of NCU10282 (aa 1425-1911) using primers CoS_10282_3/_4

4.4.4 Plasmids encoding MBP-tagged GAP constructs

Plasmids intended for expression of MBP-tagged *N. crassa* RhoGAP domain constructs in *E. coli* were generated in analogy with the GEF constructs (see previous section for general remarks applying). For all candidate RhoGAP genes only the cDNA region encoding the predicted Rho GAP domain was amplified.

cDNA encoding the GAP domain of NCU00196 (aa 224-455) was amplified using primers CoS_00196_3/_4, cut with XhoI/NotI and ligated with pNV72 cleaved with Sall/NotI, resulting in pMalc2xL_00196GAP.

For generation of pMalc2xL_00553GAP, the cDNA fragment encoding the GAP domain of NCU00553 (aa 531-742, i.e. end) was released from the respective full-length cDNA

intermediate (see section 4.4.2) using Sall/NotI making use of the internal Sall site present in the cDNA. Sall and NotI were also used to open pNV72, and fragments were ligated.

cDNA fragments encoding the GAP domains of NCU01472 (aa 88-308), NCU02524 (aa 1120-1317), NCU02915 (aa 441-678, i.e. end), NCU09537 (aa 453-669) and NCU10647 (aa 369-572) were generated by PCR with primer pairs CoS_01472_3/_4, CoS_02524_3b/_4, CoS_02915_4/_3, CoS_09537_4/_5 or CoS_10647_3/_4, respectively and inserted into pNV72 via Sall/NotI restriction sites. The plasmids created in this way were named pMalc2xL_01472GAP, pMalc2xL_02524GAP, pMalc2xL_09537GAP and pMalc2xL_10647GAP, respectively.

In case of NCU07622, presumed full-length cDNA was cleaved from the respective intermediate vector (see section 4.4.2) using EcoRI/NotI and transferred to pNV72 cut with the same enzymes. Due to changes in annotation (see Supplementary Table 1, p.104), however, the resulting plasmid is thought to encode only a part of the protein (aa 110-626, i.e. end) completely covering the predicted RhoGAP domain

EcoRI and NotI restriction sites in both insert and vector were also used for generation of pMalc2xL_07688GAP; the cDNA fragment encoding the RhoGAP domain (aa 972-1169, i.e. end) of the protein was amplified using primers NV_NCU07688_4/_2.

4.4.5 Plasmids for yeast two-hybrid analyses

Routinely, *N. crassa* cDNA for plasmids used in yeast two-hybrid analyses was amplified from reaction products of reverse transcriptions (see section 4.6.2). For convenience, aa positions given in the description below refer to the current annotation version .4 of the Broad *Neurospora crassa* Database; *Neurospora* constructs denominated as “full-length” generally lack the start codon (or first aa, respectively), to safeguard exclusive translation from the start codon giving rise to the N-terminally tagged fusion protein.

Proteins whose interaction was to be tested in this study were expressed as fusion proteins with SV40 NLS (nuclear localization signal)-GAL4 activation domain or GAL4 DNA binding domain from pGADT7, pGBKT7 (both from Clontech, USA) or two derivatives thereof which were created with the intention to decrease expression levels of fusion proteins.

pGADT7adh1sht was generated by replacing the full-length *S. cerevisiae ADH1* promoter of pGADT7 by a truncated version (410bp), which is identical to that controlling fusion protein expression in pGBT9 (Clontech, USA) and expected to result in low expression (see (Ammerer, 1983; Ruohonen et al., 1991, 1995) and unpublished data obtained at Clontech Laboratories presented at <http://www.clontech.com/images/pt/PT3024-1.pdf> for a detailed comparison of promoter versions and expression strength). To this end, a DNA fragment spanning the desired length of the promoter and part of the SV40 NLS feature was amplified from pGADT7 using primers pGADT7_adh1_s/_as, cut with SdaI/KpnI and inserted into pGADT7 from which the full-length *ADH1* promoter and part of SV40 NLS had been excised by digestion with the same enzymes.

In analogy, pGBKT7adh1sht was created by replacing the truncated *S. cerevisiae ADH1* promoter of pGBKT7 by that present in pGBT9 (Clontech, USA). Using pGBKT7 as a template, a DNA fragment ranging from the desired start of the shorter promoter into the GAL4 DNA binding domain feature was amplified with primers pGBKT7_adh1_s/_as,

cleaved with DralIII/XhoI and substituted for the DralIII/XhoI fragment released from pGBKT7. Note that, in contrast to pGBKT7, the new vector contains a truncated f1 ori only.

Positive control plasmids for the newly created vector pair offering low expression were created in the following way: cDNA encoding part of SV40 large T antigen was released from control plasmid pGADT7-T (Clontech, USA) and inserted into pGADT7adh1sht via EcoRI/XhoI, generating pGADT7adh1sht_T; similarly, cDNA encoding part of murine p53 was transferred from pGBKT7-53 (Clontech, USA) into pGBKT7adh1sht using EcoRI/BamHI to produce pGBKT7adh1sht_p53.

The 5' part of NCU01431 (*bni-1* or *sepA*) is predicted to lack any introns, so the region encoding aa 2-824 (comprising predicted GTPase binding/FH3 (formin homology 3) domains) was amplified from genomic DNA using primers CoS_01431_1/_9. The fragment was digested with Eco72I/SfiI and inserted into pGADT7adh1sht opened with SfiI/SmaI, giving rise to pGADT7adh1sht_01431N.

Full-length NCU06544 (*pkc-1*) cDNA was amplified using primers CoS_06544_1/_2, cleaved with Eco72I/SfiI and inserted into pGADT7 or pGADT7adh1sht opened with SmaI/SfiI to produce pGADT7_06544 or pGADT7adh1sht_06544, respectively. Primers CoS_06544_1/_5 were used for amplification of cDNA encoding the N-terminal part of NCU06544 (aa 2-612; covering C2 domain, HR1 repeats and C1 phorbol ester/diacylglycerol binding domain, but excluding catalytic domain). The fragment was ligated with pGADT7adh1sht as described for the full-length construct, creating pGADT7adh1sht_06544N.

For NCU06871 (GLS1), cDNA encoding the largest intracellular domain (aa 762-1352; as predicted consistently by membrane protein topology prediction programs SOSUI, TMpred and TopPred (see section 4.10.1) as of December 2008; the region coincides largely with the predicted glucan synthase domain covering aa 857-1691) was amplified with primer pair CoS_06871_1/_2 and inserted into pGADT7 or pGADT7adh1sht via EcoRI/NdeI, generating pGADT7_06871icd and pGADT7adh1sht_06871icd.

Expression plasmids employed in yeast two-hybrid assays encoded the same regions of NCU00668 as the corresponding pMalc2xL vectors (see section 4.4.3). While NCU00668DGC cDNA had to be amplified anew using primers CoS_00668_5/_7, cDNA for NCU00668GC and NCU00668GEF constructs could be used from the respective amplification reactions described in section 4.4.3. Each of the three cDNA fragments was inserted into pGADT7adh1sht via SmaI/BamHI sites, resulting in plasmids pGADT7adh1sht_00668DGC, pGADT7adh1sht_00668GC or pGADT7adh1sht_00668GEF, respectively.

The Rho GTPase constructs used for two-hybrid tests are presumed to represent dominant active (DA) or negative (DN) forms of the proteins; additionally, their putative C-terminal prenylation motif was destroyed by mutation to prevent interference with NLS-mediated nuclear localization of interacting protein pairs, which is required for reporter gene activation and thus efficient readout of interaction in the test.

Fusion PCRs were employed to create *rho-1* (NCU01484) or *rho-2* (NCU08683) cDNA constructs containing the desired mutations leading to amino acid substitutions G15V,C191S for RHO1DA, E41I,C191S for RHO1DN, G20V,CC196/197SS for RHO2DA and E46I,CC196,197SS for RHO2DN. pNV28 or pNV29 (Vogt, 2008) served as templates for

rho-1 or *rho-2* constructs, respectively. Primer combinations used to insert the desired mutations in the first rounds of PCR were CoS_Rho1_1/Rho1_GV2 and Rho1_GV1/CoS_Rho1_2 (for RHO1DA), CoS_Rho1_1/Rho1_DN2 and Rho1_DN1/CoS_Rho1_2 (for RHO1DN), CoS_Rho2_1/CoS_Rho2_DAreV and CoS_Rho2_DAFOR/CoS_Rho2_2 (for RHO2DA) and finally CoS_Rho2_1/Rho2_DN2short and Rho2_DN1short/CoS_Rho2_2 (for RHO2DN). Reaction products of the first round of amplifications were fused to give the desired full-length cDNAs in a subsequent round of PCRs employing the outer primer pairs CoS_Rho1_1/2 and CoS_Rho2_1/2 (for *rho-1* and *rho-2* constructs, respectively). The resulting DNA fragments were cleaved with EcoRI/NdeI and ligated with pGBKT7adh1sht opened accordingly, thus producing pGBKT7adh1sht_Rho1DA, pGBKT7adh1sht_Rho1DN, pGBKT7adh1sht_Rho2DA and pGBKT7adh1sht_Rho2DN.

4.4.6 Plasmids for analysis of subcellular fusion protein localization

pPgpd_YFP was designed to allow expression of N-terminally yellow fluorescent protein (YFP)-tagged proteins under the control of the *A. nidulans gpdA* promoter. The promoter was amplified from plasmid pEHN1-nat ((Dreyer et al., 2007); kindly provided by S. Pöggeler, Germany) using primers CoS_Pgpd_3/4, while *yfp* was amplified from pYFP (Bardiya et al., 2008) using primers CoS_YFP_1/CoS_YFPC_2MCS (the latter omitting the stop codon and attaching a multiple cloning site of BglII/SmaI/EcoRI/NotI to the end of the fragment). The two fragments were subjected to fusion PCR with primer pair CoS_Pgpd_3/CoS_YFPC_2MCS. The resulting amplification product was cleaved with ApaI/NotI and inserted into pYFP from which the *ccg-1* promoter and *yfp* gene had been released by digestion with the same enzymes.

pBiFC (see Supplementary Figure 16, p.119 for a map) was created as a tool for testing protein interaction *in vivo* by bimolecular fluorescence complementation (BiFC). With the help of this plasmid, which is targeted to the *his-3* locus via homologous recombination, all features required for expression of two proteins whose interaction is to be tested (one being N-terminally, the other C-terminally tagged) can be expressed from the same vector under the control of the *A. nidulans gpdA* promoter and the *N. crassa ccg-1* promoter, respectively. The plasmid is derived from the BiFC vector system consisting of pYFPN and pYFPC (Bardiya et al., 2008). In analogy to the construction of pPgpdYFP, the *gpdA* promoter was amplified from pEHN1-nat using primers CoS_Pgpd_1/2, while the portion of *yfp* encoding the C-terminal part of YFP, *yfpc*, was amplified from pYFPC using primers CoS_YFPC_1/CoS_YFPC_2MCS (the first introducing a start codon, the latter omitting the stop codon and attaching a multiple cloning site; see preceding paragraph). Both fragments were fused in a subsequent PCR with primers CoS_Pgpd_1/CoS_YFPC_2MCS. The resulting reaction product was cleaved with NotI, inserted at the corresponding site of pYFPN and its orientation determined, by analytical PCR with suitable primers, as opposing that of the other expression cassette (*ccg-1* promoter - multiple cloning site - *yfpn*) present in the vector.

For creation of plasmids allowing expression of N-terminally green fluorescent protein (GFP)-tagged RHO1 and RHO2 proteins, the corresponding coding regions were amplified from genomic DNA using primers CoS_Rho1_11/12 or CoS_Rho2_5/6, respectively and inserted into pCCG::N-GFP (Honda and Selker, 2009) via PstI/XbaI sites present both at insert termini and in the vector. Resulting plasmids pCCG_N_GFP_Rho1 and pCCG_N_GFP_Rho2 were routinely prepared for use in electroporation of *N. crassa* by linearization with NdeI or XmaJI, respectively.

Plasmid ppRho1_N_GFP_Rho1 was devised for homologous recombination-mediated N-terminal GFP-tagging of RHO1 expressed from the endogenous locus. Part of the *rho-1* 5'UTR (untranslated region) was amplified from genomic DNA using primers CoS_Rho1_13/_14, cleaved with *Adel*/*Bgl*III and used to replace the *Adel*/*Bam*HI fragment of pCCG_N-GFP_Rho1 containing the *his-3* flank and *ccg-1* promoter of the vector. In electroporation of *N. crassa*, an *Eco*RI/*Not*I fragment comprising the *rho-1* 5'UTR and *gfp-rho-1* was cotransformed with pCSN44.

Analogously, ppRho2_N_GFP_Rho2 was derived from pCCG_N_GFP_Rho2 by removing the *ccg-1* promoter by *Eco*RI/*Bam*HI digestion and inserting the partial *rho-2* 5'UTR fragment amplified from genomic DNA using primers CoS_Rho2_9/_10 and restricted correspondingly. An *Eco*RI/*Not*I fragment spanning *rho-2* 5'UTR and *gfp-rho-2* was used for cotransformation with pCSN44.

For expression of RHO1 fused to an N-terminal mCherry-tag, plasmid pJV16_Rho1MCS was conceived. The *rho-1* genomic sequence was amplified with primers CoS_Rho1_5/_6MCS (the latter of which attaches a multiple cloning site containing *Pac*I/*Bgl*III/*Eco*72I/*Eco*RI sites to the end of the construct, thus enabling further general use of the plasmid as explicated below), subjected to incomplete digestion with *Pac*I/*Eco*RI (sparing the 3'-terminal *Pac*I site) and used to replace the *gfp*-containing *Pac*I/*Eco*RI fragment of pJV_16_2_1 (kindly provided by M. Riquelme, Mexico). Note that by removal of the *rho-1* insert after restriction with *Pac*I and subsequent vector religation, a plasmid apt for expression of many other mCherry-tagged proteins could easily be generated.

For expression of Rho GTPases tagged with YFP at their N-termini, *rho-1* and *rho-2* were amplified from genomic DNA using primers CoS_Rho1_9/_10 or CoS_Rho2_3/_4 and inserted into pPgpYFP via *Bgl*III/*Eco*RI sites. For transformation by electroporation, the resulting plasmids pPgpYFP_Rho1 and pPgpYFP_Rho2 were linearized with *Hind*III. pPgpYFP_Rac and pPgpYFP_Cdc42 were generated analogously after amplification of *rac* (NCU02160) and *cdc-42* (NCU06454) using primer combinations SB_rac_5_BglIII/SB_rac_3_EcoRI and SB_cdc42_5_BglIII/SB_cdc42_3_EcoRI, respectively.

Genomic DNA encoding NCU00668 was amplified using primers CoS_00668_9/_10 (the latter omitting the stop codon) and inserted into pMF272 (Freitag et al., 2004) and pYFP via *Spe*I/*Pac*I sites to create pMF272_00668 and pYFP_00668 intended for expression of C-terminally GFP- or YFP-tagged versions, respectively, of the putative RhoGEF protein. The plasmids were linearized with *Xma*JI or *Adel*, respectively, for use in electroporation.

Vectors for expression of C-terminally GFP- or YFP-tagged fusion proteins of the putative RhoGEF CDC24 (NCU06067) were created by amplifying the genomic sequence of *cdc-24* using primers SB_cdc24_5_speI/SB_cdc24_3_pacI (the latter omitting the stop codon). The amplification product was cleaved with *Spe*I/*Pac*I and ligated with pMF272 and pYFP opened with the same enzymes, thus giving rise to plasmids pMF272_Cdc24 and pYFP_Cdc24, respectively.

In preparation of BiFC analysis to test *in vivo* interactions of RHO1 or RHO2 with NCU00668 and of RAC or CDC42 with CDC24, the corresponding combinations of genes were introduced into pBiFC to produce vectors for expression of N-terminally YFP-tagged Rho proteins and C-terminally YFP-tagged RhoGEF proteins under control of the *gpdA* or the *ccg-1* promoter, respectively. As controls for specificity of potential interactions, vectors containing only one of the two genes were also generated in parallel. Genomic amplification

products used for plasmid construction were identical to those used for creation of pPgpYFP or pYFP plasmids containing the respective DNA fragments (see above); GEF encoding DNA fragments were introduced via *SpeI/PacI* first, followed by insertion of GTPase encoding fragments at *BglII/EcoRI* sites. Resulting plasmids were named pBiFC_Rho1_00668 (for electroporation linearized with *Adel*), pBiFC_Rho2_00668 (devoid of unique restriction sites for linearization for electroporation), pBiFC_Rho1 (linearized with *NdeI*), pBiFC_Rho2 (linearized with *Paul*), pBiFC_00668 (linearized with *Adel*), pBiFC_Rac_Cdc24 and pBiFC_Cdc42_Cdc24 (both linearized with *SspI*), respectively.)

4.4.7 Plasmids for overexpression of epitope-tagged fusion proteins for phenotypic rescue and coimmunoprecipitation experiments

To create vectors for expression of 3xmyc-tagged RAC and CDC42 in phenotypic rescue experiments, the corresponding coding regions and part of their 3'UTRs were amplified from genomic DNA using primers *Rac_5_Bgl/Rac_3_Spe* and *Cdc42_5_Bgl/Cdc42_3_Spe*. Resulting DNA fragments were cleaved with *BglII/SpeI* and ligated with pNV83 (Vogt, 2008) from which the insert had been removed accordingly, thus yielding pBScpcmyc3hyg_Rac and pBScpcmyc3hyg_Cdc42, respectively. As a control, pBScpcmyc3hyg was created by removing the *cdc-42* insert from pBScpcmyc3hyg_Cdc42 by digestion with *BglII/SpeI*, digesting single-stranded restriction overhangs at the vector ends with Mung Bean Nuclease (see section 4.6.5) and subsequent religation. For electroporations, plasmids were linearized with *PsiI*.

N-terminally HA-tagged versions of RHO1 and RHO2 were expressed from pHAN1_Rho1 and pHAN1_Rho2, respectively. The first of these was kindly provided by Y. Heilig (University of Göttingen, Germany) and contained *rho-1* inserted into pHAN1 (Kawabata and Inoue, 2007). The latter was created similarly by amplifying *rho-2* from genomic DNA using primers *CoS_Rho2_7/_8* and inserting the resulting fragment into pHAN1 via *SpeI/PacI* sites. For electroporation, plasmids were digested with *SspI* or *Paul*, respectively.

For creation of plasmids encoding N-terminally 3xmyc-tagged RHO1 or RHO2 proteins, the *rho-1* and *rho-2* constructs originally amplified for insertion into pCCG::N-GFP (see section 4.4.6) were used and ligated with pCCG::N-3xMyc (Honda and Selker, 2009) via *PacI/XbaI* sites. The plasmids thus generated were named pCCG_N_3xMyc_Rho1 and pCCG_N_3xMyc_Rho2 and prepared for transformation by electroporation by digestion with *SspI* or *XmaJI*, respectively.

In an attempt to improve immunological detection of the fusion proteins, the 3xmyc epitope tag encoded by these two plasmids was expanded to a 12xmyc tag. For this, a DNA fragment encoding a 9xmyc tag was amplified from pME2865 ((Bömeke et al., 2006); kindly provided by G. Braus, Germany) using primers *CoS_myc9_1/_2* (the first one introducing a start codon), released from the subcloning vector by digestion with *BglII* and inserted into the two vectors at their respective *BamHI* sites, yielding plasmids pCCG_N_12xMyc_Rho1 and pCCG_N_12xMyc_Rho2, respectively. Desired orientation of the insert was verified by DNA sequencing. For electroporation, plasmids were digested with *SspI* or *XmaJI*, respectively.

To create plasmids for expression of N-terminally 3xFLAG-tagged NCU00668 and NCU06544 (PKC1) fusion proteins, the corresponding coding sequences were amplified from genomic DNA using primers *CoS_00668_13/_14* and *CoS_06544_6/_7*, respectively. Resulting DNA fragments were cleaved with *Eco72I/PacI* and ligated with pFLAGN1 (Kawabata and Inoue, 2007) opened with *SmaI/PacI*, thus generating pFLAGN1_00668 and

pFLAGN1_06544, respectively. For transformation by electroporation, the plasmids were linearized with *Adel* or *SspI*, respectively.

NCU06871 (GLS1) and NCU01431 (BNI1/SEPA) were expressed as C-terminally 3xFLAG-tagged fusion proteins from vectors pCCG_C_Gly_3xFLAG_06871 and pCCG_C_Gly_3xFLAG_01431, respectively. For creation of these plasmids, the corresponding coding regions were amplified from genomic DNA (omitting stop codons) using primer pairs CoS_06871_3/_4 and CoS_01431_11/_12. NCU06871 was inserted into pCCG::C-Gly::3xFLAG (Honda and Selker, 2009) via *XbaI*/*BamHI* sites, while insertion of NCU01431 was via *PacI*/*SpeI* sites. For linearization of both plasmids *NdeI* was employed.

4.5 Strains

N. crassa strains used in this work are summarized in Table 3. As indicated, several strains used in this study were obtained from the Fungal Genetics Stock Center (FGSC) at the University of Missouri, USA.

The single deletion strains used had been generated within the framework of the *Neurospora* genome project hosted at Dartmouth Medical School, Great Britain, following the procedure outlined in (Dunlap et al., 2007). A detailed description is available at <http://www.dartmouth.edu/~neurosporagenome/protocols.html>. In all cases, genes had been disrupted through targeted replacement by a hygromycin resistance cassette containing the selectable marker *hph^R*; strains had been verified by Southern blotting. For *rho-1* and NCU00668, only heterokaryotic deletion strains were available, in which both nuclei harbouring the deletion of the gene (marked by the presence of the *hph^R* gene) and nuclei of wild type are present, the latter providing shelter from the (lethal) effects of the deletion.

Conditional mutants of *cdc-24* had been generated by UV mutagenesis and identified as described in (Seiler and Plamann, 2003); *cdc-42*, *rac* and *rho-1* loss-of-function and temperature-sensitive strains had been created by S. Seiler (Germany) applying RIP (repeat induced point mutation) mutagenesis (Selker et al., 1989).

The majority of *N. crassa* strains generated in this study were obtained by transformation applying vectors targeted to the *his-3* locus (cp. Table 2 and descriptions below). These plasmids contain the respective expression cassette flanked by a region allowing homologous recombination to the *his-3* locus and concomitant restoration of a functional *his-3* allele (and thus, histidine prototrophy) in transformants obtained from *his-3* strains possessing a mutant *his-3* allele (Aramayo and Metzberg, 1996; Margolin et al., 1997).

For all strains, expression of the desired fusion protein was routinely verified by Western blotting (see section 4.7.3) using antibodies for detection of the respective epitope tag.

Generally, strains for expression of proteins fused to fluorescent proteins were generated by transforming strain *his-3* (FGSC #6103) with expression vectors targeted to the *his-3* locus (see Table 2 and section 4.4.6) and selecting histidine-prototrophic transformants. Functionality of the expressed proteins was tested by crossing the resulting strains (which still contain the endogenous wild type copy of the gene) with the respective hygromycin-resistant (heterokaryotic or homokaryotic) deletion mutant; offspring carrying the deletion nucleus were identified by their hygromycin resistance. Suppression of phenotypic defects associated with the deletion was used as evidence for functionality.

Deviating from this procedure, strain *mus52::bar his-3* (FGSC #9720) was cotransformed with a fragment of ppRho1_N_GFP_Rho1 targeted to the *rho-1* locus by homologous recombination and pCSN44 (see Table 2 and section 4.4.6) to create strain *sgfp-rho-1* (*endog.*), in which *rho-1* is *sgfp*-tagged at the endogenous locus. Cotransformants were selected by their resistance towards hygromycin (based on ectopic integration of the hygromycin resistance cassette delivered by pCSN44) and expression of GFP-RHO1, as verified by Western blotting. Crossing with wild type to remove the *mus52* mutation and verification by Southern blotting are still pending.

Strains for overexpression of myc-tagged CDC42 and RAC in the *cdc-42(18-4)* background were obtained by transforming the corresponding temperature-sensitive strain with plasmids pBScpcmyc3hyg_Cdc42 or pBScpcmyc3hyg_Rac (see Table 2 and section 4.4.7), which are thought to integrate ectopically into the genome; transformants were selected on hygromycin. As a control, a strain harbouring the empty expression vector ectopically integrated was prepared in parallel.

For expression of HA-, myc- and FLAG-tagged fusion proteins for interaction analysis by coimmunoprecipitation and pulldown experiments, strains were generated by transforming auxotrophic strains *trp-3; his-3* or *nic-3; his-3*, respectively, with the corresponding vectors (see Table 2 and section 4.4.7) targeting expression cassettes to the *his-3* locus. Resulting histidine-prototrophic transformants were isolated and fusion protein expression checked. For growth, the strains thus generated still depended on supplementation of the medium with tryptophane or nicotinamide, respectively. To prepare coimmunoprecipitation analyses, desired combinations of these strains were fused to produce prototrophic heterokaryotic strains simultaneously expressing two fusion proteins; to this end, conidia of the respective pair of strains (one Nic⁻, the other Trp⁻) were combined on VMM (see (Kawabata and Inoue, 2007) for details).

Table 3: *N. crassa* strains used in this work. (Note that heterokaryotic fusion strains used in coimmunoprecipitation analysis are not listed in the table; see text for details on their generation.) Genetic features are denoted as (EC) if ectopically integrated.

Strain	Genotype or description	Reference/source
wild type A	74-OR23-1V A	FGSC #2489
wild type a	ORS-SL6 a	FGSC #4200
<i>his-3</i>	<i>his-3</i> A	FGSC #6103
<i>mus52::bar his-3</i>	$\Delta mus52::bar^R his-3$ A	FGSC #9720
$\Delta 00668$ (<i>het</i>)	$\Delta NCU00668::hph^R + NCU00668^+$ $\Delta mus51::bar^R a$	FGSC #11488
$\Delta cdc-42$	$\Delta cdc-42::hph^R a$	FGSC #15833
Δrac microconidia	$\Delta rac::hph^R \Delta mus51::bar^R a$	FGSC #11525
$\Delta rho-1$ (<i>het</i>)	$\Delta rho-1::hph^R + rho-1^+$ $\Delta mus51::bar^R a$	<i>Neurospora</i> genome project, Dartmouth (kind gift)
$\Delta rho-2 a$	$\Delta rho-2::hph^R a$	FGSC #13322
$\Delta rho-2 A$	$\Delta rho-2::hph^R A$	FGSC #13323
<i>cdc-24(10-19)</i>	<i>cdc-24(10-19)</i> A	(Seiler and Plamann, 2003)
<i>cdc-24(19-3)</i>	<i>cdc-24(19-3)</i> A	(Seiler and Plamann, 2003)
<i>cdc-24(24-21)</i>	<i>cdc-24(24-21)</i> A	(Seiler and Plamann, 2003)
<i>cdc-42(18-4)</i>	<i>cdc-42(18-4)</i> a	S. Seiler, unpublished
<i>cdc-42(18-7)</i>	<i>cdc-42(18-7)</i>	S. Seiler, unpublished
<i>rac(7-1)</i>	<i>rac(7-1)</i> A	S. Seiler, unpublished
<i>rac(11-21)</i>	<i>rac(11-21)</i>	S. Seiler, unpublished
<i>rac(11-23)</i>	<i>rac(11-23)</i>	S. Seiler, unpublished

Strain	Genotype or description	Reference/source
<i>rac(7-1);cdc-42(18-4)</i>	<i>rac(7-1) cdc-42(18-4)</i>	S. Seiler, unpublished
<i>rho-1(9-1)</i>	<i>rho-1(9-1) a</i>	S. Seiler, unpublished
<i>rho-1(10-1)</i>	<i>rho-1(10-1) a</i>	S. Seiler, unpublished
Δ <i>rho-2; rho-1(9-1)</i>	Δ <i>rho-2::hph^R rho-1(9-1)</i>	S. Seiler (Δ <i>rho-2</i> x <i>rho-1(9-1)</i>)
<i>00668-sgfp</i>	<i>his-3⁺::Pccg-1-NCU00668⁺-sgfp A</i>	this study
<i>00668-sgfp (compl.)</i>	Δ <i>NCU00668::hph^R his-3⁺::Pccg-1-NCU00668⁺-sgfp (Δ<i>mus51::bar^R?</i>)</i>	this study (FGSC #11488 x <i>00668-sgfp</i>)
<i>00668-yfp</i>	<i>his-3⁺::Pccg-1-NCU00668-yfp A</i>	this study
<i>mCherry-rho-1</i>	<i>his-3⁺::Pccg-1-mCherry-rho-1⁺ A</i>	this study
<i>sgfp</i>	<i>his-3⁺::Pccg-1-sgfp A</i>	this study
<i>sgfp-rho-1</i>	<i>his-3⁺::Pccg-1-sgfp-rho-1⁺ A</i>	this study
<i>sgfp-rho-1 (endog.)</i>	Δ <i>mus52::bar^R his-3⁻ Prho-1-sgfp-rho-1⁺ hyg^R(EC) A</i>	this study
<i>sgfp-rho-2</i>	<i>his-3⁺::Pccg-1-sgfp-rho-2⁺ A</i>	this study
<i>yfp-cdc-42</i>	<i>his-3⁺::PgpDA-yfp-cdc-42⁺ A</i>	this study
<i>yfp-cdc-42 (compl.)</i>	Δ <i>cdc-42::hph^R his-3⁺::PgpDA-yfp-cdc-42⁺</i>	this study (FGSC #15833 x <i>yfp-cdc-42</i>)
<i>yfp-rac</i>	<i>his-3⁺::PgpDA-yfp-rac⁺ A</i>	this study
<i>yfp-rac (compl.)</i>	Δ <i>rac::hph^R his-3⁺::PgpDA-yfp-rac⁺ (Δ<i>mus51::bar^R?</i>)</i>	this study (FGSC #11525 x <i>yfp-rac</i>)
<i>yfp-rho-1</i>	<i>his-3⁺::PgpDA-yfp-rho-1⁺ A</i>	this study
<i>yfp-rho-2</i>	<i>his-3⁺::PgpDA-yfp-rho-2⁺ A</i>	this study
<i>cdc-42(18-4) 3xmyc-cdc-42</i>	<i>cdc-42(18-4) Pcp-1-3xmyc-cdc-42⁺-hph^R (EC) a</i>	this study
<i>cdc-42(18-4) 3xmyc-rac</i>	<i>cdc-42(18-4) Pcp-1-3xmyc-rac⁺-hph^R (EC) a</i>	this study
<i>cdc-42(18-4) 3xmyc control</i>	<i>cdc-42(18-4) Pcp-1-3xmyc-hph^R (EC) a</i>	this study
<i>trp-1; his-3</i>	<i>trp-1⁻; his-3⁻</i>	S. Seiler (FGSC #6103 x FGSC#4050)
<i>nic-3; his-3</i>	<i>nic-3⁻; his-3⁻</i>	S. Seiler (FGSC #6103 x FGSC#4082)
<i>HA-rho-1</i>	<i>trp-1⁻ his-3⁺::Pccg-1-ha-rho-1⁺</i>	Y. Heilig, unpublished
<i>HA-rho-2</i>	<i>trp-1⁻ his-3⁺::Pccg-1-ha-rho-2⁺</i>	this study
<i>3xmyc-rho-1</i>	<i>trp-1⁻ his-3⁺::Pccg-1-3xmyc-rho-1⁺</i>	this study
<i>3xmyc-rho-2</i>	<i>trp-1⁻ his-3⁺::Pccg-1-3xmyc-rho-2⁺</i>	this study
<i>12xmyc-rho-1</i>	<i>trp-1⁻ his-3⁺::Pccg-1-12xmyc-rho-1⁺</i>	this study
<i>3xFLAG-00668</i>	<i>nic-3⁻ his-3⁺::Pccg-1-3xflag-NCU00668⁺</i>	this study
<i>3xFLAG-pkc-1</i>	<i>nic-3⁻ his-3⁺::Pccg-1-3xflag-NCU06544⁺</i>	this study
<i>bni-1-3xFLAG</i>	<i>nic-3⁻ his-3⁺::Pccg-1-NCU01431⁺-3xflag</i>	this study
<i>06871-3xFLAG</i>	<i>nic-3⁻ his-3⁺::Pccg-1-NCU06871⁺-3xflag</i>	this study

E. coli strain DH5 α [F⁻, ϕ 80*lacZ* Δ M15, Δ (*lacZYA-argF*) U169, *phoA*, *recA1*, *endA1*, *hsdR17* (*r_K*⁻, *m_K*⁺), *supE44*, λ , *thi-1*, *gyrA96*, *relA1*] ((Woodcock et al., 1989) and Invitrogen, USA), was used for amplification of DNA. For expression of MBP- and GST-tagged fusion proteins, *E. coli* strain Rosetta™ 2(DE3) [F⁻, *ompT*, *hsdS_B* (*r_B*⁻ *m_B*⁻), *gal*, *dcm* (DE3), pRARE2 (Cam^R)] (Merck KGaA, Germany) was used.

S. cerevisiae strain AH109 [*MATa*, *trp1-901*, *leu2-3, 112*, *ura3-52*, *his3-200*, *gal4Δ*, *gal80Δ*, *LYS2::GAL1_{UAS}-GAL1_{TATA}-HIS3*, *GAL2_{UAS}-GAL2_{TATA}-ADE2*, *URA3::MEL1_{UAS}-MEL1_{TATA}-lacZ*] ((James et al., 1996) and Clontech, USA) was employed for yeast two-hybrid analyses.

4.6 General molecular biological techniques

Standard molecular biological methods were performed as described in (Sambrook and Russell, 2001; Ausubel et al., 2002) with minor modifications.

4.6.1 Isolation and analysis of nucleic acids

Plasmid DNA was purified from *E. coli* cells using the peqGOLD Plasmid Miniprep Kit II (PEQLAB Biotechnologie GmbH, Germany) according to the protocol supplied with the product.

For extraction of DNA from agarose gels or purification of DNA from enzymatic reaction mixes, the peqGOLD Gel Extraction Kit (PEQLAB Biotechnologie GmbH, Germany) was used following the product manual.

For isolation of genomic DNA from *N. crassa*, the methods of (Borges et al., 1990; Weiland, 1997) were adapted. Mycelial samples were harvested from liquid cultures by filtration, frozen in liquid nitrogen, mixed with quartz sand and ground to a fine powder with mortar and pestle. Homogenization in extraction buffer (50mM Tris, pH 8.0, 50mM ethylenediaminetetraacetic acid (EDTA), 3% sodium dodecyl sulfate (SDS), 1% β-mercaptoethanol) was ensued by an incubation step of two hours at 65°C. Afterwards, at least two extraction steps with Roti®-Phenol (Carl Roth GmbH+Co. KG, Germany)/chloroform/isoamyl alcohol (25/24/1) and one with chloroform were performed. DNA was precipitated with isopropanol (0.7 volumes added), redissolved in TE buffer (10mM Tris, pH 8.0, 1mM EDTA), and ribonucleic acid (RNA) digestion was performed by incubation with 0.1 μg/ml RNaseA (Fermentas GmbH, Germany) for 10 min at 65°C. The enzyme was removed by repeating the extraction routine as described above, DNA was precipitated by addition of 1/10 volume 3M sodium acetate and 2 volumes ethanol, washed once with 70% ethanol, air-dried and redissolved in H₂O. Solutions were stored at -20°C or 4°C.

N. crassa mycelial powder for isolation of total RNA was obtained as outlined above (without addition of sand). Essentially as described in (Chomczynski and Sacchi, 1987; Chomczynski, 1993) and the product manual, RNA was extracted from the frozen mycelium with TRIzol® Reagent (Invitrogen GmbH, Germany) followed by a phenol/chloroform/isoamyl alcohol extraction, precipitation by isopropanol and washing with 70% ethanol. After air-drying, RNA was re-dissolved in RNase-free water (Stratagene Corporation, USA) at 65°C. To remove DNA, DNase I (Fermentas GmbH, Germany) was used in accordance with the instruction manual. Samples were stored at -80°C.

Concentration and purity of nucleic acid solutions were determined with a Nanodrop spectrophotometer ND-1000 (PEQLAB Biotechnologie GmbH, Germany) applying the respective analysis mode.

4.6.2 Reverse transcription of RNA

Adhering to the protocols provided by the manufacturers, AccuScript™ High Fidelity 1st Strand cDNA Synthesis Kit (Stratagene Corporation, USA) or Transcriptor High Fidelity

cDNA Synthesis Kit (Roche Applied Science, Germany) were used for reverse transcription of RNA with the Oligo(dT) primers supplied.

4.6.3 Polymerase chain reaction (PCR)

Amplification of DNA by polymerase chain reactions with thermostable DNA polymerases (Saiki et al., 1988) was performed in accordance with standard protocols (Ausubel et al., 2002). *Taq* DNA Polymerase was used for analytical PCRs while the proofreading enzymes *Pfu* DNA Polymerase (both Fermentas GmbH, Germany) and Phusion® High-Fidelity DNA Polymerase (Finnzymes Oy, Finland) were used if the amplified DNA fragments were intended for use in plasmid construction. Oligonucleotides used as PCR primers were synthesized by Operon Biotechnologies, Invitrogen GmbH or Eurofins MWG Operon (all Germany). Depending on the purpose, plasmids, genomic DNA of *N. crassa* or reaction products from reverse transcription of RNA or preceding PCR reactions served as templates. In colony PCRs (Zon et al., 1989), which were performed to identify positive transformants of *E. coli*, *E. coli* cells of a single colony were directly transferred to the reaction tube using a sterile toothpick.

Typical analytical reaction mixes contained 200µM dNTP Mix (Fermentas GmbH, Germany), 200nM forward and reverse primers, approximately 0.5u/20µl of *Taq* DNA Polymerase and varying amounts of template in reaction buffer (20mM Tris, pH8.8, 10mM KCl, 10mM (NH₄)₂SO₄, 2.25mM MgCl₂, 0.002% NP40, 0.002% Triton X-100, 4% glycerol). A routine PCR reaction consisted of an initial template denaturation step (2 min, 94°C) followed by 30-35 cycles each consisting of denaturation (30 sec, 94°C), primer annealing (30 sec, 53-60°C depending on the primers used) and product elongation (1 min/1 kb template length, 72°C); thereafter, the reaction was completed by a final elongation step (5 min, 72°C).

For PCRs employing *Pfu* DNA Polymerase (Fermentas GmbH, Germany) or Phusion® High-Fidelity DNA Polymerase (Finnzymes Oy, Finland), reaction conditions were adapted to the manufacturers' recommendations.

4.6.4 DNA agarose gel electrophoresis

Separation of DNA fragments and plasmids by horizontal agarose gel electrophoresis was carried out following standard protocols using the Mini Sub-Cell System (Bio-Rad Laboratories GmbH, Germany). GeneRuler™ 1 kb DNA Ladder (Fermentas GmbH, Germany) was used as a DNA molecular weight marker. DNA bands stained with ethidiumbromide were visualized at 254nm using the UV transilluminators GelDoc 1000 or Molecular Imager Gel Doc XR System (Bio-Rad Laboratories GmbH, Germany).

4.6.5 Enzymatic restriction and modification of DNA

For endonucleolytic digestion of DNA, restriction enzymes and accompanying reaction buffers were obtained from Fermentas GmbH (Germany) and New England Biolabs (USA) and used in accordance with the respective product manuals.

If necessary, DNA termini of cloning vectors were dephosphorylated employing Shrimp Alkaline Phosphatase (Fermentas GmbH, Germany) following the manual to prevent vector recircularization in subsequent ligation reactions. For removal of single-stranded DNA extensions to create ligatable blunt ends, Mung Bean Nuclease (New England Biolabs, USA) was used in accordance with the manufacturer's instructions.

4.6.6 Ligation

Ligation of DNA fragments was performed in 15µl reaction volumes using T4 DNA ligase (Fermentas GmbH, Germany) in quick ligation buffer (50mM Hepes, pH7.6, 10mM MgCl₂, 2mM dithiothreitol (DTT), 2mM adenosine triphosphate (ATP), 7% polyethylene glycol 4000) modified from Quick Ligation Reaction Buffer (New England Biolabs, USA). Typically, 5u enzyme and additional 3.3mM ATP were freshly added, and the reaction was carried out at room temperature for 20 minutes.

4.7 Biochemical and immunological methods

4.7.1 Preparation of *N. crassa* crude extracts for protein analysis

Mycelia from liquid cultures were harvested by filtration using a Büchner funnel, washed once with H₂O, pulverized by grinding in liquid nitrogen and thoroughly suspended to a homogenous mixture in extraction buffer (50mM Tris, pH 8.0, 50mM KCl, 2mM EDTA; freshly added 2mM benzamidine, 2mM DTT, 0.5mM phenylmethylsulfonyl fluoride (PMSF), 0.05% Nonidet P-40 (NP-40)). The lysate was successively cleared in two centrifugation steps (4°C, 15 and 12 min, 16000xg). If applicable, protein content of the samples was determined using a Nanodrop spectrophotometer ND-1000 (analysis mode. Protein A280, 340 nm normalization on, 1OD° \approx 1mg/ml; PEQLAB Biotechnologie GmbH, Germany) before addition of 1/3 volume of 3x Laemmli sample buffer (3% SDS, 62.5mM Tris, pH6.8, 5% β -mercaptoethanol, 10% glycerol, 5M Urea, tinted with bromophenol blue; modified from (Laemmli, 1970)) and boiling at 98°C for 10 minutes.

4.7.2 Separation of proteins by SDS polyacrylamide gel electrophoresis (PAGE)

Vertical discontinuous polyacrylamide gel electrophoresis (PAGE) (Ornstein, 1964; Davis, 1964) of protein samples in the presence of sodium dodecyl sulfate (SDS) in a Tris glycine buffer system (Shapiro et al., 1967; Laemmli, 1970) was performed using the Mini-PROTEAN® 3 Cell System (Bio-Rad Laboratories GmbH, Germany) in accordance with the accompanying instruction manual. Rotiphorese® Gel 30 (acrylamide:bisacrylamide 37.5:1; Carl Roth GmbH & Co. KG, Germany) was used in casting the gels. Generally, protein samples prepared by boiling in Laemmli sample buffer (see section 4.7.1) and the molecular weight markers PageRuler™ Prestained or Unstained Protein Ladder (Fermentas GmbH, Germany) were loaded onto gels consisting of stacking gel (4.5% acrylamide in 124mM Tris, pH 6.8, 0.1% SDS, 0.04% ammonium persulfate (APS), 0.16% tetramethylethylenediamine (TEMED)) and resolving gel (7.5, 10 or 15% acrylamide in 372mM Tris pH 8.8, 0.1% SDS, 0.06% APS, 0.06% TEMED). Electrophoretic separation of protein was performed by applying a constant current of 14-15mA per gel to gels submerged in running buffer (2.5mM Tris base, 19.2mM glycine and 0.1% SDS).

Proteins separated by PAGE were visualized by staining with Coomassie Brilliant Blue (Merril, 1990); alternatively, Western blotting was performed.

4.7.3 Western blotting

Electrophoretic transfer of proteins from polyacrylamide gels to Protran® nitrocellulose membrane (Whatman GmbH, Germany) and their subsequent immunological detection (Western blotting) was based on the method described by (Towbin et al., 1979) and was performed in Mini Trans-Blot® Cells (Bio-Rad Laboratories GmbH, Germany) adhering to the manufacturer's instructions. After electroblotting (1 hour, 100V) in cooled transfer buffer (2.5mM Tris, 19.2mM glycine, 20% methanol), the membrane was subjected to reversible protein staining in 0.1% Ponceau S in 5% acetic acid essentially as described in (Salinovich and Montelaro, 1986).

5% Sucofin milk powder (TSI GmbH & Co. KG, Germany) in PBS solution (10mM sodium phosphate, 150mM NaCl, pH7.4) was used in an initial blocking step and for incubation of the membrane with antibodies; unbound antibodies were washed off with PBS solution. Polyclonal rabbit α -GST (Z-5) (Santa Cruz Biotechnology, Inc., USA) or α -Phospho-p44/42 MAPK (Erk1/2) (Thr202/Tyr204) (Cell Signaling Technology, Inc., USA), rabbit α -MBP antiserum (New England Biolabs, USA) or monoclonal mouse α -c-Myc (9E10), α -GFP (B-2) (both Santa Cruz Biotechnology, Inc., USA), α -HA (clone HA-7) or ANTI-FLAG® M2 (both Sigma-Aldrich Corporation, USA) antibodies served as primary antibodies and were detected by horseradish peroxidase-coupled secondary antibodies donkey α -rabbit IgG-HRP (Santa Cruz Biotechnology, Inc., USA), goat- α -rabbit IgG (Invitrogen GmbH, Germany) or goat- α -mouse IgG (Dianova Gesellschaft für biochemische, immunologische und mikrobiologische Diagnostik mbH, Germany). Immunolabelled protein bands were visualized using Immobilon™ Chemiluminescent Western HRP Substrate (Millipore, USA) in combination with Amersham™ Hyperfilm™ ECL (GE Healthcare Europe GmbH, Germany) according to the manufacturers' recommendations.

4.7.4 Immunoprecipitation

Immunoprecipitation experiments were performed according to (Maerz et al., 2009) with minor modifications. All buffers used contained the following additives: 25mM β -glycerophosphate, 10ng/ μ l leupeptin, 10 ng/ μ l aprotinin, 2ng/ μ l Pepstatin A (Sigma-Aldrich Corporation, USA), 2mM DTT, 1mM Na₃VO₄, 1mM PMSF, 2mM benzamide, 5mM NaF. Mycelia from liquid cultures were harvested by filtration using a Büchner funnel, washed once with H₂O, pulverized by grinding in liquid nitrogen and suspended in lysis buffer (20mM Tris pH7.4, 150mM NaCl, 10% (v/v) glycerol, 0.5mM EDTA, 0.1% (v/v) NP-40). After three centrifugation steps (4°C; 15min 3000xg, 20min and 12min 16000xg), the cleared supernatant was incubated on a rotation device for two hours with 0.8 μ g/ml lysate monoclonal mouse α -c-Myc (9E10), 1.6 μ g/ml lysate monoclonal mouse α -GFP (B-2) (both Santa Cruz Biotechnology, Inc., USA), 2.5 μ g/ml lysate α -HA or 4-10 μ g/ml lysate monoclonal mouse ANTI-FLAG® M2 (both Sigma-Aldrich Corporation, USA). 5 mg lyophilized Protein A Sepharose™ CL-4B (GE Healthcare Life Sciences, USA) per ml lysate was allowed to swell in lysis buffer and washed twice to remove stabilization agents before the lysate-antibody mixture was added to the slurry. After another hour of incubation, the suspension was centrifuged (4°C, 2min, 595xg) and the supernatant removed thoroughly. If applicable, the sepharose was washed twice with washing buffer (20mM Tris pH7.4, 500mM NaCl, 10% (v/v) glycerol, 0.5mM EDTA, 0.1% (v/v) NP-40). Recovery of immunoprecipitated proteins was achieved by boiling the sepharose for 10min at 98°C in 40 μ l 3x Laemmli sample buffer (see section 4.7.1).

4.7.5 Analysis of MAK1 phosphorylation status

For MAK1 phosphorylation analysis, liquid cultures were inoculated with conidia (4-7 days old) of the indicated strains and grown to low density at 21-22°C for 24-26 hours. Cell wall stress was induced by addition of Lysing Enzymes from *Trichoderma harzianum* (containing β -glucanase, cellulase, protease and chitinase activity; Sigma-Aldrich Corporation, USA) to a final concentration of 1mg/ml; for assessing base level phosphorylation, cultures were left untreated. After 15 min, mycelia were harvested by gentle filtration using a Büchner funnel and immediately ground in liquid nitrogen without prior rinsing.

Ensuing protein extraction was performed as described in (Jones et al., 2007) with modifications kindly communicated by L. Bennett (Department of Biology, Texas A&M University, USA): The frozen mycelial powder was transferred to a screw-top tube containing glass beads (diameter 0.25-0.5 mm), and 95% ethanol was added. After thorough mixing the samples were incubated at least overnight at -20°C. The supernatant was removed after centrifugation (4°C, 30 min, 16000xg) and the pellet vacuum-dried in a SpeedVac concentrator (Thermo Fisher Scientific, USA). Extraction buffer (100mM Tris pH7.0, 1% (w/v) SDS; supplemented with 5mM NaF, 1mM PMSF, 1mM Na₃VO₄, 25mM β -glycerophosphate, 2mM benzamidine, 2 ng/ μ l Pepstatin A, 10 ng/ μ l aprotinin, 10 ng/ μ l leupeptin) was added, the samples were mixed and incubated at 80°C for 5 minutes. After an ensuing centrifugation step (room temperature, 5 min, 16000xg) the supernatant was collected. The extraction step was repeated once, the supernatants were pooled and subjected to another centrifugation step (15 min). Protein contents of cell extracts cleared in this way were measured spectrophotometrically using a Nanodrop spectrophotometer ND-1000 as described in section 4.7.1. Finally, 3x Laemmli sample buffer (see section 4.7.1) was added to give a 1x concentration and samples were boiled at 98°C for 5 minutes.

Sample volumes corresponding to 50 or 150 μ g total protein per lane were loaded onto SDS polyacrylamide gels and electrophoresis and Western blotting were performed as described in sections 4.7.2 and 4.7.3 with the following modifications: After being blocked in 5% milk powder in PBST (PBS solution/0.05% Tween-20), membranes were rinsed three times with PBST. Polyclonal rabbit α -Phospho-p44/42 MAPK (Erk1/2) (Thr202/Tyr204) (Cell Signaling Technology, Inc., USA) in 5% bovine serum albumin/PBST (overnight incubation) and donkey α -rabbit IgG-HRP (Santa Cruz Biotechnology, Inc., USA) in 5% milk powder/PBST were used as primary and secondary antibodies for immunodetection, respectively. Except for the last step, PBST was used for washing.

For quantification of MAK1 phosphorylation levels, exposed films were scanned at a resolution of 600 dots per inch and densitometry was performed on the resulting .tiff-files employing the AIDA Image Analyzer (version 4.22; raytest Isotopenmessgeräte GmbH, Germany) in transmission mode. Intensity values [arbitrary units] measured within a region of interest of fixed size containing the MAK1 protein bands were corrected by subtraction of local background, normalized to the protein amount loaded and used for further evaluation.

In each set of experiments, basal and stress-induced MAK1 phosphorylation levels of a mutant strain were directly related to those of the wildtype by analyzing three to four individual cultures of each strain under both non-stress and stress conditions. For the *rho-1ts* strains, one such set was evaluated, for Δ *rho-2* and Δ 00668het two sets and for the double mutant Δ *rho-2*; *rho-1(9-1)* three sets were analyzed. As a consequence of the chosen

evaluation method, nine sets were available for final analysis in the case of stressed wildtype cultures.

Following the guidelines for analysis of experimental data and error propagation calculations presented in (Ait Tahar and Stollenwerk), for each of the four subgroups of a set, the absolute arithmetic mean \bar{x} and confidence interval ($p=68\%$) $\Delta\bar{x}$ (standard error of the mean corrected for small sample number by multiplication with t factor of Student's t distribution) of the experimentally determined intensity values were calculated. In a subsequent step the mean value for the untreated wildtype, $\bar{x}_{wtbasal}$, was set to 1, and relative mean values $\bar{x}_{i\ relative}$ of the other three subgroups of a set were calculated as $\bar{x}_{i\ relative} = \frac{\bar{x}_i}{\bar{x}_{wtbasal}}$. Assuming Gaussian error propagation, the corresponding confidence intervals ($p=68\%$) $\Delta\bar{x}_{i\ relative}$ (which incorporate the uncertainty of $\bar{x}_{wtbasal}$) were calculated as $\Delta\bar{x}_{i\ relative} = \sqrt{\left(\frac{\Delta\bar{x}_{wtbasal}}{\bar{x}_{wtbasal}} \bar{x}_{i\ relative}\right)^2 + \left(\frac{\Delta\bar{x}_i}{\bar{x}_i} \bar{x}_{i\ relative}\right)^2}$.

If applicable, data from different sets n of experiments were combined in the following way:

Arithmetic mean values $\bar{x}_{i\ relative\ combined}$ were calculated from $\bar{x}_{i\ relative}$ values of all sets by simple averaging, and again applying the rules of Gaussian error propagation, the final confidence intervals were calculated as $\Delta\bar{x}_{i\ relative\ combined} = \sqrt{\sum^n (\Delta\bar{x}_{i\ relative})^2} / n$.

For illustration of mean MAK1 phosphorylation levels depicted in Figure 30, samples from all individual experiments were united evenly and subjected to phospho-MAK1 immunodetection as described above.

4.7.6 Protein expression and purification from *E. coli*

N. crassa Rho GTPases RHO1 to RHO4, RAC and CDC42 and the putative RhoGEF or RhoGAP domain constructs were expressed as fusion proteins with an N-terminal maltose binding protein (MBP) tag. Additionally, the DEP domain of NCU00668 was expressed fused to an N-terminal glutathione S-transferase (GST) tag. For fusion protein purification (modified from (Vogt and Seiler, 2008)), LB⁺ medium (1% NaCl, 0.8% yeast extract, 1.8% peptone, 2% glucose) supplemented with chloramphenicol and ampicillin or kanamycin for selection was inoculated to an OD₆₀₀ of 0.1 from an overnight culture of Rosetta2(DE3) cells transformed with the respective pNV72- or pETM30-derived plasmid. Cultures were grown shaking at 20°C to an OD₆₀₀ of 0.45, and fusion protein expression was induced by addition of isopropyl β-D-thiogalactopyranoside to 0.2 mM. After 2 hours, cells were harvested by centrifugation and the pellet was resuspended in lysis buffer (50mM Tris, pH7.4, 125 mM NaCl, 5 mM MgCl₂, 10% glycerol, 0.02% NP-40, 2mM DTT, 1mM PMSF, 0.35 mg/ml benzamidine, 10μM GTP) and stored at -20°C.

Cells were disrupted by ultrasonication using a Sonopuls HD 2070 ultrasonicator (Bandelin GmbH & Co. KG, Germany); cleared lysates (4°C, 20 min, 13000xg) were incubated on a rotating wheel at 4°C with preequilibrated Amylose Resin (New England Biolabs, USA) for one hour. The resin was washed twice with washing buffer (lysis buffer with 250mM NaCl; GTP was omitted in second wash step) before elution with elution buffer (50mM Tris, pH7.4, 200 mM NaCl, 5 mM MgCl₂, 10% glycerol, 0.02% Nonidet-P40, 2mM DTT, 20mM maltose); protein-rich fractions were pooled. Eluates containing MBP-tagged GEF constructs were occasionally supplemented with glycerol to a final concentration of 33%, prefrozen at -20°C, transferred to -80°C and stored several days for subsequent use in GEF assays; in contrast,

MBP-Rho GTPase fusion proteins were always freshly purified. Eluate samples were prepared for SDS PAGE as described in section 4.7.1, and purity of fusion proteins was routinely checked by Coomassie staining of SDS gels to amount to at least 85%. Total protein concentration of the eluates was determined by Bradford analysis (Bradford, 1976) with bovine serum albumin standard solutions as a reference and using Roti®-Quant (Carl Roth GmbH+Co. KG, Germany) and a Tecan Infinite® M200 microplate reader equipped with Magellan™ software (version 6; both Tecan Group Ltd., Switzerland). For GEF assays, protein concentrations of eluates were adjusted with elution buffer (with glycerol added, if applicable).

4.7.7 *In vitro* GEF activity assays

Intrinsic and GEF-stimulated *in vitro* Rho GTPase nucleotide exchange activity was measured using the fluorescent guanine nucleotide analogue mant-GDP (2'/3'-O-(N'-methylanthraniloyl)-GDP; (Hiratsuka, 1983)), which exhibits markedly increased emission intensity upon binding to a protein (Jameson and Eccleston, 1997). Assay procedures were modified from (Leonard et al., 1994; Abe et al., 2000). If not stated otherwise, reaction mixtures contained 0.1µM mant-GDP, 10mM NaH₂PO₄/K₂HPO₄, pH7.5, 1.2µM MBP-Rho GTPase and/or 0.8µM MBP-GEF in reaction buffer (30mM Tris, pH 7.4, 5mM MgCl₂, 3mM DTT); exchange reactions were started by addition of mant-GDP and, where applicable, GEF protein. Changes in fluorescence intensity ($\lambda_{exc}=356\text{nm}$, $\lambda_{em}=448\text{nm}$; [arbitrary units]) were monitored using a Tecan Infinite M200 plate reader operated by Magellan software (see section 4.7.6) at 21°C over 24 minutes or as stated. To assess the impact of NCU00668DEP domain on intrinsic or GEF-stimulated nucleotide exchange, NCU00668 construct or RHO1 fusion proteins, respectively, were preincubated with variable concentrations of MBP-DEP (0.4 - 2.8µM) before starting the exchange reactions.

After correcting measured data for background signals determined in replicate blank buffer controls (without nucleotide analogue or proteins) for each time point, data were plotted as fluorescence intensity over time, and initial (i.e. pre-saturation) mean linear slope [per second] was calculated. For each sample, data from at least two technical replicates were then averaged and mean slope values and their variances calculated by combining data from all samples of a type.

In the absence of Rho GTPases in samples, a slight spontaneous decrease in fluorescence over time was observed, hinting at instability of mant-GDP in the solution; reduction was generally more pronounced in samples containing GEF proteins. To correct for this effect, mean values calculated for Rho GTPase-free controls without or with GEF were subtracted from the respective sample mean. In accordance with the rules of error propagation, standard deviation (SD) of each resulting value was calculated as square root of the sum of the respective variances. Finally, relative values were calculated by normalizing to the respective value of intrinsic exchange activity of each Rho GTPase. All data analysis was performed using Excel (Microsoft Corporation, USA).

Rare outliers which could have unduly influenced results, although without changing the overall conclusions, fell into two categories: Either fluorescence intensity exhibited strong random oscillations over time (evident in irregular "zigzagging" of resulting plot curves), presumably indicative of measurement errors of the platereader; or intensity values of the first few measurements were exceedingly high, hinting at a delayed equilibration of reaction mixtures. In cases where outliers of the first (I) or second (II) type were observed, the

respective technical replicate was not evaluated or the first few data points were omitted. In the following, all cases where the non-consideration of (partial) technical replicates affected results of mean relative nucleotide exchange activities are listed in the form “figure reference: Rho GTPase/GEF combination (outlier category (if applicable); mean relative nucleotide exchange activity \pm SD under consideration of all data values [%]; mean relative nucleotide exchange activity \pm SD under non-consideration of outliers [%])”: Figure 8: RHO4+00668 (II; 38 \pm 96; 91 \pm 23); Figure 10: RHO1 no GEF (I; 100 \pm 326; 100 \pm 210), RHO1+BUD3 (I; 175 \pm 226; 104 \pm 185); Figure 11: RHO1 no GEF (I; 100 \pm 222; 100 \pm 186), RHO1+10282 (63 \pm 190; 56 \pm 168); Figure 20: RHO1+DGC (I; 94 \pm 100; 73 \pm 57), RHO3+DGC(I,I,II; 54 \pm 42; 64 \pm 29); RHO4+GEF (II; 42 \pm 105; 100 \pm 25), CDC42 no GEF (I; 100 \pm 53; 100 \pm 54), CDC42+DGC (I,I,I,II; 51 \pm 49; 54 \pm 45), CDC42+GC (102 \pm 20; 103 \pm 20), CDC42+GEF (124 \pm 22; 125 \pm 22); Supplementary Figure 9: RHO1 no GEF (II; 100 \pm 108; 100 \pm 91), RHO1+DGC (I; 92 \pm 87; 69 \pm 50), RHO1+GC (194 \pm 71; 176 \pm 64), RHO1+GEF (II; 405 \pm 75; 374 \pm 66).

4.7.8 Copurification experiments

For copurification experiments, cleared lysates obtained as described in section 4.7.6 from *E. coli* cultures expressing MBP or GST (fusion) proteins were mixed in the desired combinations and incubated on a rotating wheel for 30 minutes at 4°C. Thereafter, purification was continued as outlined in section 4.7.6.

4.8 Yeast two-hybrid assays

For yeast two-hybrid assays (Fields and Song, 1989), the Matchmaker™ Two-Hybrid System 3 (Clontech, USA) was used following the manufacturer’s recommendations for yeast media formulations and handling. Combinations of plasmids encoding proteins fused to the GAL4 activation domain (cDNA constructs inserted into pGADT7 or derivatives) or the DNA-binding domain (cDNA constructs inserted into pGBKT7 or a derivative), respectively, were used for cotransformation of *S. cerevisiae* AH109 cells adhering to the protocol provided in (Schiestl and Gietz, 1989). Cotransformants were selected by their restored ability to grow on SD medium lacking leucine and tryptophane. Interaction of fusion proteins was shown by proving activation of the reporter genes *HIS3*, *LacZ* and *ADE2*. For this, cells were collected from discrete colonies, suspended in water, and serial dilutions thereof applied to SD plates additionally lacking histidine (containing 10mM 3-amino-1,2,4-triazole for enhanced selection; for *LacZ* screening, 40 μ g/ml X- α -Gal (Clontech, USA) were added) or both histidine and adenine. Colony growth and formation of blue galactosidase reaction product were assessed after three or eight days at 30°C, respectively, if not stated otherwise.

None of the fusion proteins exhibited autoactivation, i.e. interaction with the respective other GAL4 domain alone, as tested by cotransformation of yeasts with each plasmid and the empty vector of the other type. Moreover, general yeast two-hybrid competency of the DNA binding domain fusion proteins was verified by their ability to interact with Δ N-RanBPM (see (Tucker et al., 2009) for details on this control).

4.9 Microscopy

For stereomicroscopical analysis of colonial and hyphal morphology, Olympus SZX16 (Olympus, Japan) equipped with an Olympus SDF PLAPO 1xPF objective was used; photos were captured with an Olympus ColorView III camera operated by the programme Cell^D analySIS Image Processing (Olympus SoftImaging Solutions GmbH, Germany).

Live cell imaging of vegetative hyphal cells of *N. crassa* grown for 12-16 hours on thin VMM layers was performed as described in (Hickey et al., 2002); calcofluor white (2.7 µg/ml staining solution) was used for counterstaining of cell wall material.

Fluorescence microscopy was performed using a Zeiss Axiovert S100 inverted epifluorescence microscope equipped with 40x Plan Neofluar® and 63x Plan Apochromat® objectives (Carl Zeiss AG, Germany) and filter sets for EGFP, DAPI, YFP and TxRed (AHF Analysentechnik, Germany). Images were acquired with a Hamamatsu Photonics ORCA-ER camera (model C4742-12ER; Hamamatsu, Japan) using Openlab (version 5.5.0; Improvion, Great Britain).

Alternatively, images were captured using a QuantEM 512SC camera (Photometrics, USA) mounted onto an inverted Axio Observer Z1 microscope equipped with a 63x Plan Apochromat® objective (Carl Zeiss AG, Germany); microscope and camera were operated by SlideBook™ software (version 5.0; Intelligent Imaging Innovations GmbH, Germany).

Brightness and contrast of acquired .tiff files of images were mildly adjusted using ImageJ (versions 1.43s and 1.43u; public domain, available at <http://rsbweb.nih.gov/ij/>).

4.10 Bioinformatic tools

4.10.1 DNA and protein sequence analysis

DNA cloning projects were planned, documented and analyzed using DNASTAR® SeqBuilder (version 8.0.3(1), DNASTAR, Inc., USA).

Results of DNA sequencing (see section 4.4.1) were analyzed using 4Peaks (version 1.7.2; Mekentosj B.V., The Netherlands) and BLAST (Altschul et al., 1990) at NCBI (accessible via <http://blast.ncbi.nlm.nih.gov/Blast.cgi>).

Programs used for creation of alignments and phylogenetic trees are detailed in section 4.10.2 and indicated in the respective figure legends.

Predictions of protein molecular weight were performed using the Protein Molecular Weight Calculator accessible at <http://www.sciencegateway.org/tools/proteinmw.htm>.

Protein structure was analyzed with regard to conserved domains using InterProScan Sequence Search (European Bioinformatics Institute of European Molecular Biology Laboratory; available at <http://www.ebi.ac.uk/Tools/InterProScan/index.html>).

SOSUI (accessible at <http://bp.nuap.nagoya-u.ac.jp/sosui/>), TMpred (at http://www.ch.embnet.org/software/TMPRED_form.html) and Mobyle TopPred (at <http://mobyle.pasteur.fr/cgi-bin/portal.py>) were used to predict transmembrane domains and their orientation for NCU06871 (GLS1).

4.10.2 Phylogenetic analysis and alignment

Protein sequences of putative *N. crassa*, *S. cerevisiae* and *S. pombe* RhoGAPs and (DH-type) RhoGEFs used for the phylogenetic trees depicted in Figure 4 and Figure 5, respectively, were retrieved in December 2007 from the Broad *Neurospora crassa* Database (assembly 7, version .3 annotation; see section 4.4.1) or from the *Saccharomyces* Genome

Database (SGD project at <http://www.yeastgenome.org/>) and GeneDB hosted by the Wellcome Trust Sanger Institute (accessible via <http://www.genedb.org>), respectively.

Conserved domains were identified by InterProScan Sequence Search (see section 4.10.1; as of December 2007) and protein regions predicted to span RhoGEF or RhoGAP domain regions were used for alignments and phylogenetic tree building by DNASTAR® Lasergene MegAlign (version 8.0.2(13); DNASTAR, Inc., USA; settings: ClustalW, Slow/Accurate, Gonnet). Note that, while in some cases presumed gene structure has changed with new annotations and own cDNA analysis (see Supplementary Table 1, p.104), no significant changes in protein domain structure have occurred. However, a further putative *S. pombe* RhoGAP similar to Rga8, Rga9, has been annotated in the meantime in GeneDB (see also (Yang et al., 2003)).

For the alignment of fungal CDC24-like proteins in Figure 17, protein sequences of the closest homologues of *N. crassa* CDC24 were retrieved by organism specific BLAST search (Altschul et al., 1990) at NCBI (accessible via <http://blast.ncbi.nlm.nih.gov/Blast.cgi>). The retrieved sequences (*A. nidulans* hypothetical protein AN5592.2, *C. albicans* guanine nucleotide exchange factor Cdc24, *S. cerevisiae* Cdc24p, *S. pombe* RhoGEF Scd1 and *U. maydis* hypothetical protein UM02422.1) were aligned with the sequence of *N. crassa* CDC24 using the ClustalW2 program (Chenna et al., 2003) accessible at <http://www.ebi.ac.uk/Tools/msa/clustalw2/>.

For the alignment presented in Figure 25, amino acid sequences of *N. crassa* RHO1 (NCU01484.3), *S. pombe* Rho1 (SPAC1F7.04) and *S. cerevisiae* Rho1 (YPR165W) were aligned by MAFFT (version 6.083b; accessible at <http://mafft.cbrc.jp/alignment/server/>; (Kato and Toh, 2008)).

5. Results

5.1 Analysis of Rho regulator specificity in *N. crassa*

In the first part of this work, a global analysis of the specificity of putative RhoGAP and RhoGEF proteins of *N. crassa* was attempted. To this end, the proteins were compared with Rho regulators of the well-studied yeasts *S. cerevisiae* and *S. pombe*, and *in vitro* activity assays were prepared and performed.

5.1.1 Comparison with the yeast Rho regulatory machinery

Figure 4 shows a phylogenetic analysis and domain structure comparison of presumptive RhoGAP proteins of *N. crassa* and the two yeasts. Most *N. crassa* RhoGAPs possess close homologues in *S. cerevisiae* and/or *S. pombe*, although those featuring no other domains besides the RhoGAP domain generally have more distant relatives only. Note that, although the sequence alignment for generating the phylogenetic tree was based on the predicted GAP domain region of the proteins only, a clustering of proteins with similar overall structural organization can be observed in several cases. The conserved domains found in the protein sequences apart from the RhoGAP domain are ascribed diverse functions (Pfam 24.0 database at <http://pfam.sanger.ac.uk/>; (Finn et al., 2009)). Many of them are associated with phospholipid interaction and membrane targeting (PX, PH, LIM, DEP (domain found in Dishevelled, Egl-10 and Pleckstrin) domains), thought to mediate protein-protein interactions (LIM, PH, DEP domains; the latter for interaction with heterotrimeric G proteins) or implicated in regulation of cytoskeletal elements (FCH (Fes/CIP4 homology) domain). The C1 domain of Rga3, which is thought to bind phorbol esters and diacylglycerol, might serve a regulatory function, while the RasGEF domains found solely in Bem2p could constitute a direct link between Rho and Ras signalling in the cell.

An analogous comparison of putative RhoGEFs of the three fungi yields similar results (Figure 5): Alignment of DH-type RhoGEF domains of the proteins reveals different degrees of homology of *N. crassa* RhoGEFs to yeast proteins of the same type. As with the RhoGAPs, subgroups with identical domain organization can be distinguished. The two putative CZH-type RhoGEF proteins of *N. crassa* and *S. cerevisiae* are shown at the bottom of the figure; note the difference in length of the predicted Ded_cyto (dedicator of cytokinesis) domains. Many RhoGEF proteins contain conserved domains in addition to the ones associated with GEF activity (i.e. RhoGEF or DH and Ded_cyto domains). Like DEP and PH domains also found in the RhoGAP proteins, BAR (Bin/amphyphysin/Rvs) domains are presumed to play a role in membrane targeting and, like PB1 (Phox and Bem1p) domains, they constitute putative dimerization domains. Interestingly, recent findings also propose a function of BAR domains in binding to small GTPases (Habermann, 2004). The function of CNH (citron homology) and SH3 (Src homology 3) domains is less well understood, the first is presumed to have regulatory effects and to be involved in macromolecular interactions, while the latter is thought to influence subcellular localization and interaction with multiprotein complexes in signal transduction pathways.

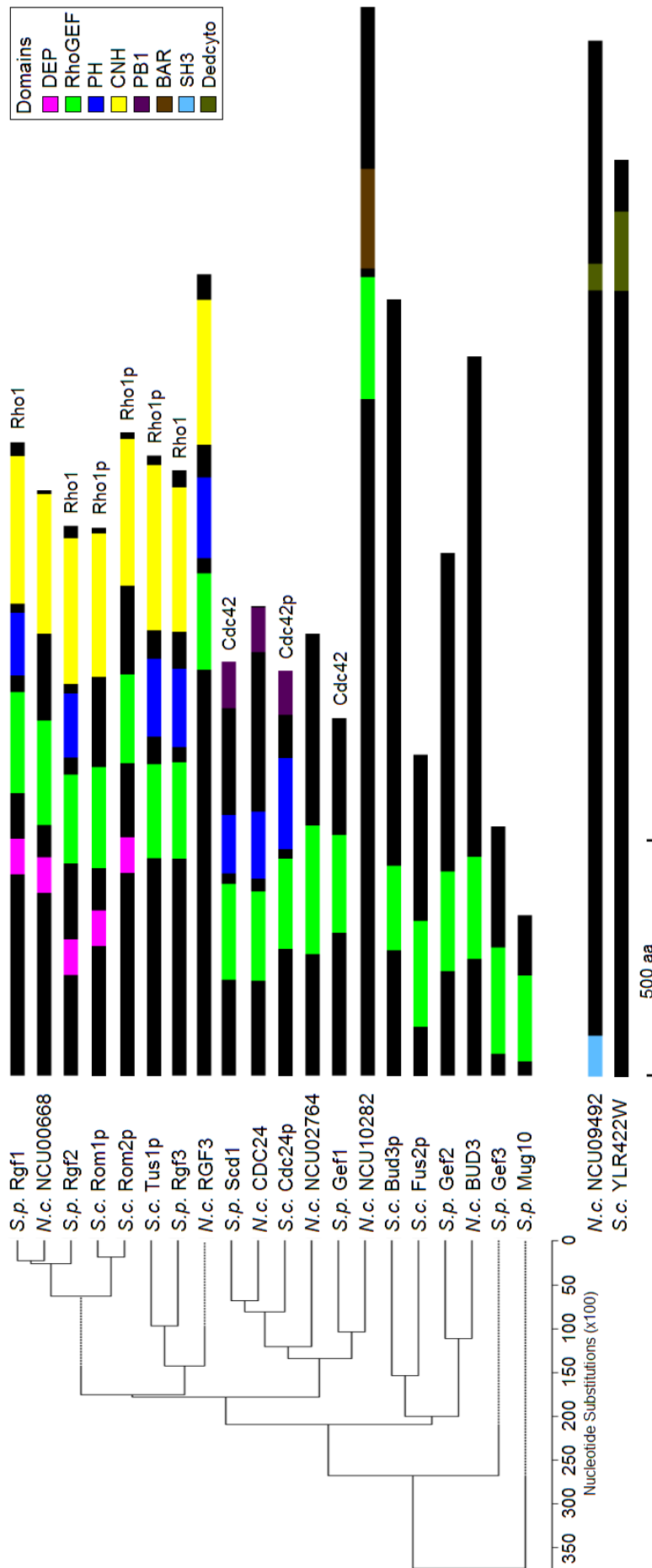


Figure 5: Comparison of putative RhoGEF proteins of *N. crassa* (*N.c.*), *S. cerevisiae* (*S.c.*) and *S. pombe* (*S.p.*). The phylogenetic tree is based on a ClustalW sequence alignment of the predicted RhoGEF domains of the DH family proteins only, while full-length proteins with all predicted domains are depicted drawn to scale. Putative CZH family RhoGEFs characterized by the presence of a Ded_cyto domain are shown at the bottom of the figure. Known target Rho GTPases are given at the end of the corresponding protein (Zheng et al., 1994; Chang et al., 1994; Ozaki et al., 1996; Schmelzle et al., 2002; Coll et al., 2003; Hirota et al., 2003; Tajadura et al., 2004; Mutoh et al., 2005). Colour coding for domains is indicated in the figure. See text and section 4.10.2 for details.

In Figure 4 and Figure 5, known target GTPases of Rho regulatory proteins are indicated. Specificity of the *N. crassa* RhoGAPs and GEFs might be deduced from that of close yeast homologues, but the reliability of such presumptions is uncertain. Moreover, the approach is limited to those proteins with close relatives; in addition, as stated, the Rho GTPase repertoires of the two yeasts and the filamentous fungus differ. Furthermore, although new findings published during the course of this work have added considerably to the current knowledge, target specificity has still only been determined for a subset of all yeast regulators. Therefore, I intended to prepare and perform comprehensive *in vitro* activity assays of putative Rho regulators of *N. crassa*.

5.1.2 Heterologous expression and purification of RhoGAP and RhoGEF constructs

In preparation of activity assays and to test *in silico* gene structure predictions by the Broad *Neurospora crassa* Database, cDNA covering the full-length coding regions of most of the *N. crassa* RhoGAP and RhoGEF genes was amplified from total RNA. Detailed results of the ensuing cDNA sequencing in comparison with the two latest annotation versions of the database, .3 and .4, are summarized in Supplementary Table 1 (p.104). With few exceptions, own findings conform to annotation version .4; deviations from the predictions are not accompanied by changes in type or order of conserved domains within the proteins encoded by the cDNAs. Full-length cDNAs were used as templates to amplify regions encoding RhoGAP or classical/non-classical RhoGEF domains (the latter sometimes in combination with PH or BAR domains) for insertion into a derivative of the pMal-c2X expression vector (New England Biolabs, USA). From the resulting vectors, RhoGAP and RhoGEF constructs (Table 4) were expressed as N-terminally maltose binding protein (MBP)-tagged fusion proteins in *E. coli* cells and enriched by affinity purification using amylose resin (see Supplementary Figure 1, p.103 for an overview of a representative purification procedure).

Table 4: RhoGAP and RhoGEF constructs expressed as MBP fusion proteins. For convenience, amino acid (aa) positions in the table refer to the current annotation version .4 of the Broad *Neurospora crassa* Database. Note that the NCU09492 non-classical GEF domain constructs are based on DHR-2 (Dock Homology Region-2) sequence alignments presented in (Côté and Vuori, 2002, 2006) rather than the less extended Ded-cyto domain predictions by InterProScan Sequence Search (see section 4.10.1).

	construct (MBP-...)	region (aa positions)
RhoGAPs	00196GAP	224-455
	00553GAP	531-742 (i.e.end)
	01472GAP	88-308
	02524GAP	1120-1317
	LRG1GAP	650-1035
	02915GAP	441-678 (i.e. end)
	07622GAP	110-626 (i.e. end)
	07688GAP	972-1169 (i.e. end)
	09537GAP	453-669
	10647GAP	369-572
RhoGEFs	00668GEF	517-928
	02764GEF	244-626
	02764GEFonly	244-530
	CDC24GEFPH (GEF/PH domains)	204-544
	BUD3GEF	230-637
	09492DHR	1290-1846
	09492DHRsht	1314-1824
	10282GEFBAR (GEF/BAR domains)	1425-1911

As shown in Figure 6, all fusion proteins can be purified in a soluble state. Only little degradation is observed, and a high degree of purity is achieved, making the proteins suitable for *in vitro* activity assays. Identity of selected fusion proteins with Coomassie stained bands was verified by performing parallel Western Blot experiments using MBP-antiserum (data not shown).

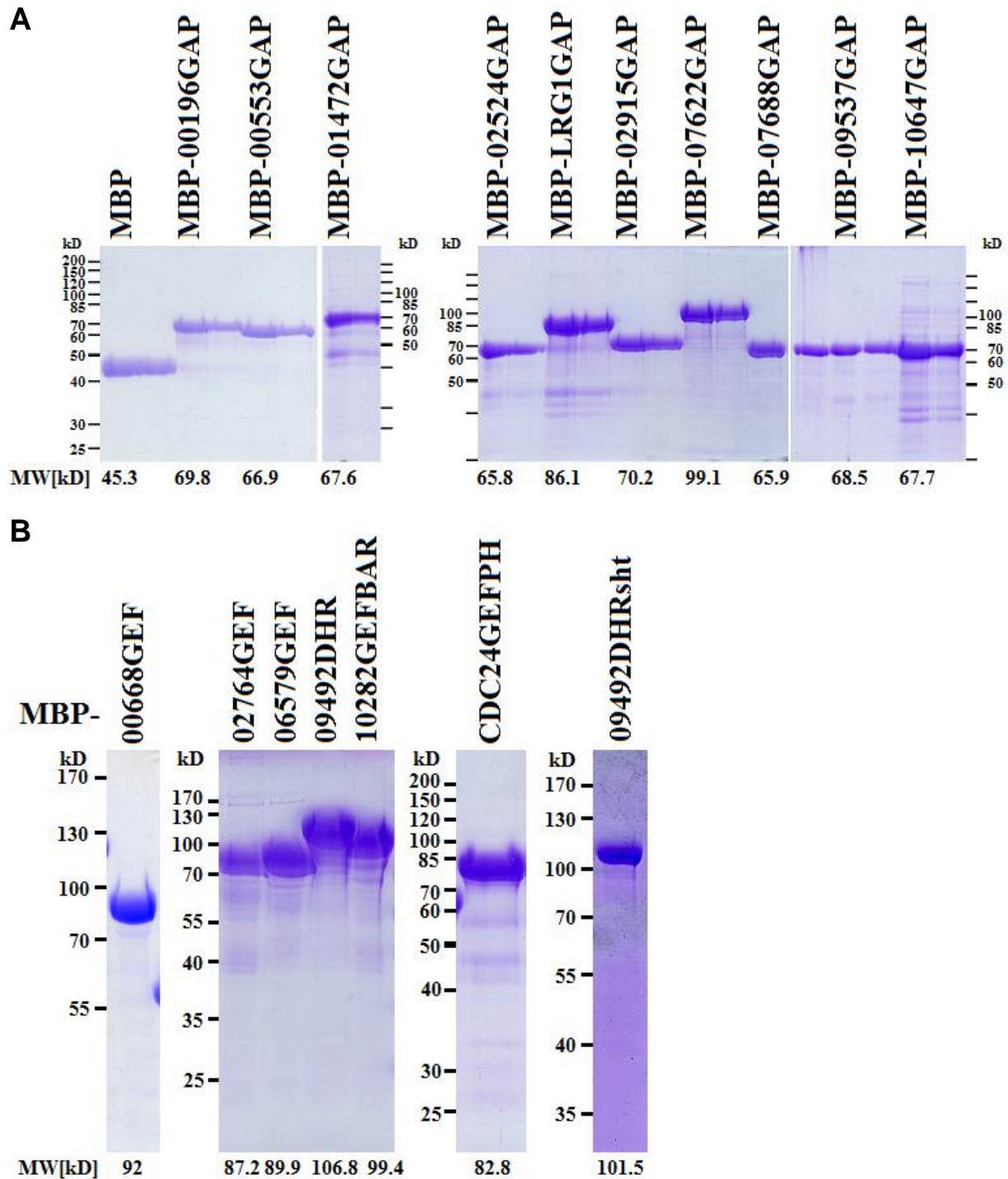


Figure 6: MBP fusion proteins of RhoGAP (A) and RhoGEF (B) constructs are soluble and can be enriched to a high degree of purity by affinity purification. Coomassie stained SDS polyacrylamide gels loaded with equal volumes of eluate fractions of the indicated constructs (two each in case of the RhoGAP constructs) are shown. Predicted fusion protein molecular weights (MW) are given below the corresponding lanes.

5.1.3 *In vitro* GEF activity assays

All RhoGEF constructs purified as described in the preceding section were tested for their ability to stimulate Rho GTPase nucleotide exchange activity *in vitro*. For this, the six *N. crassa* Rho GTPases were likewise purified as MBP fusion proteins (Figure 7 A), and their nucleotide exchange activity in the absence or presence of RhoGEF constructs (Figure 7 B) was assessed fluorospectrometrically employing mant-GDP (2'-(3'-O-(N'-methylanthraniloyl)-GDP). Presumably due to relief of quenching interactions existing in solution between the mant moiety and the nucleotide base, emission intensity of this fluorescent nucleotide analogue is enhanced two- to threefold upon binding to a protein, in this case the Rho GTPases (Scheidig et al., 1995; Jameson and Eccleston, 1997). Fluorescence emission was monitored over time, and the mean linear slopes of the kinetic curves calculated to serve as a measure for intrinsic and GEF-stimulated nucleotide exchange activity.

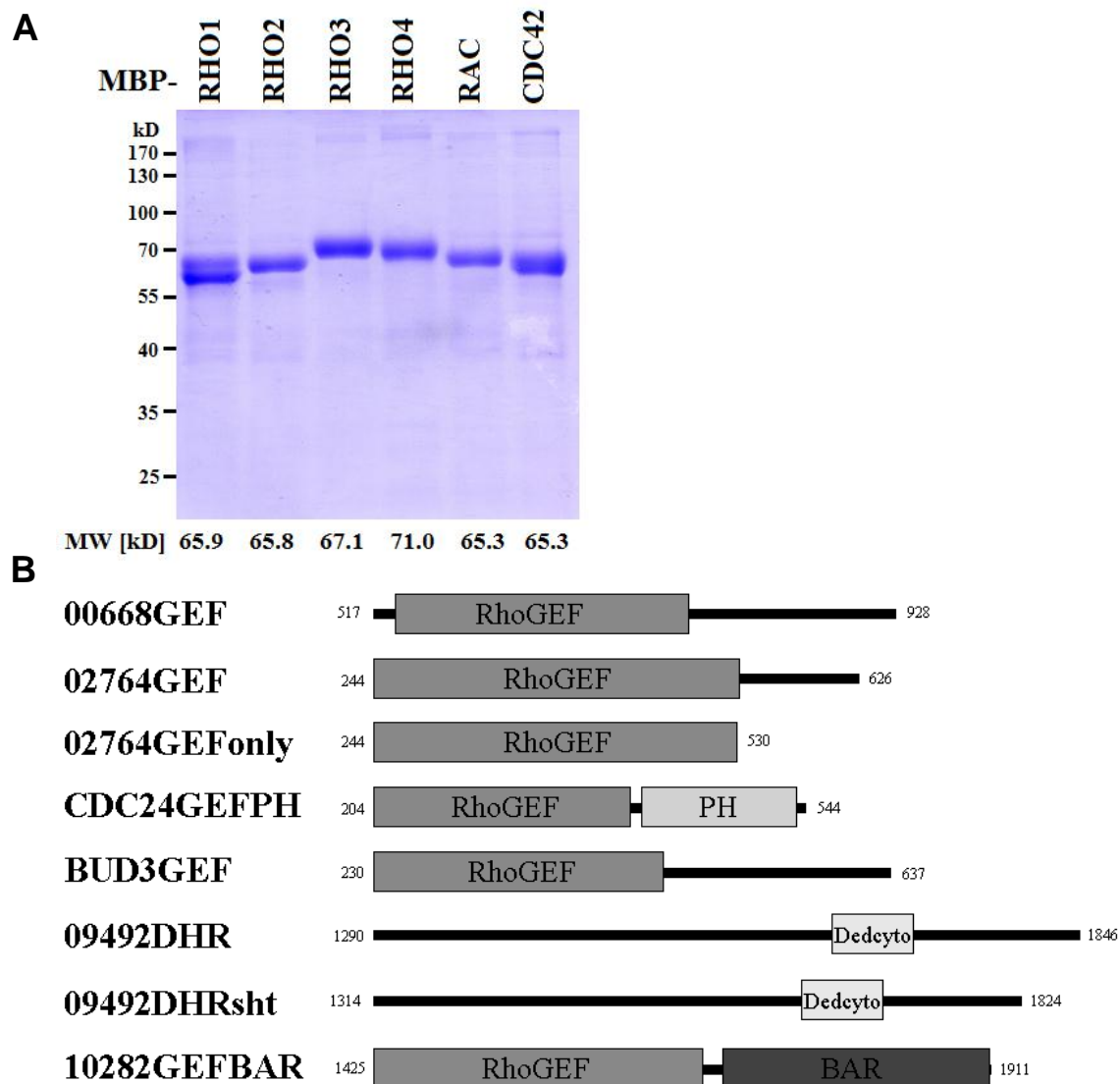


Figure 7: (A) Result of a representative purification of MBP-Rho GTPase fusion proteins used in *in vitro* GEF activity assays. A Coomassie stained SDS polyacrylamide gel loaded with equal volumes of eluate fractions of the indicated constructs is shown. Predicted fusion protein molecular weights (MW) are given below the corresponding lanes. (B) Schematic representation of RhoGEF constructs tested as MBP fusion proteins in *in vitro* activity assays. Numbers indicate amino acid positions referring to the corresponding full-length protein (annotation version .4 of Broad *Neurospora crassa* Database). Conserved domains predicted by InterProScan Sequence Search (see section 4.10.1) are depicted as boxes of varying shades of grey.

In the assays, all Rho GTPases exhibited intrinsic nucleotide exchange activity, although its extent differed considerably, with RHO1 and RHO2 displaying the lowest and RHO3 the highest exchange rates (cp. Supplementary Figures 2 to 5, p.106-109). While MBP alone had no effect on the exchange activity of any of the Rho GTPases (data not shown), several MBP-GEF fusion constructs clearly showed GEF activity towards specific Rho GTPases.

Diagrams in Figures 8 to 11 below summarize the results of the *in vitro* experiments for NCU00668, CDC24, BUD3 and NCU10282, respectively. Accompanying representative plots of fluorescence intensity over time as a measure for mant-GDP incorporation and thus nucleotide exchange activity for individual reaction samples can be found in Supplementary Figures 2 to 5 (p.106-109).

While NCU00668 functions as a RHO1-specific GEF (Figure 8), CDC24 stimulates nucleotide exchange in both RAC and CDC42 to a similar extent (Figure 9). RHO4 is the exclusive target GTPase of BUD3 (Figure 10), while NCU10282 strongly enhances nucleotide exchange in CDC42 (Figure 11 B). Note, however, that NCU10282 also increases the rate of nucleotide exchange in RAC, albeit more gradually, as evident in the curve progression when fluorescence emission intensity is plotted over time (Figure 11 A). Indeed, when calculated for a longer period of time (ca. 24 min), relative exchange activity of RAC in the presence of the GEF construct is 165 ± 37 (mean \pm SD, [%]), as compared to an intrinsic activity of 100 ± 14 .

Although two different constructs each were tested (see Figure 7 B), no *in vitro* GEF activity was observed for NCU02764 and NCU09492 (data not shown). As GEF activity of RGF3 towards RHO4 was determined in parallel to this work (Justa-Schuch et al., 2010), the complete set of putative *N. crassa* RhoGEFs has now been analyzed with regard to *in vitro* specificity (see Figure 12 for a summary).

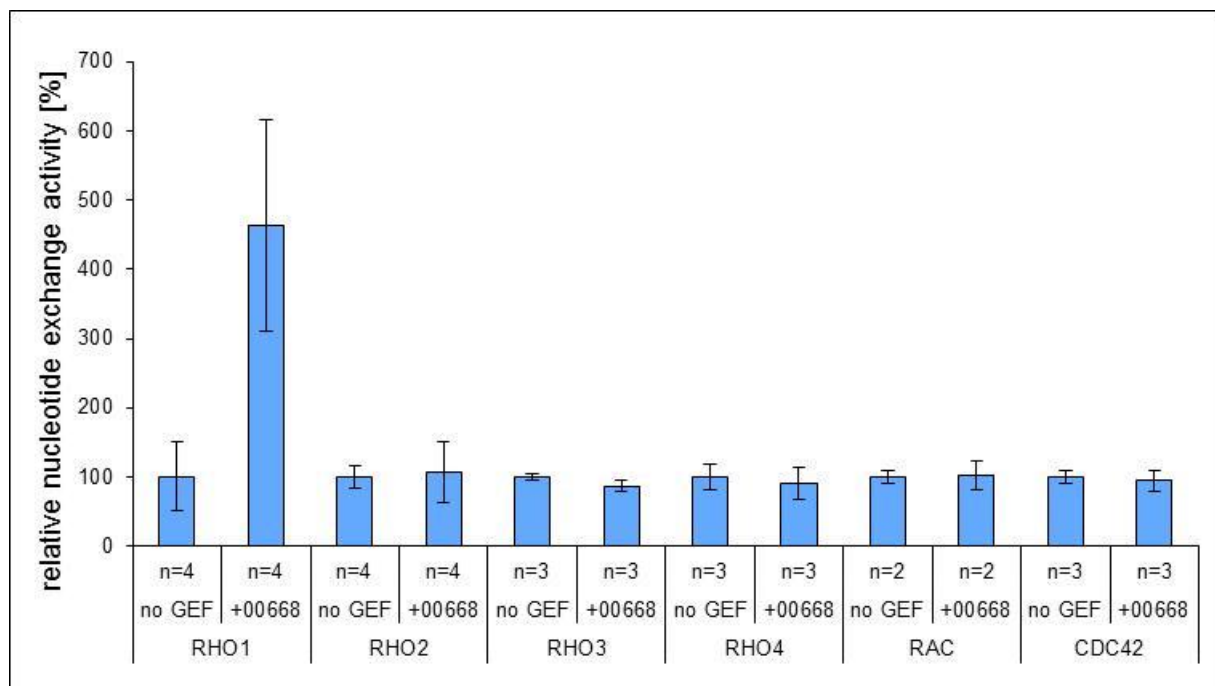


Figure 8: NCU00668 is a RHO1-specific GEF *in vitro*. Nucleotide exchange activity calculated as mean linear slope of fluorescence intensity over a period of ca. 24 minutes [arbitrary units/second] is displayed normalized to the intrinsic exchange activity (“no GEF”) of each Rho GTPase, which was set to 100% . n gives the number of independent experimental replicates, each of which was performed in technical duplicates. Error bars indicate standard deviation. See section 4.7.7 for details on data evaluation.

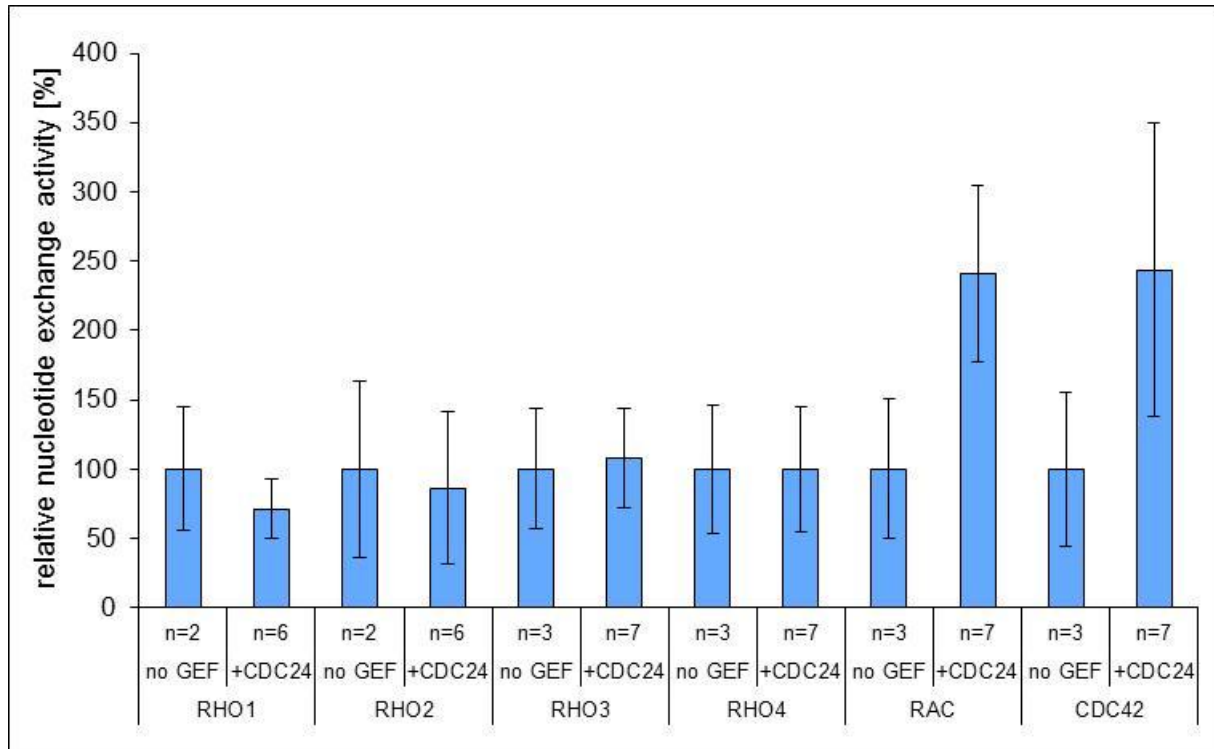


Figure 9: CDC24 specifically stimulates nucleotide exchange activity of both RAC and CDC42 *in vitro*. Nucleotide exchange activity calculated as mean linear slope of fluorescence intensity over a period of ca. 24 minutes [arbitrary units/second] is displayed normalized to the intrinsic exchange activity (“no GEF”) of each Rho GTPase, which was set to 100%. n gives the number of independent experimental replicates, each of which was performed at least in technical duplicates. Error bars indicate standard deviation. See section 4.7.7 for details on data evaluation.

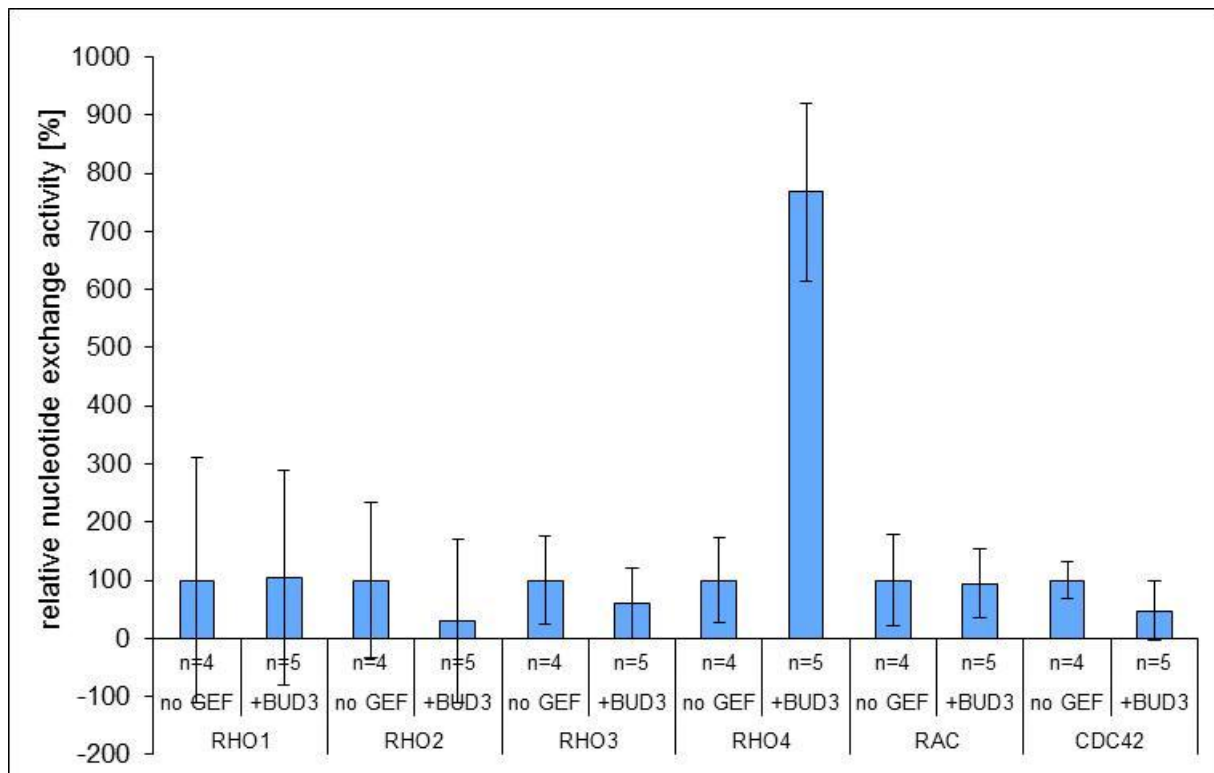


Figure 10: BUD3 is a RHO4-specific GEF *in vitro*. Nucleotide exchange activity calculated as mean linear slope of fluorescence intensity over a period of ca. 8 minutes [arbitrary units/second] is displayed normalized to the intrinsic exchange activity (“no GEF”) of each Rho GTPase, which was set to 100%. n gives the number of independent replicates, each of which was performed in technical duplicates. Error bars indicate standard deviation. See section 4.7.7 for details on data evaluation.

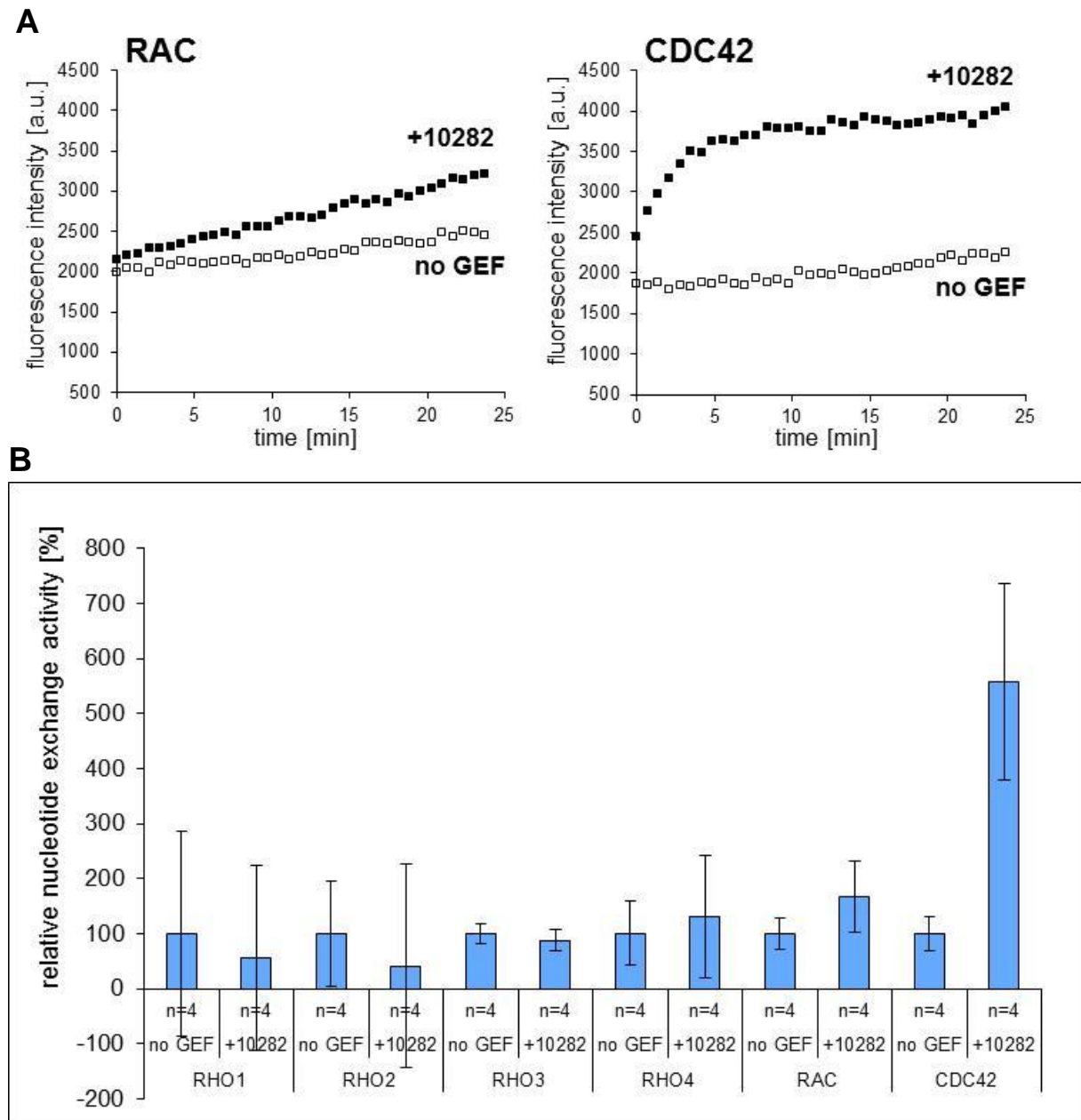


Figure 11: NCU10282 is a RhoGEF acting on CDC42 and, to a lesser extent, on RAC *in vitro*. (A) Curves of fluorescence emission intensity [a.u. =arbitrary units] plotted over time [min] for representative individual experiments testing the nucleotide exchange activity of RAC and CDC42 in the absence (“no GEF”) or presence (“+10282”) of MBP-10282GEFBAR. (B) Nucleotide exchange activity calculated as mean linear slope of fluorescence intensity over a period of ca. 8 minutes [arbitrary units/second] is displayed normalized to the intrinsic exchange activity (“no GEF”) of each Rho GTPase, which was set to 100%. n gives the number of independent replicates, each of which was performed in technical duplicates. Error bars indicate standard deviation. See section 4.7.7 for details on data evaluation.

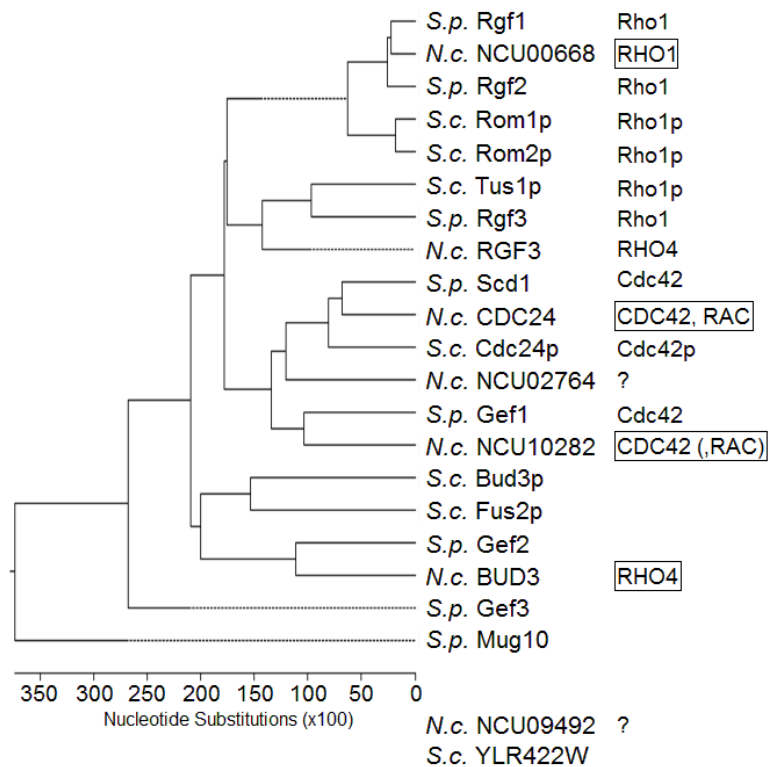


Figure 12: Summary of RhoGEF specificities in *S. cerevisiae* (*S.c.*), *S. pombe* (*S.p.*) and *N. crassa* (*N.c.*). Target GTPases newly determined in this study are highlighted by frames. Question marks denote *N. crassa* RhoGEFs showing no *in vitro* stimulatory activity under the assay conditions. See legend of Figure 5 for details on phylogenetic tree construction and references.

5.2 Analysis of the CDC42/RAC/CDC24 module in *N. crassa*

After determining *in vitro* specificity of *N. crassa* RhoGEFs, *in vivo* functions of selected GEF/Rho GTPase modules in polar growth of the fungus were to be analyzed in more detail. First, the CDC42/RAC/CDC24 module, for which several strains bearing mutations in the corresponding genes are available, was scrutinized. Unfortunately, in contrast, no mutant strains are currently available for NCU10282, preventing the study of the cellular role of this GEF in regulation of the two Rho GTPases. Preliminary plans to perform a complete gene knockout of NCU10282 were postponed as partial cDNA sequencing revealed highly repetitive sequences within the 5' part of the predicted coding region, suggesting misannotation of the translation start site (Supplementary Table 1, p.104) and thus precluding the application of the well-proven *Neurospora* standard knockout protocol (cp. section 4.5).

5.2.1 Morphological characterization of mutants

The *Neurospora* genome project (see section 4.5) had generated a heterokaryotic deletion strain of *cdc-24* (FGSC #11721); however, homokaryotic knockout ascospores obtained by backcrossing with the wild type only rarely germinated apolarly and ultimately lysed, indicating that *cdc-24* is essential for viability and making deletion mutants unsuitable to study the morphology of CDC24-deficient hyphae.

Thus, to analyze the impact of compromised CDC24 function on hyphal morphology, temperature-sensitive strains originating from a UV mutagenesis screen and thought to carry

mutant *cdc-24* alleles, as suggested by their phenotypic rescue upon transformation with the wild type *cdc-24* gene (Seiler and Plamann, 2003), were used instead. They were grown at room temperature and transferred to restrictive temperature to assess the phenotype caused by depletion of functional CDC24 (Figure 13).

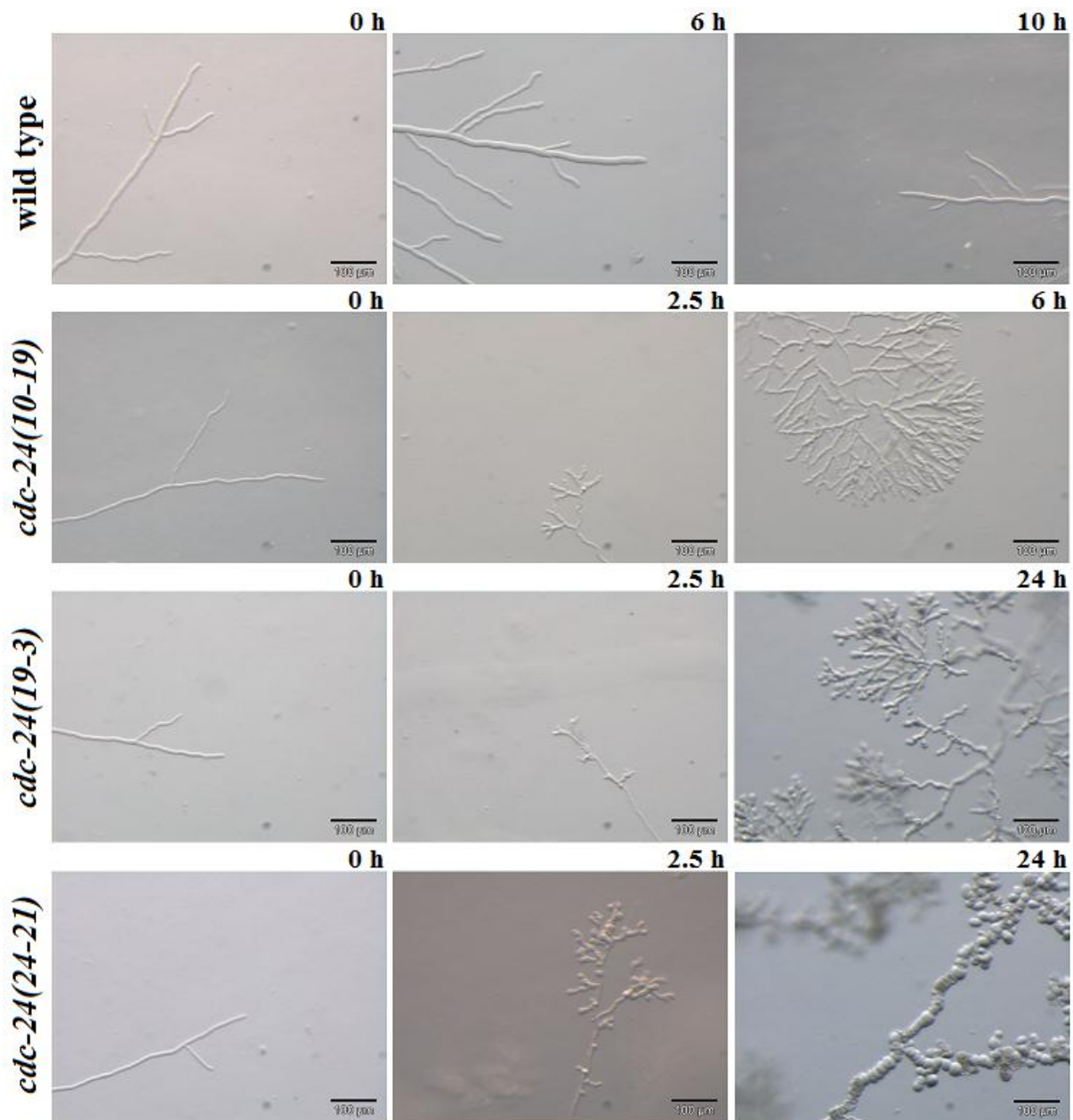


Figure 13: Hyphae of conditional *cdc-24* mutant strains *cdc-24(10-19)*, *cdc-24(19-3)* and *cdc-24(24-21)* grown under restrictive conditions exhibit polarity defects. Wild type hyphae are shown for comparison. Time points indicate hours after transfer from permissive to restrictive temperature. Scale bars are 100 µm.

When cultivated at permissive temperature, all three mutant strains exhibit a normal hyphal extension and branching pattern comparable to that of wild type (Figure 13, left column). After transfer to restrictive temperature (middle and right columns), however, polarity defects of varying severity occur. For instance, after few hours at 37°C, *cdc-24(10-19)* displays pronounced hyperbranching (especially in the vicinity of apical tips), ultimately resulting in the formation of tree-like hyphal structures. At later stages, a slight swelling of hyphae can be observed (data not shown). Likewise, *cdc-24(19-3)* hyphae branch excessively; this is

accompanied by apolar swelling of apical tips and, to a lesser extent, subapical hyphal regions after prolonged incubation at restrictive temperature. The most severe morphological defects are observed in *cdc-24(24-21)*. Already after one hour at 37°C, hyphal tips lose growth polarity and swell bulbously (data not shown). Later, hyphae exhibit hyperbranching and eventually resemble chains of spheres as apical and subapical hyphal compartments expand isotropically, with some lysing at an advanced stage.

When conidia of the mutant strains are germinated at 37°C, polarity defects of similar characteristics are observed (Figure 14). After 22 hours, *cdc24(10-19)* has formed a hyperbranched colony, while similar hyperbranching is accompanied by apical and, to a lesser degree, subapical swelling of hyphal compartments in *cdc-24(19-3)*. In accordance with the severe polarity defects of the strain, *cdc-24(24-21)* conidia are unable to give rise to colonies at restrictive temperature; growth is restricted to isotropic expansion of the conidia, but no formation of polar germ tubes occurs, which underlines the importance of CDC24 not only for maintenance but also for establishment of polarized growth.

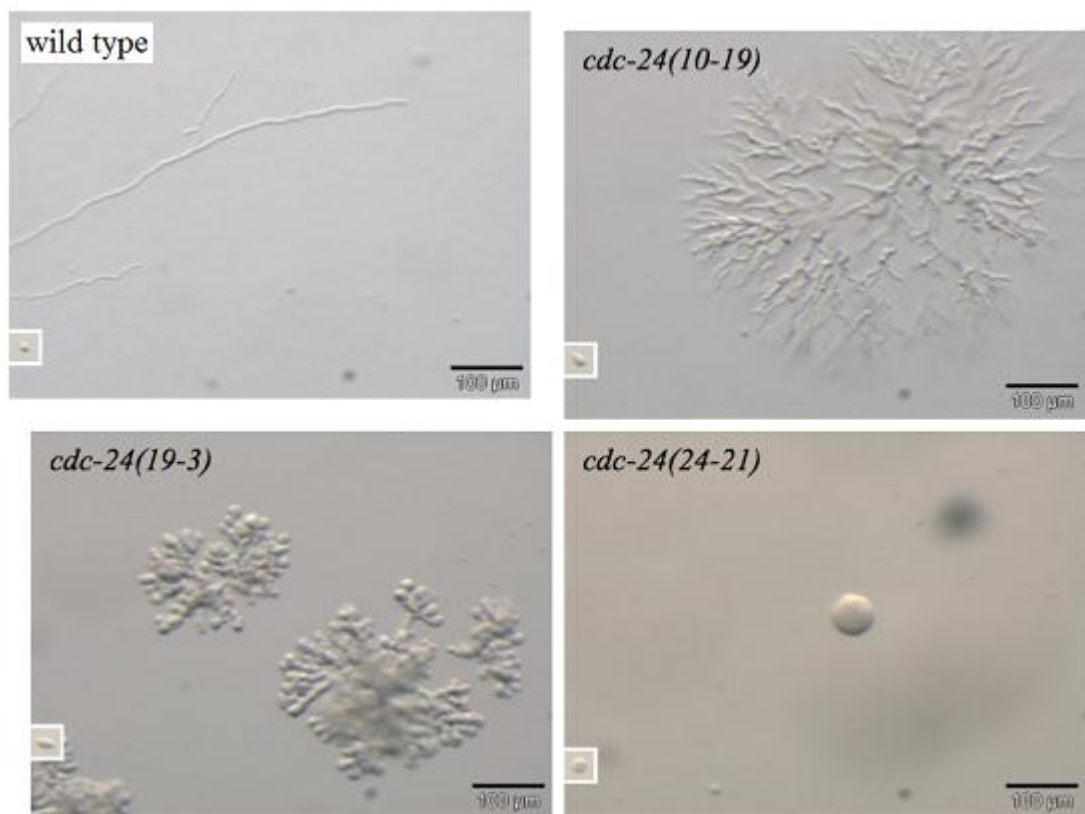


Figure 14: Conidial germination of conditional *cdc-24* mutant strains *cdc-24(10-19)*, *cdc-24(19-3)* and *cdc-24(24-21)* at restrictive temperature. Pictures were captured after 22 hours of incubation. Insets display conidia at start of incubation. Wild type (incubated for 12 hours only) is shown for comparison. Scale bars are 100 µm.

In vitro results had established CDC24 as an activator of both RAC and CDC42 (Figure 9); therefore, I was also interested in the morphology of mutants affected in function of the two target GTPases, whose phenotypic characteristics might help understand the *in vivo* regulatory influence of CDC24. For such morphological analyses, deletion mutants of *rac* and *cdc-42* as well as loss-of-function and temperature-sensitive strains with deficiencies in the GTPases were available; the latter had been generated by RIP (repeat induced point mutation) mutagenesis (see section 4.5).

As evident in Figure 15, hyphae of *Δrac microconidia* and the two loss-of-function mutants *rac(11-21)* and *rac(11-23)* are characterized by excessive tip branching, leading to the formation of overall tree-like structures. The morphology of these strains thus closely resembles that of *cdc-24(10-19)* (cp. Figures 13 and 14). Strains lacking functional CDC42, i.e. *cdc-42(18-7)* and *Δcdc-42*, on the other hand, exhibit very compact colonial growth with some irregularity in branching and slight swelling of hyphal compartments (Figure 15).

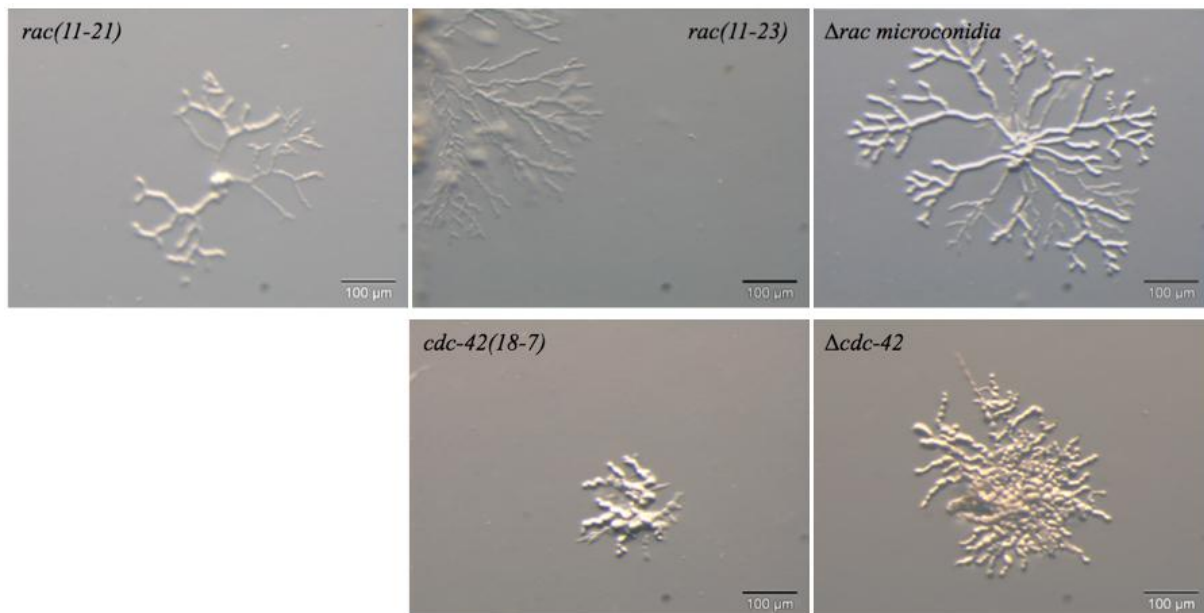


Figure 15: Hyphae of *rac* and *cdc-42* loss-of-function and deletion mutants exhibit polarity defects. Loss-of-function mutant strains *rac(11-21)*, *cdc-42(18-7)* and *rac(11-23)* and deletion mutant strains *Δrac microconidia* and *Δcdc-42* were grown at room temperature. Scale bars are 100 μm.

Consistently, hyphae of conditional *rac* and *cdc-42* mutant strains exhibit similar polarity defects upon transfer to restrictive temperature (Figure 16), while their morphology is more or less indistinguishable from that of wild type when grown at permissive temperature. After shift of colonies to 37°C, marked hyperbranching at the apex of hyphae is observed for *rac(7-1)*, effecting a tree-like structure of hyphae towards the edge of the colony. Some *cdc-42(18-4)* hyphae also exhibit excessive apical tip branching (cp. Supplementary Figure 6, p.110, and data not shown); additionally, extensive formation of subapical branches, themselves usually not further ramified, gives hyphae of the strain an overall barbed wire appearance.

The isolation of a double deletion strain of *rac* and *cdc-42* by crossing the two single deletion strains had not been possible despite several attempts, suggesting synthetic lethality of the two GTPases. However, a strain bearing conditional mutant alleles of both GTPase genes, *rac(7-1); cdc-42(18-4)*, had been successfully generated (S. Seiler, unpublished). In accordance with the proposed requirement of at least RAC or CDC42 function for viability, this double mutant strain shows strong synthetic defects in growth and polarity upon transfer to 37°C (Figure 16). Soon after the temperature shift, pronounced apical hyperbranching and concomitant swelling of apical and subapical hyphal compartments occur; at later stages, frequent lysis of the unusually short compartments is observed. Intriguingly, this phenotype resembles that of the most severely affected *cdc-24* temperature-sensitive mutant strain, *cdc-24(24-21)* (Figure 13).

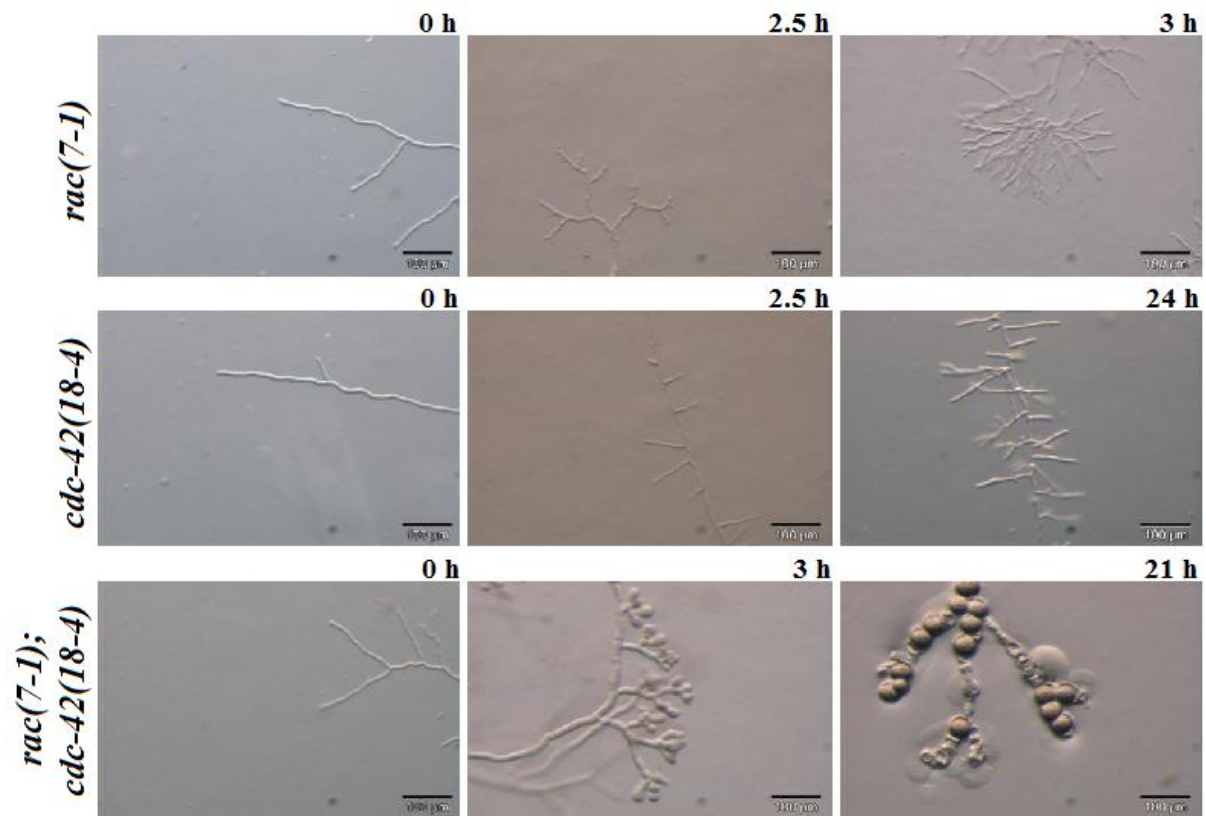


Figure 16: Conditional *rac* and *cdc-42* mutant strains *rac(7-1)* and *cdc-42(18-4)* grown under restrictive conditions exhibit polarity defects, which are markedly exacerbated in the double mutant *rac(7-1); cdc-42(18-4)*. Time points indicate hours after transfer from permissive to restrictive temperature. Scale bars are 100 μm .

The impossibility to obtain a double deletion mutant of *rac* and *cdc-42* as well as the synthetic effect of the temperature-sensitive mutations revealed in the exacerbated polarity defects of the conditional double mutant compared to the parental strains hint at a shared important, possibly essential function of the two GTPases in polar growth. At the same time, sheer redundancy of function seems unlikely in face of differences in the nature of morphological defects exhibited by the single mutants.

In order to test if overexpression of one GTPase can compensate for deficiency in the other, plasmids for expression of N-terminally 3xmyc-tagged RAC and CDC42 were generated and used to transform the conditional mutant strains. As shown in Supplementary Figure 6 (p.110), the morphological defects of *cdc-42(18-4)* are specifically suppressed by overexpression of CDC42, but not RAC (or the 3xmyc tag alone), which supports the notion of distinct functions of the two GTPases. While the converse test of phenotypic rescue of *rac(7-1)* is still under way, it should be noted that the 3xmyc-RAC fusion protein is expected to be functional, because a similar N-terminally YFP-tagged construct is able to complement a *rac* deletion mutant strain (see section 5.2.3).

5.2.2 *In vitro* GEF activity of mutant CDC24 versions

Morphological defects of the three temperature-sensitive *cdc-24* strains introduced above were specifically suppressed by overexpression of RAC, but not CDC42 (S. Seiler, personal communication). In addition, the *cdc-24* mutant strains less strongly affected in growth appeared more similar to *rac* than to *cdc-42* mutants, although the most severely impaired strain resembled the double mutant deficient in function of both CDC24 target

GTPases. Therefore we wondered if the GEF proteins encoded by the mutant alleles, in contrast to wild type CDC24, might stimulate nucleotide exchange of these GTPases with different efficiency. To test this hypothesis, partial cDNA encoding the GEF and PH domains of CDC24 (aa 204-544) was prepared from the mutant strains to generate bacterial expression plasmids.

cdc-24(10-19): F254S* *cdc-24(19-3): L444S* *cdc-24(24-21): Q264R

<i>N. crassa</i>	TTGFVKVTSVINYLVDLAEKRGLLQLTLPYPEDDIT-----QFGSKMTHRDIYIVRELV	219
<i>A. nidulans</i>	TIGFTKVIKMNVRVLDILEIQGQLKKPS-DTAMAAP-----AAGRKLTKREHILKELL	187
<i>U. maydis</i>	TNGFVKVVRTINRLLDVFEERGLLIETN--RKSDND-----DLDHPSSDDRAKVIRELL	282
<i>S. pombe</i>	TAPLVRALQTIELLLKYEVSNTTKSSSTPSPSTDDNVPTG--TLNSLIASGRRVTAELY	237
<i>C. albicans</i>	AQDLIKIIDVINKLLAEYS DASDSGGGDEDVNM DVQ-----ITDERSKVFREII	286
<i>S. cerevisiae</i>	TSQLVKVLEVVELTMNSSPTIFPSKSKTQQIMNAENQHRHQPPQSSKKNHEYVKIIEFV	287
:	: : : : : :	: * :
<i>N. crassa</i>	DTERKYVQDLENLHDLKRTLEHRSVIPGEFIHDIFFLNINAILDHRKFLIRVETTNSMPQ	279
<i>A. nidulans</i>	ETERDYVHHLQNLQALKKELEDTGALTGDASHQIFLNLNLLDFSRFLIRLEQHYARPE	247
<i>U. maydis</i>	TTERKYVQDLEVMQNYARALAQYDILPPTLHNLFFGNLNKLVDFQRRFLICVEENVR RTP	342
<i>S. pombe</i>	ETELKYIQDLEYSNYMVILQQKQILSQDTILSIFINLNEILDFQRRFLVGLMNLSPV	297
<i>C. albicans</i>	ETERKYVQDLELMCKYRQDLIEAENLSSEQIHLFFPNLNEIIDFQRRFLNGLECNINVP I	346
<i>S. cerevisiae</i>	ATERKYVHDLEILDKYRQQLDSNLITSEELYMLFFPNLGDAIDFQRRFLISLEINALVEP	347
**	*.:*: : * . : : : * * : : * : : * * : *	
RhoGEF		
<i>N. crassa</i>	ARQEWGSLFVTAEEN-FGIYQPFIANQ-RKAAQVATQVFDKIQEAG-----HPVACDFNT	332
<i>A. nidulans</i>	EQQNWGELEFIQH EEA-FRQYEPFIANQ-MRCDKTCQKEWDKIQAAPRSPDLQMQVAQPAT	305
<i>U. maydis</i>	DEQHFHGHVFMTEED-FSVYEPFCANYNLALDLINQEAHNLIRLKGMPSAEGCYLDPAYE	401
<i>S. pombe</i>	EEQRLGALFIALEEG-FSVYQVFCNFPNAQQLIIDNQNQLLKVAN-----LLEPSYE	349
<i>C. albicans</i>	RYQRIGSVFIHASLGFNAYEPWTIGQLTAIDLINKEAANLKKSS-----LLDPGFE	399
<i>S. cerevisiae</i>	SKQRIGALFMHSHKF-FKLYEPWSIGQNAAEFLSSTLHKMRVDES----QRFIINNKLE	402
*	* . * : * : . * * : : 	
<i>N. crassa</i>	LDGFLLKPMQRLVKYPLLLKDLLKKS-EDEHT-----KEDLAAGIAAAERVL MKA	381
<i>A. nidulans</i>	LNGFFVKPFQRLTKYPLMLSELRKQI-EDPDL-----QADISRAIDSIQSVLDAA	354
<i>U. maydis</i>	LPTFMIKPVQRICKYPLLEQLLKKTSDDAPR-----YQELQNGLEV MRITDKV	451
<i>S. pombe</i>	LPALLIKPIQRICKYPLLNQLLKGTPSGYQY-----EEELKQGMACVVRVANQV	399
<i>C. albicans</i>	LQSYILKPIQRICKYPLLLKELIKTSPEYSKQDPHGSSSSTSFNELLVAKTAMKELANQV	459
<i>S. cerevisiae</i>	LQSFYKPVQRLCRYPLLVKELLAESSDDNNT-----KELEAALDISKNIARSI	451
*	: * * : * : : * * : * : : * * : : * * : : * * : : * * :	
<i>N. crassa</i>	NSAVDKNILEEALQDLIHRVDDWKS HKVDNFGSLL LHGVYTVITGKSEQEKD-QYEIYLF	440
<i>A. nidulans</i>	NDAIDKEQLAAAFVELDERVDDWKALKIETFGELLRFGTFTVIKNDNNKDSEREYHIYLF	414
<i>U. maydis</i>	NETSRLQGNAQLVKELEFRVEDWKGHNIKTFGLLLSDVFMVAKS----DTEREYHVYLF	507
<i>S. pombe</i>	NETRIHENRNAIIELEQRVIDWKGYSLQYFGQLLVWDVVNVCKA----DIEREYHVYLF	455
<i>C. albicans</i>	NEAQRRAENIEHLEKLERVGNWRGFNLDAQGELLFHGQVGVKDA----ENEKEYVAYLF	515
<i>S. cerevisiae</i>	NENQRRTENHQVVKLYGRVVNWKGYRISKFGELLYFDKVFISTTSSSEPEREFVYLF	511
*	. . * . . * * * : * : : . * * * . : : : : * * *	
PH		
<i>N. crassa</i>	ENILLCCKELTTTKAKD-----KKDKTRSSVPKLRNKFALQLKGRIFMNTVDV	491
<i>A. nidulans</i>	ERILLCCKDINPNKQKS-----RLVGGSKDKPNTSGKGPRLVLKGRIFYMANVTDIV	465
<i>U. maydis</i>	EKILLCCKELAPAAQKSNKNSLLKQKNGLGAATAGGKKPKTTLQLKGRIFINVTGAF	567
<i>S. pombe</i>	EKILLCCKEMSTLKRQAR-----SISMNKKTKRLDSLQLKGRILTSNITTV	502
<i>C. albicans</i>	EKIVFFFTIIDDNKKSD-----KQEKSKFSTRKRSTSSNLSSST	555
<i>S. cerevisiae</i>	EKIIILFSEVVTKKSAS-----SLILKKSSTASISASNITDNN	551
*	*.:* : : : : : : :	* : :

Figure 17: Multiple sequence alignment of CDC24 homologues of various fungi. The alignment was produced using ClustalW2 (<http://www.ebi.ac.uk/Tools/msa/clustalw2/>). RhoGEF and part of the PH domain regions predicted for *N. crassa* CDC24 by InterProScan Sequence Search (see section 4.10.1) are indicated with a red and grey bar, respectively. Amino acid substitutions resulting from the mutations identified in *cdc-24* alleles (10-19), (19-3) and (24-21) are summarized above and their positions are highlighted within the alignment in blue, pink and green, respectively. Note that only the central part of the alignment is shown.

Sequence analysis of the cDNAs revealed mutations causing substitutions of highly conserved amino acids located within the predicted RhoGEF domain (*cdc-24(10-19)* and *cdc-24(24-21)*) or the adjacent PH domain (*cdc-24(19-3)*) of CDC24 (Figure 17). None of the amino acid substitutions affected sites predicted by the NCBI Conserved Domains Database (accessible at <http://www.ncbi.nlm.nih.gov/sites/entrez?db=cdd>) to be directly involved in GTPase interaction.

The two target GTPases RAC and CDC42 and the wild type and mutant versions of CDC24 fragments were purified as MBP fusion proteins (Supplementary Figure 7, p.111) and subjected to *in vitro* GEF assays as described above. In addition to standard tests at 21°C, GEF activity was also evaluated at 37°C to account for a putative temperature-sensitivity of the mutant proteins.

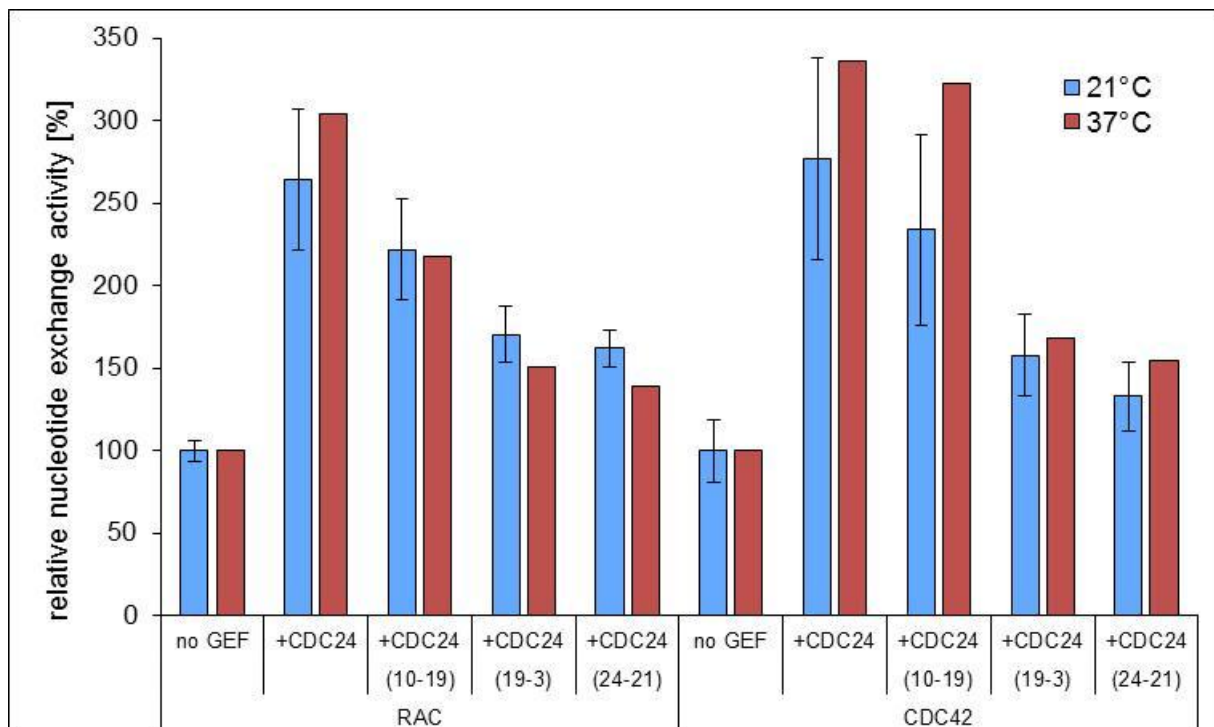


Figure 18: Mutant RhoGEF-PH fragments CDC24(10-19), (19-3) and (24-21) exhibit reduced *in vitro* GEF activity towards both RAC and CDC42 compared to the wild type construct. Nucleotide exchange activity calculated as mean linear slope of fluorescence intensity over time [arbitrary units/second] is displayed normalized to the intrinsic exchange activity (“no GEF”) of each Rho GTPase, which was set to 100%. For 21°C (blue columns), data from two independent measurements (with two technical replicates of each sample) over a period of ca. 20 minutes were evaluated; for 37°C (red columns), results are based on one experiment performed in technical triplicates, with data points of the first ca. 8 minutes included in calculations. Error bars indicate standard deviation. See 4.7.7 for details on data evaluation.

As apparent in Figure 18 and Supplementary Figure 8 (p.112), alteration of single amino acids in the CDC24 mutant constructs affects their ability to enhance nucleotide exchange in RAC and CDC42. Notably, the extent of reduction in GEF competency of the mutant proteins correlates well with the severeness of morphological defects observed in the corresponding mutant strains (cp. Figure 13): While CDC24(10-19) GEF activity is only slightly impaired, the stimulatory effect of the other two mutant proteins is reduced to about one third of that of the wild type. Contrary to initial expectations, however, none of the mutant proteins shows altered selectivity with regard to the two target GTPases. Although saturation of exchange reaction was reached faster and absolute values of exchange activities were about doubled

in comparison with those calculated for 21°C (data not shown), the same general findings applied when the GEF assay was performed at elevated temperature.

5.2.3 Analysis of the subcellular localization of RAC and CDC42

To further elucidate the relationship and cellular functions of CDC24, RAC and CDC42, I aimed to analyze and compare the subcellular localization of these proteins fused to a fluorescent protein tag. The vectors generated for this purpose generally target the respective expression cassette to the *his-3* locus and enable restoration of histidine prototrophy of a *his-3⁻* strain used for transformation (see sections 4.4.6 and 4.5 for details).

Plasmids intended for expression of C-terminally YFP- or GFP-tagged versions of CDC24 under control of the *ccg-1* promoter were constructed, but so far no transformants with detectable expression levels of the fusion proteins could be recovered.

For localization analysis of RAC and CDC42, a vector (pPgpd_YFP) allowing expression of YFP fusion proteins tagged at their N-termini was devised to foreclose interference of a C-terminal tag with the utilization of the putative C-terminal prenylation motifs present in both GTPases. In plasmids based on this vector, the *gpdA* promoter of *A. nidulans* (Punt et al., 1988) controls fusion protein expression.

Transformants exhibiting distinct YFP fluorescence clearly above background (data not shown) were readily obtained, but confirmation of fusion protein expression in these and various positive control strains by immunodetection was not possible using the α -GFP antibody available. Primary transformants were backcrossed to the corresponding Δ *rac* *microconidia* and Δ *cdc-42* deletion strains to eliminate the untagged wild type copy of the gene; suppression of the knockout-associated growth defects (cp. Figure 15) in the resulting hygromycin-resistant offspring (bearing the deletion mutation at the endogenous gene locus) proved functionality of the YFP-tagged fusion proteins.

When YFP-RAC is expressed in the wild type background, fluorescence is distributed throughout the cytoplasm with accumulation at septa and vacuolar membranes (data not shown). In the deletion background, additional signals are regularly observed at the apical membrane of growing hyphal tips (Figure 19 A).

Interestingly, in line with the proposed functional overlap between the two GTPases, YFP-CDC42 shows a highly similar localization pattern (Figure 19 B). Both in the wild type (not shown) and knockout background, it localizes diffusely throughout the cytoplasm; accumulation is observed at septa and at vacuolar membranes, and in several hyphae fluorescence is also visible as an apical cap.

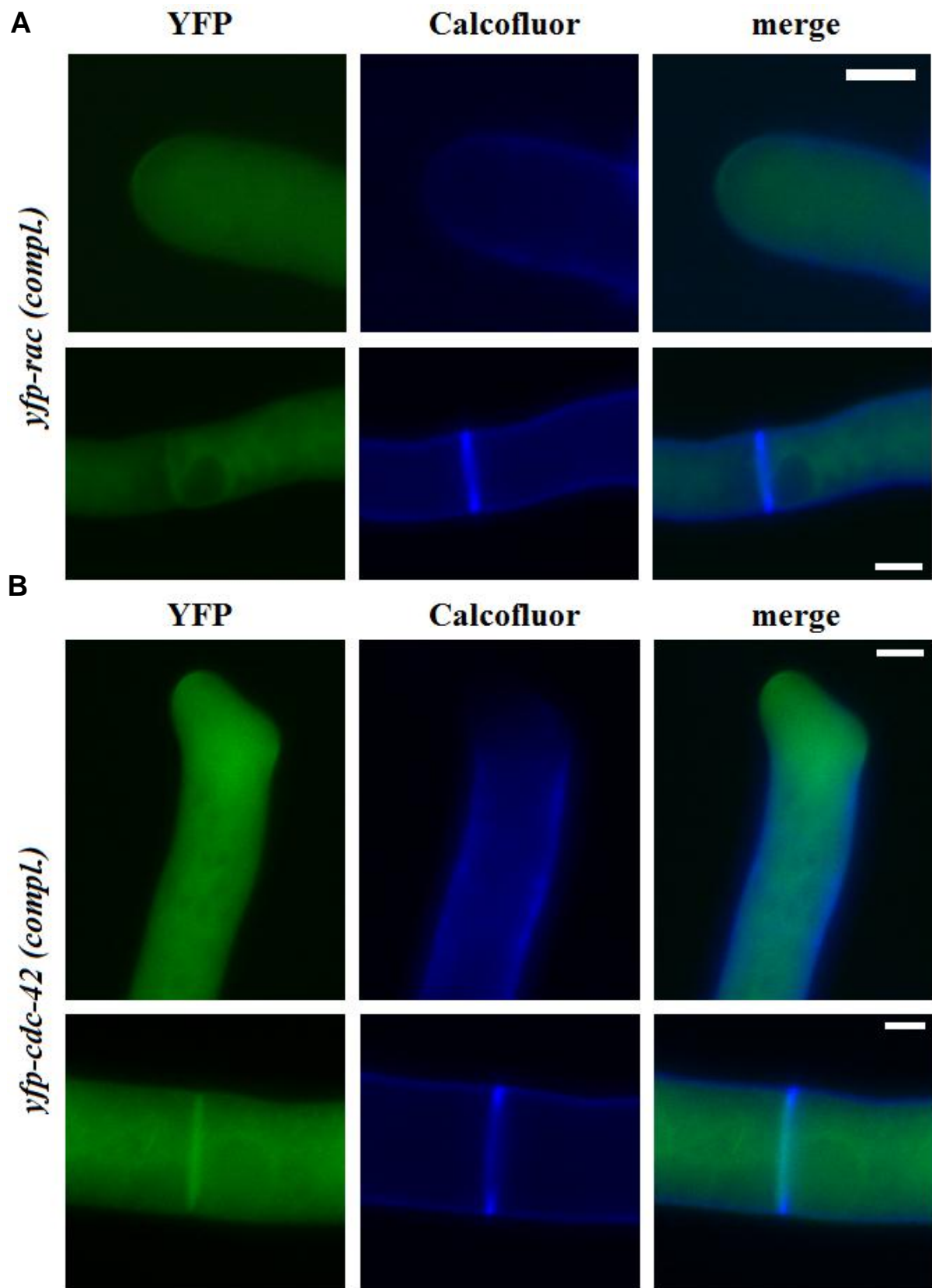


Figure 19: Both YFP-RAC and YFP-CDC42 localize throughout the cytoplasm and accumulate at septa, at the vacuolar membrane and as cap-like structures at the apical membrane. Images show distribution of YFP-RAC (A) and YFP-CDC42 (B) in the respective deletion background. Cell wall and septa stained with calcofluor white (DAPI filter) are shown for orientation. Scale bars are 5 μ m.

5.3 Analysis of the RHO1/RHO2/NCU00668 module in *N. crassa*

5.3.1 Potential autoregulatory effect of the DEP domain on GEF activity of NCU00668

As outlined above, the GEF domain of the *N. crassa* RhoGEF NCU00668 specifically enhances *in vitro* nucleotide exchange in RHO1 (Figure 8). In contrast, in initial GEF activity assays, a construct comprising the DEP, GEF and CNH domains of the RhoGEF protein had never been able to activate the GTPase. An intermediate length construct encompassing the GEF and CNH domains, on the other hand, clearly exhibits GEF activity, too, although its stimulatory effect is less pronounced than that of the shortest construct (Figure 20).

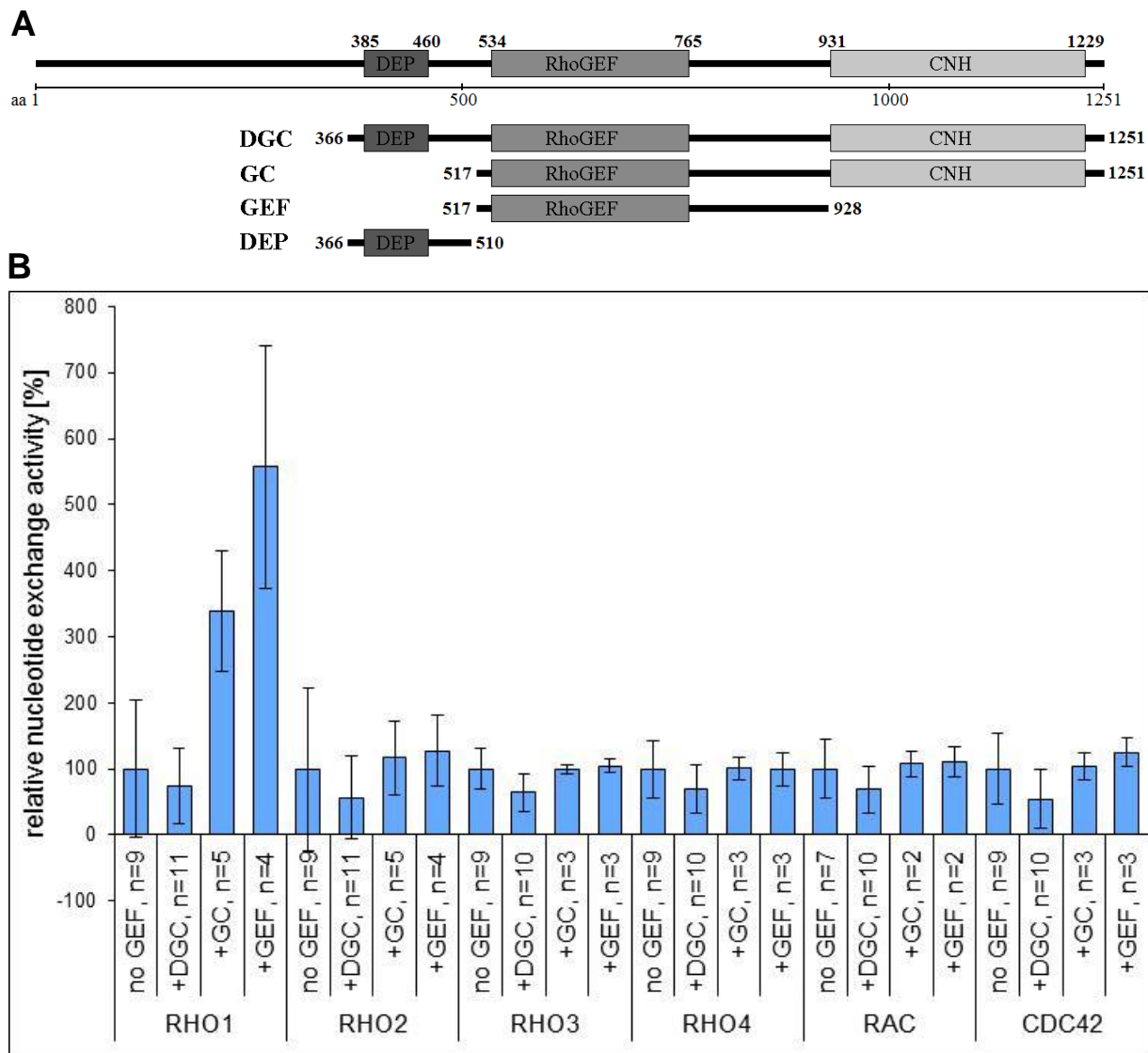


Figure 20: A NCU00668 construct containing the DEP domain (DGC) shows no *in vitro* GEF activity, while two constructs restricted to the GEF and CNH domain (GC) or the GEF domain alone (GEF) specifically activate RHO1. (A) Schematic representation of full-length NCU00668 and the constructs used as MBP fusion proteins in *in vitro* activity assays. Numbers indicate amino acid positions (annotation version .4 of Broad *Neurospora crassa* Database). Conserved domains predicted by InterProScan Sequence Search (see section 4.10.1) are depicted as boxes of varying shades of grey. (B) Nucleotide exchange activity calculated as mean linear slope of fluorescence intensity over a period of ca. 24 minutes [arbitrary units/second] is displayed normalized to the intrinsic exchange activity (“no GEF”) of each Rho GTPase, which was set to 100%. n gives the number of independent experimental replicates, each of which was performed in technical duplicates. DGC was used at 0.4 μ M, whereas GC and GEF concentrations were adjusted to 0.8 μ M. Error bars indicate standard deviation. See section 4.7.7 for details on data evaluation.

Due to the lower protein yield from purifications of the 00668DGC construct (Supplementary Figure 9 A, p.113), it had been used at half the concentration compared to the two shorter constructs in *in vitro* assays. To exclude that the observed differences in GEF activity might be merely attributable to differences in concentrations, I performed further assays with all NCU00668 constructs used at the same concentrations of 0.4 or 0.8 μ M, respectively. As expected, the two shorter constructs still stimulate nucleotide exchange in RHO1 when used at lower concentration, while 00668DGC remains inactive at higher concentration, too (Supplementary Figure 9 B-D, p.113).

The function of DEP domains is generally poorly understood, although they are thought to be involved in intracellular protein targeting and stability and mediate membrane and protein-protein interactions (Pfam 24.0 database at <http://pfam.sanger.ac.uk/>; (Finn et al., 2009)). As a DEP domain had been ascribed an autoregulatory effect on the *in vivo* function of a RasGEF protein in *D. discoideum* (Mondal et al., 2008), I wondered whether the DEP domain of NCU00668 might in some way interfere with the GEF activity of the protein, which would explain the lack of GEF activity seen for NCU00668DGC.

If this assumption was true and the inhibitory effect was exercised by binding of the DEP domain to the RhoGEF or the GTPase in a way that masks regions necessary for their fruitful interaction, addition of excess purified DEP domain (Figure 20 A, Figure 21 A) to the reaction samples should inhibit *in vitro* nucleotide exchange. Figure 21 B shows that this is not the case: The presence of the DEP domain does not influence the nucleotide exchange reactions *in vitro*. Although I tested several ratios of DEP construct to Rho GTPase and GEF constructs and diverse preincubation schemes, I never observed a specific effect of DEP domain addition on intrinsic or GEF-stimulated RHO1 activity (data not shown).

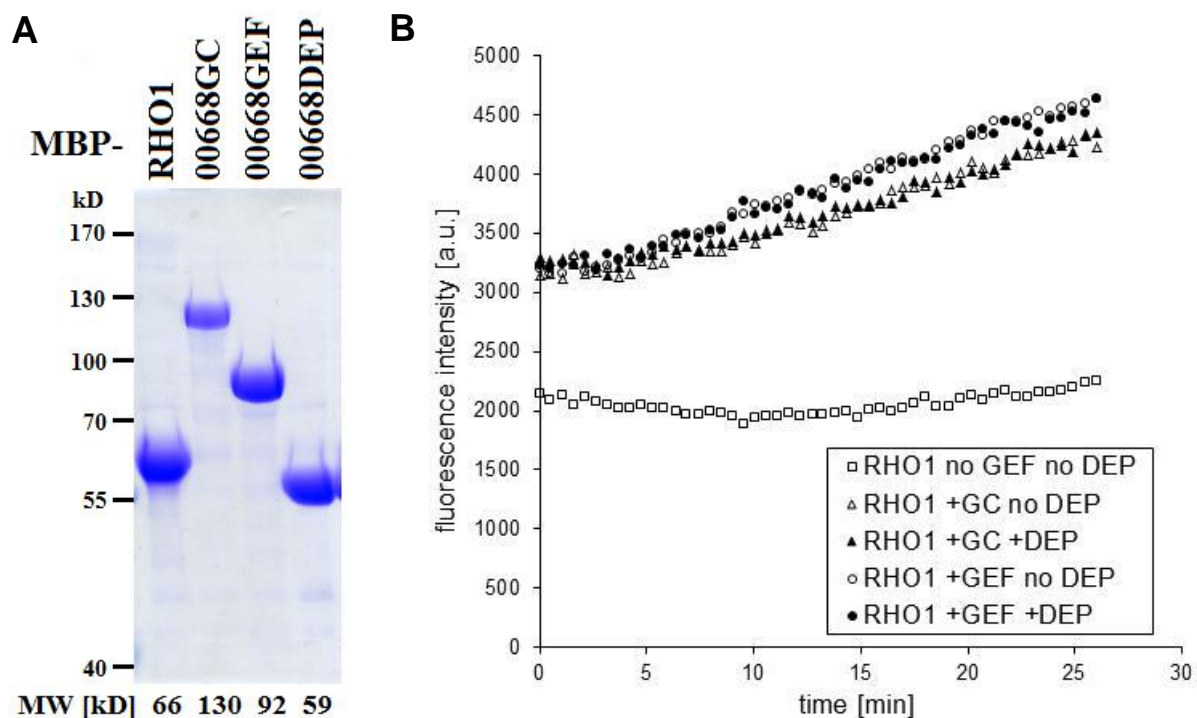


Figure 21: Addition of DEP domain does not influence the NCU00668-stimulated *in vitro* nucleotide exchange activity of RHO1. (A) Result of a representative purification of MBP-Rho GTPase and NCU00668 fusion proteins used in *in vitro* GEF activity assays. A Coomassie stained SDS polyacrylamide gel loaded with equal volumes of eluate fractions of the indicated constructs is shown. Predicted fusion protein molecular weights (MW) are given below the corresponding lanes. (B) An exemplary set of curves representing fluorescence emission intensity [a.u. =arbitrary units] plotted over time [min] is shown. MBP fusion protein concentrations in this assay were 1.2 μ M RHO1, 0.8 μ M 00668GC or 00668GEF and 1.0 μ M DEP. DEP and RhoGEF constructs were preincubated together before start of the reaction.

Although the DEP domain expressed as a separate fusion protein exerts no direct influence on nucleotide exchange activity in *in vitro* assays, it does show physical interaction with MBP-tagged RHO1 and, even stronger, with all three other NCU00668 constructs in copurification experiments (Figure 22). The interaction is not mediated by the MBP tag, as MBP alone does not interact with GST-DEP; a control testing the role of the GST tag is still pending. GST-DEP does not exclusively copurify with RHO1, but probably possesses general affinity towards Rho GTPases, as indicated by its copurification with RHO2 and CDC42. As stated, strength of interaction is higher for the RhoGEF constructs, but there is no clear preference for any of them.

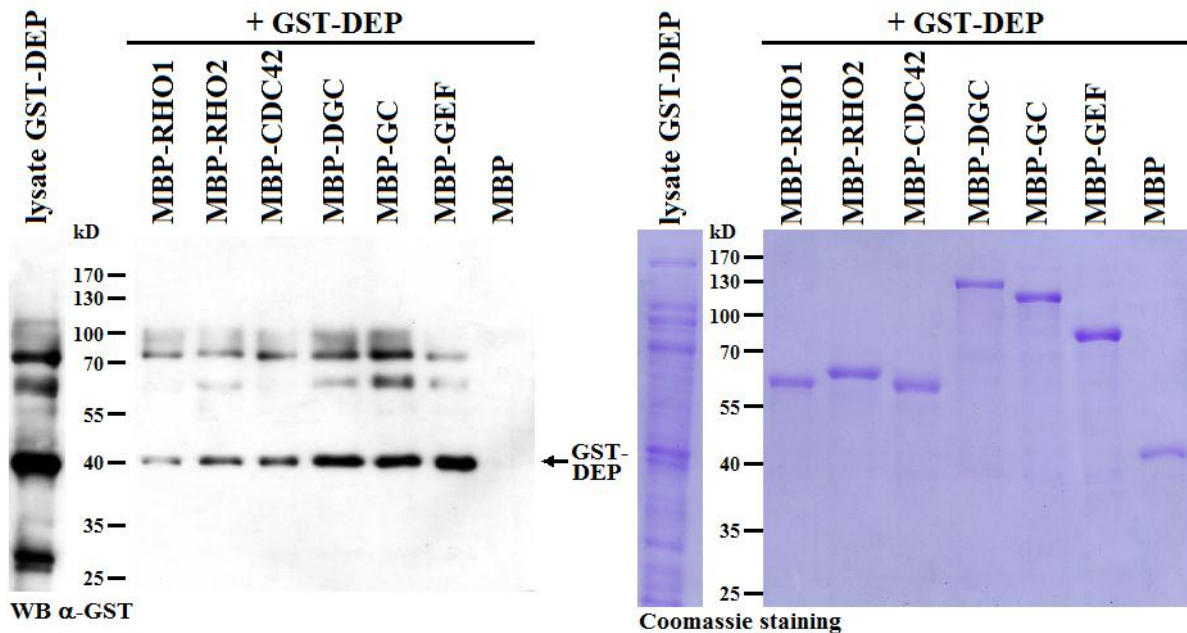


Figure 22: The DEP domain of NCU00668 interacts physically with Rho GTPases and various fragments of NCU00668. GST-DEP (predicted MW=46 kD) copurifies with MBP fusions of RHO1, RHO2 and CDC42 and fragments of NCU00668, but not with MBP alone. Lysates of *E. coli* cells expressing the GST-DEP construct (see also left lanes) or the indicated MBP fusion proteins were combined and subjected to affinity purification using amylose resin. Eluate fraction samples, whose protein content corresponds to equimolar amounts of the respective MBP fusion proteins, were separated by SDS PAGE. Copurified GST-DEP was detected by Western blotting (WB) using α -GST antibody (left), and purified MBP-fusion proteins were visualized by Coomassie staining (right).

5.3.2 Morphological characterization of *rho-1*, *rho-2* and NCU00668 mutants

The *in vitro* findings implying a role of NCU00668 as an activator of RHO1 are corroborated by the identical phenotype of mutants in the corresponding genes. Conidia (which are multinucleate) of the heterokaryotic deletion strains $\Delta\rho\text{-}1$ (*het*) or Δ00668 (*het*) seeded on medium selecting for the presence of the hygromycin resistance knockout cassette develop in three different ways (Figure 23): Some do not grow at all, indicating complete absence of the hygromycin resistance knockout cassette; some only expand isotropically, suggesting severe defects associated with the mutations that prevent polarized growth altogether; others, which presumably harbor both deletion and sheltering wild type nuclei, form slow-growing hyphae, many of which meander unusually and display swollen tips. In accordance with the defects observed in conidia devoid of sheltering wild type nuclei, ascospores produced in crosses with the wild type that bear the respective gene deletion rarely germinate at all, and if so in an apolar manner, with growth soon ceasing and cell lysis occurring. These observations suggest that, like *rho-1* (Vogt and Seiler, 2008), NCU00668 is an essential gene in *N. crassa*.

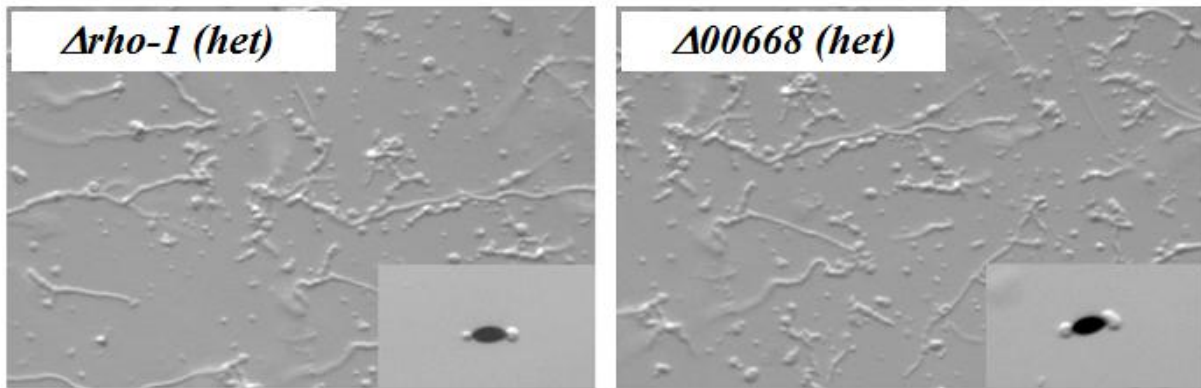


Figure 23: Heterokaryotic deletion mutants of *rho-1* and NCU00668 exhibit identical phenotypes, and homokaryotic deletion mutants are not viable. Conidia of the two strains were germinated on VMM supplemented with hygromycin and incubated for 12 hours. Insets show rare apolar ascospore germination.

Hypomorphic conditional mutants of *rho-1* generated by RIP mutagenesis (S. Seiler, unpublished) allowed the investigation of fungal growth in the absence of fully functional RHO1 (Figure 24). When grown at room temperature, *rho-1(9-1)* and *rho-1(10-1)* exhibit largely normal, albeit slightly slowed, growth (cp. also Figure 27); shifting cultures to 37°C, however, quickly leads to pronounced swelling of apical tips, which resume polarized growth in short time, although extension proceeds at a reduced pace (cp. also Figure 26).

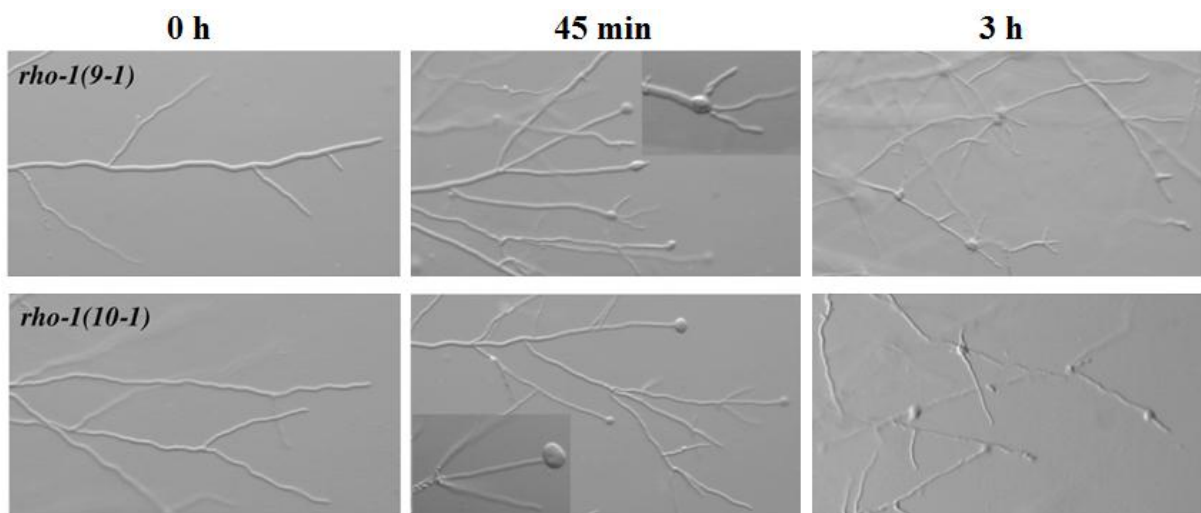
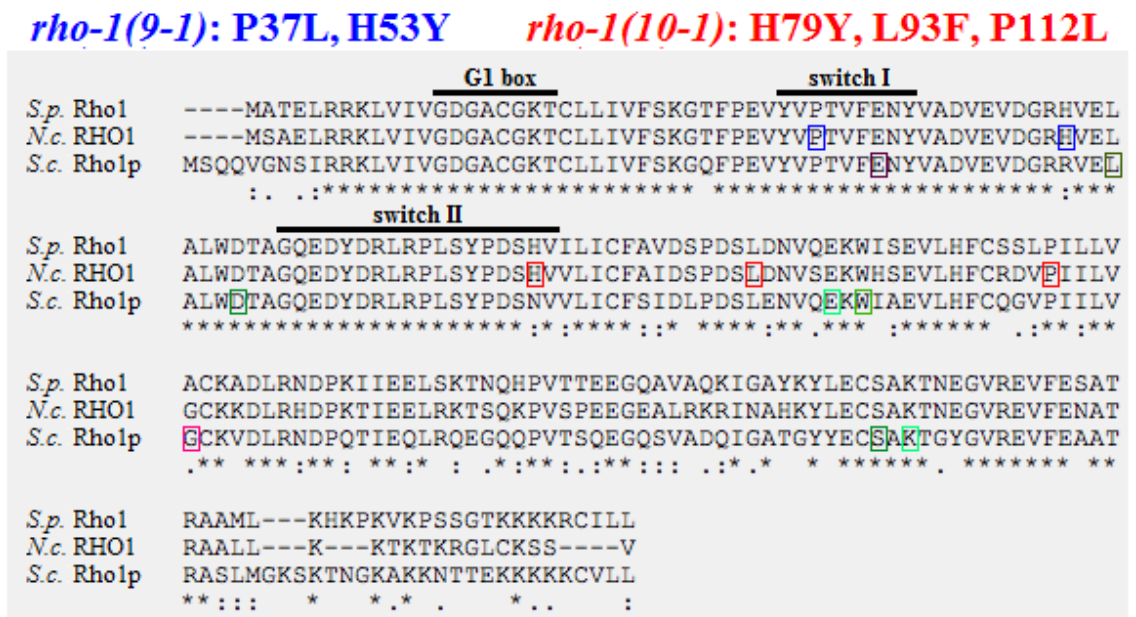


Figure 24: Temperature-sensitive mutant strains of *rho-1* exhibit apolar tip growth. When grown under permissive conditions, *rho-1(9-1)* and *rho-1(10-1)* display a largely normal morphology; after shift to 37°C (time points indicated), apical tips initially swell in an apolar fashion (compare magnified insets), while later polarized growth is resumed.

Sequencing of the *rho-1* coding region amplified from genomic DNA of the two mutant strains revealed several silent mutations and mutations translated to two or three amino acid substitutions in the encoded proteins, respectively (Figure 25). An alignment of *N. crassa* RHO1 with its homologues in *S. pombe* and *S. cerevisiae* shows that the substitutions are all located at conserved positions. Intriguingly, both RHO1(9-1) and RHO1(10-1) have one amino acid substitution each within one of the two highly conserved switch domain regions essential for regulation and function of the GTPase; proline at position 37 replaced by leucine in RHO1(9-1) is even predicted to be a direct interaction site for RhoGAPs by the the NCBI Conserved Domains Database (<http://www.ncbi.nlm.nih.gov/sites/entrez?db=cdd>). None of the amino acid substitutions coincides with any of those encoded by *S. cerevisiae rho1*

alleles associated with specific impairment of different Rho1p effector pathways (Saka et al., 2001).



S.c.* complementation group *rho1A (Pkc1p/Mpk1p and actin defects) ***S.c.* complementation group *rho1B*** (glucan synthase activity defects)

rho1-2: E45V

rho1-5: G121C

rho1-3: L60P

rho1-4: W104R

rho1-10: D70G, S165P

rho1-11: E102K, K167E

Figure 25: Alignment of *N. crassa* (*N.c.*) RHO1 with its homologues from the yeasts *S. pombe* (*S.p.*) and *S. cerevisiae* (*S.c.*). The alignment was generated by MAFFT (version 6.083b). Conserved features predicted by the NCBI Conserved Domains Database (see text) are indicated with black bars. Amino acid substitutions resulting from the mutations identified in *rho-1* mutant alleles (*9-1*) and (*10-1*) are given above and their positions are highlighted within the alignment in blue and red, respectively. For comparison, amino acids altered in Rho1p proteins of *S. cerevisiae* strains forming the two complementation groups *rho1A* and *rho1B*, which are characterized by distinct Rho1p effector defects (Saka et al., 2001), are highlighted in varying shades of pink and green, respectively.

N. crassa rho-1 possesses a highly similar putative paralogue, *rho-2*; identity between the encoded proteins is as high as 64%, as determined by sequence alignment with BLAST (<http://blast.ncbi.nlm.nih.gov/Blast.cgi>). Despite this close relation to RHO1, RHO2 had not been a target of NCU00668 in *in vitro* GEF activity assays. Nevertheless, I tested the physical interaction of the proteins in copurification experiments (Supplementary Figure 10, p.114). Indeed, just like RHO1, RHO2 could be copurified with all three NCU00668 constructs used; however, it also bound to the GEF-PH domain construct of CDC24, and all NCU00668 constructs were enriched in parallel to the GTPase CDC42, too. Thus, there is obviously a general affinity between RhoGEFs and Rho GTPases, so mere physical interaction cannot serve as evidence for a specific regulatory relationship.

Interestingly, while the *rho-2* gene is not essential and the homokaryotic deletion mutant is mostly inconspicuous under standard conditions - although growth speed and directionality are slightly affected -, the double mutant $\Delta\rho\text{-}2;\rho\text{-}1(9-1)$ exhibits strong synthetic growth and polarity defects both at room temperature and at 37°C (Figure 26): From most conidia polarized germ tubes never emerge, and the rare hyphae that are formed resemble pearls on

a string, with several subapical and apical compartments swollen in an apolar manner. Additionally, growth speed, formation of aerial hyphae and conidiation are highly reduced (data not shown).

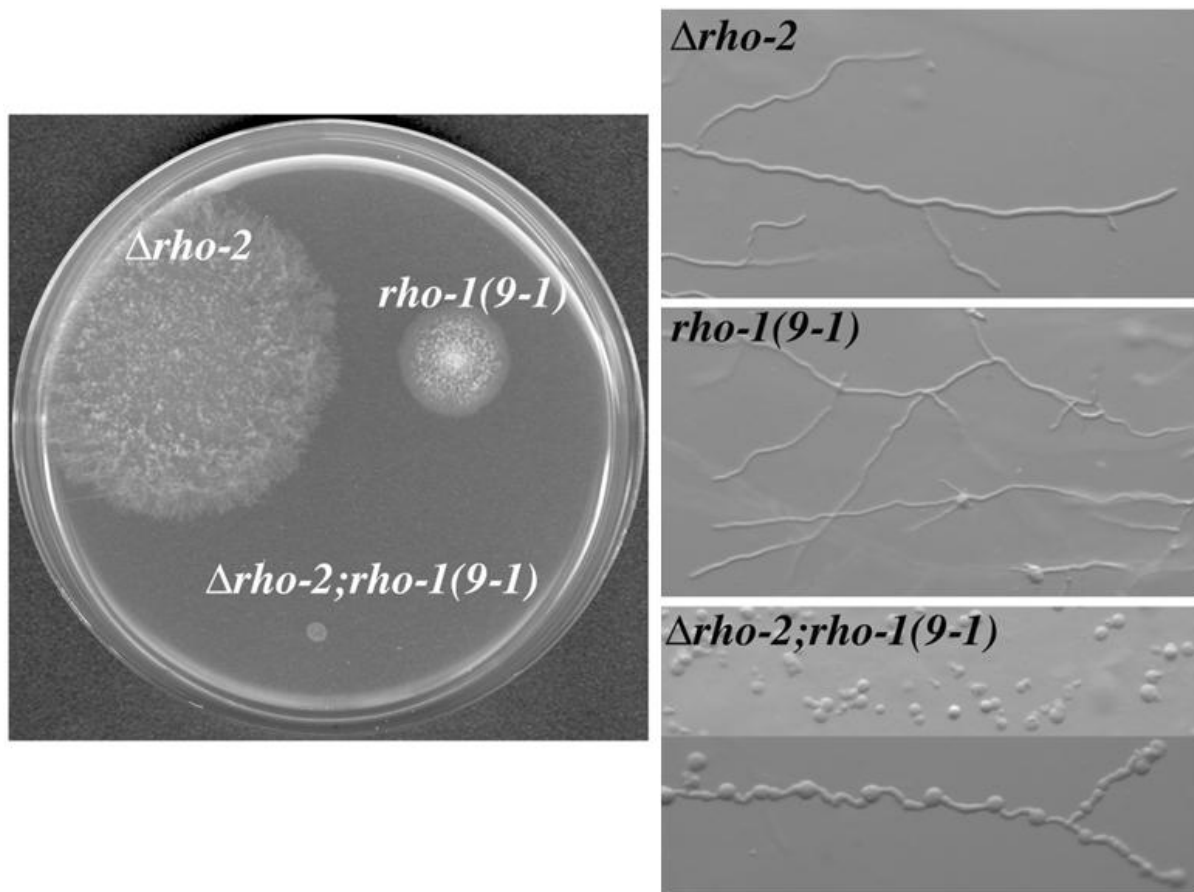


Figure 26: Mutations in *rho-1* and *rho-2* have synthetic effects. While the deletion of *rho-2* has little effect on hyphal growth and morphology, a $\Delta\rho\text{-}2;\rho\text{-}1(9-1)$ double mutant exhibits strong synthetic polarity and growth defects. Conidia of the indicated strains were incubated on VMM for 15 hours at 37°C.

The finding that lack of RHO2 markedly aggravates the effects of deficiency in RHO1 hints at overlapping functions of the two Rho GTPases, while RHO1 must possess at least one additional essential function, as indicated by the fact that deletion of *rho-1* is lethal, whereas knockout of *rho-2* has only mild effects.

5.3.3 Effector pathways regulated by RHO1 and RHO2 in *N. crassa*

To distinguish between these proposed shared and distinct cellular functions of RHO1 and RHO2, mutant strains were treated with inhibitors of putative downstream effectors inferred from yeast models (Figure 27). In comparison to the wild type, the temperature-sensitive *rho-1* and the *rho-2* deletion mutant strains display no markedly increased sensitivity towards latrunculin A, which disrupts the actin cytoskeleton (Spector et al., 1999). However, they are clearly hypersusceptible towards cell wall damage by lysing enzymes or caspofungin, an irreversible inhibitor of β -1,3-glucan synthase (Hoang, 2001). While cell wall integrity thus seems to be equally compromised as a result of deficiency in RHO1 or RHO2, only *rho-1(9-1)*, but not $\Delta\rho\text{-}2$, shows reduced sensitivity towards cercosporamide, a selective inhibitor of protein kinase C (Sussman et al., 2004). Hyposensitivity pointing towards increased activity of PKC1 is even more pronounced in the double deletion strain, possibly suggesting the existence of an alternative, RHO1/2-independent PKC1 activation pathway when cell wall integrity is compromised.

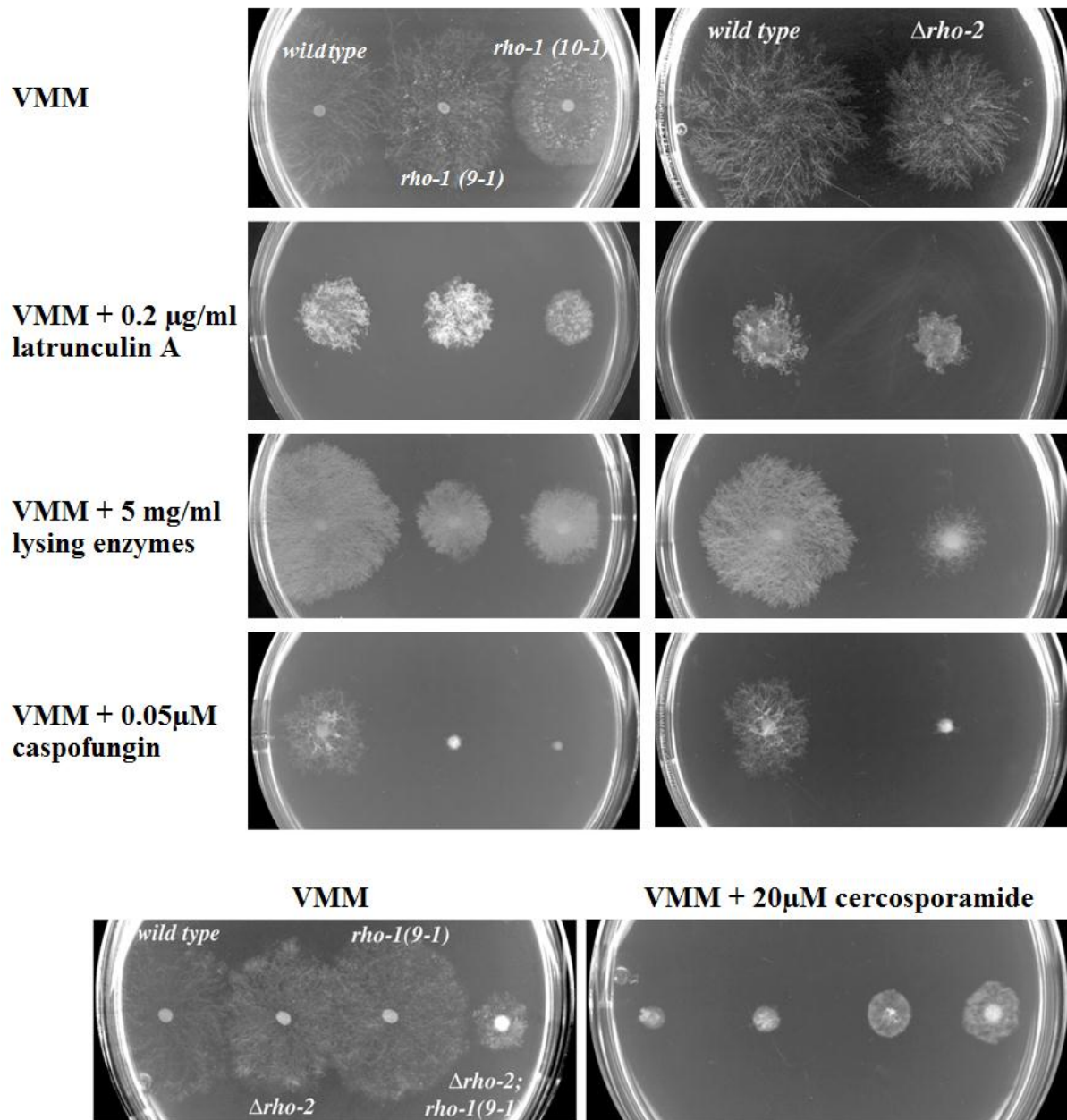


Figure 27: Cell wall integrity is compromised in mutants of both *rho-1* and *rho-2*, while only mutation of *rho-1* or the double mutation effects hyposensitivity towards inhibition of PKC1. Actin organization is not clearly affected in any of the mutants tested. Wild type and mutant strains were incubated for 24 hours at room temperature on VMM supplemented with the actin-depolymerizing drug latrunculin A, cell wall damaging agents lysing enzymes or caspofungin (kindly provided by MSD Sharp & Dohme GmbH, Germany) or the protein kinase C inhibitor cercosporamide.

Next, I sought to directly analyze physical interaction between the two GTPases and their putative effectors and regulators by yeast two-hybrid analyses (Figure 28).

The RHO1 and RHO2 constructs expressed in the two-hybrid tests are presumed to represent dominant active (DA) or negative (DN) forms of the proteins, as homologous proteins of other organisms bearing analogous changes at conserved amino acid positions have been shown to have altered signalling properties: Equivalent mutations have been reported to significantly decrease GTPase activity (Marshall et al., 1991; Longenecker et al., 2003) or are thought to interfere with effector interaction by perturbing the switch I region (Drgonová et al., 1996; Tomić et al., 2007), respectively; moreover, analogous *rho1* alleles affect polar growth and cell wall integrity in various fungi (Guest et al., 2004).

Initially, bait and prey proteins were expressed as fusions to the GAL4 DNA-binding (BD) or activation (AD) domain from the vectors of the Matchmaker™ Two-Hybrid System 3 (Clontech, USA). In this way, however, I was not able to detect reproducible interaction between any pair of fusion proteins, presumably because expression of the dominant activated form of RHO1 and some other fusion proteins was harmful to yeasts, as evident in very poor transformation efficiency and growth.

To overcome this problem, I generated vectors in which fusion protein expression was no longer controlled by the full-length and intermediately truncated *ADH1* promoters associated with high expression levels but by a shorter promoter fragment which results in low expression (for comparison of promoter versions and expression strength, see (Ammerer, 1983; Ruohonen et al., 1991, 1995) and unpublished data by Clontech, USA, presented at <http://www.clontech.com/images/pt/PT3024-1.pdf>).

Yeast cells tolerated expression of all fusion proteins from the new vectors. None of the fusion proteins used in the assay exhibited autoactivation, i.e. interaction with the respective other GAL4 domain alone (data not shown). General yeast two-hybrid competency of all RHO1 and RHO2 fusion proteins was verified by their ability to interact with Δ N-RanBPM (see Supplementary Figure 11, p.115).

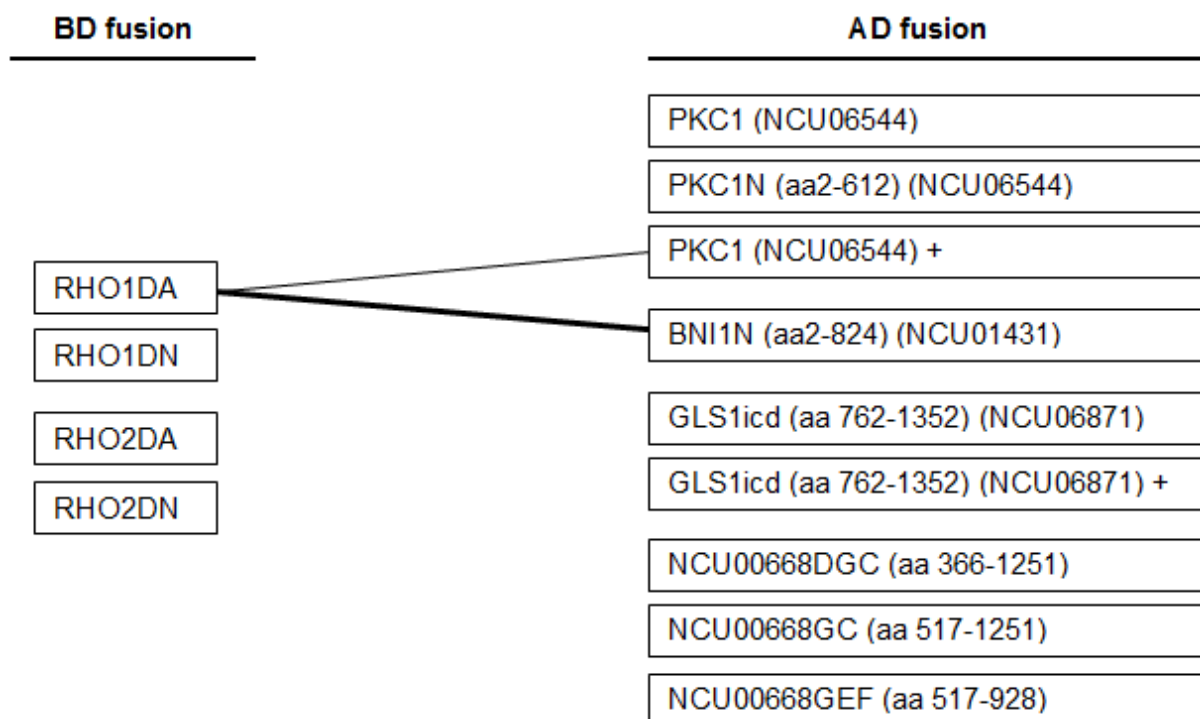


Figure 28: Overview of combinations of fusion proteins tested for interaction in yeast two-hybrid assays. All possible pairwise combinations between GAL4 BD and AD fusion constructs (left and right column, respectively) were coexpressed; only the two pairs connected by lines exhibited weak (fine line) or strong (thick line) interaction. All proteins were expressed at low levels under control of a short truncated version of the *ADH1* promoter except those denoted by a plus sign, whose expression was controlled by the full-length promoter associated with high expression. See text for details.

As evident in Figure 29, the dominant active version of RHO1, but not its dominant negative counterpart or any RHO2 construct, interacted strongly with the N-terminus of the formin BNI1, which comprises the predicted GTPase binding and FH3 domains but lacks the actin-binding FH2 and autoregulatory domains. RHO1DA was also the only GTPase construct

engaging in weak interaction with PKC1; interestingly, the protein kinase had to be expressed at high levels for detectable interaction.

No interaction of any of the GTPase constructs with the largest intracellular domain of the glucan synthase NCU06871 (which coincides largely with its predicted catalytic domain) or any of the NCU00668 fragments was observed (data not shown).

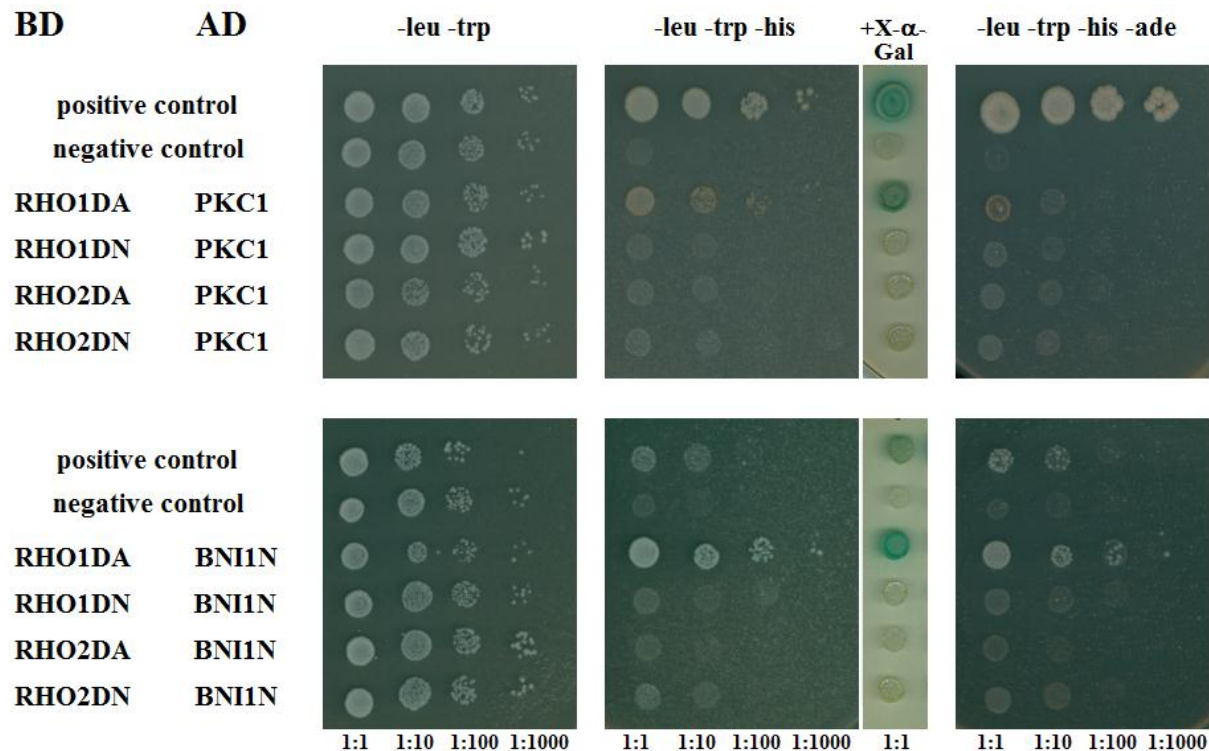


Figure 29: An activated form of RHO1, but not RHO2, interacts specifically with PKC1 and the N-terminus of BNI1 in yeast two-hybrid experiments. The Rho GTPase and putative effector constructs indicated where coexpressed as fusions to the GAL4 DNA binding (BD) or activation (AD) domain in the reporter yeast strain AH109. Growth of colonies on medium lacking histidine and adenine and formation of a blue galactosidase reaction product from X- α -Gal reveal interaction between fusion protein pairs. Fusion proteins for positive and negative controls were expressed under control of the same *ADH1* promoter versions as the corresponding test pairs. Note that growth on selective medium for the combination RHO1DA-PKC1 was poor and only visible after prolonged incubation at 30°C (eight days instead of three). Dilution factors of cell suspensions used for inoculation are indicated.

Intending to confirm and expand the findings of the yeast two-hybrid analyses, I attempted to identify interaction partners of RHO1 and RHO2 by coimmunoprecipitation experiments using *N. crassa* strains which coexpress epitope-tagged versions of the potential binding partners. For this purpose, I have already created plasmids encoding FLAG-tagged BNI1, PKC1, NCU06871 and NCU00668 and generated auxotrophic *N. crassa* strains stably expressing these constructs (data not shown; cp. sections 4.4.7 and 4.5). Likewise, I have constructed plasmids for expression of HA- and 3xmyc-tagged RHO1 and RHO2 and used them to generate complementary auxotrophic strains. Unfortunately, expression levels of the GTPase constructs, in particular that of RHO2, have turned out to be very low; indeed, GTPase fusion proteins are almost immunologically undetectable in lysates of the forced heterokaryon strains coexpressing both putative interactor constructs, even after enrichment (data not shown). Therefore, I am currently working on improving the detectability of the epitope-tagged GTPase proteins by testing new vector constructs (section 4.4.7).

Inhibitor tests and yeast two-hybrid studies presented above suggest that RHO1 influences PKC1 signalling in *N. crassa*, while RHO2 only plays a minor, if any, role. In yeasts, protein

kinase C has been established as a regulator of the cell wall integrity MAPK pathway (reviewed in (Levin, 2005)). A homologous tripartite kinase cascade consisting of MIK1, MEK1 and MAK1 has been described in *N. crassa* (Park et al., 2008). Activating signals are thought to be passed on along the cascade by sequential phosphorylation of the three component kinases, and phosphorylation of the MAPK MAK1, the last kinase in the row, can be detected using a phospho-specific p42/44 antibody (ibid.).

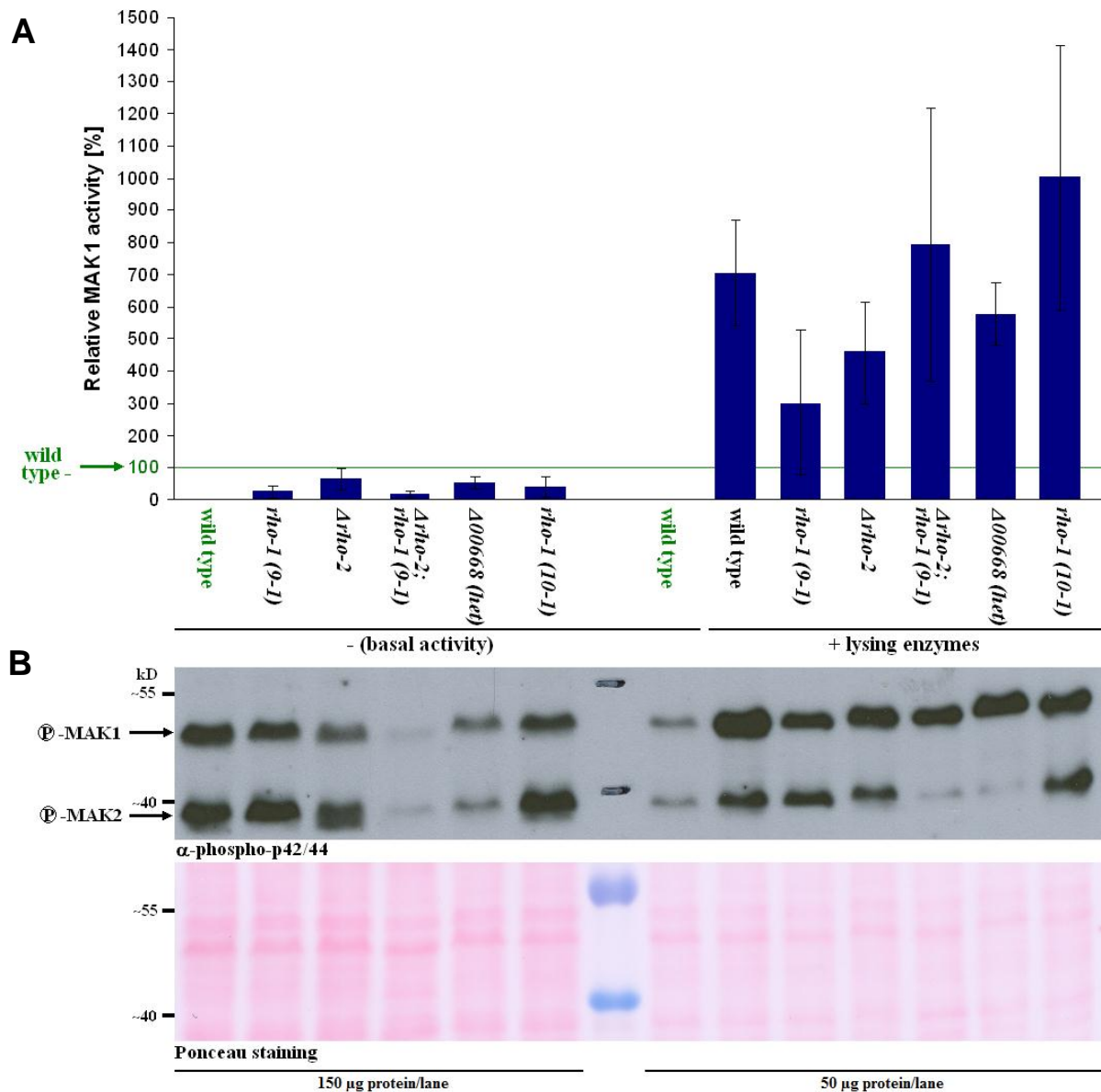


Figure 30: Mutants of the RHO1/RHO2 GTPase module exhibit reduced basal activity of the MAPK MAK1, while they are still able to respond to cell wall stress by activation of the cell wall integrity pathway. (A) Summary of mean relative MAK1 activity levels in the different strains. Cell lysates prepared from unstressed or stressed *N. crassa* cultures of the indicated strains were subjected to SDS PAGE and ensuing Western blotting, and phosphorylated MAK1 was detected using a phospho-specific p42/44 antibody. MAK1 phosphorylation levels were quantified by densitometric analysis of MAK1 band intensity and normalized to the values obtained for the unstressed wild type ("wild type -"). Error bars are confidence intervals ($p=68\%$). See section 4.7.5 for details on data acquisition and evaluation. (B) Immunoblot illustrating mean MAK1 phosphorylation levels. Lysate samples of the indicated strains corresponding to 150 or 50 μ g total protein were subjected to SDS PAGE, and phospho-MAK1 and -MAK2 were immunodetected as described in (A). Bands corresponding to the two MAPK proteins (predicted MW=47/41 kD), as verified by their absence in lysate samples of the respective deletion mutants (data not shown), are indicated. Equal loading is confirmed by Ponceau S staining.

As seen in Figure 30, basal MAK1 activity of mutants affected in components of the RHO1/RHO2 GTPase module is reduced compared to that of wild type. On average, reduction is most pronounced in the two temperature-sensitive *rho-1* mutants and especially the $\Delta\rho-2$; *rho-1(9-1)* double mutant, while $\Delta\rho-2$ and $\Delta\text{NCU00668}$ (*het*) exhibit a MAK1 phosphorylation status more similar to that of the wild type.

In wild type, the pathway is reliably induced by addition of lysing enzymes to the culture medium. Such cell wall stress still elicits MAK1 activation in all of the mutants analyzed; unfortunately, further conclusions about differences regarding the strength of the response are prevented by the high variability of the assay.

5.3.4 Analysis of the subcellular localization of NCU00668, RHO1 and RHO2

To obtain further clues about shared and distinct cellular roles of RHO1, its activator NCU00668 and its close homologue RHO2, subcellular localization of the three proteins was analyzed. For this, they were expressed as fusions to different fluorescent proteins from constructs integrated at the *his-3* locus.

NCU00668 was expressed as a C-terminally tagged GFP or YFP fusion protein under control of the *ccg-1* promoter. For the GFP version, protein expression and stability could be verified by immunoblot analysis (Supplementary Figure 12 B, p.115), and functionality of the fusion protein has already been confirmed by its ability to complement the otherwise lethal deletion mutation of NCU00668. Analogous crosses of strain *00668-yfp* with the Δ00668 (*het*) mutant strain are pending. In spite of its good detectability in immunoblots, fluorescence of NCU00668-GFP is weak both when expressed in the wild type (data not shown) and the deletion background. Signal intensity is slightly higher for *00668-yfp*, although still low. Nevertheless, the strains show fluorescence clearly above background levels of the wild type (data not shown).

Both the YFP- and GFP-tagged versions of the RhoGEF localize in a diffuse manner throughout the hyphal cytoplasm. Occasionally, accumulation at septa is observed (Figure 31 and Supplementary Figure 12 A, p.115). As GFP alone expressed in a control strain is markedly excluded from septa (Supplementary Figure 13, p.116), this distinct septal localization must reflect a genuine property of NCU00668.

In contrast to NCU00668, RHO1 and RHO2 were fused to the C-terminus of fluorescent proteins to preserve the function of the putative C-terminal prenylation motifs of the GTPases. Expression of GFP and mCherry fusion proteins was controlled by the *ccg-1* promoter, while expression of YFP-tagged RHO1 and RHO2 was governed by the *gpdA* promoter, just like that of the analogous constructs of RAC and CDC42 presented above. Although expression constructs for the GFP fusions of RHO1 and RHO2 were created in identical ways, expression levels of the resulting fusion proteins turned out to differ widely: While GFP-RHO1 was readily immunodetected in lysates prepared from the corresponding strain (Supplementary Figure 14 B, p.117), GFP-RHO2 was only detectable after enrichment by immunoprecipitation (Supplementary Figure 15 B, p.118).

Several attempts to backcross strains expressing a tagged version of RHO1 to the heterokaryotic deletion strain $\Delta\rho-1$ (*het*) yielded no viable hygromycin-resistant offspring, indicating that fusion protein expression from the chosen constructs is not suitable to overcome the lethality associated with the deletion of *rho-1*. Functionality of GFP- and YFP-RHO2 by analogous complementation analyses remains to be tested, although it is

suggested by the ability of an overexpressed N-terminally myc-tagged RHO2 construct to rescue the cell wall defects of $\Delta rho-2$ (data not shown).

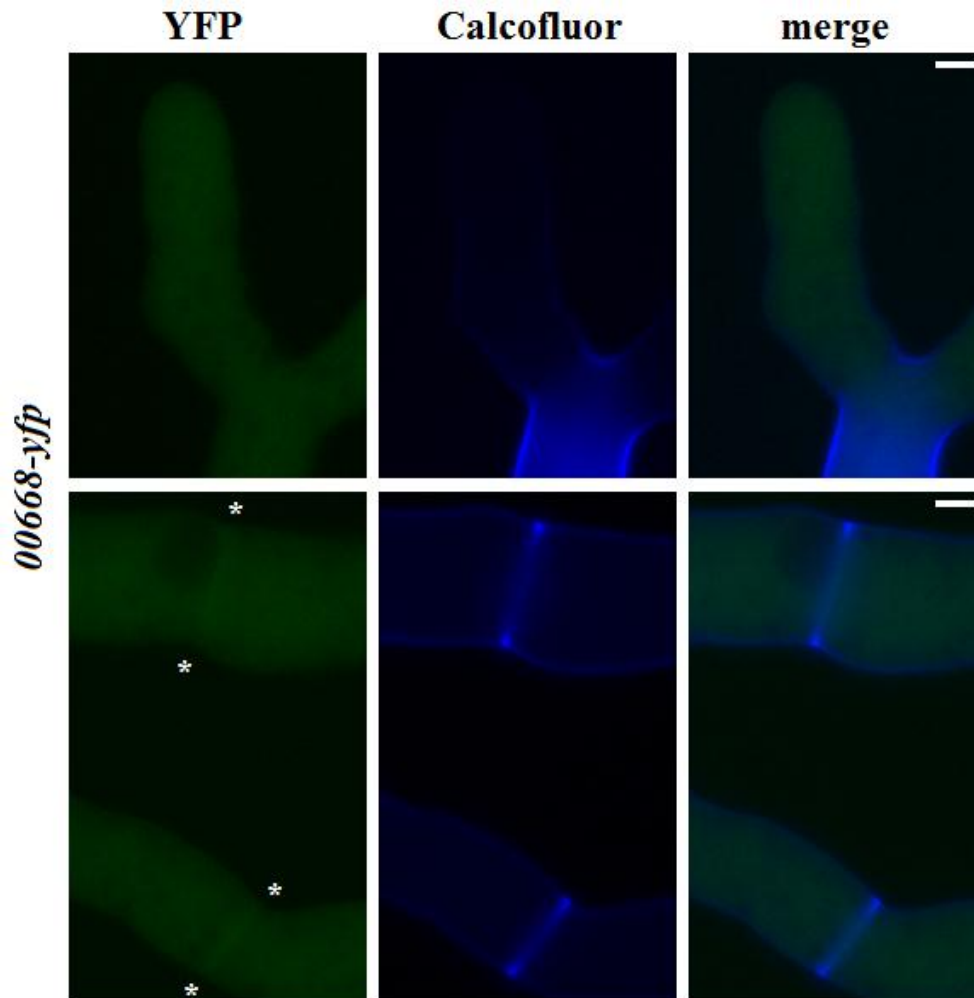


Figure 31: NCU00668 localizes to septa and throughout the cytoplasm. Micrographs showing localization of NCU00668-YFP in wild type background are displayed. Cell wall and septa stained with calcofluor white (DAPI filter) are shown for orientation. Asterisks mark fusion protein accumulation at the septa. Scale bars are 5 μ m.

Fluorescence intensity is markedly higher for strains expressing YFP and mCherry fusions of the GTPases than those in which RHO1 or RHO2 are GFP-labelled. Nevertheless, also the latter show fluorescence considerably higher than background fluorescence of the wild type (data not shown). As expected, the overall localization pattern of the Rho GTPases is independent of the fluorescent protein tag used, although more details are visible in the strains exhibiting brighter fluorescence.

RHO1 fusion proteins are observed throughout the cytoplasm with accumulation at septa and at vacuolar membranes. Furthermore, the plasma membrane is clearly labelled. In addition, a vesicular-reticulate patchy structure that extends throughout the hyphae with exception of apical tips is regularly observed in the corresponding strains. RHO1 has never been seen specifically enriched at hyphal tips (Figure 32 A and Supplementary Figure 14, p.117).

Localization of RHO2 is largely identical to that of RHO1, although it differs in minor aspects. RHO2, too, is visible throughout the cytoplasm and accumulates strongly at septa and along the plasma membrane; additionally, it localizes in a structure which, resembling that seen for RHO1, does not extend into hyphal tips. Contrasting to the rather diffuse network seen for

RHO1, however, this structure is more distinct and more reticulate in nature, although some patches and vesicles are also observed (Figure 32 B and Supplementary Figure 15, p.118).

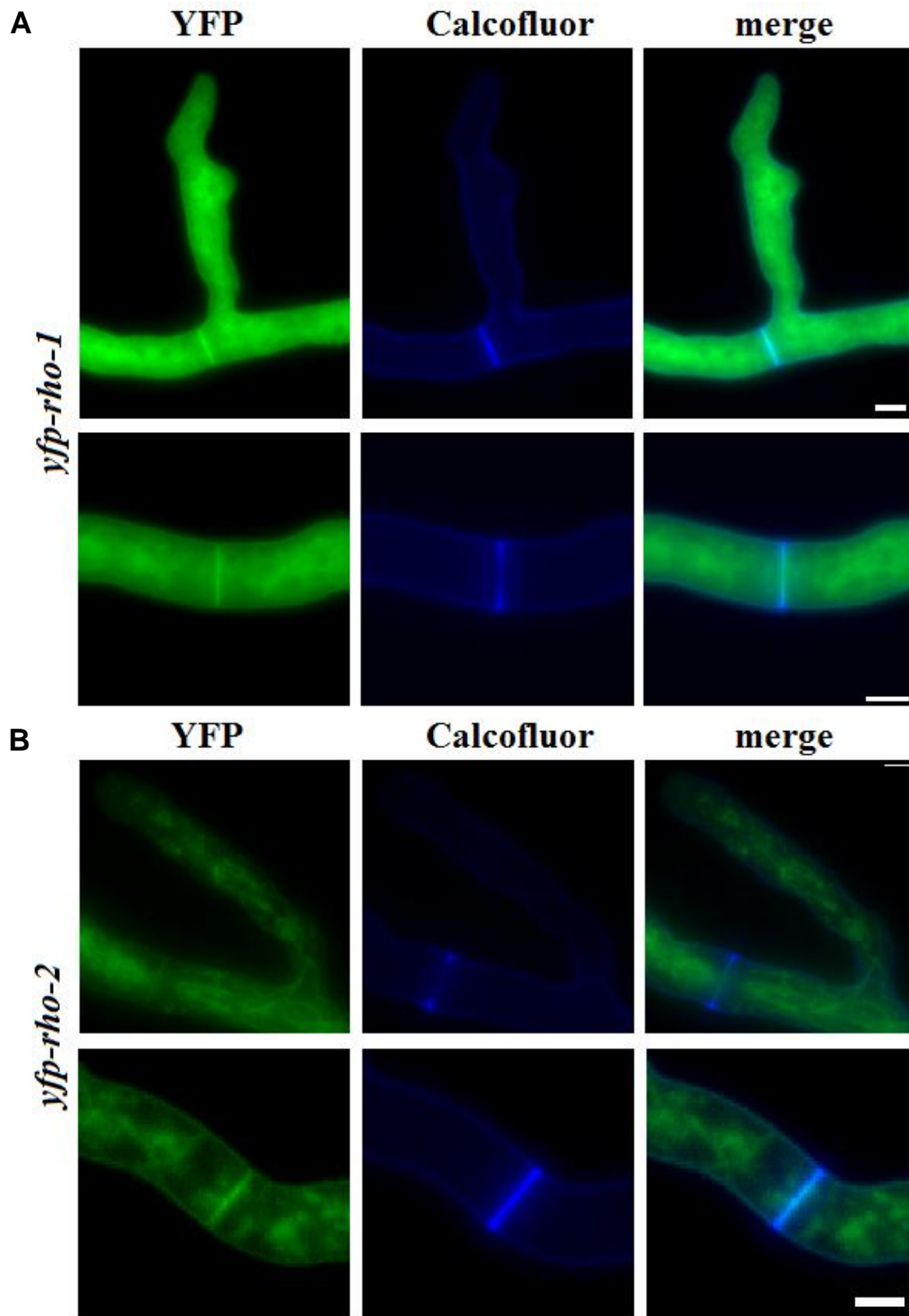


Figure 32: RHO1 and RHO2 exhibit a similar localization pattern: They accumulate at septa and membranes and are distributed throughout the cytoplasm, sometimes in reticulate-vesicular structures absent from apical regions. Micrographs of strains expressing YFP-RHO1 (A) or YFP-RHO2 (B) in the wild type background are displayed. Images of cell wall and septa stained with calcofluor white (DAPI filter) are shown for orientation. Scale bars are 5 μ m.

6. Discussion

6.1 Lessons from the *in vitro* assays

The study of the molecular basis underlying establishment and maintenance of polarized growth in fungi has long been mostly restricted to the unicellular members of this kingdom, although the hyphae of filamentous fungi, together with pollen tubes and neurons, are acknowledged as the most extremely polarized cells, making them prime candidates for investigations of these fundamental processes (Harris, 2006). As stated in the introduction, adapted wiring of conserved components and the incorporation of novel factors into the basic toolbox of the polarity machinery are presumed to be responsible for the markedly different morphogenetic outcomes of yeast and hyphal growth. Given the importance of Rho GTPases as key integrators of polarity signalling, it is conceivable that their differential regulation might contribute considerably to the differences in spatial and temporal patterns of yeast-like and hyphal growth.

Therefore this work attempts to lay the basis for a comprehensive analysis of all putative RhoGEFs and RhoGAPs present in *N. crassa*. As seen in Figure 4 and Figure 5, most of the Rho regulatory proteins found in the two yeasts *S. pombe* and *S. cerevisiae* are conserved in *N. crassa*, although, like other components of the polarity machinery, to varying degree, and with some missing (e.g. NCU00668 is the only Rho GEF in *Neurospora* similar to the pairs Rgf1/2 and Rom1/2p in the yeasts); others are apparently present in the filamentous fungus only (e.g. the GAPs NCU02915 and NCU07622).

Using *in vitro* assays, I tested each putative GEF for its activity towards the full set of Rho GTPases, which is in contrast to the work in the two yeasts, where in most cases only a subset of the six GTPases was included in the analysis.

I identified Rho1 as the unique target of the GEF NCU00668 (Figure 8), which is in accordance with the specificity displayed by its closest yeast homologues Rom1/2p and Rgf1/2. It did not come as a surprise, either, that CDC24 of *N. crassa*, like its yeast counterparts Cdc24p and Scd1, activates CDC42 *in vitro* (Figure 9). Interestingly, however, it additionally stimulates nucleotide exchange equally well in RAC, the GTPase absent altogether in the yeasts. Support for the proposed dual specificity of CDC24 and the link between NCU00668 and RHO1 signalling comes from corresponding *in vivo* analyses (see below for discussion).

NCU10282, too, shares with its close relative *S. pombe* Gef1 the specificity for CDC42; however, it also slightly stimulates nucleotide exchange in RAC (Figure 11). It will be interesting to test if and in how far simultaneous activation of both CDC42 and RAC might play a role *in vivo* in *N. crassa*; unfortunately, as stated, no knockout strain is available so far for NCU10282. The apparent misannotation of its translation start site complicates the generation of a full deletion mutant and suggests a partial deletion of the GEF and BAR domains as an alternative approach.

Budding yeast has no close homologue of NCU10282. In *S. pombe*, the related Gef1 is one of two Cdc42-specific GEFs, sharing an essential function with the other Cdc42 activator Scd1; it has been mainly implicated in regulation of its target GTPase during septum formation (Coll et al., 2003; Hirota et al., 2003). Interestingly, the BAR domain found in

NCU10282 is absent in Gef1, while its presence is predicted for the closest (still uncharacterized) homologues of NCU10282 in filamentously growing fungi such as *A. nidulans*, *A. fumigatus*, *P. marneffeii* and *U. maydis*. This is noteworthy as it has recently been shown that Hob3, a separate *S. pombe* BAR domain protein, is required for concentrating Cdc42p at the division area; it forms a complex with the GTPase and Gef1 and thus facilitates their localized stimulatory interaction (Coll et al., 2007; Rincon et al., 2007). Therefore it is possible that the BAR domains of NCU10282 and its relatives in filamentous fungi mediate an analogous function in localizing the GEF activity towards areas of high membrane curvature. Notably, this could resemble the mode of action of Tuba, a mammalian Cdc42-specific GEF, which also features combined DH and BAR domains (Salazar et al., 2003; Cestra et al., 2005; Rincon et al., 2007). In this regard, localization studies of fluorescent protein-tagged NCU10282 deleted for the BAR domain in comparison to the full length protein could give valuable insights.

This study identifies BUD3 as a RHO4-specific GEF in *N. crassa* (Figure 10). Notably, no GEF activity has been reported so far for any of its yeast homologues. While the cellular role of *S. pombe* Gef2 has not been characterized, *S. cerevisiae* Fus2p has been implicated in cell fusion (Elion et al., 1995; Gammie et al., 1998), and Bud3p is considered a marker for axial bud site selection (Chant and Herskowitz, 1991; Chant et al., 1995). Similarly, the closest homologue of BUD3 in the filamentous fungus *A. gossypii*, Bud3, acts as a landmark that tags future septal sites and is involved in the positioning of the contractile actin ring (Wendland, 2003). In line with and expanding these findings, our group has recently shown that BUD3, together with the other RHO4 activator RGF3, regulates septum formation in *N. crassa*, combining the functions of septation site marker protein and RhoGEF (Justa-Schuch et al., 2010). In the meantime, conservation of this dual role has been corroborated for *A. nidulans* AnBud3 (Si et al., 2010), and it will be interesting to see if the cellular functions of the corresponding yeast proteins also rely on their putative GEF activity.

As evident in the results of the GEF activity assays presented in this study (cp. Figure 12), prediction of Rho regulatory protein target specificity based on conservation of the catalytic domain is possible in some cases. However, it is of course limited to those candidates having a close homologue which has already been assigned to a target (and, ideally, excluded as a regulator of others), and its applicability is further restricted if the Rho GTPase repertoires of the organisms compared differ, as is the case here. Therefore, the experimental determination of *N. crassa* RhoGAP activity prepared in this study is expected to yield further interesting results, only some of which could have been deduced from the available yeast data, and will in turn, as has already been the case for BUD3, provide a basis for better understanding of Rho regulation in other filamentous fungi.

In the *in vitro* assays, I did not observe GEF activity for NCU02764, which is rather distantly related to the Cdc24-like subgroup of RhoGEFs (Figure 5), and for the CZH-family GEF NCU09492, whose cousin YLR422W in budding yeast is still uncharacterized but has been shown to interact with mammalian Rac (Brugnera et al., 2002). While I cannot rule out the possibility that the purified proteins were not functional due to *in vitro* folding problems, this seems rather unlikely, as I used two different constructs each, and all of them were readily solubly expressed. Alternatively, their putative GEF domains could have generally lost their catalytic functions. For NCU02764 this is improbable, as it exhibits a high degree of conservation of residues predicted to be involved in GTPase interaction by NCBI Conserved Domains Database (data not shown). NCU02764 is identical to the gene *Rsp* (*Roundspore*), whose dominant deletion mutants produce spherical instead of spindle-shaped ascospores

when crossed to wild type (Mitchell, 1966; Srb et al., 1973; Pratt et al., 2004), while at the same time they exhibit largely inconspicuous vegetative hyphae (S. Seiler, personal communication). Given its implication in the sexual development, it is easily conceived that NCU02764 could require a stimulatory posttranslational modification by a pathway active during the sexual phase of the *N. crassa* life cycle. There are numerous examples of GEFs that are posttranslationally modified, although the physiological significance of the modifications has seldom been clarified so far (reviewed in (Zheng, 2001; Rossman et al., 2005)). For NCU09492, on the other hand, partial alignments with other CZH-family members reveal that conservation of the rather vaguely defined putative DHR-2 domain (see (Côté and Vuori, 2002, 2006)) is less pronounced, although the key valine residue implicated in the catalytic mechanism (Yang et al., 2009) appears to be conserved (data not shown). While NCU09492 might consequently well be non-functional as a GEF, other evidence suggests that it could instead rely on a cofactor for activity: It has been shown that the mammalian Dock180, a CZH-type GEF, requires the accessory protein ELMO1 for full GEF activity towards Rac (Brugnera et al., 2002; Lu et al., 2004). Likewise, in the dimorphic fungus *C. albicans*, a similar complex made up of the CZH-type GEF Dck1 and the ELMO homologue Lmo1 has been proposed to regulate Rac function in invasive filamentous growth and cell wall integrity (Hope et al., 2008, 2010). *N. crassa*, too, possesses a putative ELMO homologue, NCU03264, and it is conceivable that NCU09492 and this protein constitute an extreme example of an analogous bipartite GEF, where the accessory ELMO-like protein is absolutely needed for GEF activity. An activity assay in the presence of purified NCU03264 could be a way to test this hypothesis; alternatively, CRIB domain pulldown experiments (cp. e.g. (van Triest et al., 2001; Bassilana and Arkowitz, 2006)) to determine changes in the levels of active RAC and/or CDC42 in the corresponding deletion backgrounds in comparison to wild type could help assess the putative GEF function of the two proteins. It is especially tempting to speculate that NCU09492 and the ELMO homologue, like their counterparts in mammals and *Candida*, could cooperately regulate RAC, because this would complement the set of RAC/CDC42 activators so far composed of the dual-specific CDC24 and the largely CDC42-specific NCU10282. In any case, analysis of genetic interactions and suppressors of mutants could aid in identifying the cellular targets of the two still enigmatic putative RhoGEFs NCU02764 and NCU09492.

Interestingly, none of the regulators tested positive in the GEF assays was active on RHO2 or RHO3. How, then, would their activity be regulated? A hint for RHO2 comes from my studies of HA-, myc- or GFP-tagged versions of the protein expressed in the fungus. In all cases, RHO2 expression levels were markedly below those of an analogously tagged RHO1 construct expressed from the same system (cp. Supplementary Figure 15, p.118 and data not shown). Control of expression and/or protein stability, also observed for other Rho GTPases (Bustelo et al., 2007), might therefore play an important role in regulating RHO2 levels. Strikingly, RHO3, whose homologues in *C. albicans* and *Trichoderma reesei* have been implicated in maintenance of cell polarity and secretion, respectively (Wendland and Philippsen, 2001; Vasara et al., 2001a, 2001b; Dünkler and Wendland, 2007), persistently exhibits the highest intrinsic exchange rates *in vitro*. Notably, no Rho3-specific GEFs have been characterized so far in other fungi, including the yeasts, either. Recently, RNA transport processes suggesting local translation of *rho3* mRNAs in *U. maydis* have been uncovered (König et al., 2009), possibly providing an alternative mechanism for localized activation of the GTPase. Nevertheless it seems plausible that yet-to-be discovered GEFs or some of the ones tested, possibly with the aid of cofactors or upon specific modifications, participate *in vivo* in regulating the activity of RHO2 and RHO3, too.

6.2 CDC42 and RAC have overlapping functions in polarized growth of *N. crassa*

The most obvious distinction between the Rho repertoires in yeasts and filamentous fungi is the presence of a Rac homologue in the latter organisms only. Rac is considered the founding member of the Rho GTPase family, from which the closely related Cdc42 and the more distantly related Rho proteins descended, a process associated with concomitant specialization of function (Boueux et al., 2007). In yeasts, Rac was probably lost later (ibid.) and its roles taken over by Cdc42. This scenario would explain why *S. cerevisiae* and *S. pombe* cells devoid of Cdc42 are not viable (Johnson and Pringle, 1990; Miller and Johnson, 1994), while its depletion in some filamentous fungi is not lethal but becomes so upon simultaneous disruption of the Rac-encoding gene (Mahlert et al., 2006; Virag et al., 2007). Initially it was suspected that Rac might play a major role in hyphal growth (Harris and Momany, 2004). However, as outlined in the introduction, several recent studies have shown that the general functions and the relative importance of Cdc42 and Rac in hyphal growth differ widely, even between closely related species or species of comparable life style, which highlights the flexibility of adaptation mechanisms.

The results presented here show that in the ascomycete *N. crassa*, both RAC and CDC42 are dispensable for viability, but deletion and loss-of-function mutants as well as conditional mutants at restrictive temperature are severely affected in polarized growth (Figure 15 and Figure 16). Cells devoid of either of the two GTPases are still able to germinate, but have a clear growth and polarity defect evident in the formation of small compact colonies with morphological aberrancies. This signifies that establishment of a primary axis of polarity is possible, albeit delayed, in the absence of CDC42 or RAC, but subsequent hyphal extension is highly compromised in distinct ways. Strains deficient in RAC are characterized by dichotomous tip splitting and massive apical hyperbranching; this is also observed to a lower extent in mutants affected in CDC42 function, but their most prominent feature is the emergence of numerous subapical branches. Thus, the two GTPases appear to function jointly in polarity establishment and maintenance of a stable polarity axis at the hyphal tip, with a greater impact of RAC on the latter process, whereas CDC42 is in addition required to negatively control subapical lateral branching. This notion of both overlapping and individual roles of the two GTPases in hyphal morphogenesis is corroborated by the findings that the simultaneous depletion of RAC and CDC42 appears to be synthetically lethal and conditional double mutants incubated at non-permissive temperature show drastically exacerbated defects and loss of polarity almost incompatible with viability; on the other hand, overexpression of *rac* cannot rescue the polarity defects of a *cdc-42* mutant strain (Supplementary Figure 6, p.110). Therefore, *N. crassa* constitutes another example of a filamentous fungus whose Rac and Cdc42 homologues have at least one common essential function, as is also the case for *A. nidulans*, *A. niger* and *U. maydis* (Mahlert et al., 2006; Virag et al., 2007; Kwon et al., 2010). In contrast to these species, however, the redundancy of functions of RAC and CDC42 appears to be a lot higher in *N. crassa*, thereby more resembling the situation in *P. marneffeii*, where both CflA and CflB are more or less equally involved in hyphal growth (Boyce et al., 2001, 2003). However, while similar hyperbranching phenotypes of deletion mutants suggest that the two Rac homologues of *N. crassa* and *P. marneffeii* might indeed have analogous roles in securing apical dominance, loss of *N. crassa* CDC42 results in a hyphal phenotype rather similar to that of *C. purpurea* strains expressing a dominant negative allele of *cdc42* (Scheffer et al., 2005). Unfortunately, none of

the downstream effectors of the corresponding GTPases have been identified so far in these two fungi.

The proposed overlap in function of *N. crassa* RAC and CDC42 is also reflected in their similar localization pattern; both GTPases appear to be present all over the cytoplasm and are regularly found concentrated at the apical membrane of growing cells, at vacuolar membranes and at septa (Figure 19). Accumulation of Rac and Cdc42 homologues at the apex of growing hyphal tips, often in a crescent-like structure as in this study, has been reported for several filamentous fungi such as *P. marneffeii* (Boyce et al., 2003, 2005), *A. nidulans* (Virag et al., 2007), *A. niger* (Kwon et al., 2010) or *C. albicans* (Hazan and Liu, 2002; Bassilana et al., 2005) and underlines the importance of the GTPases for proper tip elongation. Likewise, septal localization has also been observed for CflA and CflB in *P. marneffeii*, where loss of the latter leads to inappropriate septation (Boyce et al., 2003, 2005), as well as for Cdc42 in *C. albicans* (Bassilana et al., 2005) and, rarely, for RacA in *A. niger* (Kwon et al., 2010). However, with the exception of *U. maydis* Cdc42, which appears to be highly specialized for control of cell separation (Böhmer et al., 2008), potential contributions of Rac and Cdc42 to septation or septum-related processes in filamentous fungi such as *N. crassa* remain to be elucidated.

While a more detailed analysis of *N. crassa* RAC and CDC42 subcellular localization with respect to spatial and temporal resolution, for instance during lateral branch emergence, might reveal the subtle differences accounting for partially different morphological outcome of deficiency in one of the two GTPases, the identification of shared and unique downstream effector proteins could help even more in clarifying their distinct roles. Potential candidates for interaction with the two GTPases include CRIB domain containing proteins, three of which are predicted by PROSITE (<http://expasy.org/prosite/>, entry PS50108) to be encoded by *N. crassa*. One of them, NCU00142, is a predicted protein with no other conserved domains and only uncharacterized homologues, all of which are found in close relatives of *Neurospora* only; the other two, NCU00406 and NCU03894, are homologues of the yeast PAK family kinases Cla4p and Ste20p, respectively. In both budding and fission yeast, Cdc42-interacting PAK kinases play a role in actin organization and MAPK cascade activation (reviewed in (Perez and Rincón, 2010)), and additionally, *S. cerevisiae* Cla4p has been implicated in septin organization (Dobbelaere et al., 2003; Versele and Thorner, 2004). Among filamentous fungi, too, PAK kinases have been identified as putative effectors of Cdc42, and of Rac. Interactions between Cdc42 and the CRIB domains of Cla4 and Ste20 homologues of *C. albicans* have been studied extensively (Su et al., 2005); in *C. purpurea*, Cla4 has been proposed to interact with Rac1 for ROS homeostasis (Rolke and Tudzynski, 2008), the *Magnaporthe grisea* Cla4 homologue Chm1 and Rac1 appear to jointly activate conidiogenesis (Chen et al., 2008), and *U. maydis* Cla4 is presumed to be one of the Rac1 effectors required for cell wall extension during filament formation (Mahlert et al., 2006). It is very likely that analogous interactions with PAK kinases also mediate some of the functions of *N. crassa* CDC42 and RAC. Interestingly, the Cla4-like NCU00406 has been found to be maximally expressed at the periphery of *N. crassa* colonies (Kasuga and Glass, 2008), indicating its involvement in active growth; furthermore, an, albeit non-functional, GFP-tagged version of the protein accumulated at septa (Justa-Schuch, 2010), suggesting that it might engage there with RAC and/or CDC42 in regulation of septum-associated processes. Other potential effectors inferred from the filamentous relatives of *N. crassa* include components of the ROS production machinery, which have been implicated in regulating differentiation processes and apical dominance in hyphae (see introduction and (Scott and

Eaton, 2008)); after all, at least the latter process is clearly affected in the *N. crassa rac* and, less severely, *cdc-42* mutants. Indeed, two NADPH oxidases, NOX-1 and NOX-2, as well as an orthologue of the regulatory subunit NoxR, NOR-1, are present in *N. crassa* and have been shown to be involved in hyphal growth, although their main functions appear to be in regulating asexual and sexual development (Cano-Domínguez et al., 2008). Interestingly, however, the study reports that ascospores devoid of NOX-2 fail to germinate, which could be a result of impaired polarity establishment. Apart from PAK kinases and Nox factors, proteins directly implicated in organizing the actin cytoskeleton as one of the main determinants of directional growth are likely part of RAC/CDC42 downstream signalling. Intriguingly, the tip branching phenotype of *rac* and *cdc-42* mutant strains observed in this study is highly reminiscent of conditional actin mutants (Seiler and Plamann, 2003). Consistently, strains deleted for Rac homologues characterized by apical hyperbranching in *A. niger* and *P. marneffeii* exhibit defects in actin localization, indicating that the inability to efficiently focus actin polymerization may result in the establishment of multiple axes of polarity (Boyce et al., 2003; Kwon et al., 2010). The sole formin BNI1 of *N. crassa* might well be an important effector engaged by RAC and/or CDC42 for safeguarding directed actin structures needed for proper tip elongation, as judged from similar interactions proposed for the two yeasts and the filamentous fungi *A. gossypii* and *A. nidulans* (Schmitz et al., 2006; Virag et al., 2007; Perez and Rincón, 2010). In light of the multitude of morphogenetic factors possibly acting downstream of RAC and CDC42, much work will certainly be needed to elucidate the common and individual output pathways, which ultimately determine the pattern of redundancy and specialization observed for the two GTPases in *N. crassa*.

6.3 CDC24 acts as a GEF of RAC and CDC42

In budding and fission yeasts, Cdc42 activity in polarity establishment is regulated by the RhoGEF Cdc24p or its close homologue Scd1, respectively (Zheng et al., 1994; Chang et al., 1994). Cdc24 homologues have also been implicated in regulation of Cdc42 homologues in *A. gossypii* and *C. albicans*, while *U. maydis* Cdc24 has been proposed to be an activator of Rac1 (Wendland and Philippsen, 2001; Bassilana et al., 2003; Mahlert et al., 2006; Castillo-Lluya et al., 2007). However, for none of the filamentous fungi GEF activity of Cdc24 towards the presumed target GTPase has been directly demonstrated. Thus, this study presents the first such evidence, showing that *N. crassa* CDC24 stimulates *in vitro* nucleotide exchange in both RAC and CDC42 (Figure 9). Consistent with this result, the polarity defects observed in conditional *cdc-24* mutants at restrictive temperature (Figure 13 and Figure 14) bear similarity to those seen for mutants deficient in RAC and CDC42 function. The less affected mutants *cdc-24(10-19)* and *cdc-24(19-3)* exhibit clear apical hyperbranching as seen for *rac* and, less pronounced, for *cdc-42* mutants, while the hyphal morphology of the most severely impaired strain *cdc-24(24-21)* is reminiscent of the complete loss of polarity evident in the conditional double mutant devoid of functions of both GTPases. Moreover, *cdc-24(24-21)* conidia are unable to perform the isotropic-polar switch required for spore germination, and ascospores homokaryotic for deletion of *cdc-24* also fail to establish polarity. This indicates that CDC24 function, like presence of at least one of its two target GTPases, is essential for growth. Similarly, depletion of Cdc24 appears to be incompatible with viability in *A. gossypii*, *C. albicans* and *U. maydis* (Wendland and Philippsen, 2001; Bassilana et al., 2003; Castillo-Lluya et al., 2007). Likewise, disruption of *S. cerevisiae* CDC24 is lethal (Coleman et al., 1986), while, strikingly, *S. pombe* strains devoid of Scd1 are viable and largely unaffected in growth rate, although mutant cells become spherical, are unable to mate and exhibit defects in endocytosis (Chang et al., 1994; Murray and Johnson, 2001). In *S. pombe*, the second

Cdc42-specific GEF Gef1 appears to be able to provide sufficient essential Cdc42 activity in the absence of Scd1, as indicated by synthetic lethality of their double deletion (Coll et al., 2003; Hirota et al., 2003). In *N. crassa*, in contrast, the second proposed CDC42 (and possibly RAC) activator, the Gef1-homologue NCU10282, is obviously not able to sufficiently substitute for CDC24 in the same way, hinting at a higher degree of regulator specialization in the filamentous fungus.

The *in vitro* GEF activity assays have shown that *N. crassa* CDC24 exhibits equal GEF activity towards RAC and CDC42. Nevertheless, in previous experiments, only overexpression of *rac*, but not *cdc-42*, had been able to suppress the morphological defects observed in the three conditional *cdc-24* mutant strains. In addition, these strains do not show pronounced subapical hyperbranching indicative of specific CDC42 impairment, thus suggesting that the CDC24 proteins encoded by the respective alleles might be preferentially impaired in activation of RAC. Specificity of GEF-GTPase interactions has been the subject of several studies, but so far research has mostly focused on selectivity determinants found in the GTPases (e.g. (Li and Zheng, 1997; Karnoub et al., 2001; Movilla et al., 2001; Rossman et al., 2002; Oleksy et al., 2006)), while little is known about the residues of RhoGEFs allowing discrimination between highly similar GTPases. Therefore, the mutant *cdc-24* alleles analyzed in this study appeared to offer the chance to identify residues contributing to the dual specificity of *N. crassa* CDC24, so far the only GEF of a filamentous fungus shown to be active on both RAC and CDC42.

However, contrary to our expectations, the three CDC24 variants did not exhibit significantly altered target specificity *in vitro*, neither at permissive nor at restrictive temperature (Figure 18). Nevertheless, the results prove that GEF activity of CDC24 is required for proper polarized growth, as the three CDC24 variants show reductions in GEF activity directly correlated with the severity of polarity defects observed in the corresponding mutant strains. Moreover, the results indicate that it is indeed the intrinsic GEF activity of each of the three proteins that is affected by the respective substitutions of conserved amino acids within the GEF or PH domain, although it cannot be excluded that secondary effects, for example mediated by altered protein-protein interactions, might add to the defects observed *in vivo*.

The unexpected result of the *in vitro* assays leaves open the question why in the original phenotypic rescue experiment, only RAC turned out to act as an extragenic suppressor of the *cdc-24* mutant defects. While dosage effects might have played a role, recommending a repetition of the experiment including careful control of expression levels of the two GTPases, other possible explanations could apply. The Gef1-homologue NCU10282, which preferentially activates CDC42 *in vitro*, might be able to substitute at least partially for loss of CDC24 stimulatory activity towards CDC42, providing a residual activity of this GTPase which alone is not enough to secure vital functions, but in combination with overexpressed RAC suffices to suppress the polarity phenotype. In this model, NCU10282 would predominantly, but not exclusively, regulate the non-essential unique functions of CDC42, while CDC24 would be the main activator controlling the shared essential functions of RAC and CDC42 (and possibly non-essential functions of RAC), which is also consistent with the proposed lethality of deletion of *cdc-24* or combined depletion of the two GTPases. At the same time, this notion would rather speak against a function of the uncharacterized CZH family member NCU09492 as a RAC-specific GEF or at least assume that it exclusively channels RAC activity towards non-essential individual output pathways. Intriguingly, an alternative, almost converse model is equally imaginable. If NCU10282 only possessed a highly output-specific or spatially restricted role in activation of CDC42, e.g. during septation,

even increasing the amount of cellular CDC42 would, in the absence of CDC24, not result in markedly increased levels of active CDC42 at the hyphal tip or other regions where it is needed; on the other hand, the putative RAC activator NCU09492 might be able to provide enough general RAC stimulatory activity to ensure that the GTPase, when overexpressed, can alone fulfill the shared essential functions. Rescue experiments employing constitutively active RAC and CDC42 might help clarify some of the questions still remaining - in *P. marneffeii*, for instance, the overexpression of constitutively active, but not wild type CflA partially rescues the defects of a *cfIB* deletion mutant (Boyce et al., 2003). However, they might also fail to produce new insights, as it is becoming increasingly clear that GTP-locked Rho proteins are not always able to substitute for their cycling-competent counterparts (cp. e.g. (Irazoqui et al., 2004)).

Rather, further work should probably focus on the role of the upstream regulators in localizing the GTPases to specific sites or, as recently also proposed for *U. maydis* Rac1 and Cdc42 (Hlubek et al., 2008), codetermining their putative output pathways. Unfortunately, my attempts to assess the subcellular distribution of *N. crassa* CDC24 have not been successful so far; however, given the ostensibly identical localization pattern of its two target GTPases, knowing its localization would scarcely help in judging if CDC24 might after all, if not by molecular discrimination, still exhibit some level of differentiation between RAC and CDC42 based on spatially discrete activation. Therefore, I have already constructed a plasmid for bimolecular fluorescence complementation (BiFC) analysis (see Supplementary Figure 16, p.119 and section 6.5) and am currently trying to investigate potential colocalization between the GEF and its target GTPases. However, it might well turn out that CDC24 really does not discriminate between RAC and CDC42; upstream signalling specificity of the two GTPases contributing to their proposedly distinct functions might instead be achieved by other regulatory components such as NCU10282, NCU09492 or the scaffold protein BEM1, whose deficiency has been shown to cause defects similar to those observed in *cdc-24* mutants (Seiler and Plamann, 2003). In any case, a detailed analysis not only of putative effectors but also of the regulatory network above RAC and CDC42 will be needed to really understand how these two GTPases cooperately act in hyphal growth of *N. crassa*, and this study has provided promising candidates for further investigations.

6.4 RHO1 and RHO2 share a function in maintaining cell wall integrity in *N. crassa*

In budding and fission yeasts, Rho1 plays a key role in securing cell wall integrity and also influences actin cytoskeleton polarization (reviewed in (Perez and Rincón, 2010)); prominent functions of Rho1 homologues in maintaining cell wall structure and cell polarization have been shown to be conserved in filamentously growing fungi such as *A. gossypii*, *C. albicans* and various *Aspergillus* species (Kondoh et al., 1997; Wendland and Philippsen, 2001; Beauvais et al., 2001; Guest et al., 2004; Kwon et al., 2010). In contrast, even for the well-studied yeast *S. cerevisiae*, few analyses of Rho2 functions have been published. Initial characterization of a *S. cerevisiae rho2Δ* mutant strain had not yielded any detectable phenotype (Madaule et al., 1987), but subsequently a slight hypersensitivity towards benomyl was observed, and consistently *RHO2* acts as a high copy suppressor of mutants defective in microtubule-based processes (Manning et al., 1997). Genetic interactions also implicate Rho2p in organization of the actin cytoskeleton ((Marcoux et al., 2000) and references therein). More evidence has been collected disclosing *S. pombe* Rho2 as a regulator of α -D-glucan synthesis and cell wall integrity MAPK signalling (Calonge et al., 2000; Ma et al.,

2006), and the only report on functions of a Rho2 homologue in filamentous fungi suggests that, similarly, *A. niger* RhoB might play a role in cell wall integrity and, moreover, in sporulation (Kwon et al., 2010).

This work shows that both RHO1 and RHO2 are involved in polarized growth in *N. crassa* and must share an overlapping function, because combined deficiency in the two proteins elicits pronounced synthetic defects in growth and polarity. As *rho-1* is essential (Vogt and Seiler, 2008), hypomorphic conditional mutants bearing amino acid substitutions at conserved positions within their RHO1 proteins were analyzed; they exhibit slowed extension and reversible depolarization of tip growth upon shift to restrictive temperature (Figure 24). In contrast, a *rho-2* deletion mutant is only mildly affected in growth speed and directionality; however, germination rates of a double mutant are clearly decreased under restrictive conditions, and their very slowly expanding hyphae are characterized by marked subapical and apical apolar swelling of compartments (Figure 26). Inhibitor growth tests were used to identify the putative pathways impaired in the absence of functional RHO1 and/or RHO2. In these, both *rho-1* and *rho-2* mutants turned out to be hypersensitive towards cell wall affecting agents, indicating that maintenance of cell wall integrity is the shared function of the two GTPases (Figure 27). In contrast, none of the mutants appears to be clearly affected in actin cytoskeleton organization, as judged from largely unaltered sensitivity towards latrunculin A. *rho-1* and *rho-2* mutants differ with regard to PKC1 activity, which is presumed to be enhanced in *rho-1* and double mutants only, while, notably, downstream basal MAPK activity is downregulated in all mutants of the RHO1/RHO2 GTPases module (Figure 30). Moreover, yeast two-hybrid assays have established direct interactions of activated RHO1, but not RHO2, with BNI1 and PKC1 (Figure 29).

These results suggest that the polarity and growth defects of *rho-1* and *rho-2* mutants are mostly a consequence of impaired cell wall functions. Action through both cell wall directed pathways known from yeasts, the direct regulation of β -1,3,-glucan synthase activity and the indirect control of cell wall biosynthetic enzymes via the PKC1-MAPK cell wall integrity pathway, is conceivable for RHO1. In contrast, the yeast two-hybrid data seem to exclude the latter route for RHO2, as no interaction with PKC1 was found. On the other hand, lack of RHO2 results in decreased MAK1 activity (Figure 30), suggesting that, like in *S. pombe*, *N. crassa* RHO2 could after all play a role in activating the MAPK pathway. Similarly, the findings that PKC1 activity is increased in *rho-1* and double mutants, while at the same time MAK1 phosphorylation levels are reduced in these strains, are difficult to reconcile. Interestingly, the same counterintuitive combination of hyperactive PKC1 and hypophosphorylated MAK1 (at least under heat stress) has also been reported for a mutant deficient in the only RHO1-specific GAP characterized so far, LRG1 (Vogt and Seiler, 2008). The same study has also produced evidence that COT1, a nuclear Dbf2 related kinase implicated in hyphal morphogenesis (see (Maerz and Seiler, 2010) for review), whose deficiency leads to a hyperbranching phenotype indistinguishable from that of a *Irg-1* mutant, negatively regulates MAK1 activation independent of RHO1-PKC1 signalling. Recently, our group has established physical interactions between COT1 and MIK1 and MEK1, the upper kinases of the cell wall integrity MAPK cascade (A. Dettmann, Göttingen, unpublished results). This suggests that COT1 might interfere with MAK1 activation at these levels, although the physiological relevance of this pathway interface is still unknown. In addition, for *S. cerevisiae*, negative feedback loops involving phosphatases such as Ptp2p have been suggested to terminate prolonged Slp2p/Mpk1p activation (Mattison et al., 1999; Levin, 2005). Therefore, the observed downregulation of basal MAK1 activity in strains exhibiting PKC1

hyperactivity might reflect a general mechanism used by cells to adapt to chronic cell wall stress. Nevertheless, it remains to be determined how PKC1 can be hyperactive when its presumed activator RHO1 is compromised. Firstly, a still unidentified RHO1/2-independent pathway might activate the kinase under conditions of cell wall stress. Secondly, residual RHO1 activity might suffice to provide hyperstimulation of PKC1 in response to the experienced cell wall defects. After all, growth tests were performed at room temperature, at which RHO1 in the temperature-sensitive mutants is active enough to sustain largely normal growth; it might also be able to activate PKC1 signalling and thus trigger diverse PKC1-mediated functions counteracting the stress effects (summarized for *S. cerevisiae* in (Levin, 2005)). In addition, disruption of negative feedback mechanisms might add to the observed PKC1 hyperactivity. A negative feedback loop protruding from the MAPK Slt2p onto the Rho1p-GEF Rom2p has recently been reported to downregulate Pkc1p signalling in budding yeast (Guo et al., 2009); an analogous mechanism possibly existing in *N. crassa* might fail to work given the downregulation of MAK1 activity in the strains concerned.

As MAK1 activity assays had to be performed at non-restrictive temperature, too, residual RHO1 activity could also account for the MAK1 phosphorylation response still efficiently induced in the respective mutants upon treatment with lysing enzymes. In this regard it could, however, also be of note that for *S. cerevisiae* evidence for a Rho1p-independent stimulation of the MAPK Slt2p by Cdc42p has been reported (Rodríguez-Pachón et al., 2002). Similarly, Cdc42 or Rac1, respectively, have been implicated in activating Slt2p homologues in *S. pombe* and *C. albicans* (Merla and Johnson, 2001; Hope et al., 2010); thus, another GTPase might well enable MAPK signalling even in the absence of RHO1 in *N. crassa*, too.

The strong two-hybrid interaction with BNI1 supports a direct impact of RHO1 on actin organization apart from the presumed indirect route via PKC1, but, inconsistently, no hypersensitivity towards latrunculin A treatment was noticed. Again, the conditional nature of the *rho-1* mutants might provide an explanation for this discrepancy, but in addition it should be noted that also in *S. cerevisiae* only a small subset of temperature-sensitive *rho-1* mutants exhibits disorganized actin even under restrictive conditions (Helliwell et al., 1998). Furthermore, although none of the mutations identified in the two *rho-1* alleles alters residues corresponding to those responsible for output specific defects in yeast Rho1p (Figure 25, (Saka et al., 2001)), the conditional *N. crassa* mutants might still be analogously affected in distinct downstream signalling pathways only. To test this possibility, their ability to complement the respective yeast mutants (see also below) should be assessed. In addition, actin staining analyses might help detect abnormal localization patterns of the cytoskeleton in the mutants.

The notion of partial functional overlap between RHO1 and RHO2 is further supported by the similar subcellular localization pattern of the two GTPases (Figure 32, Supplementary Figure 14, Supplementary Figure 15, p.117f). As stated, they are both found at plasma and vacuolar membranes, persistent at septa and in slightly different dynamic vesicular-reticulate structures within subapical regions of hyphae. In contrast to findings in yeasts (Yamochi et al., 1994; Arellano et al., 1997; Nakano et al., 1997; Yoshida et al., 2009) and the filamentous fungi *A. gossypii*, *A. fumigatus* and *U. maydis* (Köhli et al., 2008; Pham et al., 2009; Dichtl et al., 2010), I did not observe concentration of RHO1 at growing cell tips. This might be a physiologically relevant difference, but given the presumed function of the GTPase in polarized apical extension deduced from mutant phenotypes, this seems rather unlikely. Instead, the amounts of localized RHO1 required for efficient tip elongation in *N. crassa* might be so low that no specific tip accumulation is detected when the GTPase is

overexpressed. Alternatively, the RHO1 fusion constructs used might fail to localize correctly, which could also explain their non-functionality evident in the inability to allow ascospore germination in a deletion background. To further elucidate the influence of abnormal expression strength on localization and, possibly, functionality, I am currently in the process of generating a strain in which GFP-RHO1 is expressed from the endogenous locus. In addition, I plan to test the functions of a C-terminally GFP-tagged RHO1 version; in contrast to Rho1 homologues in the two yeasts and other filamentous fungi such as *U. maydis*, various *Aspergilli*, *C. albicans*, *Podospora anserina* (but not *Sordaria macrospora*), *N. crassa* RHO1 does not contain a classical CaaX box, but terminates in CKSSV, suggesting that its membrane localization might be independent of C-terminal prenylation. Apart from the lack of tip accumulation, the observed localization of RHO1 appears plausible: Plasma membrane and vacuole/endomembrane staining has also been reported for *S. cerevisiae* GFP-Rho1p (Yoshida et al., 2009), and cortical and septal localization of Rho1 homologues is also observed in *U. maydis* and *A. gossypii* (Köhli et al., 2008; Pham et al., 2009), further suggesting conserved roles for RHO1 in cell wall maintenance and in cell division. Likewise, the only other study on fungal Rho2 localization reports that in *S. pombe*, GFP-tagged Rho2 is observed all along the plasma membrane and at the septum (Ma et al., 2006), which is in partial accordance with our own observations of *N. crassa* RHO2 localization. However, it will be of special interest to identify the prominent vesicular-reticulate structures observed for RHO1 and RHO2, e.g. by counterstaining or using marker proteins to visualize different cellular compartments (cp. e.g. (Araujo-Palomares et al., 2007)). Interestingly, GFP-LRG1, besides its apical and septal accumulation, has also been reported to localize in a vesicular-reticulate structure not dissimilar to that seen for its target GTPase (Vogt and Seiler, 2008); in addition, said structure is also reminiscent of the localization pattern of CHS3 and, above all, CHS6, although these two chitin synthases are also found in the Spitzenkörper (Riquelme et al., 2007). It is tempting to speculate that, as suggested by several lines of evidence for budding yeast (Qadota et al., 1996; Abe et al., 2003; Valdivia and Schekman, 2003), inactive RHO1, and possibly RHO2, colocalizing with cell wall biosynthetic enzymes in secretory organelles might serve as pools to supply sites of active growth at the plasma membrane. However, more work is clearly needed to validate this hypothesis.

In parallel, my research efforts in the near future will focus on confirming the physical interactions found in two-hybrid experiments between RHO1 and its putative effectors PKC1 and BNI1 by coimmunoprecipitation and pulldown analyses, two methods also used to validate some of the corresponding interactions in yeasts (Kamada et al., 1996; Kohno et al., 1996; Arellano et al., 1999). As stated in section 5.3.3, RHO2 will also be included in the investigations, especially to clarify whether PKC1 might after all represent an effector of the GTPase, similar to the situation in *S. pombe* (Arellano et al., 1999). This would help determine if RHO2 employs the PKC1 pathway to impact cell wall integrity, as suggested by reduced basal MAK1 activity in the $\Delta\rho\text{-}2$ mutant, or only uses other yet-to-determined routes such as direct control of cell wall biosynthetic enzymes. In this context, analysis of interaction between the sole Fks1p homologue NCU06871 (Schimoler-O'Rourke et al., 2003) and the two Rho proteins using the same methods will be of special interest. In this study, no interaction between any of the GTPases and the catalytic subunit of β -1,3-glucan synthase was found in yeast two-hybrid assays; however, this was not too surprising, as the same technique had also yielded negative results for *S. cerevisiae* and *A. gossypii* Rho1 and glucan synthase homologues, and because prenylation of the GTPase has been proposed to be required for interaction of the two *S. cerevisiae* proteins (Inoue et al., 1999; Köhli et al., 2008).

Besides these continued attempts to define more clearly the effectors utilized by RHO1 and/or RHO2, I intend to analyze the degree of functional overlap between them by testing their ability to substitute for each other. For this, I have already cloned overexpression plasmids encoding 3xmyc-tagged wild type and dominant positive or negative versions of the two GTPases, which I will use for transformation of mutant strains. Another way to dissect the shared and individual roles of RHO1 and RHO2 in polarized morphogenesis could be phenotypic rescue experiments employing *S. cerevisiae* strains harbouring *RHO1* mutant alleles belonging to either one of the two complementation groups specifically impaired in distinct output pathways (see Figure 25 and (Saka et al., 2001)). As even human RhoA partially complements a *S. cerevisiae rho1* deletion mutant (Qadota et al., 1994) and, as stated in the introduction, Rho1 homologues of numerous filamentous fungi can substitute for budding yeast Rho1p, I expect to experience no general problem in this trans-species approach, which together with the other pending experiments will hopefully help in shaping a clearer picture of RHO1 and RHO2 signalling pathways in *N. crassa*.

6.5 NCU00668 is a RHO1-specific GEF and might be autoregulated

While experimental evidence clearly indicates that RHO1 and RHO2 have an overlapping role in cell wall maintenance, activity of the two highly similar GTPases must be regulated in distinct ways, because, like the RhoGAP LRG1 (Vogt and Seiler, 2008), the RhoGEF NCU00668 acts specifically on RHO1, but not on RHO2 or any of the other Rho GTPases. Although the three partial constructs of NCU00668 do not exhibit yeast two-hybrid interactions with their target GTPase, they bind RHO1 in copurification experiments (Supplementary Figure 10, p.114), and, most importantly, two of them unambiguously enhance RHO1 nucleotide exchange activity *in vitro* (Figure 8). As a fine-balanced expression ratio between binding partners appeared to be essential for interactions to be detected in the two-hybrid experiments in this study (cp. the contrasting data for RHO1 and PKC1N expressed from different vectors, Figure 28), failure to produce positive binding interactions in this system could be attributable to inadequate protein levels. Moreover, two-hybrid interactions between wild type, GDP- and GTP-bound versions of Rho GTPases with their respective DH-type GEFs have been demonstrated (e.g. (Weinzierl et al., 2002; Mutoh et al., 2005)); yet for other GTPase-GEF pairs detectable interactions are obviously limited to the nucleotide-free form of the Rho protein, which mimicks the transition state of the nucleotide exchange reaction (e.g. (Ozaki et al., 1996; Schmelzle et al., 2002)), or they require the concomitant overexpression of a scaffold protein to stabilize the interaction in the reporter strain (Chang et al., 1994). Therefore, the negative yeast two-hybrid results do in no way challenge the establishment of NCU00668 as a RHO1-specific GEF.

Furthermore, *in vivo* observations corroborate the role of NCU00668 as a positive regulator of RHO1: Mutants deleted for NCU00668 are indistinguishable from analogous *rho-1* deletion mutants, exhibiting clear polarity and growth defects in the heterokaryotic state and lethality in homokaryotic ascospores (Figure 23). In addition, basal MAK1 activity is reduced in the heterokaryotic knockout strain, indicating involvement of the putative GEF in the cell wall integrity signalling pathway (Figure 30). Unfortunately, weak fluorescence intensities in strains expressing GFP- or YFP-tagged NCU00668 so far prevent detailed conclusions about the distribution of the RhoGEF within growing hyphae. Nevertheless, I have demonstrated that it localizes to septa (Figure 31); there, RHO1 is also found, which suggests a function of the GEF-GTPase module during septation or in other septum-associated processes such as septal pore plugging in response to hyphal lesions (see (Markham and Collinge, 1987)).

Based on the findings in budding and fission yeasts, where its close relatives Rom2p and Rgf1/2 accumulate at sites of polarized growth (Manning et al., 1997; Mutoh et al., 2005; García et al., 2006a), and on its evident impact on polarized growth, NCU00668 is also expected to concentrate at the apex of growing hyphae; however, more studies will be needed to verify this prediction. To analyze the anticipated dynamic *in vivo* interactions between NCU00668 and its target GTPase RHO1, I am also pursuing attempts to establish the exact sites of their colocalization by BiFC, a technique previously successfully applied in *N. crassa* to prove interaction between components of a meiotic silencing pathway (Bardiya et al., 2008). In preparation for this, I have already constructed the required plasmids (see section 4.4.6) and started to perform transformations. As a caveat it should be noted, however, that due to the assumed non-functionality of an N-terminally tagged RHO1 construct the intended experiments might require further refinement.

NCU00668 is the first Rho1 GEF identified in any filamentous fungus, and based on my comprehensive GEF specificity screen it is most likely the only activator of RHO1 in *N. crassa*. In the yeasts *S. cerevisiae* and *S. pombe*, in contrast, its homologue pairs Rom1/2p and Rgf1/2, and a third GEF each, Tus1p or Rgf3, respectively, share the function as positive regulators of the respective RHO1 homologue (Perez and Rincón, 2010). This striking difference in the number of GEFs might in part be explained by the fact that at least one of the cellular functions of yeast Rho1 appears to be fulfilled by another GTPase in *N. crassa*. While budding yeast Rho1p is responsible for the assembly of the contractile actin ring needed for cytokinesis (Tolliday et al., 2002), the GTPase upon which this function is bestowed in *N. crassa* is RHO4, whose activity is consistently essential for septation (Rasmussen and Glass, 2005). In *S. pombe*, the functions of Rho GTPases in cytokinesis are less well understood, but Rho1 has likewise been implicated in actin ring assembly (Pinar et al., 2008), although in this organism Rho4, too, appears to play a more important role in cytokinesis than in *S. cerevisiae* (reviewed in (Perez and Rincón, 2010)). The transfer of function between the GTPases appears to have been accompanied by a concomitant transfer of regulator specificity: RGF3, the *N. crassa* homologue of Tus1p and Rgf3, the two GEFs identified as the main regulators of Rho1 functions in actin ring assembly and cytokinesis in the two yeasts (Mutoh et al., 2005; Yoshida et al., 2006), acts on RHO4 but not on RHO1 (Justa-Schuch et al., 2010). Apparently, NCU00668 suffices to control activity of RHO1 for its further output pathways affecting polarity and cell wall integrity in *N. crassa*; in contrast, in the two yeasts two highly similar paralogues with overlapping functions, as evident in synthetic lethality of the corresponding double mutants (Ozaki et al., 1996; Morrell-Falvey et al., 2005), are presumed to fulfill the same task. It is conceivable that a more complex upstream modulation of NCU00668 activity or localization compensates for it being the sole RHO1-GEF in the filamentous fungus.

Remarkably, the *in vitro* GEF activity assays performed in this study produced evidence indicating a possible inhibition of NCU00668 GEF activity by its DEP domain. The function of DEP domains, which are likewise present in the homologous GEFs of the two yeasts (Figure 5), is poorly understood, but DEP domains in other proteins have been implicated in membrane targeting and interaction with heterotrimeric GTPases (Chen and Hamm, 2006; Narayanan et al., 2007). The notion of an autoregulatory role of the DEP domain is based on the finding that a NCU00668 construct containing it exhibits no GEF activity towards RHO1, while constructs lacking this part of the protein serve as efficient stimulators of nucleotide exchange (Figure 20). The possibility that the longer construct is merely inactive due to protein folding problems cannot be ruled out, but the finding that the DEP domain copurifies

with different partial NCU00668 constructs (and Rho GTPases) further supports the existence of an autoinhibition mechanism (Figure 22). However, the putative interference with GEF activity does not function *in trans*, since the presence of excess purified DEP domain constructs does not abolish *in vitro* GEF activity of the shorter NCU00668 constructs (Figure 21). Intriguingly, our findings are in accordance with another report proposing an autoregulatory function of the DEP domain of RasGEF Q, a *Dictyostelium discoideum* exchange factor stimulating the small GTPase RasB (Mondal et al., 2008). In said study, physical interaction between the DEP and GEF domains of RasGEF Q was demonstrated, and cells overexpressing a RasGEF Q construct lacking the DEP domain were shown to exhibit increased activity levels of the target GTPase. Based on these and related findings, the authors suggested a model in which a G protein-coupled receptor, in response to an external stimulus, induces a conformational change in RasGEF Q, thereby relieving the autoinhibitory intramolecular interaction between its DEP and GEF domains and making the regulator competent for activation of its target GTPase. It is attractive to envision a similar mechanism controlling GEF activity of NCU00668 and possibly coupling its activation to upstream signalling pathways. To test this idea, I am planning to perform an overexpression experiment analogous to the one conducted in the amoeba, employing a NCU00668 construct devoid of the DEP domain. However, similar to the aforementioned CRIB domain pulldown experiments, a system allowing specific pulldown of activated RHO1 from *N. crassa* lysates by a Rho binding domain (RBD) construct will first have to be implemented; the existence of strains expressing epitope-tagged versions of the GTPase and successful utilization of the RBD pulldown technique to analyze GTPase activity levels in other fungi (e.g. (Villar-Tajadura et al., 2008; Yoshida et al., 2009)) give reason to hope for a relatively quick outcome. In addition to this approach, *in vitro* activity assays testing if mutations of conserved residues within the DEP domain of the longest NCU00668 construct influence its ability to activate RHO1 might help in providing further evidence for the proposed intramolecular interaction.

Likewise, the conserved CNH domain might influence the regulatory activity of NCU00668 towards RHO1. Its presence in NCU00668 constructs used for *in vitro* assays also resulted in decreased GEF activity (Figure 20), and in the *N. crassa* RHO4-GEF RGF3, for instance, the CNH domain appears to be required for proper localization (Justa-Schuch et al., 2010). Therefore, analyzing its function could give valuable insights in the fine-tuning of NCU00668-mediated RHO1 regulation and its impact on polarized growth.

Together with continued efforts to further elucidate the shared and distinct effector pathways of RHO1 and RHO2, these investigations will hopefully allow us to improve the still fragmentary model on the roles of these two GTPases in hyphal morphogenesis of *N. crassa* (Figure 33). Moreover, future work should address the question how the various GTPase modules, some of whose components and their wiring have been identified in this study, interact to secure polarization of the hyphae.

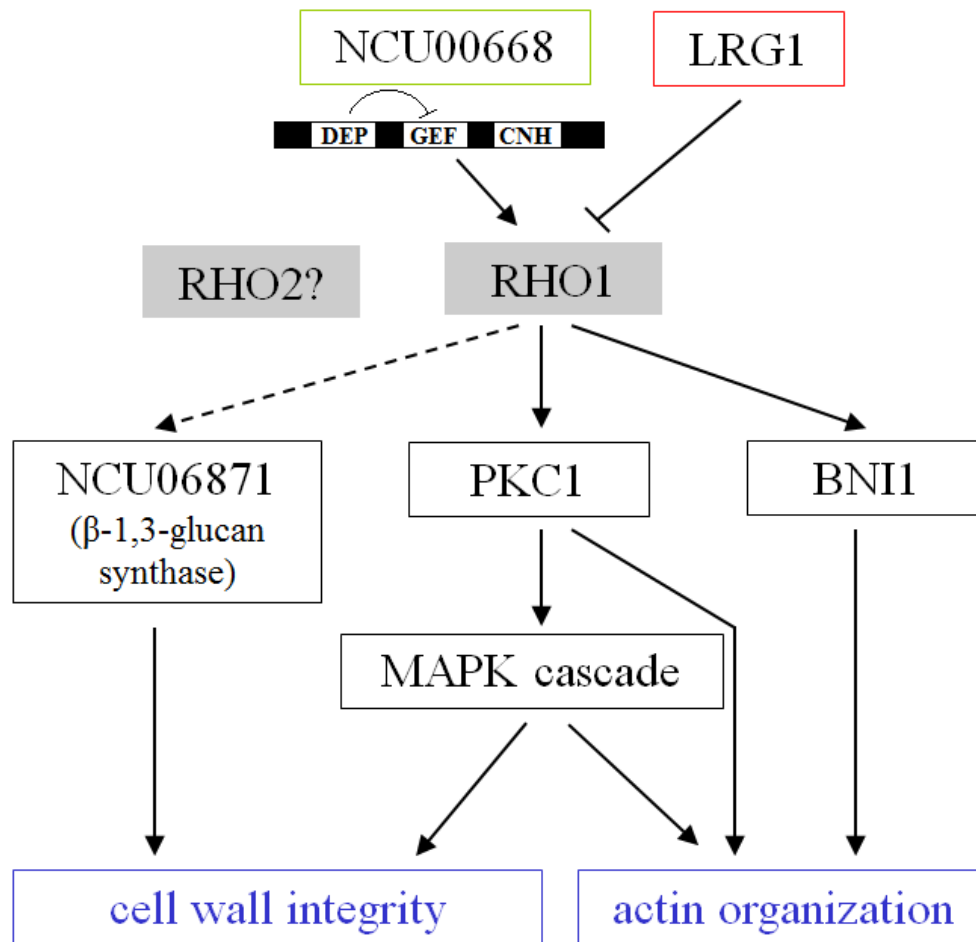
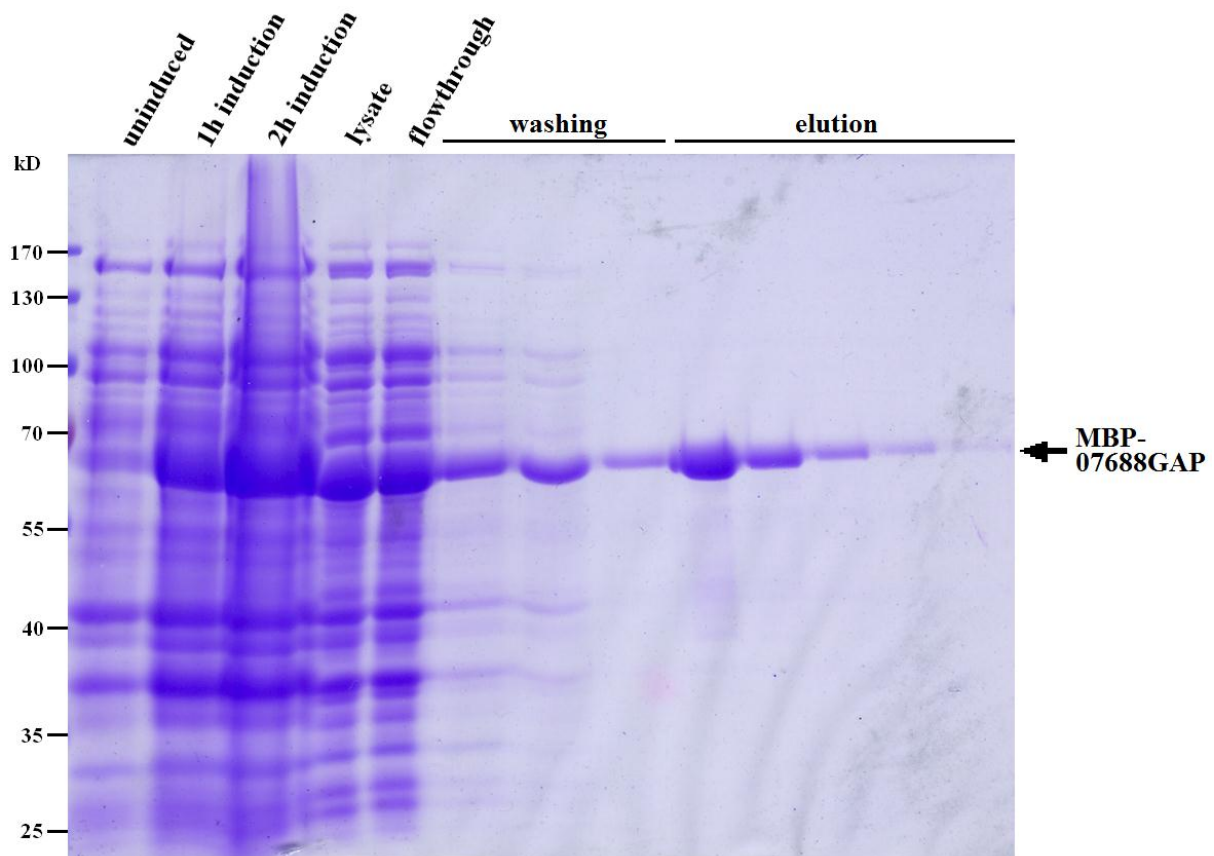


Figure 33: Model of the RHO1/RHO2 GTPase module and its proposed regulation and functions in *N. crassa*. While PKC1 and BNI1 have been established as RHO1 effectors by yeast two-hybrid assays, no interaction partners mediating the influence of RHO2 on cell wall integrity have been identified so far. See text for details.

7. Supplemental material



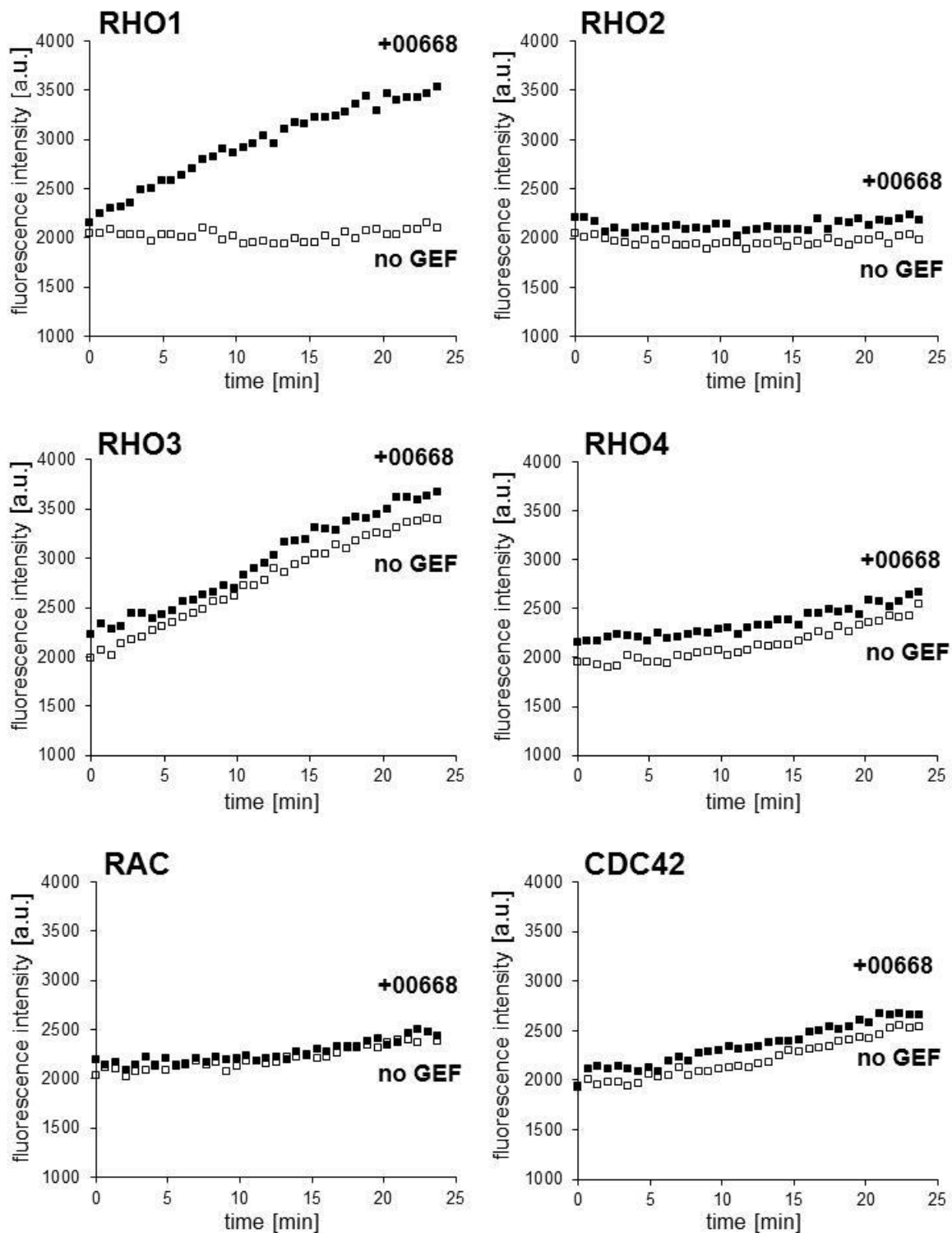
Supplementary Figure 1: Monitoring of MBP-07688GAP fusion protein expression in uninduced and induced *E. coli* cultures and its sequential enrichment during the amylose resin-based affinity purification procedure applied. Samples taken during the indicated steps were subjected to SDS PAGE, and proteins were stained with Coomassie. Protein bands corresponding to MBP-07688GAP (predicted MW=66 kD) are indicated.

Supplementary Table 1: Comparison of gene structures predicted by Broad (annotation versions .3 and .4) and found in own cDNA sequencing. Nucleotide positions in columns 4-8 refer to (translation) start (= nd 1) predicted by .3. See text for details. LG= linkage group.

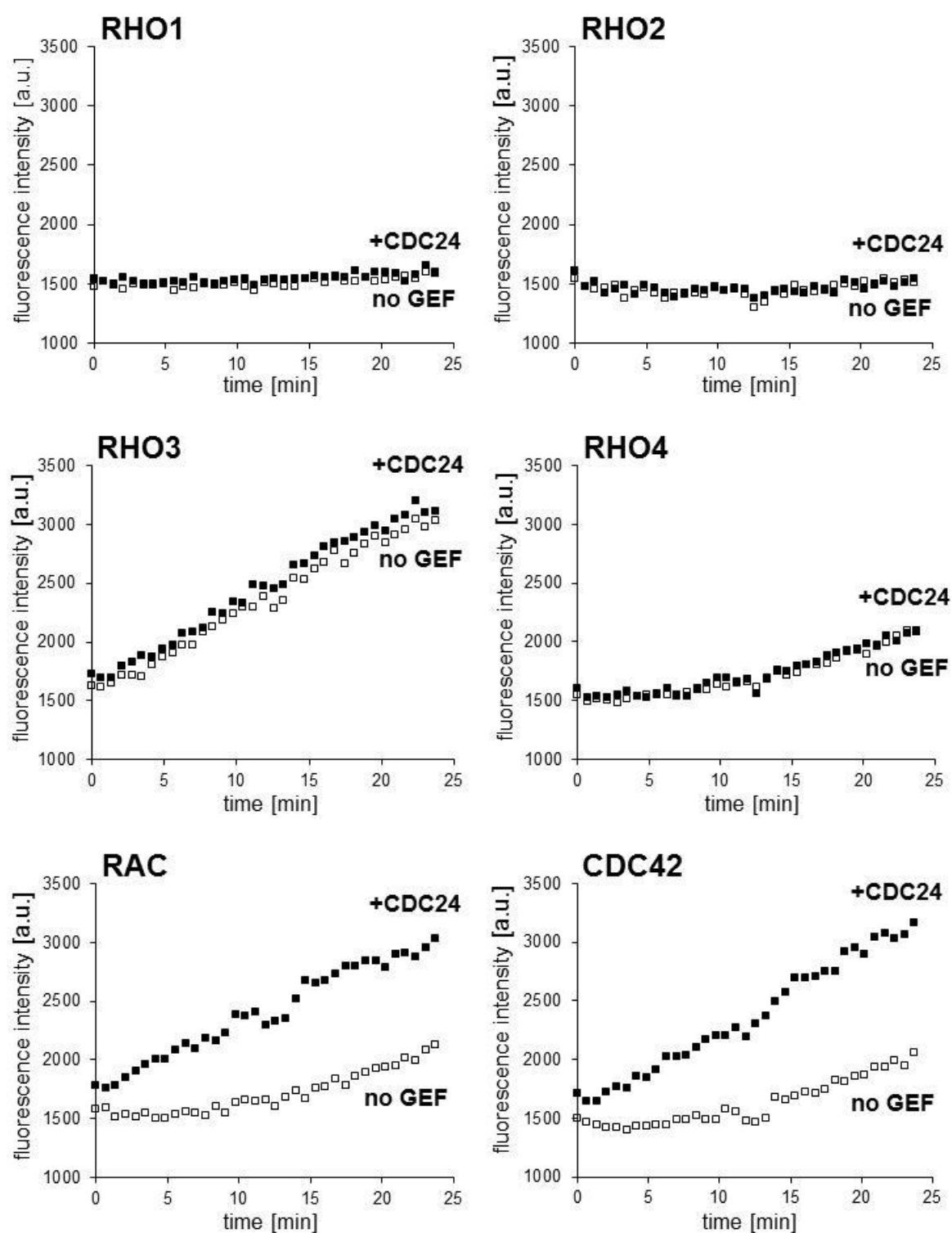
Gene NCU...	LG, strand, start (.3)	Length [nd] (.3)	Predicted introns (.3)	Predicted introns (.4)	cDNA region sequenced	Introns found (own)	Remarks
00196	III, -, 2962447	3365	830-909	unchanged	4-3365	341-667; 830-909	own: protein shorter (no frameshift)
00553	I, +, 8026582	2653	148-219; 274-382; 1002-1060; 1252-1308; 2093-2153; 2304-2369	unchanged	4-2653	as predicted by .3 and .4	-
00668	I, -, 7631108	3874	2819-2877; 3672-3784	2819-2877; 3726-3784	4-3874	as predicted by .4	.4/own: protein longer (no frameshift)
01431 (<i>bni-1</i>)	V, +, 4770295	5511	3722-3778	unchanged	3513-5511	as predicted by .3 and .4 (partial cDNA only)	-
01472	V, -, 4628245	4753	81-141; 187-268; 559-617; 1530-1586	unchanged	4-4753	81-141; 187-242; 559-617; 1530-1586	own: protein longer (putative new start at -229), frameshift at start of sequence
02131 (<i>rgf-3</i>)	I, +, 1140090	5287	1977-2144; 3592-3643	3592-3643	-	-	.4: protein longer (no frameshift)
02524	I, +, 2615368	4928	123-554; 783-883	unchanged	4-4928	as predicted by .3 and .4	-
02689 (<i>lrg-1</i>)	I, -, 3213889	4036	376-433; 1126-1197; 1287-1334; 3221-3286	376-433; 1126-1197; 3221-3286	4-4036	as predicted by .4	.4/own: protein longer (no frameshift)
02764 (<i>Rsp</i>)	I, -, 9284564	3090	853-913; 1944-2005; 2231-2294; 2900-3006	853-913; 1439-1489; 1944-2005; 2231-2294; (3' extended; new stop 3292)	4-3090	853-913; 1439-1489; 1944-2005; 2231-2294	.4/own: protein longer (short internal stretch deleted, no frameshift, but 3' extended), frameshift at end of sequence
02915	I, +, 8706272	2386	81-200; 594-678; 1353-1496	unchanged	4-2386	81-200; 594-669	own: protein longer (no frameshift)
06067 (<i>cdc-24</i>)	VII, -, 2335035	3199	517-602; 1143-1203; 1447-1528	517-602; 1143-1203; 1447-1531; 1719-1772; 2115-2231	695-1918	as predicted by .4 (partial cDNA only)	.4/(own): protein shorter (no frameshifts)

Supplementary Table 1 (continued)

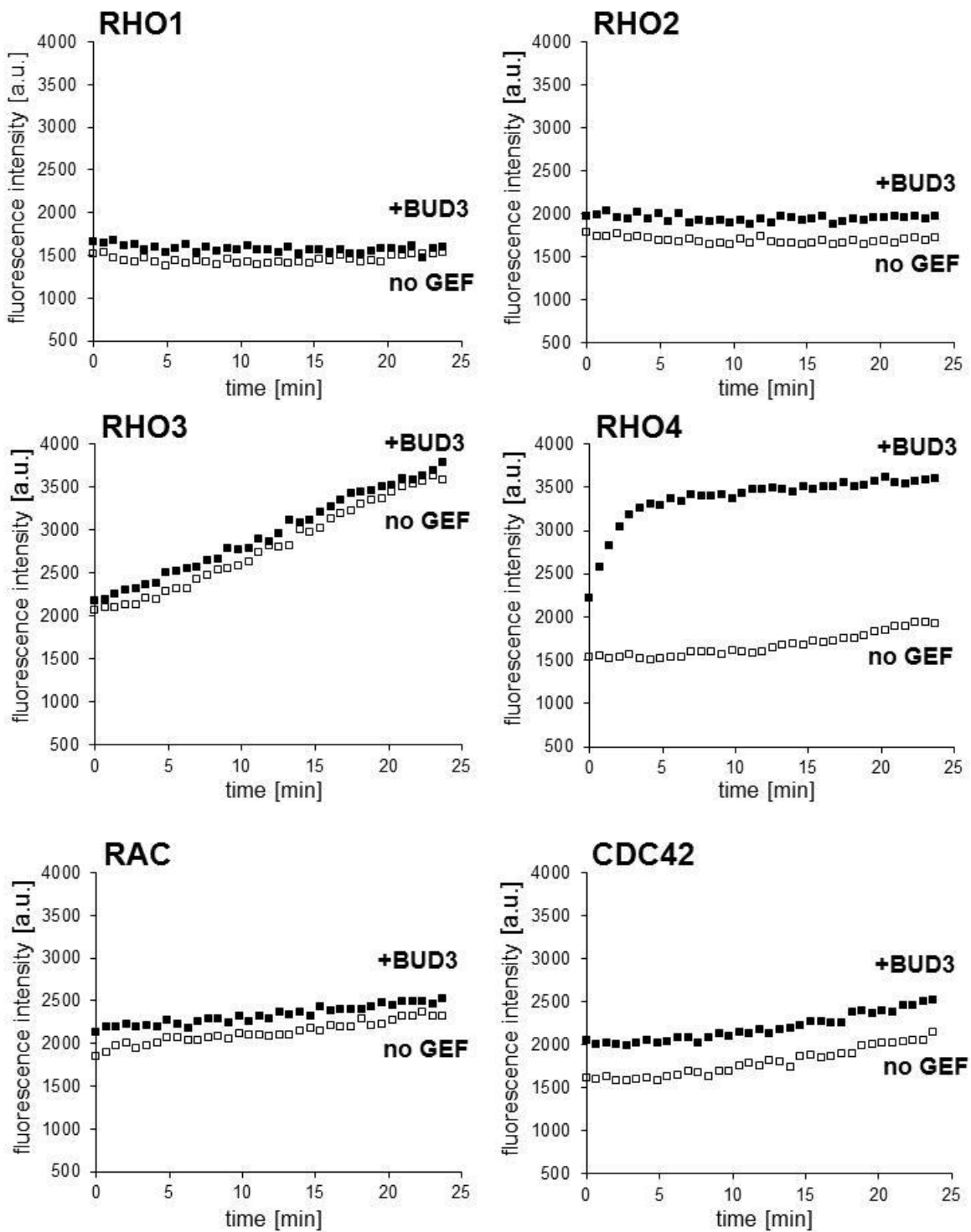
Gene NCU...	LG, strand, start (.3)	Length [nd] (.3)	Predicted introns (.3)	Predicted introns (.4)	cDNA region sequenced	Introns found (own)	Remarks
06544 (<i>pkc-1</i>)	IV, +, 1591451	3744	437-510; 775-842; 1818-1870; 2955-3007 3616-3682	unchanged	4-3744 (i.e end)	as predicted by .3 and .4	-
06579 (<i>bud-3</i>)	IV, -, 1695391	4812	3358-3621	no introns	4-4812	3422-3476	.4: protein longer (no frameshift); own: protein shorter (new stop 3565), frameshift at end of sequence
06871 (<i>g/s-1</i>)	VII, +, 3648268	6007	177-251; 5577-5640	unchanged	2359-4131	as predicted by .3 and .4 (partial cDNA only)	-
07622	IV, +, 304073	1629	821-892	introns unchanged; new start -324	4-1629	as predicted by .3 (and .4)	.4: Protein longer (coding sequence 5' extended in same frame)
07688	IV, +, 2226145	3911	62-184; 270-432; 1599-1661; 3510-3565; 3700-3767	67-124; 156-311; 1599-1661; 3510-3565; 3700-3767	4-3911	as predicted by .4	.4/own: protein longer (short internal stretch near start with altered frame)
09492	II, +, 4458486	6604	5489-5543	unchanged	4-6604	as predicted by .3 and .4	-
09537	V, -, 4523157	2851	47-114; 297-376; 1830-1892	unchanged	4-2851	as predicted by .3 and .4	-
10282	I, -, 9161704	7250	1344-1625; 6925-7136	unchanged	4-7250 (but internal gaps)	as predicted by .3 and .4 (partial cDNA only)	different internal gaps (812/897-3439; no intron consensus!) in cDNAs sequenced
10647	I, -, 351481	2561	557-844; 942-1076; 1451-1509; 2235-2552	557-703; 1451-1509; new stop 2354	4-2561	557-703; 1451-1509; 2235-2552	.4: protein longer (internal insertions, no frameshift; stop at 2354 not removed by splicing); own: protein longer (internal insertions, no frameshift)



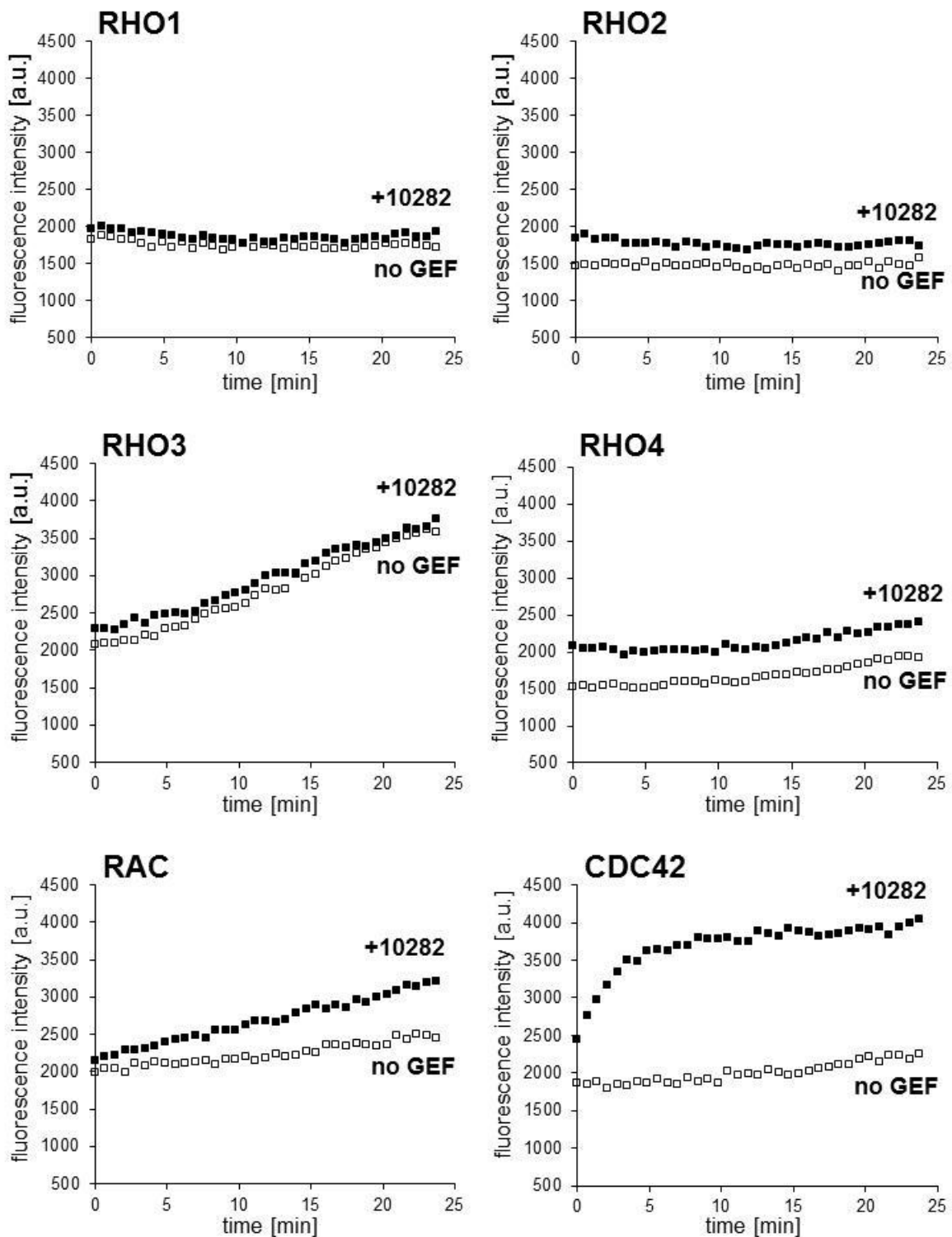
Supplementary Figure 2: Representative plots of fluorescence intensity [a.u.= arbitrary units] over time [min] as a measure for mant-GDP incorporation and thus in vitro nucleotide exchange activity of the six Rho GTPases in the absence (open squares) or presence (filled squares) of the MBP-00668GEF construct.



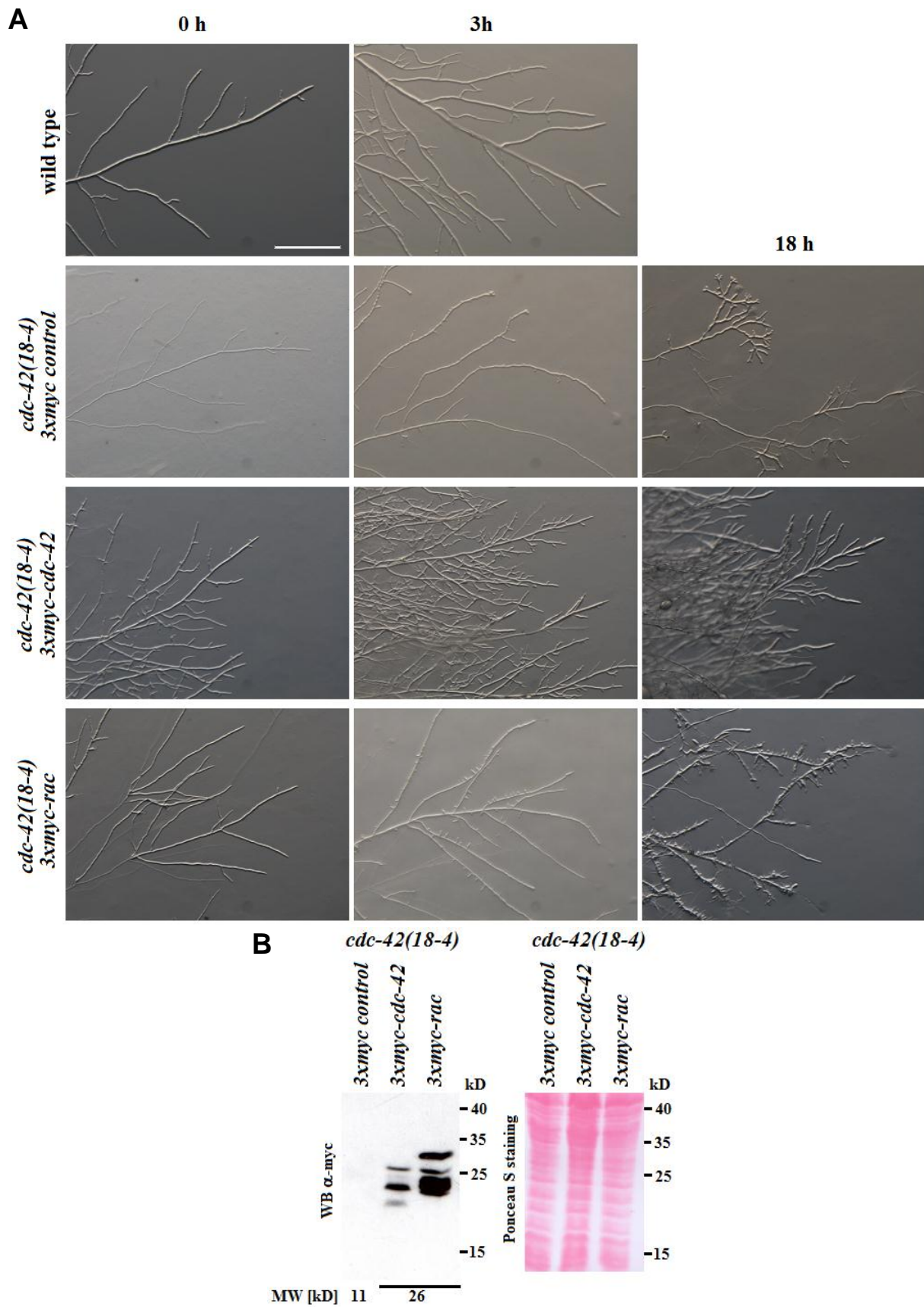
Supplementary Figure 3: Representative plots of fluorescence intensity [a.u.= arbitrary units] over time [min] as a measure for mant-GDP incorporation and thus in vitro nucleotide exchange activity of the six Rho GTPases in the absence (open squares) or presence (filled squares) of the MBP-CDC24GEFP construct.



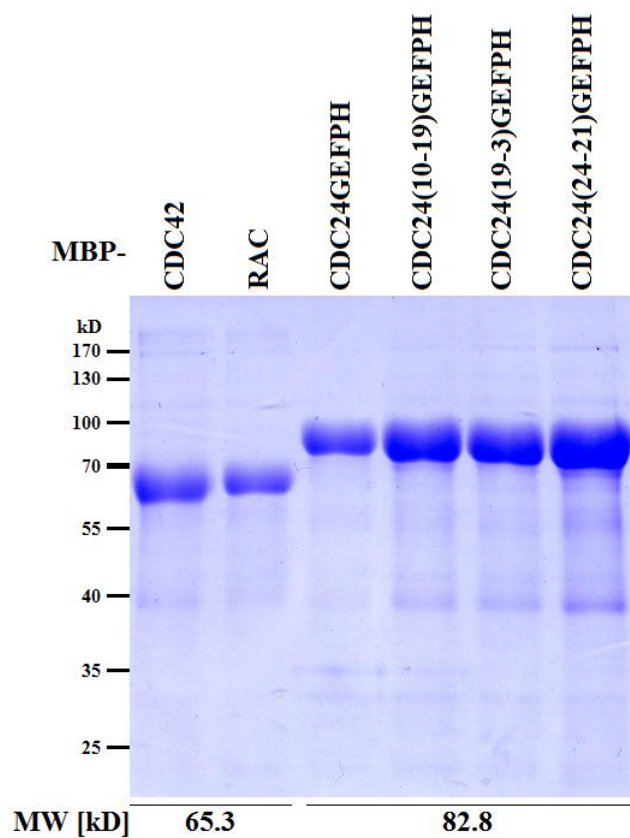
Supplementary Figure 4: Representative plots of fluorescence intensity [a.u.= arbitrary units] over time [min] as a measure for mant-GDP incorporation and thus in vitro nucleotide exchange activity of the six Rho GTPases in the absence (open squares) or presence (filled squares) of the MBP-BUD3GEF construct.



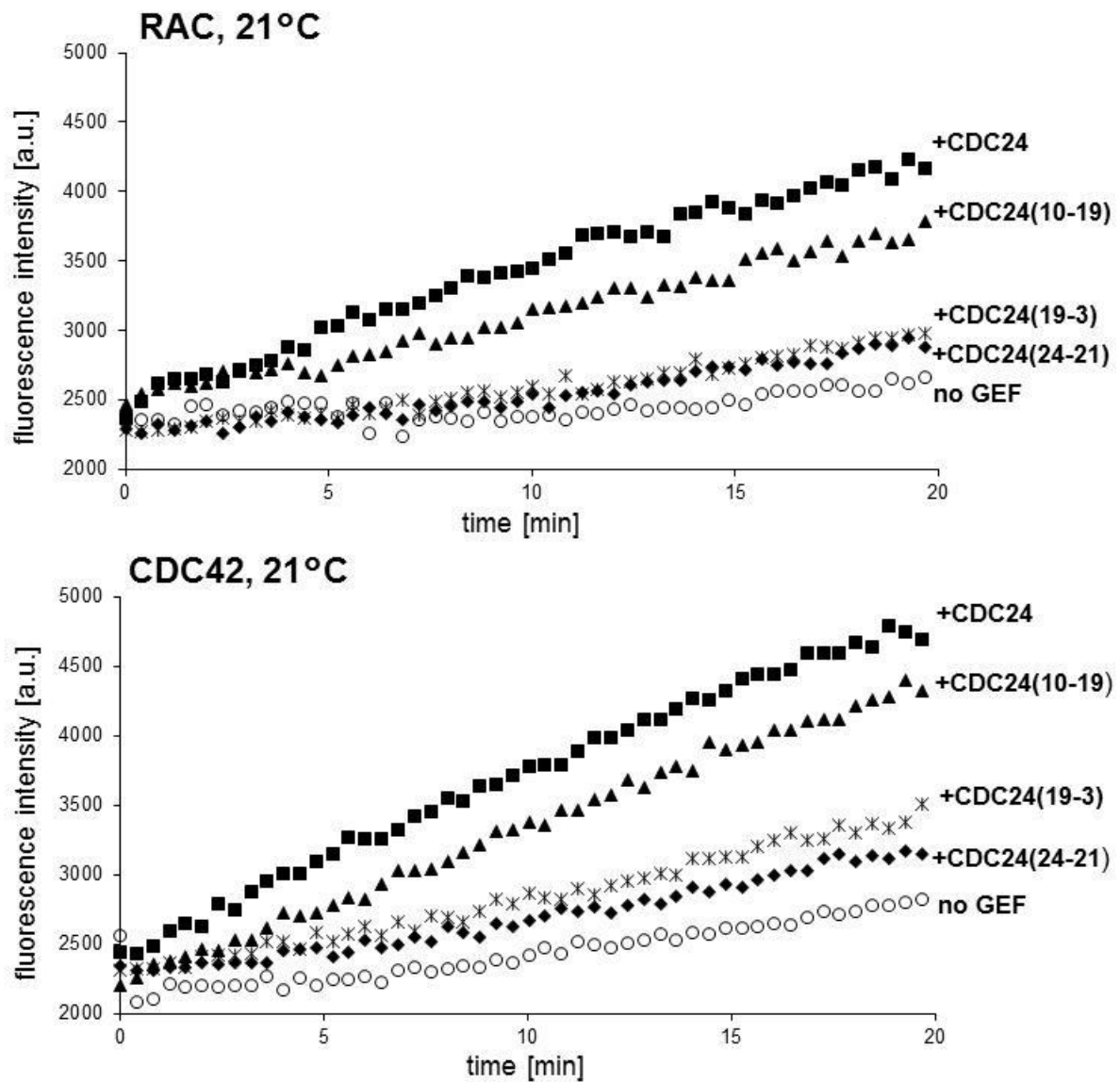
Supplementary Figure 5: Representative plots of fluorescence intensity [a.u.= arbitrary units] over time [min] as a measure for mant-GDP incorporation and thus in vitro nucleotide exchange activity of the six Rho GTPases in the absence (open squares) or presence (filled squares) of the MBP-10282GEFBAR construct.



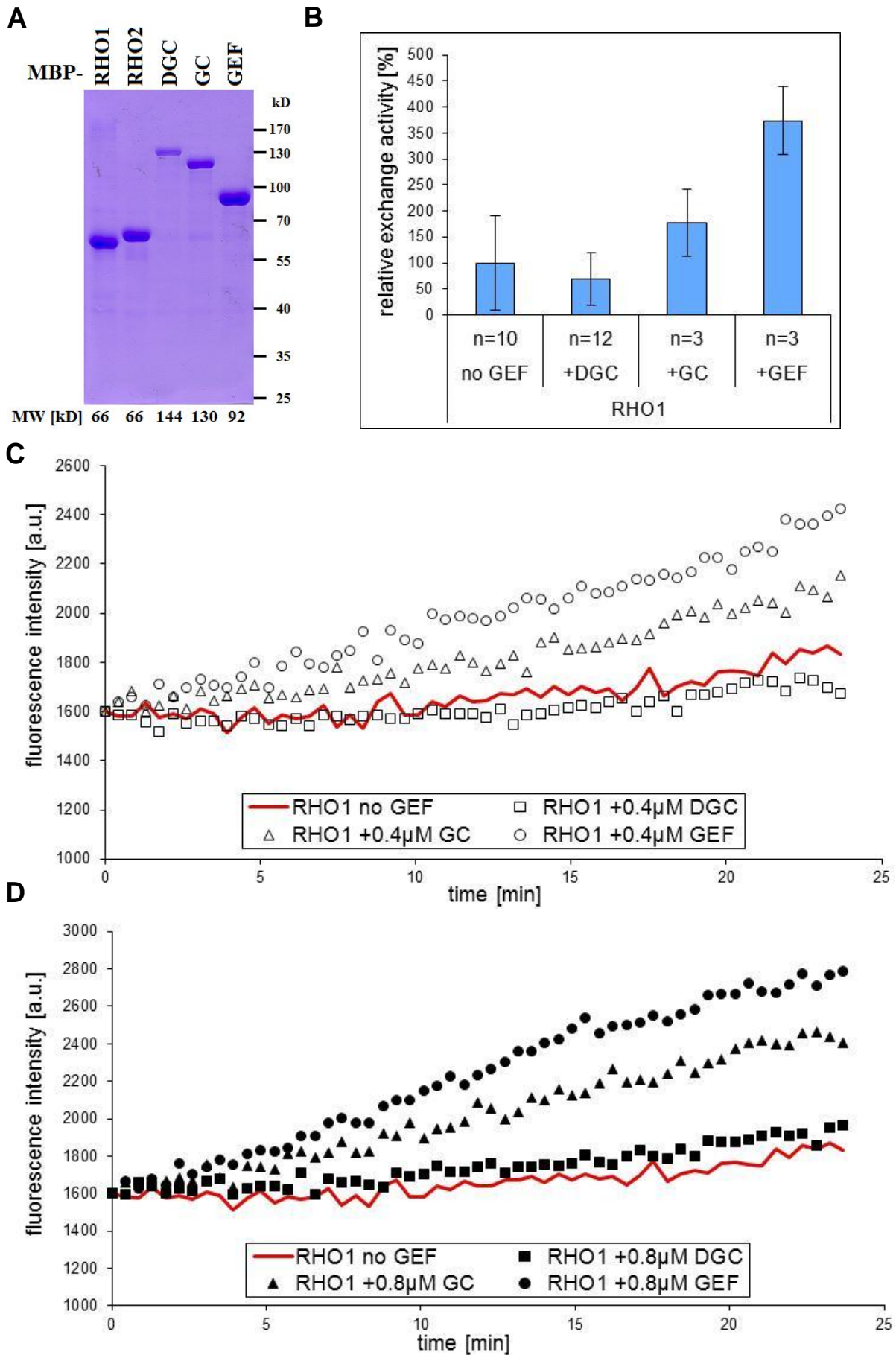
Supplementary Figure 6: Overexpression of CDC42, but not RAC, rescues the morphological defects of *cdc-42(18-4)*. (A) *cdc-42(18-4)* strains transformed with vectors encoding N-terminally 3xmyc-tagged CDC42 or RAC or the empty control vector were cultivated at room temperature and transferred to 37°C. Wild type is shown for comparison. Time points given indicate hours after temperature shift. Scale bar is 500 μ m. (B) Expression of the fusion proteins is verified by immunodetection with α -myc antibody in Western blotting. Ponceau S. staining is shown as a loading control.



Supplementary Figure 7: Result of a representative purification of MBP-tagged Rho GTPase and CDC24GEFPH constructs used to analyze GEF activity of mutant CDC24 versions *in vitro*. A Coomassie stained SDS polyacrylamide gel loaded with eluate fractions of the indicated constructs is shown. Predicted fusion protein molecular weights (MW) are given below the corresponding lanes.

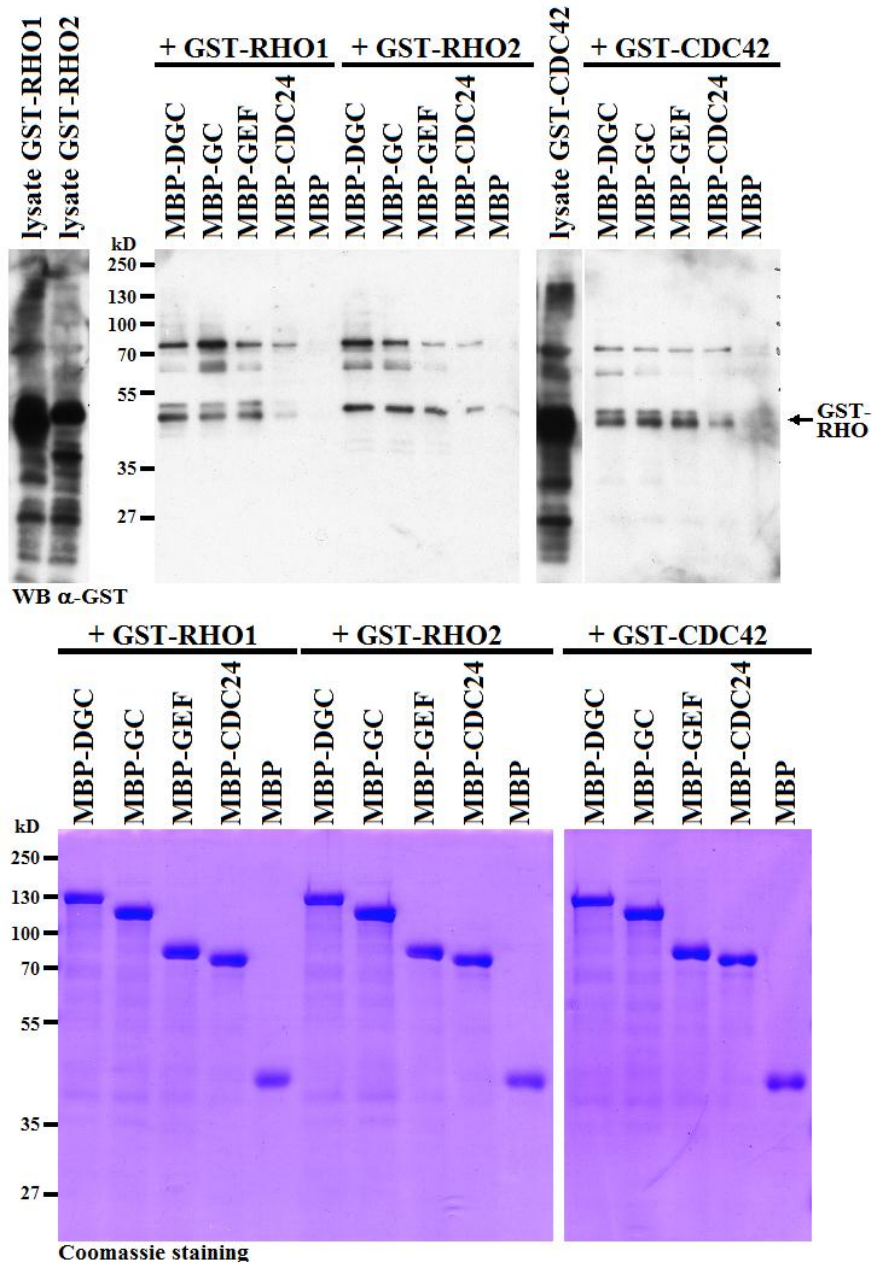


Supplementary Figure 8: Mutant RhoGEF fragments CDC24(10-19), (19-3) and (24-21) exhibit reduced *in vitro* GEF activity towards both RAC and CDC42 compared to the wild type construct. Diagrams show curves of fluorescence emission intensity [a.u. =arbitrary units] plotted over time [min] for representative experiments performed at 21°C. Nucleotide exchange activity of RAC and CDC42 was assessed in the absence of GEF and in the presence of different MBP-CDC24GEFPH constructs.

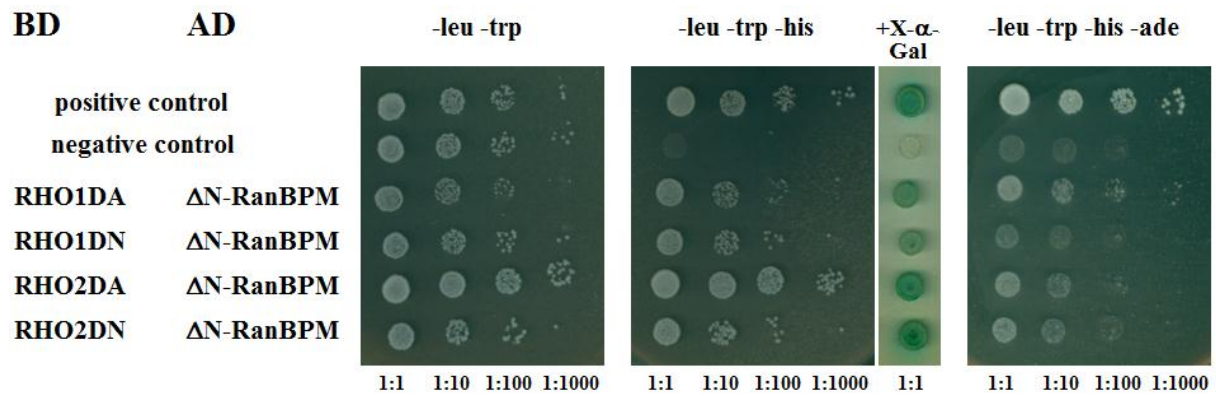


Supplementary Figure 9: Concentration differences are not responsible for differences in GEF activity observed for NCU00668 DGC versus GC and GEF constructs. (A) Result of a representative purification of MBP-Rho GTPase and NCU00668 fusion proteins used in *in vitro* GEF activity assays. A Coomassie

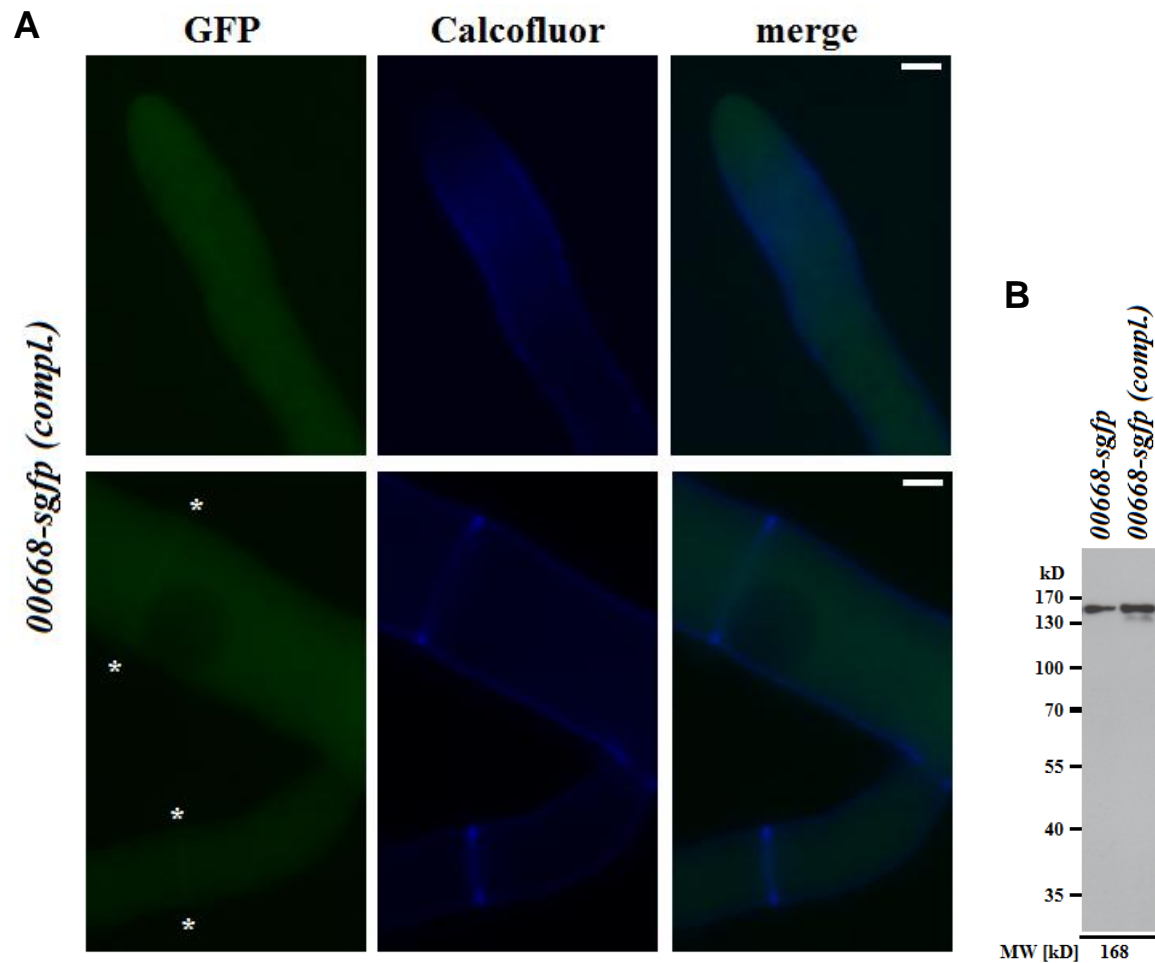
stained SDS polyacrylamide gel loaded with equal volumes of eluate fractions of the indicated constructs is shown. Predicted fusion protein molecular weights (MW) are given below the corresponding lanes. (B), (C): 00668GC and GEF constructs are still active at lower concentration. Mean relative nucleotide exchange activity during first ca. 24 minutes is displayed in (B). Scale bars represent standard deviation, and n gives the number of independent measurements performed in technical duplicate. (C) shows curves of fluorescence emission intensity [a.u. =arbitrary units] plotted over time [min] for representative individual experiments. Each RhoGEF construct was used at 0.4 μ M. (D): The 00668DGC construct is not active at higher concentration. Curves of fluorescence emission intensity [a.u.] plotted over time [min] for representative individual experiments are shown. 0.8 μ M of each RhoGEF construct were used. For better comparability, graphs in (C) and (D) are translated to the same point of origin on the y axis.



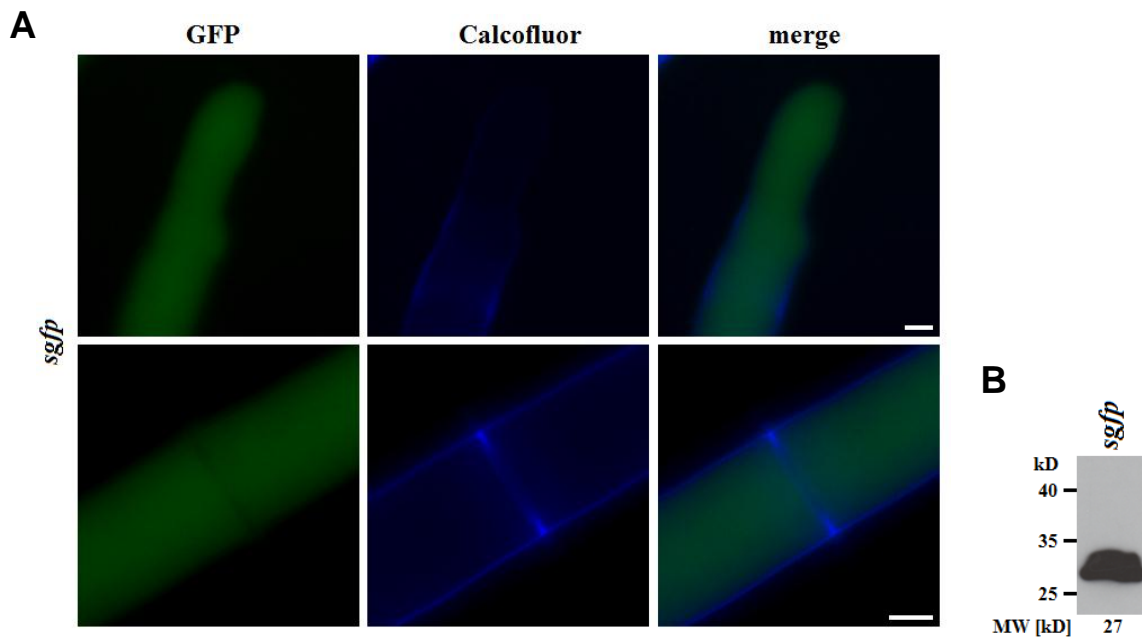
Supplementary Figure 10: Rho GTPases interact physically with various fragments of NCU00668 and CDC24. GST-tagged RHO1, RHO2 and CDC42 (predicted MW=51 kD) copurify with MBP fusions of different fragments of NCU00668 and the GEFPH domain construct of CDC24, but not with MBP alone. Lysates of *E. coli* cells expressing GST and MBP-fusions of the indicated constructs were combined and subjected to affinity purification using amylose resin. Lysate samples and eluate fractions, the latter adjusted to equimolar amounts of the respective MBP fusion proteins, were separated by SDS PAGE. Copurified GST-DEP was detected by Western blotting using α -GST antibody (upper panel), and purified MBP-fusion proteins were visualized by Coomassie staining (lower panel).



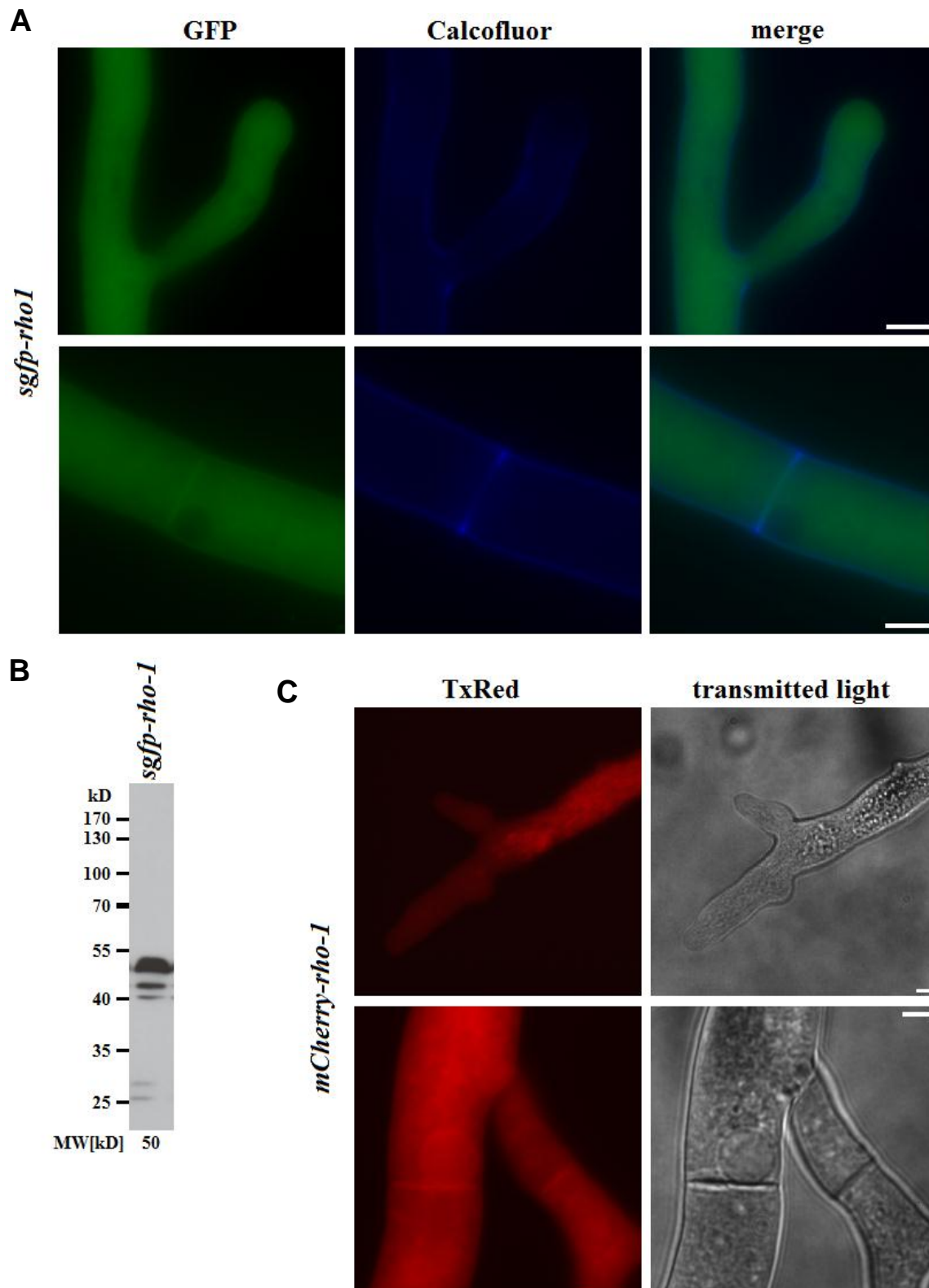
Supplementary Figure 11: All four Rho GTPase constructs used in yeast two-hybrid assays possess general bait competency. The Rho GTPases fused to the GAL4 DNA binding domain (BD) are expressed appropriately for interaction to occur in the assays, as suggested by their interaction with an activation domain (AD) fusion of Δ N-RanBPM. Coexpression of Δ N-RanBPM with GAL4 BD fusion proteins yields positive results if the latter are expressed at sufficient levels and localize to the nucleus (Tucker et al., 2009). See legend of Figure 29 for further information.



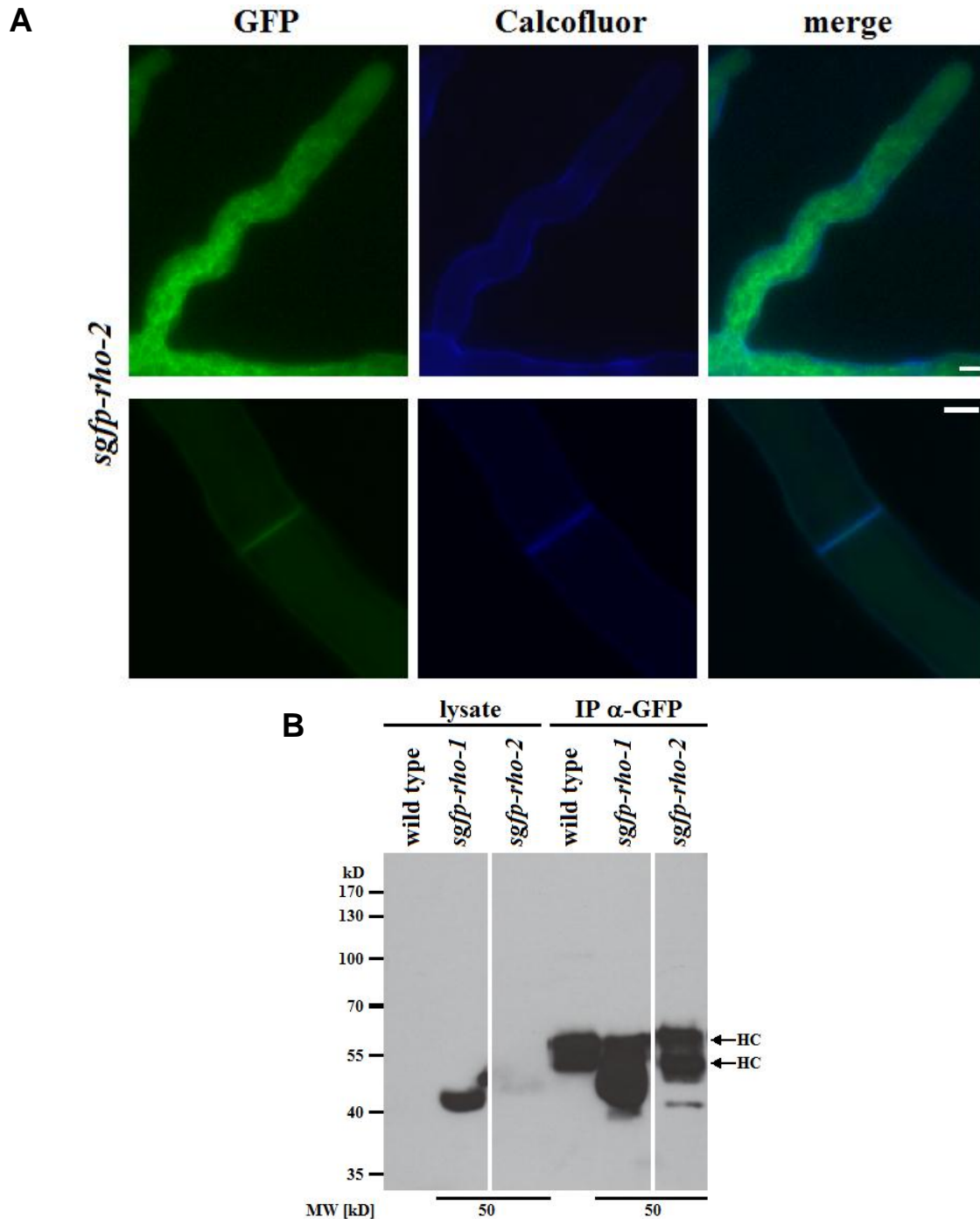
Supplementary Figure 12: NCU00668 localizes to septa and throughout the cytoplasm. (A) Micrographs showing localization of NCU00668-GFP in the deletion background are displayed. Cell wall and septa stained with calcofluor white (DAPI filter) are shown for orientation. Asterisks mark fusion protein accumulation at the septa. Scale bars are 5 μ m. (B) depicts an immunoblot probed with α -GFP antibody verifying expression of NCU00668-GFP in the indicated strains; predicted molecular weight is given.



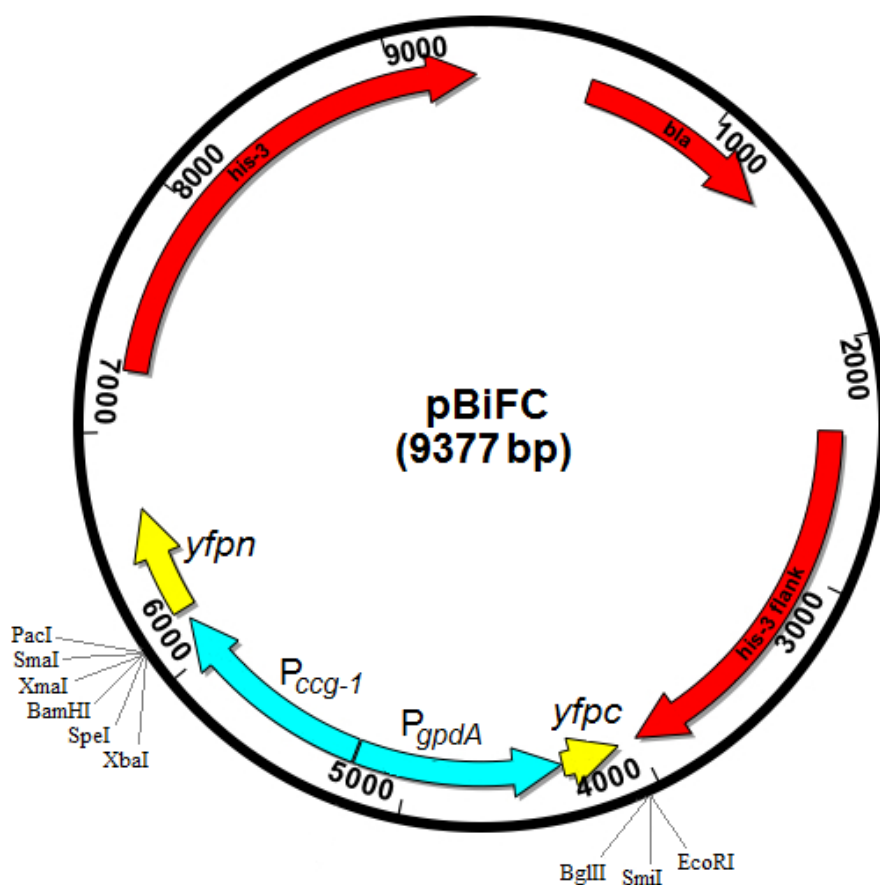
Supplementary Figure 13: GFP is distributed uniformly throughout the hyphal cytoplasm and is absent from septa or membranes. (A) Micrographs showing even distribution of fluorescence in hyphae of strain *sgfp*. Images of cell wall and septa stained with calcofluor white are shown for orientation. Scale bars are 5 μ m. (B) Immunoblot probed with α -GFP verifying expression of GFP in strain *sgfp*; predicted molecular weight is indicated.



Supplementary Figure 14: RHO1 localizes to septa and membranes and is distributed throughout the cytoplasm, sometimes in a reticulate-vesicular structure which is absent from apical regions. Micrographs of strains expressing (A) GFP-RHO1 or (C) mCherry-RHO1 (TxRed Filter was used) in the wild type background are displayed. Images of cell wall and septa stained with calcofluor white (DAPI filter) or transmitted light micrographs are shown for orientation. Scale bars are 5 μ m. (B) depicts an immunoblot probed with α -GFP antibody verifying expression of GFP-RHO1 in strain *sgfp-rho-1*; predicted molecular weight is indicated.



Supplementary Figure 15: RHO2 accumulates at septa, the plasma membrane and is distributed in a reticulate structure extending throughout the hyphae but not into apical regions. Furthermore, hyphae exhibit diffuse cytoplasmic fluorescence. (A) Micrographs of strains expressing GFP-RHO2 in the wild type background are displayed. Images of cell wall and septa stained with calcofluor white (DAPI filter) are shown for orientation. Scale bars are 5 μ m. (B) GFP-RHO2 can be immunodetected in lysates prepared from strain *sgfp-rho-2* only after immunoprecipitation with α -GFP antibody. Lysate and precipitate samples of *sgfp-rho-2* and the indicated control strains were loaded on a SDS PAGE gel; α -GFP antibody was used for detection of proteins in subsequent Western blotting analysis. Predicted molecular weights of fusion proteins are indicated, so are bands representing IgG heavy chains (HC). Lanes shown originate from the same membrane probed with α -GFP antibody



Supplementary Figure 16: Plasmid map of pBiFC. Location of promoters P_{ccg-1} and P_{gpdA} , the two fragments encoding the N- and C-terminal portions of YFP (*yfpn* and *yfpc*) as well as unique restriction sites within the two multiple cloning sites are shown. Additional features for targeting the vector to the *his-3* locus and selection in *E. coli* are indicated in red. The map was generated using DNASTAR® SeqBuilder (version 8.0.3(1), DNASTAR, Inc., USA) and further edited.

8. References

- Abe, K., Rossman, K. L., Liu, B., Ritola, K. D., Chiang, D., Campbell, S. L., Burrridge, K., and Der, C. J. (2000). Vav2 is an activator of Cdc42, Rac1, and RhoA. *J. Biol. Chem* 275, 10141-10149.
- Abe, M., Qadota, H., Hirata, A., and Ohya, Y. (2003). Lack of GTP-bound Rho1p in secretory vesicles of *Saccharomyces cerevisiae*. *J. Cell Biol* 162, 85-97.
- Adamo, J. E., Rossi, G., and Brennwald, P. (1999). The Rho GTPase Rho3 Has a Direct Role in Exocytosis That Is Distinct from Its Role in Actin Polarity. *Mol. Biol. Cell* 10, 4121-4133.
- Adams, A. E., Johnson, D. I., Longnecker, R. M., Sloat, B. F., and Pringle, J. R. (1990). CDC42 and CDC43, two additional genes involved in budding and the establishment of cell polarity in the yeast *Saccharomyces cerevisiae*. *J. Cell Biol* 111, 131-142.
- Adams, A. E., and Pringle, J. R. (1984). Relationship of actin and tubulin distribution to bud growth in wild-type and morphogenetic-mutant *Saccharomyces cerevisiae*. *J. Cell Biol* 98, 934-945.
- Adamson, P., Paterson, H. F., and Hall, A. (1992). Intracellular localization of the P21rho proteins. *The Journal of Cell Biology* 119, 617-627.
- Adrio, J. L., and Demain, A. L. (2003). Fungal biotechnology. *Int. Microbiol* 6, 191-199.
- Ait Tahar, M., and Stollenwerk, J. *Physikalisches Praktikum: Einführung in die Fehlerrechnung*. Available at: <http://www.physik.fh-koeln.de/physik/fehler/fehlerrechnung.pdf> [Accessed August 18, 2010].
- Alberts, A. S., Bouquin, N., Johnston, L. H., and Treisman, R. (1998). Analysis of RhoA-binding proteins reveals an interaction domain conserved in heterotrimeric G protein beta subunits and the yeast response regulator protein Skn7. *J. Biol. Chem* 273, 8616-8622.
- Altschul, S. F., Gish, W., Miller, W., Myers, E. W., and Lipman, D. J. (1990). Basic local alignment search tool. *J. Mol. Biol* 215, 403-410.
- Alvarez-Tabarés, I., and Pérez-Martín, J. (2008). Cdk5 kinase regulates the association between adaptor protein Bem1 and GEF Cdc24 in the fungus *Ustilago maydis*. *J. Cell. Sci* 121, 2824-2832.
- Ammerer, G. (1983). Expression of genes in yeast using the ADCl promoter. *Meth. Enzymol* 101, 192-201.
- Andrews, P. D., and Stark, M. J. (2000). Dynamic, Rho1p-dependent localization of Pkc1p to sites of polarized growth. *J. Cell. Sci* 113 (Pt 15), 2685-2693.
- Annan, R. B., Wu, C., Waller, D. D., Whiteway, M., and Thomas, D. Y. (2008). Rho5p is involved in mediating the osmotic stress response in *Saccharomyces cerevisiae*, and its activity is regulated via Msi1p and Npr1p by phosphorylation and ubiquitination. *Eukaryotic Cell* 7, 1441-1449.
- Aramayo, R., and Metzenberg, R. L. (1996). Gene replacements at the his-3 locus of *Neurospora crassa*. *Fungal Genetics Newsletter* 43, 9-13.
- Araujo-Palomares, C. L., Castro-Longoria, E., and Riquelme, M. (2007). Ontogeny of the Spitzenkörper in germlings of *Neurospora crassa*. *Fungal Genet. Biol* 44, 492-503.
- Arellano, M., Duran, A., and Perez, P. (1997). Localisation of the *Schizosaccharomyces pombe* rho1p GTPase and its involvement in the organisation of the actin cytoskeleton. *J. Cell. Sci* 110 (Pt 20), 2547-2555.
- Arellano, M., Durán, A., and Pérez, P. (1996). Rho 1 GTPase activates the (1-3)beta-D-glucan synthase and is involved in *Schizosaccharomyces pombe* morphogenesis. *EMBO J* 15, 4584-4591.
- Arellano, M., Valdivieso, M. H., Calonge, T. M., Coll, P. M., Duran, A., and Perez, P. (1999). *Schizosaccharomyces pombe* protein kinase C homologues, pck1p and pck2p, are targets of rho1p and rho2p and differentially regulate cell integrity. *J. Cell. Sci* 112 (Pt 20), 3569-3578.
- Audhya, A., and Emr, S. D. (2002). Stt4 PI 4-Kinase Localizes to the Plasma Membrane and Functions in the Pkc1-Mediated MAP Kinase Cascade. *Developmental Cell* 2, 593-605.
- Ausubel, F. M., Brent, R., Kingston, R. E., Moore, D. D., Seidman, J. G., Smith, J. A., and Struhl, K. eds. (2002). *Short protocols in molecular biology: a compendium of methods from Current protocols in molecular biology* 5th ed. (New York: Wiley).
- Banuett, F., Quintanilla, R. H., and Reynaga-Peña, C. G. (2008). The machinery for cell polarity, cell morphogenesis, and the cytoskeleton in the Basidiomycete fungus *Ustilago maydis*-a survey of the genome sequence. *Fungal Genet. Biol* 45 Suppl 1, S3-S14.
- Barale, S., McCusker, D., and Arkowitz, R. A. (2006). Cdc42p GDP/GTP cycling is necessary for efficient cell fusion during yeast mating. *Mol. Biol. Cell* 17, 2824-2838.
- Barba, G., Soto, T., Madrid, M., Núñez, A., Vicente, J., Gacto, M., and Cansado, J. (2008). Activation of the cell integrity pathway is channelled through diverse signalling elements in fission yeast. *Cell. Signal* 20, 748-757.
- Bardiya, N., Alexander, W. G., Perdue, T. D., Barry, E. G., Metzenberg, R. L., Pukkila, P. J., and Shiu, P. K. T. (2008). Characterization of Interactions Between and Among Components of the Meiotic Silencing by Unpaired DNA Machinery in *Neurospora crassa* Using Bimolecular Fluorescence Complementation. *Genetics* 178, 593-596.

- Bassilana, M., and Arkowitz, R. A. (2006). Rac1 and Cdc42 Have Different Roles in *Candida albicans* Development. *Eukaryot Cell* 5, 321-329.
- Bassilana, M., Blyth, J., and Arkowitz, R. A. (2003). Cdc24, the GDP-GTP exchange factor for Cdc42, is required for invasive hyphal growth of *Candida albicans*. *Eukaryotic Cell* 2, 9-18.
- Bassilana, M., Hopkins, J., and Arkowitz, R. A. (2005). Regulation of the Cdc42/Cdc24 GTPase module during *Candida albicans* hyphal growth. *Eukaryotic Cell* 4, 588-603.
- Beauvais, A., Bruneau, J. M., Mol, P. C., Buitrago, M. J., Legrand, R., and Latgé, J. P. (2001). Glucan Synthase Complex of *Aspergillus fumigatus*. *J Bacteriol* 183, 2273-2279.
- Bender, A., and Pringle, J. R. (1989). Multicopy suppression of the *cdc24* budding defect in yeast by CDC42 and three newly identified genes including the ras-related gene RSR1. *Proc. Natl. Acad. Sci. U.S.A* 86, 9976-9980.
- Bender, A., and Pringle, J. R. (1991). Use of a screen for synthetic lethal and multicopy suppressor mutants to identify two new genes involved in morphogenesis in *Saccharomyces cerevisiae*. *Mol. Cell. Biol* 11, 1295-1305.
- Bertani, G. (1951). Studies on lysogenesis. I. The mode of phage liberation by lysogenic *Escherichia coli*. *J. Bacteriol* 62, 293-300.
- Bishop, A. L., and Hall, A. (2000). Rho GTPases and their effector proteins. *Biochem J* 348, 241-255.
- Böhmer, C., Böhmer, M., Bölker, M., and Sandrock, B. (2008). Cdc42 and the Ste20-like kinase Don3 act independently in triggering cytokinesis in *Ustilago maydis*. *J. Cell. Sci* 121, 143-148.
- Bömeke, K., Pries, R., Korte, V., Scholz, E., Herzog, B., Schulze, F., and Braus, G. H. (2006). Yeast Gcn4p Stabilization Is Initiated by the Dissociation of the Nuclear Pho85p/Pcl5p Complex. *Mol. Biol. Cell* 17, 2952-2962.
- Borges, M. I., Azevedo, M. O., Bonatelli Jr., R., Felipe, M. S. S., and Astolfi-Filho, S. (1990). A practical method for the preparation of total DNA from filamentous fungi. *Fungal Genetics Newsletter* 37.
- Borkovich, K. A., Alex, L. A., Yarden, O., Freitag, M., Turner, G. E., Read, N. D., Seiler, S., Bell-Pedersen, D., Paietta, J., Plesofsky, N., et al. (2004). Lessons from the Genome Sequence of *Neurospora crassa*: Tracing the Path from Genomic Blueprint to Multicellular Organism. *Microbiol Mol Biol Rev* 68, 1-108.
- Bos, J. L., Rehmann, H., and Wittinghofer, A. (2007). GEFs and GAPs: critical elements in the control of small G proteins. *Cell* 129, 865-877.
- Bose, I., Irazoqui, J. E., Moskow, J. J., Bardes, E. S. G., Zyla, T. R., and Lew, D. J. (2001). Assembly of Scaffold-mediated Complexes Containing Cdc42p, the Exchange Factor Cdc24p, and the Effector Cla4p Required for Cell Cycle-regulated Phosphorylation of Cdc24p. *Journal of Biological Chemistry* 276, 7176-7186.
- Boureux, A., Vignal, E., Faure, S., and Fort, P. (2007). Evolution of the Rho Family of Ras-Like GTPases in Eukaryotes. *Molecular Biology and Evolution* 24, 203-216.
- Bourne, H. R., Sanders, D. A., and McCormick, F. (1991). The GTPase superfamily: conserved structure and molecular mechanism. *Nature* 349, 117-127.
- Boyce, K. J., Hynes, M. J., and Andrianopoulos, A. (2001). The CDC42 homolog of the dimorphic fungus *Penicillium marneffei* is required for correct cell polarization during growth but not development. *J. Bacteriol* 183, 3447-3457.
- Boyce, K. J., and Andrianopoulos, A. (2007). A p21-Activated Kinase Is Required for Conidial Germination in *Penicillium marneffei*. *PLoS Pathog* 3.
- Boyce, K. J., Hynes, M. J., and Andrianopoulos, A. (2003). Control of morphogenesis and actin localization by the *Penicillium marneffei* RAC homolog. *J. Cell. Sci* 116, 1249-1260.
- Boyce, K. J., Hynes, M. J., and Andrianopoulos, A. (2005). The Ras and Rho GTPases genetically interact to coordinately regulate cell polarity during development in *Penicillium marneffei*. *Mol. Microbiol* 55, 1487-1501.
- Bradford, M. M. (1976). A rapid and sensitive method for the quantitation of microgram quantities of protein utilizing the principle of protein-dye binding. *Anal. Biochem* 72, 248-254.
- Bretscher, A. (2003). Polarized growth and organelle segregation in yeast: the tracks, motors, and receptors. *J. Cell Biol* 160, 811-816.
- Brockman, H. E., and de Serres, F. J. (1963). "Sorbose Toxicity" in *Neurospora*. *American Journal of Botany* 50, 709-714.
- Brown, J. L., Jaquenoud, M., Gulli, M. P., Chant, J., and Peter, M. (1997). Novel Cdc42-binding proteins Gic1 and Gic2 control cell polarity in yeast. *Genes Dev* 11, 2972-2982.
- Brugnera, E., Haney, L., Grimsley, C., Lu, M., Walk, S. F., Tosello-Tramont, A., Macara, I. G., Madhani, H., Fink, G. R., and Ravichandran, K. S. (2002). Unconventional Rac-GEF activity is mediated through the Dock180-ELMO complex. *Nat. Cell Biol* 4, 574-582.
- Bustelo, X. R., Sauzeau, V., and Berenjano, I. M. (2007). GTP-binding proteins of the Rho/Rac family: regulation, effectors and functions in vivo. *Bioessays* 29, 356-370.
- Butty, A., Perrinjaquet, N., Petit, A., Jaquenoud, M., Segall, J. E., Hofmann, K., Zwahlen, C., and Peter, M.

- (2002). A positive feedback loop stabilizes the guanine-nucleotide exchange factor Cdc24 at sites of polarization. *EMBO J* 21, 1565-1576.
- Calonge, T. M., Nakano, K., Arellano, M., Arai, R., Katayama, S., Toda, T., Mabuchi, I., and Perez, P. (2000). *Schizosaccharomyces pombe* rho2p GTPase regulates cell wall alpha-glucan biosynthesis through the protein kinase pck2p. *Mol. Biol. Cell* 11, 4393-4401.
- Calonge, T. M., Arellano, M., Coll, P. M., and Perez, P. (2003). Rga5p is a specific Rho1p GTPase-activating protein that regulates cell integrity in *Schizosaccharomyces pombe*. *Mol. Microbiol* 47, 507-518.
- Cano-Domínguez, N., Alvarez-Delfín, K., Hansberg, W., and Aguirre, J. (2008). NADPH oxidases NOX-1 and NOX-2 require the regulatory subunit NOR-1 to control cell differentiation and growth in *Neurospora crassa*. *Eukaryotic Cell* 7, 1352-1361.
- Castillo-Lluva, S., Alvarez-Tabarés, I., Weber, I., Steinberg, G., and Pérez-Martín, J. (2007). Sustained cell polarity and virulence in the phytopathogenic fungus *Ustilago maydis* depends on an essential cyclin-dependent kinase from the Cdk5/Pho85 family. *J. Cell. Sci* 120, 1584-1595.
- Cestra, G., Kwiatkowski, A., Salazar, M., Gertler, F., and De Camilli, P. (2005). Tuba, a GEF for CDC42, links dynamin to actin regulatory proteins. *Meth. Enzymol* 404, 537-545.
- Chang, E. C., Barr, M., Wang, Y., Jung, V., Xu, H. P., and Wigler, M. H. (1994). Cooperative interaction of *S. pombe* proteins required for mating and morphogenesis. *Cell* 79, 131-141.
- Chang, F., and Martin, S. G. (2009). Shaping fission yeast with microtubules. *Cold Spring Harb Perspect Biol* 1, a001347.
- Chang, Y. C., and Penoyer, L. A. (2000). Properties of various Rho1 mutant alleles of *Cryptococcus neoformans*. *J. Bacteriol* 182, 4987-4991.
- Chant, J., and Herskowitz, I. (1991). Genetic control of bud site selection in yeast by a set of gene products that constitute a morphogenetic pathway. *Cell* 65, 1203-1212.
- Chant, J., Mischke, M., Mitchell, E., Herskowitz, I., and Pringle, J. R. (1995). Role of Bud3p in producing the axial budding pattern of yeast. *J. Cell Biol* 129, 767-778.
- Chardin, P., Boquet, P., Madaule, P., Popoff, M. R., Rubin, E. J., and Gill, D. M. (1989). The mammalian G protein rhoC is ADP-ribosylated by *Clostridium botulinum* exoenzyme C3 and affects actin microfilaments in Vero cells. *EMBO J* 8, 1087-1092.
- Chen, C., and Dickman, M. B. (2004). Dominant active Rac and dominant negative Rac revert the dominant active Ras phenotype in *Colletotrichum trifolii* by distinct signalling pathways. *Mol. Microbiol* 51, 1493-1507.
- Chen, C., Ha, Y., Min, J., Memmott, S. D., and Dickman, M. B. (2006). Cdc42 is required for proper growth and development in the fungal pathogen *Colletotrichum trifolii*. *Eukaryotic Cell* 5, 155-166.
- Chen, G. C., Kim, Y. J., and Chan, C. S. (1997). The Cdc42 GTPase-associated proteins Gic1 and Gic2 are required for polarized cell growth in *Saccharomyces cerevisiae*. *Genes Dev* 11, 2958-2971.
- Chen, J., Zheng, W., Zheng, S., Zhang, D., Sang, W., Chen, X., Li, G., Lu, G., and Wang, Z. (2008). Rac1 is required for pathogenicity and Chm1-dependent conidiogenesis in rice fungal pathogen *Magnaporthe grisea*. *PLoS Pathog* 4, e1000202.
- Chen, S., and Hamm, H. E. (2006). DEP domains: More than just membrane anchors. *Dev. Cell* 11, 436-438.
- Chenevert, J., Corrado, K., Bender, A., Pringle, J., and Herskowitz, I. (1992). A yeast gene (BEM1) necessary for cell polarization whose product contains two SH3 domains. *Nature* 356, 77-79.
- Chenna, R., Sugawara, H., Koike, T., Lopez, R., Gibson, T. J., Higgins, D. G., and Thompson, J. D. (2003). Multiple sequence alignment with the Clustal series of programs. *Nucleic Acids Res* 31, 3497-3500.
- Chomczynski, P. (1993). A reagent for the single-step simultaneous isolation of RNA, DNA and proteins from cell and tissue samples. *BioTechniques* 15, 532-534, 536-537.
- Chomczynski, P., and Sacchi, N. (1987). Single-step method of RNA isolation by acid guanidinium thiocyanate-phenol-chloroform extraction. *Anal. Biochem* 162, 156-159.
- Coleman, K. G., Steensma, H. Y., Kaback, D. B., and Pringle, J. R. (1986). Molecular cloning of chromosome I DNA from *Saccharomyces cerevisiae*: isolation and characterization of the CDC24 gene and adjacent regions of the chromosome. *Mol. Cell. Biol* 6, 4516-4525.
- Coll, P. M., Rincon, S. A., Izquierdo, R. A., and Perez, P. (2007). Hob3p, the fission yeast ortholog of human BIN3, localizes Cdc42p to the division site and regulates cytokinesis. *EMBO J* 26, 1865-1877.
- Coll, P. M., Trillo, Y., Ametzazurra, A., and Perez, P. (2003). Gef1p, a new guanine nucleotide exchange factor for Cdc42p, regulates polarity in *Schizosaccharomyces pombe*. *Mol. Biol. Cell* 14, 313-323.
- Collinge, A. J., and Trinci, A. P. (1974). Hyphal tips of wild-type and spreading colonial mutants of *Neurospora crassa*. *Arch. Microbiol* 99, 353-368.
- Côté, J., and Vuori, K. (2002). Identification of an evolutionarily conserved superfamily of DOCK180-related proteins with guanine nucleotide exchange activity. *J. Cell. Sci* 115, 4901-4913.
- Côté, J., and Vuori, K. (2006). In vitro guanine nucleotide exchange activity of DHR-2/DOCKER/CZH2 domains. *Meth. Enzymol* 406, 41-57.
- Court, H., and Sudbery, P. (2007). Regulation of Cdc42 GTPase activity in the formation of hyphae in *Candida*

- albicans. *Mol. Biol. Cell* 18, 265-281.
- Cvrcková, F., De Virgilio, C., Manser, E., Pringle, J. R., and Nasmyth, K. (1995). Ste20-like protein kinases are required for normal localization of cell growth and for cytokinesis in budding yeast. *Genes Dev* 9, 1817-1830.
- Das, M., Wiley, D. J., Medina, S., Vincent, H. A., Larrea, M., Oriolo, A., and Verde, F. (2007). Regulation of cell diameter, For3p localization, and cell symmetry by fission yeast Rho-GAP Rga4p. *Mol. Biol. Cell* 18, 2090-2101.
- Davis, B. J. (1964). DISC ELECTROPHORESIS – II METHOD AND APPLICATION TO HUMAN SERUM PROTEINS. *Annals of the New York Academy of Sciences* 121, 404-427.
- Davis, R. H. (2000). *Neurospora: contributions of a model organism* (Oxford University Press).
- Davis, R. H., and de Serres, F. J. (1970). Genetic and microbiological research techniques for *Neurospora crassa*. *Methods in Enzymology Volume 17, Part 1*, 79-143.
- Delley, P., and Hall, M. N. (1999). Cell Wall Stress Depolarizes Cell Growth via Hyperactivation of Rho1. *The Journal of Cell Biology* 147, 163-174.
- Dichtl, K., Ebel, F., Dirr, F., Routier, F. H., Heesemann, J., and Wagener, J. (2010). Farnesol misplaces tip-localized Rho proteins and inhibits cell wall integrity signalling in *Aspergillus fumigatus*. *Mol. Microbiol* 76, 1191-1204.
- Dobbelaere, J., Gentry, M. S., Hallberg, R. L., and Barral, Y. (2003). Phosphorylation-dependent regulation of septin dynamics during the cell cycle. *Dev. Cell* 4, 345-357.
- Doignon, F., Weinachter, C., Roumanie, O., and Crouzet, M. (1999). The yeast Rgd1p is a GTPase activating protein of the Rho3 and rho4 proteins. *FEBS Lett* 459, 458-462.
- Dong, Y., Pruyne, D., and Bretscher, A. (2003). Formin-dependent actin assembly is regulated by distinct modes of Rho signaling in yeast. *J. Cell Biol* 161, 1081-1092.
- Dreyer, J., Eichhorn, H., Friedlin, E., Kurnsteiner, H., and Kuck, U. (2007). A Homologue of the *Aspergillus* velvet Gene Regulates both Cephalosporin C Biosynthesis and Hyphal Fragmentation in *Acremonium chrysogenum*. *Appl. Environ. Microbiol.* 73, 3412-3422.
- Drgonová, J., Drgon, T., Tanaka, K., Kollár, R., Chen, G. C., Ford, R. A., Chan, C. S., Takai, Y., and Cabib, E. (1996). Rho1p, a yeast protein at the interface between cell polarization and morphogenesis. *Science* 272, 277-279.
- Dünkler, A., and Wendland, J. (2007). *Candida albicans* Rho-type GTPase-encoding genes required for polarized cell growth and cell separation. *Eukaryotic Cell* 6, 844-854.
- Dunlap, J. C., Borkovich, K. A., Henn, M. R., Turner, G. E., Sachs, M. S., Glass, N. L., McCluskey, K., Plamann, M., Galagan, J. E., Birren, B. W., et al. (2007). Enabling a community to dissect an organism: overview of the *Neurospora* functional genomics project. *Adv. Genet* 57, 49-96.
- Dvorsky, R., and Ahmadian, M. R. (2004). Always look on the bright site of Rho: structural implications for a conserved intermolecular interface. *EMBO Rep* 5, 1130-1136.
- Elion, E. A., Trueheart, J., and Fink, G. R. (1995). Fus2 localizes near the site of cell fusion and is required for both cell fusion and nuclear alignment during zygote formation. *J. Cell Biol* 130, 1283-1296.
- Endo, M., Shirouzu, M., and Yokoyama, S. (2003). The Cdc42 binding and scaffolding activities of the fission yeast adaptor protein Scd2. *J. Biol. Chem* 278, 843-852.
- Etienne-Manneville, S., and Hall, A. (2002). Rho GTPases in cell biology. *Nature* 420, 629-635.
- Evangelista, M., Blundell, K., Longtine, M. S., Chow, C. J., Adames, N., Pringle, J. R., Peter, M., and Boone, C. (1997). Bni1p, a yeast formin linking cdc42p and the actin cytoskeleton during polarized morphogenesis. *Science* 276, 118-122.
- Evangelista, M., Klebl, B. M., Tong, A. H., Webb, B. A., Leeuw, T., Leberer, E., Whiteway, M., Thomas, D. Y., and Boone, C. (2000). A role for myosin-I in actin assembly through interactions with Vrp1p, Bee1p, and the Arp2/3 complex. *J. Cell Biol* 148, 353-362.
- Fidyk, N., Wang, J., and Cerione, R. A. (2006). Influencing cellular transformation by modulating the rates of GTP hydrolysis by Cdc42. *Biochemistry* 45, 7750-7762.
- Fields, S., and Song, O. (1989). A novel genetic system to detect protein-protein interactions. *Nature* 340, 245-246.
- Finn, R. D., Mistry, J., Tate, J., Coggill, P., Heger, A., Pollington, J. E., Gavin, O. L., Gunasekaran, P., Ceric, G., Forslund, K., et al. (2009). The Pfam protein families database. *Nucleic Acids Research* 38, D211-D222.
- Fischer, R., Zekert, N., and Takeshita, N. (2008). Polarized growth in fungi--interplay between the cytoskeleton, positional markers and membrane domains. *Mol. Microbiol* 68, 813-826.
- Fitch, P. G., Gammie, A. E., Lee, D. J., de Candal, V. B., and Rose, M. D. (2004). Lrg1p Is a Rho1 GTPase-activating protein required for efficient cell fusion in yeast. *Genetics* 168, 733-746.
- Freitag, M., Hickey, P. C., Raju, N. B., Selker, E. U., and Read, N. D. (2004). GFP as a tool to analyze the organization, dynamics and function of nuclei and microtubules in *Neurospora crassa*. *Fungal Genet. Biol* 41, 897-910.
- Galagan, J. E., Calvo, S. E., Borkovich, K. A., Selker, E. U., Read, N. D., Jaffe, D., FitzHugh, W., Ma, L., Smirnov,

- S., Purcell, S., et al. (2003). The genome sequence of the filamentous fungus *Neurospora crassa*. *Nature* **422**, 859-868.
- Gammie, A. E., Brizzio, V., and Rose, M. D. (1998). Distinct morphological phenotypes of cell fusion mutants. *Mol. Biol. Cell* **9**, 1395-1410.
- García, P., Tajadura, V., and Sanchez, Y. (2009). The Rho1p exchange factor Rgf1p signals upstream from the Pmk1 mitogen-activated protein kinase pathway in fission yeast. *Mol. Biol. Cell* **20**, 721-731.
- García, P., Tajadura, V., García, I., and Sánchez, Y. (2006a). Rgf1p is a specific Rho1-GEF that coordinates cell polarization with cell wall biogenesis in fission yeast. *Mol. Biol. Cell* **17**, 1620-1631.
- García, P., Tajadura, V., García, I., and Sánchez, Y. (2006b). Role of Rho GTPases and Rho-GEFs in the regulation of cell shape and integrity in fission yeast. *Yeast* **23**, 1031-1043.
- Girbardt, M. (1957). Der Spitzenkörper von *Polystictus versicolor* (L.). *Planta* **50**, 47-59.
- Guest, G. M., Lin, X., and Momany, M. (2004). *Aspergillus nidulans* RhoA is involved in polar growth, branching, and cell wall synthesis. *Fungal Genet. Biol* **41**, 13-22.
- Guo, S., Shen, X., Yan, G., Ma, D., Bai, X., Li, S., and Jiang, Y. (2009). A MAP kinase dependent feedback mechanism controls Rho1 GTPase and actin distribution in yeast. *PLoS ONE* **4**, e6089.
- Guo, W., Tamanoi, F., and Novick, P. (2001). Spatial regulation of the exocyst complex by Rho1 GTPase. *Nat. Cell Biol* **3**, 353-360.
- Habermann, B. (2004). The BAR-domain family of proteins: a case of bending and binding? *EMBO Rep* **5**, 250-255.
- Hakoshima, T., Shimizu, T., and Maesaki, R. (2003). Structural basis of the Rho GTPase signaling. *J. Biochem* **134**, 327-331.
- Hancock, J. F., Cadwallader, K., Paterson, H., and Marshall, C. J. (1991). A CAAX or a CAAL motif and a second signal are sufficient for plasma membrane targeting of ras proteins. *EMBO J* **10**, 4033-4039.
- Harris, S. D. (2006). Cell polarity in filamentous fungi: shaping the mold. *Int. Rev. Cytol* **251**, 41-77.
- Harris, S. D., and Momany, M. (2004). Polarity in filamentous fungi: moving beyond the yeast paradigm. *Fungal Genet. Biol* **41**, 391-400.
- Harris, S. D., Read, N. D., Roberson, R. W., Shaw, B., Seiler, S., Plamann, M., and Momany, M. (2005). Polarisome meets Spitzenkörper: microscopy, genetics, and genomics converge. *Eukaryotic Cell* **4**, 225-229.
- Harris, S. D., Turner, G., Meyer, V., Espeso, E. A., Specht, T., Takeshita, N., and Helmstedt, K. (2009). Morphology and development in *Aspergillus nidulans*: a complex puzzle. *Fungal Genet. Biol* **46 Suppl 1**, S82-S92.
- Hazan, I., and Liu, H. (2002). Hyphal tip-associated localization of Cdc42 is F-actin dependent in *Candida albicans*. *Eukaryotic Cell* **1**, 856-864.
- Helliwell, S. B., Schmidt, A., Ohya, Y., and Hall, M. N. (1998). The Rho1 effector Pkc1, but not Bni1, mediates signalling from Tor2 to the actin cytoskeleton. *Curr. Biol* **8**, 1211-1214.
- Henchoz, S., Chi, Y., Catarin, B., Herskowitz, I., Deshaies, R. J., and Peter, M. (1997). Phosphorylation- and ubiquitin-dependent degradation of the cyclin-dependent kinase inhibitor Far1p in budding yeast. *Genes & Development* **11**, 3046-3060.
- Hickey, P. C., Jacobson, D., Read, N. D., and Louise Glass, N. L. G. (2002). Live-cell imaging of vegetative hyphal fusion in *Neurospora crassa*. *Fungal Genet. Biol* **37**, 109-119.
- Hiratsuka, T. (1983). New ribose-modified fluorescent analogs of adenine and guanine nucleotides available as substrates for various enzymes. *Biochim. Biophys. Acta* **742**, 496-508.
- Hirota, K., Tanaka, K., Ohta, K., and Yamamoto, M. (2003). Gef1p and Scd1p, the Two GDP-GTP exchange factors for Cdc42p, form a ring structure that shrinks during cytokinesis in *Schizosaccharomyces pombe*. *Mol. Biol. Cell* **14**, 3617-3627.
- Hlubek, A., Schink, K. O., Mahlert, M., Sandrock, B., and Bölker, M. (2008). Selective activation by the guanine nucleotide exchange factor Don1 is a main determinant of Cdc42 signalling specificity in *Ustilago maydis*. *Mol. Microbiol* **68**, 615-623.
- Hoang, A. (2001). Caspofungin acetate: an antifungal agent. *Am J Health Syst Pharm* **58**, 1206-1214.
- Honda, S., and Selker, E. U. (2009). Tools for fungal proteomics: multifunctional *Neurospora* vectors for gene replacement, protein expression and protein purification. *Genetics* **182**, 11-23.
- Hope, H., Bogliolo, S., Arkowitz, R. A., and Bassilana, M. (2008). Activation of Rac1 by the guanine nucleotide exchange factor Dck1 is required for invasive filamentous growth in the pathogen *Candida albicans*. *Mol. Biol. Cell* **19**, 3638-3651.
- Hope, H., Schmauch, C., Arkowitz, R. A., and Bassilana, M. (2010). The *Candida albicans* ELMO homologue functions together with Rac1 and Dck1, upstream of the MAP Kinase Cek1, in invasive filamentous growth. *Mol. Microbiol* **76**, 1572-1590.
- Hurtado, C. A., Beckerich, J. M., Gaillardin, C., and Rachubinski, R. A. (2000). A rac homolog is required for induction of hyphal growth in the dimorphic yeast *Yarrowia lipolytica*. *J. Bacteriol* **182**, 2376-2386.

- Ihara, K., Muraguchi, S., Kato, M., Shimizu, T., Shirakawa, M., Kuroda, S., Kaibuchi, K., and Hakoshima, T. (1998). Crystal structure of human RhoA in a dominantly active form complexed with a GTP analogue. *J. Biol. Chem* 273, 9656-9666.
- Imai, J., Toh-e, A., and Matsui, Y. (1996). Genetic analysis of the *Saccharomyces cerevisiae* RHO3 gene, encoding a rho-type small GTPase, provides evidence for a role in bud formation. *Genetics* 142, 359-369.
- Inoue, H., Nojima, H., and Okayama, H. (1990). High efficiency transformation of *Escherichia coli* with plasmids. *Gene* 96, 23-28.
- Inoue, S. B., Qadota, H., Arisawa, M., Watanabe, T., and Ohya, Y. (1999). Prenylation of Rho1p is required for activation of yeast 1, 3-beta-glucan synthase. *J. Biol. Chem* 274, 38119-38124.
- Irazoqui, J. E., Gladfelter, A. S., and Lew, D. J. (2004). Cdc42p, GTP hydrolysis, and the cell's sense of direction. *Cell Cycle* 3, 861-864.
- Irazoqui, J. E., Gladfelter, A. S., and Lew, D. J. (2003). Scaffold-mediated symmetry breaking by Cdc42p. *Nat. Cell Biol* 5, 1062-1070.
- Irazoqui, J. E., Howell, A. S., Theesfeld, C. L., and Lew, D. J. (2005). Opposing roles for actin in Cdc42p polarization. *Mol. Biol. Cell* 16, 1296-1304.
- Iwase, M., Luo, J., Nagaraj, S., Longtine, M., Kim, H. B., Haarer, B. K., Caruso, C., Tong, Z., Pringle, J. R., and Bi, E. (2006). Role of a Cdc42p effector pathway in recruitment of the yeast septins to the presumptive bud site. *Mol. Biol. Cell* 17, 1110-1125.
- Jackson, S. L., and Heath, I. B. (1993). Roles of calcium ions in hyphal tip growth. *Microbiol. Rev* 57, 367-382.
- Jaffe, A. B., and Hall, A. (2005). Rho GTPases: biochemistry and biology. *Annu. Rev. Cell Dev. Biol* 21, 247-269.
- James, P., Halladay, J., and Craig, E. A. (1996). Genomic libraries and a host strain designed for highly efficient two-hybrid selection in yeast. *Genetics* 144, 1425-1436.
- Jameson, D. M., and Eccleston, J. F. (1997). [18] Fluorescent nucleotide analogs: Synthesis and applications. In *Fluorescence Spectroscopy* (Academic Press), pp. 363-390. Available at: <http://www.sciencedirect.com/science/article/B7CV2-4B5XKMV-FD/2/2eb472858a00089b52f35898cf291a59> [Accessed December 23, 2010].
- Johnson, D. I. (1999). Cdc42: An essential Rho-type GTPase controlling eukaryotic cell polarity. *Microbiol. Mol. Biol. Rev* 63, 54-105.
- Johnson, D. I., and Pringle, J. R. (1990). Molecular characterization of CDC42, a *Saccharomyces cerevisiae* gene involved in the development of cell polarity. *J. Cell Biol* 111, 143-152.
- Jones, C. A., Greer-Phillips, S. E., and Borkovich, K. A. (2007). The Response Regulator RRG-1 Functions Upstream of a Mitogen-activated Protein Kinase Pathway Impacting Asexual Development, Female Fertility, Osmotic Stress, and Fungicide Resistance in *Neurospora crassa*. *Mol. Biol. Cell* 18, 2123-2136.
- Justa-Schuch, D. (2010). Regulation of septum formation by RHO4 GTPase signalling in *Neurospora crassa*. Available at: http://webdoc.sub.gwdg.de/diss/2010/justa_schuch/ [Accessed October 27, 2010].
- Justa-Schuch, D., Heilig, Y., Richthammer, C., and Seiler, S. (2010). Septum formation is regulated by the RHO4-specific exchange factors BUD3 and RGF3 and by the landmark protein BUD4 in *Neurospora crassa*. *Mol. Microbiol* 76, 220-235.
- Kamada, Y., Qadota, H., Python, C. P., Anraku, Y., Ohya, Y., and Levin, D. E. (1996). Activation of yeast protein kinase C by Rho1 GTPase. *J. Biol. Chem* 271, 9193-9196.
- Kang, P. J., Sanson, A., Lee, B., and Park, H. O. (2001). A GDP/GTP exchange factor involved in linking a spatial landmark to cell polarity. *Science* 292, 1376-1378.
- Kang, P. J., Béven, L., Hariharan, S., and Park, H. (2010). The Rsr1/Bud1 GTPase interacts with itself and the Cdc42 GTPase during bud-site selection and polarity establishment in budding yeast. *Mol. Biol. Cell* 21, 3007-3016.
- Karnoub, A. E., Worthylake, D. K., Rossman, K. L., Pruitt, W. M., Campbell, S. L., Sondek, J., and Der, C. J. (2001). Molecular basis for Rac1 recognition by guanine nucleotide exchange factors. *Nat. Struct. Biol* 8, 1037-1041.
- Karnoub, A. E., Symons, M., Campbell, S. L., and Der, C. J. (2004). Molecular basis for Rho GTPase signaling specificity. *Breast Cancer Res. Treat* 84, 61-71.
- Karpova, T. S., Reck-Peterson, S. L., Elkind, N. B., Mooseker, M. S., Novick, P. J., and Cooper, J. A. (2000). Role of actin and Myo2p in polarized secretion and growth of *Saccharomyces cerevisiae*. *Mol. Biol. Cell* 11, 1727-1737.
- Kasuga, T., and Glass, N. L. (2008). Dissecting colony development of *Neurospora crassa* using mRNA profiling and comparative genomics approaches. *Eukaryotic Cell* 7, 1549-1564.
- Katoh, K., and Toh, H. (2008). Recent developments in the MAFFT multiple sequence alignment program. *Briefings in Bioinformatics* 9, 286-298.
- Kawabata, T., and Inoue, H. (2007). Detection of physical interactions by immunoprecipitation of FLAG- and HA-tagged proteins expressed at the his-3 locus in *Neurospora crassa*. *Fungal Genetics Newsletter* 54, 5-8.
- Kim, H., Yang, P., Catanuto, P., Verde, F., Lai, H., Du, H., Chang, F., and Marcus, S. (2003). The kelch repeat

- protein, Tea1, is a potential substrate target of the p21-activated kinase, Shk1, in the fission yeast, *Schizosaccharomyces pombe*. *J. Biol. Chem* 278, 30074-30082.
- Knaus, M., Pelli-Gulli, M., van Drogen, F., Springer, S., Jaquenoud, M., and Peter, M. (2007). Phosphorylation of Bem2p and Bem3p may contribute to local activation of Cdc42p at bud emergence. *EMBO J* 26, 4501-4513.
- Koch, G., Tanaka, K., Masuda, T., Yamochi, W., Nonaka, H., and Takai, Y. (1997). Association of the Rho family small GTP-binding proteins with Rho GDP dissociation inhibitor (Rho GDI) in *Saccharomyces cerevisiae*. *Oncogene* 15, 417-422.
- Köhli, M., Buck, S., and Schmitz, H. (2008). The function of two closely related Rho proteins is determined by an atypical switch I region. *J. Cell. Sci* 121, 1065-1075.
- Kohno, H., Tanaka, K., Mino, A., Umikawa, M., Imamura, H., Fujiwara, T., Fujita, Y., Hotta, K., Qadota, H., Watanabe, T., et al. (1996). Bni1p implicated in cytoskeletal control is a putative target of Rho1p small GTP binding protein in *Saccharomyces cerevisiae*. *EMBO J* 15, 6060-6068.
- Kondoh, O., Tachibana, Y., Ohya, Y., Arisawa, M., and Watanabe, T. (1997). Cloning of the RHO1 gene from *Candida albicans* and its regulation of beta-1,3-glucan synthesis. *J. Bacteriol* 179, 7734-7741.
- König, J., Baumann, S., Koepke, J., Pohlmann, T., Zarnack, K., and Feldbrügge, M. (2009). The fungal RNA-binding protein Rrm4 mediates long-distance transport of ubi1 and rho3 mRNAs. *EMBO J* 28, 1855-1866.
- Kozma, R., Ahmed, S., Best, A., and Lim, L. (1995). The Ras-related protein Cdc42Hs and bradykinin promote formation of peripheral actin microspikes and filopodia in Swiss 3T3 fibroblasts. *Mol. Cell. Biol* 15, 1942-1952.
- Kozminski, K. G., Beven, L., Angerman, E., Tong, A. H. Y., Boone, C., and Park, H. (2003). Interaction between a Ras and a Rho GTPase couples selection of a growth site to the development of cell polarity in yeast. *Mol. Biol. Cell* 14, 4958-4970.
- Kwon, M. J., Arentshorst, M., Roos, E. D., van den Hondel, C. A. M. J. J., Meyer, V., and Ram, A. F. J. (2010). Functional characterization of Rho GTPases in *Aspergillus niger* uncovers conserved and diverged roles of Rho proteins within filamentous fungi. *Mol. Microbiol.* Available at: <http://www.ncbi.nlm.nih.gov/pubmed/21205013> [Accessed January 11, 2011].
- Laemmli, U. K. (1970). Cleavage of structural proteins during the assembly of the head of bacteriophage T4. *Nature* 227, 680-685.
- Leberer, E., Harcus, D., Broadbent, I. D., Clark, K. L., Dignard, D., Ziegelbauer, K., Schmidt, A., Gow, N. A., Brown, A. J., and Thomas, D. Y. (1996). Signal transduction through homologs of the Ste20p and Ste7p protein kinases can trigger hyphal formation in the pathogenic fungus *Candida albicans*. *Proc. Natl. Acad. Sci. U.S.A* 93, 13217-13222.
- Leberer, E., Wu, C., Leeuw, T., Fourest-Lieuvain, A., Segall, J. E., and Thomas, D. Y. (1997a). Functional characterization of the Cdc42p binding domain of yeast Ste20p protein kinase. *EMBO J* 16, 83-97.
- Leberer, E., Ziegelbauer, K., Schmidt, A., Harcus, D., Dignard, D., Ash, J., Johnson, L., and Thomas, D. Y. (1997b). Virulence and hyphal formation of *Candida albicans* require the Ste20p-like protein kinase CaCla4p. *Curr. Biol* 7, 539-546.
- Lechler, T., Jonsdottir, G. A., Klee, S. K., Pellman, D., and Li, R. (2001). A two-tiered mechanism by which Cdc42 controls the localization and activation of an Arp2/3-activating motor complex in yeast. *J. Cell Biol* 155, 261-270.
- Lechler, T., Shevchenko, A., and Li, R. (2000). Direct involvement of yeast type I myosins in Cdc42-dependent actin polymerization. *J. Cell Biol* 148, 363-373.
- León, M., Jaafar, L., and Zueco, J. (2003). RHO1 (YIRHO1) is a non-essential gene in *Yarrowia lipolytica* and complements rho1Delta lethality in *Saccharomyces cerevisiae*. *Yeast* 20, 343-350.
- Leonard, D. A., Evans, T., Hart, M., Cerione, R. A., and Manor, D. (1994). Investigation of the GTP-binding/GTPase cycle of Cdc42Hs using fluorescence spectroscopy. *Biochemistry* 33, 12323-12328.
- Leveleki, L., Mahlert, M., Sandrock, B., and Bölker, M. (2004). The PAK family kinase Cla4 is required for budding and morphogenesis in *Ustilago maydis*. *Mol. Microbiol* 54, 396-406.
- Levin, D. E., Bowers, B., Chen, C. Y., Kamada, Y., and Watanabe, M. (1994). Dissecting the protein kinase C/MAP kinase signalling pathway of *Saccharomyces cerevisiae*. *Cell. Mol. Biol. Res* 40, 229-239.
- Levin, D. E. (2005). Cell wall integrity signaling in *Saccharomyces cerevisiae*. *Microbiol. Mol. Biol. Rev* 69, 262-291.
- Li, R., and Zheng, Y. (1997). Residues of the Rho family GTPases Rho and Cdc42 that specify sensitivity to Dbp-like guanine nucleotide exchange factors. *J. Biol. Chem* 272, 4671-4679.
- Li, S., Dean, S., Li, Z., Horecka, J., Deschenes, R. J., and Fassler, J. S. (2002). The eukaryotic two-component histidine kinase Sln1p regulates OCH1 via the transcription factor, Skn7p. *Mol. Biol. Cell* 13, 412-424.
- Longenecker, K., Read, P., Lin, S., Somlyo, A. P., Nakamoto, R. K., and Derewenda, Z. S. (2003). Structure of a constitutively activated RhoA mutant (Q63L) at 1.55 Å resolution. *Acta Crystallogr. D Biol. Crystallogr* 59, 876-880.
- Loo, T., and Balasubramanian, M. (2008). *Schizosaccharomyces pombe* Pak-related protein, Pak1p/Orb2p,

- phosphorylates myosin regulatory light chain to inhibit cytokinesis. *J. Cell Biol* 183, 785-793.
- Lu, M., Kinchen, J. M., Rossman, K. L., Grimsley, C., deBakker, C., Brugnera, E., Tosello-Tramont, A., Haney, L. B., Klingele, D., Sondek, J., et al. (2004). PH domain of ELMO functions in trans to regulate Rac activation via Dock180. *Nat. Struct. Mol. Biol* 11, 756-762.
- Ma, Y., Kuno, T., Kita, A., Asayama, Y., and Sugiura, R. (2006). Rho2 is a target of the farnesyltransferase Cpp1 and acts upstream of Pmk1 mitogen-activated protein kinase signaling in fission yeast. *Mol. Biol. Cell* 17, 5028-5037.
- Madaule, P., and Axel, R. (1985). A novel ras-related gene family. *Cell* 41, 31-40.
- Madaule, P., Axel, R., and Myers, A. M. (1987). Characterization of two members of the rho gene family from the yeast *Saccharomyces cerevisiae*. *Proc. Natl. Acad. Sci. U.S.A* 84, 779-783.
- Madrid, M., Soto, T., Khong, H. K., Franco, A., Vicente, J., Pérez, P., Gacto, M., and Cansado, J. (2006). Stress-induced response, localization, and regulation of the Pmk1 cell integrity pathway in *Schizosaccharomyces pombe*. *J. Biol. Chem* 281, 2033-2043.
- Maerz, S., Dettmann, A., Ziv, C., Liu, Y., Valerius, O., Yarden, O., and Seiler, S. (2009). Two NDR kinase-MOB complexes function as distinct modules during septum formation and tip extension in *Neurospora crassa*. *Mol. Microbiol* 74, 707-723.
- Maerz, S., and Seiler, S. (2010). Tales of RAM and MOR: NDR kinase signaling in fungal morphogenesis. *Current Opinion in Microbiology* 13, 663-671.
- Mahlert, M., Leveleki, L., Hlubek, A., Sandrock, B., and Bölker, M. (2006). Rac1 and Cdc42 regulate hyphal growth and cytokinesis in the dimorphic fungus *Ustilago maydis*. *Mol. Microbiol* 59, 567-578.
- Manning, B. D., Padmanabha, R., and Snyder, M. (1997). The Rho-GEF Rom2p localizes to sites of polarized cell growth and participates in cytoskeletal functions in *Saccharomyces cerevisiae*. *Mol. Biol. Cell* 8, 1829-1844.
- Marcoux, N., Cloutier, S., Zakrzewska, E., Charest, P. M., Bourbonnais, Y., and Pallotta, D. (2000). Suppression of the profilin-deficient phenotype by the RHO2 signaling pathway in *Saccharomyces cerevisiae*. *Genetics* 156, 579-592.
- Marcus, S., Polverino, A., Chang, E., Robbins, D., Cobb, M. H., and Wigler, M. H. (1995). Shk1, a homolog of the *Saccharomyces cerevisiae* Ste20 and mammalian p65PAK protein kinases, is a component of a Ras/Cdc42 signaling module in the fission yeast *Schizosaccharomyces pombe*. *Proc. Natl. Acad. Sci. U.S.A* 92, 6180-6184.
- Margolin, B. S., Freitag, M., and Selker, E. U. (1997). Improved plasmids for gene targeting at the his-3 locus of *Neurospora crassa* by electroporation. *Fungal Genetics Newsletter* 44.
- Markham, P., and Collinge, A. J. (1987). Woronin bodies of filamentous fungi. *FEMS Microbiology Letters* 46, 1-11.
- Marquitz, A. R., Harrison, J. C., Bose, I., Zyla, T. R., McMillan, J. N., and Lew, D. J. (2002). The Rho-GAP Bem2p plays a GAP-independent role in the morphogenesis checkpoint. *EMBO J* 21, 4012-4025.
- Marshall, M. S., Davis, L. J., Keys, R. D., Mosser, S. D., Hill, W. S., Scolnick, E. M., and Gibbs, J. B. (1991). Identification of amino acid residues required for Ras p21 target activation. *Mol Cell Biol* 11, 3997-4004.
- Martin, S. G. (2009). Microtubule-dependent cell morphogenesis in the fission yeast. *Trends Cell Biol* 19, 447-454.
- Martin, S. G., Rincón, S. A., Basu, R., Pérez, P., and Chang, F. (2007). Regulation of the formin for3p by cdc42p and bud6p. *Mol. Biol. Cell* 18, 4155-4167.
- Martínez-Rocha, A. L., Roncero, M. I. G., López-Ramírez, A., Mariné, M., Guarro, J., Martínez-Cadena, G., and Di Pietro, A. (2008). Rho1 has distinct functions in morphogenesis, cell wall biosynthesis and virulence of *Fusarium oxysporum*. *Cell. Microbiol* 10, 1339-1351.
- Matsui, Y., and Toh-e, A. (1992a). Isolation and characterization of two novel ras superfamily genes in *Saccharomyces cerevisiae*. *Gene* 114, 43-49.
- Matsui, Y., and Toh-e, A. (1992b). Yeast RHO3 and RHO4 ras superfamily genes are necessary for bud growth, and their defect is suppressed by a high dose of bud formation genes CDC42 and BEM1. *Mol. Cell. Biol* 12, 5690-5699.
- Mattison, C. P., Spencer, S. S., Kresge, K. A., Lee, J., and Ota, I. M. (1999). Differential regulation of the cell wall integrity mitogen-activated protein kinase pathway in budding yeast by the protein tyrosine phosphatases Ptp2 and Ptp3. *Mol. Cell. Biol* 19, 7651-7660.
- Mazur, P., and Baginsky, W. (1996). In vitro activity of 1,3-beta-D-glucan synthase requires the GTP-binding protein Rho1. *J. Biol. Chem* 271, 14604-14609.
- Mazzoni, C., Zarov, P., Rambourg, A., and Mann, C. (1993). The SLT2 (MPK1) MAP kinase homolog is involved in polarized cell growth in *Saccharomyces cerevisiae*. *The Journal of Cell Biology* 123, 1821-1833.
- Meller, N., Irani-Tehrani, M., Kiosses, W. B., Del Pozo, M. A., and Schwartz, M. A. (2002). Zizimin1, a novel Cdc42 activator, reveals a new GEF domain for Rho proteins. *Nat. Cell Biol* 4, 639-647.
- Meller, N., Merlot, S., and Guda, C. (2005). CZH proteins: a new family of Rho-GEFs. *J. Cell. Sci* 118, 4937-4946.
- Merla, A., and Johnson, D. I. (2001). The *Schizosaccharomyces pombe* Cdc42p GTPase signals through Pak2p

- and the Mkh1p-Pek1p-Spm1p MAP kinase pathway. *Curr. Genet* 39, 205-209.
- Merril, C. R. (1990). Gel-staining techniques. *Meth. Enzymol* 182, 477-488.
- Miller, P. J., and Johnson, D. I. (1994). Cdc42p GTPase is involved in controlling polarized cell growth in *Schizosaccharomyces pombe*. *Mol. Cell. Biol* 14, 1075-1083.
- Mionnet, C., Bogliolo, S., and Arkowitz, R. A. (2008). Oligomerization regulates the localization of Cdc24, the Cdc42 activator in *Saccharomyces cerevisiae*. *J. Biol. Chem* 283, 17515-17530.
- Mishra, N. C., and Tatum, E. L. (1972). Effect of L-Sorbose on Polysaccharide Synthetases of *Neurospora crassa*. *Proc Natl Acad Sci U S A* 69, 313-317.
- Mitchell, M. B. (1966). A round-spore character in *N. crassa*. *Neurospora Newsletter* 10.
- Momany, M. (2005). Growth control and polarization. *Med. Mycol* 43 Suppl 1, S23-25.
- Momany, M. (2002). Polarity in filamentous fungi: establishment, maintenance and new axes. *Curr. Opin. Microbiol* 5, 580-585.
- Mondal, S., Bakthavatsalam, D., Steimle, P., Gassen, B., Rivero, F., and Noegel, A. A. (2008). Linking Ras to myosin function: RasGEF Q, a *Dictyostelium* exchange factor for RasB, affects myosin II functions. *J. Cell Biol* 181, 747-760.
- Morrell-Falvey, J. L., Ren, L., Feoktistova, A., Haese, G. D., and Gould, K. L. (2005). Cell wall remodeling at the fission yeast cell division site requires the Rho-GEF Rgf3p. *J. Cell. Sci* 118, 5563-5573.
- Movilla, N., Dosil, M., Zheng, Y., and Bustelo, X. R. (2001). How Vav proteins discriminate the GTPases Rac1 and RhoA from Cdc42. *Oncogene* 20, 8057-8065.
- Murray, J. M., and Johnson, D. I. (2001). The Cdc42p GTPase and its regulators Nrf1p and Scd1p are involved in endocytic trafficking in the fission yeast *Schizosaccharomyces pombe*. *J. Biol. Chem* 276, 3004-3009.
- Mutoh, T., Nakano, K., and Mabuchi, I. (2005). Rho1-GEFs Rgf1 and Rgf2 are involved in formation of cell wall and septum, while Rgf3 is involved in cytokinesis in fission yeast. *Genes Cells* 10, 1189-1202.
- Nakano, K., Arai, R., and Mabuchi, I. (1997). The small GTP-binding protein Rho1 is a multifunctional protein that regulates actin localization, cell polarity, and septum formation in the fission yeast *Schizosaccharomyces pombe*. *Genes Cells* 2, 679-694.
- Nakano, K., Mutoh, T., and Mabuchi, I. (2001). Characterization of GTPase-activating proteins for the function of the Rho-family small GTPases in the fission yeast *Schizosaccharomyces pombe*. *Genes Cells* 6, 1031-1042.
- Nakano, K., Arai, R., and Mabuchi, I. (2005). Small GTPase Rho5 is a functional homologue of Rho1, which controls cell shape and septation in fission yeast. *FEBS Lett* 579, 5181-5186.
- Nakano, K., Imai, J., Arai, R., Toh-E, A., Matsui, Y., and Mabuchi, I. (2002). The small GTPase Rho3 and the diaphanous/formin For3 function in polarized cell growth in fission yeast. *J. Cell. Sci* 115, 4629-4639.
- Nakano, K., Mutoh, T., Arai, R., and Mabuchi, I. (2003). The small GTPase Rho4 is involved in controlling cell morphology and septation in fission yeast. *Genes Cells* 8, 357-370.
- Narayanan, V., Sandiford, S. L., Wang, Q., Keren-Raifman, T., Levay, K., and Slepak, V. Z. (2007). Intramolecular interaction between the DEP domain of RGS7 and the Gbeta5 subunit. *Biochemistry* 46, 6859-6870.
- Nelson, W. J. (2003). Adaptation of core mechanisms to generate cell polarity. *Nature* 422, 766-774.
- Nern, A., and Arkowitz, R. A. (1999). A Cdc24p-Far1p-Gβγ Protein Complex Required for Yeast Orientation during Mating. *The Journal of Cell Biology* 144, 1187 -1202.
- Ness, F., Prouzet-Mauleon, V., Vieillehard, A., Lefebvre, F., Noël, T., Crouzet, M., Doignon, F., and Thoraval, D. (2010). The *Candida albicans* Rgd1 is a RhoGAP protein involved in the control of filamentous growth. *Fungal Genet. Biol* 47, 1001-1011.
- Nonaka, H., Tanaka, K., Hirano, H., Fujiwara, T., Kohno, H., Umikawa, M., Mino, A., and Takai, Y. (1995). A downstream target of RHO1 small GTP-binding protein is PKC1, a homolog of protein kinase C, which leads to activation of the MAP kinase cascade in *Saccharomyces cerevisiae*. *EMBO J* 14, 5931-5938.
- Oleksy, A., Opaliński, Ł., Derewenda, U., Derewenda, Z. S., and Otlewski, J. (2006). The molecular basis of RhoA specificity in the guanine nucleotide exchange factor PDZ-RhoGEF. *J. Biol. Chem* 281, 32891-32897.
- Ornstein, L. (1964). DISC ELECTROPHORESIS – I BACKGROUND AND THEORY. *Annals of the New York Academy of Sciences* 121, 321-349.
- Ottillie, S., Miller, P. J., Johnson, D. I., Creasy, C. L., Sells, M. A., Bagrodia, S., Forsburg, S. L., and Chernoff, J. (1995). Fission yeast pak1+ encodes a protein kinase that interacts with Cdc42p and is involved in the control of cell polarity and mating. *EMBO J* 14, 5908-5919.
- Ozaki, K., Tanaka, K., Imamura, H., Hihara, T., Kameyama, T., Nonaka, H., Hirano, H., Matsuura, Y., and Takai, Y. (1996). Rom1p and Rom2p are GDP/GTP exchange proteins (GEPs) for the Rho1p small GTP binding protein in *Saccharomyces cerevisiae*. *EMBO J* 15, 2196-2207.
- Ozaki-Kuroda, K., Yamamoto, Y., Nohara, H., Kinoshita, M., Fujiwara, T., Irie, K., and Takai, Y. (2001). Dynamic localization and function of Bni1p at the sites of directed growth in *Saccharomyces cerevisiae*. *Mol. Cell. Biol* 21, 827-839.
- Park, G., Pan, S., and Borkovich, K. A. (2008). Mitogen-Activated Protein Kinase Cascade Required for

- Regulation of Development and Secondary Metabolism in *Neurospora crassa*. *Eukaryot Cell* 7, 2113-2122.
- Park, H. O., Bi, E., Pringle, J. R., and Herskowitz, I. (1997). Two active states of the Ras-related Bud1/Rsr1 protein bind to different effectors to determine yeast cell polarity. *Proc. Natl. Acad. Sci. U.S.A* 94, 4463-4468.
- Park, H. O., Chant, J., and Herskowitz, I. (1993). BUD2 encodes a GTPase-activating protein for Bud1/Rsr1 necessary for proper bud-site selection in yeast. *Nature* 365, 269-274.
- Park, H., and Bi, E. (2007). Central roles of small GTPases in the development of cell polarity in yeast and beyond. *Microbiol. Mol. Biol. Rev* 71, 48-96.
- Paterson, H. F., Self, A. J., Garrett, M. D., Just, I., Aktories, K., and Hall, A. (1990). Microinjection of recombinant p21rho induces rapid changes in cell morphology. *J. Cell Biol* 111, 1001-1007.
- Pechlivanis, M., and Kuhlmann, J. (2006). Hydrophobic modifications of Ras proteins by isoprenoid groups and fatty acids--More than just membrane anchoring. *Biochim. Biophys. Acta* 1764, 1914-1931.
- Perez, P., and Rincón, S. A. (2010). Rho GTPases: regulation of cell polarity and growth in yeasts. *Biochem. J* 426, 243-253.
- Pertz, O. (2010). Spatio-temporal Rho GTPase signaling - where are we now? *J. Cell. Sci* 123, 1841-1850.
- Peter, M., Neiman, A. M., Park, H. O., van Lohuizen, M., and Herskowitz, I. (1996). Functional analysis of the interaction between the small GTP binding protein Cdc42 and the Ste20 protein kinase in yeast. *EMBO J* 15, 7046-7059.
- Peterson, J., Zheng, Y., Bender, L., Myers, A., Cerione, R., and Bender, A. (1994). Interactions between the bud emergence proteins Bem1p and Bem2p and Rho-type GTPases in yeast. *J. Cell Biol* 127, 1395-1406.
- Pham, C. D., Yu, Z., Sandrock, B., Böcker, M., Gold, S. E., and Perlin, M. H. (2009). *Ustilago maydis* Rho1 and 14-3-3 homologues participate in pathways controlling cell separation and cell polarity. *Eukaryotic Cell* 8, 977-989.
- Philip, B., and Levin, D. E. (2001). Wsc1 and Mid2 are cell surface sensors for cell wall integrity signaling that act through Rom2, a guanine nucleotide exchange factor for Rho1. *Mol. Cell. Biol* 21, 271-280.
- Pinar, M., Coll, P. M., Rincón, S. A., and Pérez, P. (2008). *Schizosaccharomyces pombe* Pxl1 is a paxillin homologue that modulates Rho1 activity and participates in cytokinesis. *Mol. Biol. Cell* 19, 1727-1738.
- Pratt, R. J., Lee, D. W., and Aramayo, R. (2004). DNA methylation affects meiotic trans-sensing, not meiotic silencing, in *Neurospora*. *Genetics* 168, 1925-1935.
- Pruyne, D., and Bretscher, A. (2000). Polarization of cell growth in yeast. *J. Cell. Sci* 113 (Pt 4), 571-585.
- Pruyne, D. W., Schott, D. H., and Bretscher, A. (1998). Tropomyosin-containing Actin Cables Direct the Myo2p-dependent Polarized Delivery of Secretory Vesicles in Budding Yeast. *The Journal of Cell Biology* 143, 1931 -1945.
- Punt, P. J., Dingemans, M. A., Jacobs-Meijsing, B. J., Pouwels, P. H., and van den Hondel, C. A. (1988). Isolation and characterization of the glyceraldehyde-3-phosphate dehydrogenase gene of *Aspergillus nidulans*. *Gene* 69, 49-57.
- Qadota, H., Anraku, Y., Botstein, D., and Ohya, Y. (1994). Conditional lethality of a yeast strain expressing human RHOA in place of RHO1. *Proc. Natl. Acad. Sci. U.S.A* 91, 9317-9321.
- Qadota, H., Python, C. P., Inoue, S. B., Arisawa, M., Anraku, Y., Zheng, Y., Watanabe, T., Levin, D. E., and Ohya, Y. (1996). Identification of yeast Rho1p GTPase as a regulatory subunit of 1,3-beta-glucan synthase. *Science* 272, 279-281.
- Qyang, Y., Yang, P., Du, H., Lai, H., Kim, H., and Marcus, S. (2002). The p21-activated kinase, Shk1, is required for proper regulation of microtubule dynamics in the fission yeast, *Schizosaccharomyces pombe*. *Mol. Microbiol* 44, 325-334.
- Ramírez-Ramírez, N., García-Soto, J., González-Hernández, A., and Martínez-Cadena, G. (1999). The small GTP-binding protein Rho is expressed differentially during spore germination of *Phycomyces blakesleeanus*. *Microbiology (Reading, Engl.)* 145 (Pt 5), 1097-1104.
- Rasmussen, C. G., and Glass, N. L. (2005). A Rho-type GTPase, rho-4, is required for septation in *Neurospora crassa*. *Eukaryotic Cell* 4, 1913-1925.
- Rasmussen, C. G., and Glass, N. L. (2007). Localization of RHO-4 indicates differential regulation of conidial versus vegetative septation in the filamentous fungus *Neurospora crassa*. *Eukaryotic Cell* 6, 1097-1107.
- Rasmussen, C. G., Morgenstein, R. M., Peck, S., and Glass, N. L. (2008). Lack of the GTPase RHO-4 in *Neurospora crassa* causes a reduction in numbers and aberrant stabilization of microtubules at hyphal tips. *Fungal Genet. Biol* 45, 1027-1039.
- Ridley, A. J. (2001). Rho GTPases and cell migration. *J. Cell. Sci* 114, 2713-2722.
- Ridley, A. J., and Hall, A. (1992). The small GTP-binding protein rho regulates the assembly of focal adhesions and actin stress fibers in response to growth factors. *Cell* 70, 389-399.
- Ridley, A. J., Paterson, H. F., Johnston, C. L., Diekmann, D., and Hall, A. (1992). The small GTP-binding protein rac regulates growth factor-induced membrane ruffling. *Cell* 70, 401-410.
- Rincon, S., Coll, P. M., and Perez, P. (2007). Spatial regulation of Cdc42 during cytokinesis. *Cell Cycle* 6, 1687-

- 1691.
- Rincón, S. A., Santos, B., and Pérez, P. (2006). Fission yeast Rho5p GTPase is a functional paralogue of Rho1p that plays a role in survival of spores and stationary-phase cells. *Eukaryotic Cell* 5, 435-446.
- Riquelme, M., Bartnicki-García, S., González-Prieto, J. M., Sánchez-León, E., Verdín-Ramos, J. A., Beltrán-Aguilar, A., and Freitag, M. (2007). Spitzenkörper localization and intracellular traffic of green fluorescent protein-labeled CHS-3 and CHS-6 chitin synthases in living hyphae of *Neurospora crassa*. *Eukaryotic Cell* 6, 1853-1864.
- Robinson, N. G., Guo, L., Imai, J., Toh-E, A., Matsui, Y., and Tamanoi, F. (1999). Rho3 of *Saccharomyces cerevisiae*, which regulates the actin cytoskeleton and exocytosis, is a GTPase which interacts with Myo2 and Exo70. *Mol. Cell. Biol* 19, 3580-3587.
- Rodríguez-Pachón, J. M., Martín, H., North, G., Rotger, R., Nombela, C., and Molina, M. (2002). A Novel Connection between the Yeast Cdc42 GTPase and the Slit2-mediated Cell Integrity Pathway Identified through the Effect of Secreted Salmonella GTPase Modulators. *Journal of Biological Chemistry* 277, 27094-27102.
- Rolke, Y., and Tudzynski, P. (2008). The small GTPase Rac and the p21-activated kinase Cla4 in *Claviceps purpurea*: interaction and impact on polarity, development and pathogenicity. *Mol. Microbiol* 68, 405-423.
- Rossman, K. L., Der, C. J., and Sondek, J. (2005). GEF means go: turning on RHO GTPases with guanine nucleotide-exchange factors. *Nat. Rev. Mol. Cell Biol* 6, 167-180.
- Rossman, K. L., Worthylake, D. K., Snyder, J. T., Cheng, L., Whitehead, I. P., and Sondek, J. (2002). Functional analysis of cdc42 residues required for Guanine nucleotide exchange. *J. Biol. Chem* 277, 50893-50898.
- Roumanie, O., Weinachter, C., Larrieu, I., Crouzet, M., and Doignon, F. (2001). Functional characterization of the Bag7, Lrg1 and Rgd2 RhoGAP proteins from *Saccharomyces cerevisiae*. *FEBS Lett* 506, 149-156.
- Roumanie, O., Wu, H., Molk, J. N., Rossi, G., Bloom, K., and Brennwald, P. (2005). Rho GTPase regulation of exocytosis in yeast is independent of GTP hydrolysis and polarization of the exocyst complex. *J. Cell Biol* 170, 583-594.
- Ruohonen, L., Aalto, M. K., and Keränen, S. (1995). Modifications to the ADH1 promoter of *Saccharomyces cerevisiae* for efficient production of heterologous proteins. *J. Biotechnol* 39, 193-203.
- Ruohonen, L., Penttilä, M., and Keränen, S. (1991). Optimization of *Bacillus alpha*-amylase production by *Saccharomyces cerevisiae*. *Yeast* 7, 337-346.
- Saiki, R. K., Gelfand, D. H., Stoffel, S., Scharf, S. J., Higuchi, R., Horn, G. T., Mullis, K. B., and Erlich, H. A. (1988). Primer-directed enzymatic amplification of DNA with a thermostable DNA polymerase. *Science* 239, 487-491.
- Saka, A., Abe, M., Okano, H., Minemura, M., Qadota, H., Utsugi, T., Mino, A., Tanaka, K., Takai, Y., and Ohya, Y. (2001). Complementing yeast rho1 mutation groups with distinct functional defects. *J. Biol. Chem* 276, 46165-46171.
- Salazar, M. A., Kwiatkowski, A. V., Pellegrini, L., Cestra, G., Butler, M. H., Rossman, K. L., Serna, D. M., Sondek, J., Gertler, F. B., and De Camilli, P. (2003). Tuba, a novel protein containing bin/amphiphysin/Rvs and Dbl homology domains, links dynamin to regulation of the actin cytoskeleton. *J. Biol. Chem* 278, 49031-49043.
- Salinovich, O., and Montelaro, R. C. (1986). Reversible staining and peptide mapping of proteins transferred to nitrocellulose after separation by sodium dodecylsulfate-polyacrylamide gel electrophoresis. *Analytical Biochemistry* 156, 341-347.
- Sambrook, J., and Russell, D. (2001). *Molecular Cloning: A Laboratory Manual* 3rd ed. (New York: Cold Spring Harbor Laboratory Press).
- Santos, B., Gutiérrez, J., Calonge, T. M., and Pérez, P. (2003). Novel Rho GTPase involved in cytokinesis and cell wall integrity in the fission yeast *Schizosaccharomyces pombe*. *Eukaryotic Cell* 2, 521-533.
- Santos, B., Martín-Cuadrado, A. B., Vázquez de Aldana, C. R., del Rey, F., and Pérez, P. (2005). Rho4 GTPase is involved in secretion of glucanases during fission yeast cytokinesis. *Eukaryotic Cell* 4, 1639-1645.
- Scheffer, J., Chen, C., Heidrich, P., Dickman, M. B., and Tudzynski, P. (2005). A CDC42 homologue in *Claviceps purpurea* is involved in vegetative differentiation and is essential for pathogenicity. *Eukaryotic Cell* 4, 1228-1238.
- Scheidig, A. J., Franken, S. M., Corrie, J. E. T., Reid, G. P., Wittinghofer, A., Pai, E. F., and Goody, R. S. (1995). X-ray Crystal Structure Analysis of the Catalytic Domain of the Oncogene Product p21H-ras Complexed with Caged GTP and Mant dGppNHp. *Journal of Molecular Biology* 253, 132-150.
- Schiestl, R. H., and Gietz, R. D. (1989). High efficiency transformation of intact yeast cells using single stranded nucleic acids as a carrier. *Curr. Genet* 16, 339-346.
- Schimoler-O'Rourke, R., Renault, S., Mo, W., and Selitrennikoff, C. P. (2003). *Neurospora crassa* FKS protein binds to the (1,3)beta-glucan synthase substrate, UDP-glucose. *Curr. Microbiol* 46, 408-412.
- Schink, K. O., and Bölker, M. (2009). Coordination of cytokinesis and cell separation by endosomal targeting of a Cdc42-specific guanine nucleotide exchange factor in *Ustilago maydis*. *Mol. Biol. Cell* 20, 1081-1088.
- Schmelzle, T., Helliwell, S. B., and Hall, M. N. (2002). Yeast protein kinases and the RHO1 exchange factor TUS1 are novel components of the cell integrity pathway in yeast. *Mol. Cell. Biol* 22, 1329-1339.

- Schmidt, A., Bickle, M., Beck, T., and Hall, M. N. (1997). The yeast phosphatidylinositol kinase homolog TOR2 activates RHO1 and RHO2 via the exchange factor ROM2. *Cell* 88, 531-542.
- Schmitz, H., Huppert, S., Lorberg, A., and Heinisch, J. J. (2002). Rho5p downregulates the yeast cell integrity pathway. *J. Cell. Sci* 115, 3139-3148.
- Schmitz, H., Kaufmann, A., Köhli, M., Laissue, P. P., and Philippsen, P. (2006). From function to shape: a novel role of a formin in morphogenesis of the fungus *Ashbya gossypii*. *Mol. Biol. Cell* 17, 130-145.
- Scott, B., and Eaton, C. J. (2008). Role of reactive oxygen species in fungal cellular differentiations. *Curr. Opin. Microbiol* 11, 488-493.
- Seiler, S., and Plamann, M. (2003). The genetic basis of cellular morphogenesis in the filamentous fungus *Neurospora crassa*. *Mol. Biol. Cell* 14, 4352-4364.
- Selker, E., Cambareri, E., Garrett, P., Jensen, B., Haack, K., Foss, E., Turpen, C., Singer, M., and Kinsey, J. (1989). Use of RIP to inactivate genes in *Neurospora crassa*. *Fungal Genetics Newsletter* 36, 76.
- Semighini, C. P., and Harris, S. D. (2008). Regulation of apical dominance in *Aspergillus nidulans* hyphae by reactive oxygen species. *Genetics* 179, 1919-1932.
- Shapiro, A. L., Viñuela, E., and V. Maizel, J. (1967). Molecular weight estimation of polypeptide chains by electrophoresis in SDS-polyacrylamide gels. *Biochemical and Biophysical Research Communications* 28, 815-820.
- Shear, C. L., and Dodge, B. O. (1927). Life Histories and Heterothallism of the Red Bread-Mold Fungi of the *Monilia sitophila* Group. *Journal of Agricultural Research* 34, 1019-1042.
- Sheu, Y. J., Santos, B., Fortin, N., Costigan, C., and Snyder, M. (1998). Spa2p interacts with cell polarity proteins and signaling components involved in yeast cell morphogenesis. *Mol. Cell. Biol* 18, 4053-4069.
- Shimada, Y., Gulli, M. P., and Peter, M. (2000). Nuclear sequestration of the exchange factor Cdc24 by Far1 regulates cell polarity during yeast mating. *Nat. Cell Biol* 2, 117-124.
- Si, H., Justa-Schuch, D., Seiler, S., and Harris, S. D. (2010). Regulation of Septum Formation by the Bud3-Rho4 GTPase Module in *Aspergillus nidulans*. *Genetics* 185, 165-176.
- Singh, K., Kang, P. J., and Park, H. (2008). The Rho5 GTPase is necessary for oxidant-induced cell death in budding yeast. *Proc. Natl. Acad. Sci. U.S.A* 105, 1522-1527.
- Smith, G. R., Givan, S. A., Cullen, P., and Sprague, G. F. (2002a). GTPase-activating proteins for Cdc42. *Eukaryotic Cell* 1, 469-480.
- Smith, S. E., Csank, C., Reyes, G., Ghannoum, M. A., and Berlin, V. (2002b). *Candida albicans* RHO1 is required for cell viability in vitro and in vivo. *FEMS Yeast Res* 2, 103-111.
- Soto, T., Villar-Tajadura, M. A., Madrid, M., Vicente, J., Gacto, M., Pérez, P., and Cansado, J. (2010). Rga4 modulates the activity of the fission yeast cell integrity MAPK pathway by acting as a Rho2 GTPase-activating protein. *J. Biol. Chem* 285, 11516-11525.
- Spector, I., Braet, F., Shochet, N. R., and Bubb, M. R. (1999). New anti-actin drugs in the study of the organization and function of the actin cytoskeleton. *Microsc. Res. Tech* 47, 18-37.
- Srb, A. M., Basl, M., Bobst, M., and Leary, J. V. (1973). Mutations in *Neurospora crassa* Affecting Ascus and Ascospore Development. *Journal of Heredity* 64, 243 -246.
- Staben, C., Jensen, B., Singer, M., Pollock, J., Schechtman, M., Kinsey, J., and Selker, E. (1989). Use of a bacterial hygromycin B resistance gene as a dominant selectable marker in *Neurospora crassa* transformation. *Fungal Genetics Newsletter* 36, 79-81.
- Stevenson, B. J., Ferguson, B., De Virgilio, C., Bi, E., Pringle, J. R., Ammerer, G., and Sprague, G. F. (1995). Mutation of RGA1, which encodes a putative GTPase-activating protein for the polarity-establishment protein Cdc42p, activates the pheromone-response pathway in the yeast *Saccharomyces cerevisiae*. *Genes & Development* 9, 2949 -2963.
- Su, Z., Osborne, M. J., Xu, P., Xu, X., Li, Y., and Ni, F. (2005). A bivalent dissectional analysis of the high-affinity interactions between Cdc42 and the Cdc42/Rac interactive binding domains of signaling kinases in *Candida albicans*. *Biochemistry* 44, 16461-16474.
- Sussman, A., Huss, K., Chio, L., Heidler, S., Shaw, M., Ma, D., Zhu, G., Campbell, R. M., Park, T., Kulanthaivel, P., et al. (2004). Discovery of Cercosporamide, a Known Antifungal Natural Product, as a Selective Pkc1 Kinase Inhibitor through High-Throughput Screening. *Eukaryot Cell* 3, 932-943.
- Szabo, R. (2001). Cla4 protein kinase is essential for filament formation and invasive growth of *Yarrowia lipolytica*. *Mol. Genet. Genomics* 265, 172-179.
- Tajadura, V., García, B., García, I., García, P., and Sánchez, Y. (2004). *Schizosaccharomyces pombe* Rgf3p is a specific Rho1 GEF that regulates cell wall beta-glucan biosynthesis through the GTPase Rho1p. *J. Cell. Sci* 117, 6163-6174.
- Takada, H., Nishida, A., Domae, M., Kita, A., Yamano, Y., Uchida, A., Ishiwata, S., Fang, Y., Zhou, X., Masuko, T., et al. (2010). The cell surface protein gene *ecm33+* is a target of the two transcription factors Atf1 and Mbx1 and negatively regulates Pmk1 MAPK cell integrity signaling in fission yeast. *Mol. Biol. Cell* 21, 674-685.
- Takada, H., Nishimura, M., Asayama, Y., Mannse, Y., Ishiwata, S., Kita, A., Doi, A., Nishida, A., Kai, N., Moriuchi,

- S., et al. (2007). Atf1 is a target of the mitogen-activated protein kinase Pmk1 and regulates cell integrity in fission yeast. *Mol. Biol. Cell* 18, 4794-4802.
- Takemoto, D., Tanaka, A., and Scott, B. (2006). A p67Phox-like regulator is recruited to control hyphal branching in a fungal-grass mutualistic symbiosis. *Plant Cell* 18, 2807-2821.
- Takemoto, D., Tanaka, A., and Scott, B. (2007). NADPH oxidases in fungi: diverse roles of reactive oxygen species in fungal cellular differentiation. *Fungal Genet. Biol.* 44, 1065-1076.
- Tanaka, A., Takemoto, D., Hyon, G., Park, P., and Scott, B. (2008). NoxA activation by the small GTPase RacA is required to maintain a mutualistic symbiotic association between *Epichloë festucae* and perennial ryegrass. *Mol. Microbiol.* 68, 1165-1178.
- Tatebe, H., Nakano, K., Maximo, R., and Shiozaki, K. (2008). Pom1 DYRK regulates localization of the Rga4 GAP to ensure bipolar activation of Cdc42 in fission yeast. *Curr. Biol.* 18, 322-330.
- Tcherkezian, J., and Lamarche-Vane, N. (2007). Current knowledge of the large RhoGAP family of proteins. *Biol. Cell* 99, 67-86.
- Tiedje, C., Sakwa, I., Just, U., and Höfken, T. (2008). The Rho GDI Rdi1 regulates Rho GTPases by distinct mechanisms. *Mol. Biol. Cell* 19, 2885-2896.
- Toda, T., Shimanuki, M., and Yanagida, M. (1993). Two novel protein kinase C-related genes of fission yeast are essential for cell viability and implicated in cell shape control. *EMBO J* 12, 1987-1995.
- Toenjes, K. A., Sawyer, M. M., and Johnson, D. I. (1999). The guanine-nucleotide-exchange factor Cdc24p is targeted to the nucleus and polarized growth sites. *Curr. Biol.* 9, 1183-1186.
- Tolliday, N., VerPlank, L., and Li, R. (2002). Rho1 directs formin-mediated actin ring assembly during budding yeast cytokinesis. *Curr. Biol.* 12, 1864-1870.
- Tomić, S., Bertosa, B., Wang, T., and Wade, R. C. (2007). COMBINE analysis of the specificity of binding of Ras proteins to their effectors. *Proteins* 67, 435-447.
- Towbin, H., Staehelin, T., and Gordon, J. (1979). Electrophoretic transfer of proteins from polyacrylamide gels to nitrocellulose sheets: procedure and some applications. *Proc. Natl. Acad. Sci. U.S.A.* 76, 4350-4354.
- van Triest, M., de Rooij, J., and Bos, J. L. (2001). Measurement of GTP-bound Ras-like GTPases by activation-specific probes. *Meth. Enzymol.* 333, 343-348.
- Tucker, C. L., Peteya, L. A., Pittman, A. M. C., and Zhong, J. (2009). A genetic test for yeast two-hybrid bait competency using RanBPM. *Genetics* 182, 1377-1379.
- Ushinsky, S. C., Harcus, D., Ash, J., Dignard, D., Marcil, A., Morchhauser, J., Thomas, D. Y., Whiteway, M., and Leberer, E. (2002). CDC42 Is Required for Polarized Growth in Human Pathogen *Candida albicans*. *Eukaryotic Cell* 1, 95-104.
- Valdivia, R. H., and Schekman, R. (2003). The yeasts Rho1p and Pkc1p regulate the transport of chitin synthase III (Chs3p) from internal stores to the plasma membrane. *Proc. Natl. Acad. Sci. U.S.A.* 100, 10287-10292.
- Vanni, C., Ottaviano, C., Guo, F., Puppo, M., Varesio, L., Zheng, Y., and Eva, A. (2005). Constitutively active Cdc42 mutant confers growth disadvantage in cell transformation. *Cell Cycle* 4, 1675-1682.
- Vasara, T., Saloheimo, M., Keränen, S., and Penttilä, M. (2001a). *Trichoderma reesei* rho3 a homologue of yeast RH03 suppresses the growth defect of yeast sec15-1 mutation. *Curr. Genet.* 40, 119-127.
- Vasara, T., Salusjärvi, L., Raudaskoski, M., Keränen, S., Penttilä, M., and Saloheimo, M. (2001b). Interactions of the *Trichoderma reesei* rho3 with the secretory pathway in yeast and *T. reesei*. *Mol. Microbiol.* 42, 1349-1361.
- Versele, M., and Thorner, J. (2004). Septin collar formation in budding yeast requires GTP binding and direct phosphorylation by the PAK, Cla4. *J. Cell Biol.* 164, 701-715.
- Vetter, I. R., and Wittinghofer, A. (2001). The guanine nucleotide-binding switch in three dimensions. *Science* 294, 1299-1304.
- Villar-Tajadura, M. A., Coll, P. M., Madrid, M., Cansado, J., Santos, B., and Pérez, P. (2008). Rga2 is a Rho2 GAP that regulates morphogenesis and cell integrity in *S. pombe*. *Mol. Microbiol.* 70, 867-881.
- Vink, E., Rodriguez-Suarez, R. J., Gérard-Vincent, M., Ribas, J. C., de Nobel, H., van den Ende, H., Durán, A., Klis, F. M., and Bussey, H. (2004). An in vitro assay for (1 → 6)-beta-D-glucan synthesis in *Saccharomyces cerevisiae*. *Yeast* 21, 1121-1131.
- Virag, A., and Harris, S. D. (2006). The Spitzenkörper: a molecular perspective. *Mycol. Res.* 110, 4-13.
- Virag, A., Lee, M. P., Si, H., and Harris, S. D. (2007). Regulation of hyphal morphogenesis by cdc42 and rac1 homologues in *Aspergillus nidulans*. *Mol. Microbiol.* 66, 1579-1596.
- Vogel, H. J. (1956). A convenient growth medium for *Neurospora* (Medium N). *Microbiol. Genet. Bull.* 13, 42-43.
- Vogel, H. J. (1964). Distribution of Lysine Pathways Among Fungi: Evolutionary Implications. *The American Naturalist* 98, 435-446.
- Vogt, N. (2008). Governing fungal polar cell extension: Analysis of Rho GTPase and NDR kinase signalling in *Neurospora crassa*. Available at: <http://webdoc.sub.gwdg.de/diss/2008/vogt/> [Accessed October 27, 2010].

- Vogt, N., and Seiler, S. (2008). The RHO1-specific GTPase-activating protein LRG1 regulates polar tip growth in parallel to Ndr kinase signaling in *Neurospora*. *Mol. Biol. Cell* 19, 4554-4569.
- Vollmer, S. J., and Yanofsky, C. (1986). Efficient cloning of genes of *Neurospora crassa*. *Proc. Natl. Acad. Sci. U.S.A* 83, 4869-4873.
- Wai, S. C., Gerber, S. A., and Li, R. (2009). Multisite phosphorylation of the guanine nucleotide exchange factor Cdc24 during yeast cell polarization. *PLoS ONE* 4, e6563.
- Walther, A., and Wendland, J. (2005). Initial molecular characterization of a novel Rho-type GTPase RhoH in the filamentous ascomycete *Ashbya gossypii*. *Curr. Genet* 48, 247-255.
- Wang, H., Tang, X., and Balasubramanian, M. K. (2003). Rho3p regulates cell separation by modulating exocyst function in *Schizosaccharomyces pombe*. *Genetics* 164, 1323-1331.
- Wei, Y., Zhang, Y., Derewenda, U., Liu, X., Minor, W., Nakamoto, R. K., Somlyo, A. V., Somlyo, A. P., and Derewenda, Z. S. (1997). Crystal structure of RhoA-GDP and its functional implications. *Nat. Struct. Biol* 4, 699-703.
- Weiland, J. J. (1997). Rapid procedure for the extraction of DNA from fungal spores and mycelia. *Fungal Genetics Newsletter* 44, 60-63.
- Weinzierl, G., Leveleki, L., Hassel, A., Kost, G., Wanner, G., and Bölker, M. (2002). Regulation of cell separation in the dimorphic fungus *Ustilago maydis*. *Mol. Microbiol* 45, 219-231.
- Wendland, J., and Philippsen, P. (2001). Cell polarity and hyphal morphogenesis are controlled by multiple rho-protein modules in the filamentous ascomycete *Ashbya gossypii*. *Genetics* 157, 601-610.
- Wendland, J. (2003). Analysis of the landmark protein Bud3 of *Ashbya gossypii* reveals a novel role in septum construction. *EMBO Rep* 4, 200-204.
- Wendland, J. (2001). Comparison of Morphogenetic Networks of Filamentous Fungi and Yeast. *Fungal Genetics and Biology* 34, 63-82.
- Wennerberg, K., Rossman, K. L., and Der, C. J. (2005). The Ras superfamily at a glance. *J Cell Sci* 118, 843-846.
- Woodcock, D. M., Crowther, P. J., Doherty, J., Jefferson, S., DeCruz, E., Noyer-Weidner, M., Smith, S. S., Michael, M. Z., and Graham, M. W. (1989). Quantitative evaluation of *Escherichia coli* host strains for tolerance to cytosine methylation in plasmid and phage recombinants. *Nucleic Acids Res* 17, 3469-3478.
- Wu, C., Lee, S. F., Furmaniak-Kazmierczak, E., Côté, G. P., Thomas, D. Y., and Leberer, E. (1996). Activation of myosin-I by members of the Ste20p protein kinase family. *J. Biol. Chem* 271, 31787-31790.
- Wu, C., Lytvyn, V., Thomas, D. Y., and Leberer, E. (1997). The phosphorylation site for Ste20p-like protein kinases is essential for the function of myosin-I in yeast. *J. Biol. Chem* 272, 30623-30626.
- Yamochi, W., Tanaka, K., Nonaka, H., Maeda, A., Musha, T., and Takai, Y. (1994). Growth site localization of Rho1 small GTP-binding protein and its involvement in bud formation in *Saccharomyces cerevisiae*. *J. Cell Biol* 125, 1077-1093.
- Yang, J., Zhang, Z., Roe, S. M., Marshall, C. J., and Barford, D. (2009). Activation of Rho GTPases by DOCK exchange factors is mediated by a nucleotide sensor. *Science* 325, 1398-1402.
- Yang, P., Kansra, S., Pimental, R. A., Gilbreth, M., and Marcus, S. (1998). Cloning and characterization of shk2, a gene encoding a novel p21-activated protein kinase from fission yeast. *J. Biol. Chem* 273, 18481-18489.
- Yang, P., Qyang, Y., Bartholomeusz, G., Zhou, X., and Marcus, S. (2003). The novel Rho GTPase-activating protein family protein, Rga8, provides a potential link between Cdc42/p21-activated kinase and Rho signaling pathways in the fission yeast, *Schizosaccharomyces pombe*. *J. Biol. Chem* 278, 48821-48830.
- Yoshida, S., Bartolini, S., and Pellman, D. (2009). Mechanisms for concentrating Rho1 during cytokinesis. *Genes & Development* 23, 810-823.
- Yoshida, S., Kono, K., Lowery, D. M., Bartolini, S., Yaffe, M. B., Ohya, Y., and Pellman, D. (2006). Polo-like kinase Cdc5 controls the local activation of Rho1 to promote cytokinesis. *Science* 313, 108-111.
- Zhang, X., Bi, E., Novick, P., Du, L., Kozminski, K. G., Lipschutz, J. H., and Guo, W. (2001). Cdc42 interacts with the exocyst and regulates polarized secretion. *J. Biol. Chem* 276, 46745-46750.
- Zheng, X., Lee, R. T. H., Wang, Y., Lin, Q., and Wang, Y. (2007). Phosphorylation of Rga2, a Cdc42 GAP, by CDK/Hgc1 is crucial for *Candida albicans* hyphal growth. *EMBO J* 26, 3760-3769.
- Zheng, Y. (2001). Dbl family guanine nucleotide exchange factors. *Trends Biochem. Sci* 26, 724-732.
- Zheng, Y., Bender, A., and Cerione, R. A. (1995). Interactions among proteins involved in bud-site selection and bud-site assembly in *Saccharomyces cerevisiae*. *J. Biol. Chem* 270, 626-630.
- Zheng, Y., Cerione, R., and Bender, A. (1994). Control of the yeast bud-site assembly GTPase Cdc42. Catalysis of guanine nucleotide exchange by Cdc24 and stimulation of GTPase activity by Bem3. *J. Biol. Chem* 269, 2369-2372.
- Zheng, Y., Hart, M. J., Shinjo, K., Evans, T., Bender, A., and Cerione, R. A. (1993). Biochemical comparisons of the *Saccharomyces cerevisiae* Bem2 and Bem3 proteins. Delineation of a limit Cdc42 GTPase-activating protein domain. *J. Biol. Chem* 268, 24629-24634.
- Zon, L. I., Dorfman, D. M., and Orkin, S. H. (1989). The polymerase chain reaction colony miniprep. *BioTechniques* 7, 696-698.

9. Acknowledgements

I would like to thank my thesis committee members Dr. Stephan Seiler, Prof. Dr. Stefanie Pöggeler and Prof. Dr. Andreas Wodarz for their advice and encouragement during the course of this work. I am especially indebted to the first two committee members for agreeing to be the reviewers of the dissertation, and to my supervisor Dr. Stephan Seiler for giving me the opportunity to work in his group and for his constant support. I am also grateful to Dr. Stefan Irniger, Dr. Wilfried Kramer and Dr. Hans Dieter Schmitt for their willingness to be further members of my examination committee. Moreover, I would like to thank Prof. Dr. Gerhard Braus for letting me use the equipment of his department.

Special thanks go to Lindsay Bennett (Texas A&M University, USA) for kindly sharing the protocol for MAK1 Western blots and to Prof. Dr. Stefanie Pöggeler, Prof. Dr. Gerhard Braus, Yvonne Heilig, Florian Schulze, Oliver Voigt (all Georg-August-Universität Göttingen, Germany) and Meritxell Riquelme (CICESE, Mexico) for plasmid gifts.

In addition, I highly appreciate the contributions of my diploma student Sonja Braun to the RAC/CDC42 section of this work and thank her cordially for the enjoyable cooperation.

Furthermore, I would like to thank the many past and present members of the AGs Seiler, Braus and Pöggeler at the Institute of Microbiology and Genetics of the Georg-August-Universität Göttingen who with their scientific input, advice, help and friendliness contributed to the progression of this thesis in a pleasant working environment.

My deepest thanks go to my friends and family for their care and loving support and especially to my husband Thomas for his love and his boundless patience in private statistics lessons and proofreading.

10. Curriculum vitae

Persönliche Daten

Name	Corinna Ute Richthammer, geb. Schmitz
Geburtsdatum und –ort	06.10.1981, Nürnberg
Staatsangehörigkeit	deutsch

Schulbildung

1988-1992	Grundschule Altenfurt, Nürnberg
1992-2001	Willstätter-Gymnasium Nürnberg
29.06.2001	Abitur

Studium

01.10.2001-31.03.2007	Ludwig-Maximilians-Universität (LMU) München Studium der Biologie (Hauptfach: Zellbiologie; Nebenfächer: Biochemie, Genetik)
10.10.2003	Diplom-Vorprüfung
31.07.2006	Diplom; Titel der Diplomarbeit: „Untersuchungen zur Funktion von PSR im Zellkern“
01.08.2007-voraussichtlich 03.2011	Promotion in Biologie an der Georg-August- Universität Göttingen im Rahmen des Promo- tionsprogramms „Molecular Biology of Microbial, Animal and Plant Cells“ der Göttingen Graduate School for Neurosciences and Molecular Bio- sciences (GGNB)

Beruflicher Werdegang

01.10.2006-30.11.2006	Studentische Hilfskraft, LMU Biozentrum, Department Biologie
01.03.2007-30.11.2010	Wissenschaftliche Mitarbeiterin, Georg-August- Universität Göttingen, Institut für Mikrobiologie und Genetik